CROSSTALK BETWEEN EPITHELIAL CELLS AND MACROPHAGES IN THE GUT: THE ROLE OF TNFR2

A thesis submitted for the degree of Ph. D.

By

Maja Kristek, M. Pharm.

JANUARY 2014

Based on research carried out at:
School of Biotechnology
Dublin City University
Dublin 9
Ireland

Under the supervision of Dr. Christine Loscher

Declaration

I hereby certify that this material, which I now submit for assessment on the programme of study leading to the award of Doctor of Philosophy is entirely my own work, and that I have exercised reasonable care to ensure that the work is original, and does not to the best of my knowledge breach any law of copyright, and has not been taken from the work of others save and to the extent that such work has been cited and acknowledged within the text of my work.

Signed: _____ (Candidate) ID No.: _____ Date: _____

TABLE OF CONTENTS

ABSTRACT

Crosstalk between epithelial cells and macrophages in the gut: the role of TNFR2 – Maja Kristek

In order to cope with the overwhelming amount of commensal bacteria, dietary and environmental antigens, homeostasis in the intestine relies upon the fine tuned crosstalk between the immune cells and their environment. One of the key regulators of homeostasis in the intestine are macrophages. Unlike other macrophage populations in the body, intestinal macrophages are in a state of partial activation showing no response to inflammatory stimuli, no production of pro-inflammatory cytokines and low expression levels of innate response receptors. Although their phenotype is largely characterised, it still remains unclear how they acquire this phenotype and thus exert these anti-inflammatory properties.

We optimised a method using cell sorting to isolate intestinal macrophages and characterised their phenotype in homeostasis and inflammation. Furthermore, in order to explore how intestinal macrophages acquire this phenotype we investigated the influence of intestinal epithelial cells on macrophages *in vitro* by conditioning J774A.1 macrophages with supernatants from the murine colonic epithelial cell line, CMT-93. Conditioned macrophages acquired a regulatory phenotype that resembles the intestinal macrophages, with decreased production of IL-12p40, IL-6 and other pro-inflammatory mediators. Furthermore, conditioned macrophages became less responsive to Toll-like receptor stimulation, while they kept their phagocytic abilities and maintained TNF-α production. Interestingly, higher expression of TNF receptor 2 (TNFR2) was observed in conditioned macrophages. This receptor has been linked with anti-inflammatory and immunosuppressive effects of TNF-α. Our *in vivo* study on DSS-induced colitis in mice also demonstrated regulation of TNFR2 in the later stage of colitis, correlating with disease resolution. Furthermore, we provide evidence that TNFR2 is also involved in the resolution of disease in the *Clostridium difficile* model of infection.

Our findings show that intestinal epithelial cells can produce factors that change and shape macrophage response and implicate TNFR2 as one of the mechanisms by which intestinal macrophages exert their homeostatic properties.

ABBREVIATIONS

APC	allophycocyanin
BMMØ	bone marrow-derived macrophage
BSA	bovine serum albumin
CD	cluster of differentiation
DC	dendritic cell
DMEM	Dulbecco's modified eagle medium
DNA	deoxyribonucleic acid
dNTP	deoxyribonucleotide triphosphates
DSS	dextran sulphate sodium
EDTA	ethylenediaminetetraacetic acid
ELISA	enzyme-linked immunosorbent assay
FACS	fluorescence activated cell sorting
FBS	foetal bovine serum
FCS	foetal calf serum
FITC	fluorescein isothiocyanate
FSC	forward scatter
HBSS	Hank's balanced salt solution
IBD	inflammatory bowel disease
IL	interleukin
IκB	inhibitor of kappa B
LPS	lipopolysaccharide
MCP	monocyte chemoattractant protein
M-CSF	macrophage colony stimulating factor
MHC	major histocompatibility complex
MIP	macrophage inflammatory protein
MØ	macrophage
mRNA	messenger ribonucleic acid
mTNF	membrane bound TNF
MyD88	myeloid differentiation primary response gene 88
NF-κB	nuclear factor kappa-light-chain-enhancer of activated B cells

NLR	Nod-like receptor
NO	nitric oxide
PAMP	pathogen-associated molecular pattern
PBS	phosphate buffered saline
PI	propidium iodide
PRR	pattern recognition receptor
qRT-PCR	quantitative real time polymerase chain reaction
RLR	Rig-I like receptor
RNA	ribonucleic acid
RPMI	Roswell Park Memorial Institute medium
RT	room temperature
SSC	side scatter
sTNF	soluble TNF
TGF	transforming growth factor
TLR	Toll-like receptor
TNF	tumour necrosis factor
TNFR	tumour necrosis factor receptor
Treg	regulatory T-cells
TSLP	thymic stromal lymphopoietin

PUBLICATIONS

Soluble factors from colonic epithelial cells contribute to gut homeostasis by modulating macrophage phenotype (2013)

Kristek M*, Collins LE, DeCourcey J, McEvoy FA, Loscher CE*

Innate Immunity, Manuscript ID INI-13-0125, resubmitted following revisions, December 2013

Surface Layer Proteins Isolated from *Clostridium difficile* Induce Clearance Responses in Macrophages (2013)

Collins LE, Lynch M, Marszalowska I, ***Kristek M****, Rochfort K, O'Connell M, Windle H, Kelleher D, Loscher CE*

Microbes and Infection, Manuscript ID MICINF-D-13-00278, resubmitted following revisions, December 2013

The role of macrophage TNFR2 in the resolution of intestinal inflammation

Kristek M*, DeCourcey J, Lynch M, Darby T, Quinlan A, Murphy CT, Casey P, Hill C, Melgar S, Loscher CE* (manuscript in preparation)

***Clostridium difficile* ribotype 027 induces a more severe infection *in vivo* compared to ribotype 001**

Lynch M, ***Kristek M****, DeCourcey J, Casey P, MacAogain M, Rodgers T, Loscher CE* (manuscript in preparation)

Syntaxin 11 negatively regulates IFN-γ secretion in early Th17 differentiation

DeCourcey J, Lynch M, ***Kristek M****, Collins LE, Darby T, Murphy CT, Quinlan A, Melgar S, Sur-Stadt U, Bulfone-Paus S and Loscher CE* (manuscript in preparation)

PRESENTATIONS

Irish Society of Immunology Annual Meeting, Dublin, October 2010

A model to examine the role of colonic macrophages in inflammatory disease

Maja Kristek, Arman Rahman, Mary Canavan, Christine E. Loscher

British Society of Immunology Annual Meeting, Liverpool, December 2010

A model to examine the role of colonic macrophages in inflammatory disease

Maja Kristek, Arman Rahman, Mary Canavan, Christine E. Loscher

Source: IMMUNOLOGY Volume: **131** Supplement: **1** Pagers **174-174** Published: **DEC 2010**

School of Biotechnology Annual Research Day, Dublin, January 2011

A model to examine the role of colonic macrophages in inflammatory disease

Maja Kristek, Arman Rahman, Mary Canavan, Christine E. Loscher

Irish Society of Immunology Annual Meeting, Galway, September 2011

Crosstalk between colonic epithelial cells and macrophages

Maja Kristek, Arman Rahman, Christine E. Loscher

American Association of Immunologists Annual Meeting, Boston, May 2012

Crosstalk between colonic epithelial cells and macrophages

Maja Kristek, Arman Rahman, Christine E. Loscher

Source: JOURNAL OF IMMUNOLOGY Volume: **188** Published: **MAY 1 2012**

European Mucosal Immunology Group Meeting, Dublin, October 2012

Crosstalk between colonic epithelial cells and macrophages

Maja Kristek, Arman Rahman, Christine E. Loscher

School of Biotechnology Annual Research Day, Dublin, January 2013

Crosstalk between epithelial cells and macrophages in the gut

Maja Kristek, Aoife Quinlan, Silvia Melgar, Christine E. Loscher

Irish Society of Immunology Annual Meeting, Dublin, September 2013

The role of macrophage TNFR2 in gut homeostasis

Maja Kristek, Trevor Darby, Aoife Quinlan, Silvia Melgar, Christine E. Loscher

CHAPTER 1

GENERAL INTRODUCTION

1 The intestinal immune system

The gastrointestinal tract consists of the small intestine, the caecum, the large intestine (colon) and the rectum. The small intestine is divided into the duodenum, the jejunum, and the ileum. The majority of digestion takes place in the small intestine, whereas the colon is primarily responsible for reabsorbing water. Immediately after birth, the intestine is colonised by a vast microbial community that reaches 10^{13}-10^{14} bacteria per gram of luminal content (Ley *et al.*, 2006, Gill *et al.*, 2006). Alongside the exposure to these commensal bacteria the intestine is also exposed to a variety of food proteins and pathogenic organisms, which means that it constantly encounters more antigens that any other part of the body (Ley *et al.*, 2006). In order to protect against infection but at the same time avoid the unnecessary inflammatory responses to beneficial microbiota and food, the immune system in the intestine has evolved into the largest and most complex part of the host immune system. The homeostasis here is balanced through a strict hierarchy of mechanisms that include many immune and non-immune cells.

The gut-associated lymphoid tissue (GALT) protects the gastrointestinal tract from the stomach to the colon. It comprises of lymphoid tissues such as Peyer's patches, isolated lymphoid follicles and mesenteric lymph nodes. Peyer's patches lie in the small intestine, while isolated lymphoid follicles, which resemble Peyer's patches, can be found in the colon (Jung *et al.*, 2010). The role of these tissues is in immune surveillance and the induction of immune response. The effector sites of the intestine are the mucosal epithelium and underlying lamina propria. Lamina propria contains many different immune cells, including macrophages, dendritic cells, plasma cells, mast cells, T and B lymphocytes (Doe, 1989).

The first line of defence in the intestine are epithelial cells and macrophages that lie just underneath the epithelium. In this introduction we will concentrate on the functions and adaptations of these two cell types and their role in homeostasis and disease. The second part of the introduction focuses on the important macrophage cytokine, TNF-α, its receptors and their role in inflammation as well as protective aspects of macrophage biology.

1.1 Intestinal epithelial cells

A single layer of intestinal epithelial cells forms a barrier between the lumen which is colonised by bacteria and the sub-epithelial tissue that contains immune cells. Apart from providing this physical barrier, intestinal epithelial cells can communicate with their environment, influencing and being influenced by both commensal bacteria and the cells of intestinal immune system (Goto and Ivanov, 2013).

1.1.1 Intestinal epithelial cells as a barrier

The entire epithelium is renewed every 5 days in humans, through differentiation and proliferation of pluripotent stem cells that are located in the base of intestinal crypts. These cells differentiate into three different cell lineages: enterocytes, enteroendocrine cells and goblet cells (Pinto *et al.*, 2003) **[Figure 1.1]**. In the small intestine, stem cells also differentiate into Paneth cells (Salzman *et al.*, 2007). The most abundant intestinal surface cell is the enterocyte. Enterocytes form tight junctions with their neighbouring cells which prevents bacterial penetration, while

allowing nutrient flux into host tissue. They also secrete a variety of antimicrobial proteins, such as defensins, cathelicidins and C-type lectins (Mukherjee *et al.*, 2008). These antimicrobial proteins are natural antibiotics that promote bacterial killing through enzymatic attack of the bacterial cell wall or by disrupting the bacterial inner membrane (Mukherjee *et al.*, 2008). In the small intestine Paneth cells also produce antimicrobial proteins such as defensines and lyzozyme (Salzman *et al.*, 2007). The enterocyte monolayer is interrupted by the presence of enteroendocrine cells and goblet cells. Enteroendocrine cells produce peptide hormones involved in cellular trophism, tissue repair, angiogenesis and enterocyte differentiation (Roda *et al.*, 2010). Goblet cells secrete large quantities of mucin glycoproteins. These glycoproteins assemble into a viscous, protective layer that extends up to 150μm from the epithelial surface (Gum *et al.*, 1994) and forms two distinct strata (Johansson *et al.*, 2008); the outer and the inner layer. The outer layer is colonised by bacteria, while the inner layer is resistant to bacterial penetration and forms a protected zone just above the epithelial surface (Johansson *et al.*, 2008). Mice that lack mucin are unable to maintain the outer layer and suffer from intestinal inflammation (Johansson *et al.*, 2008).

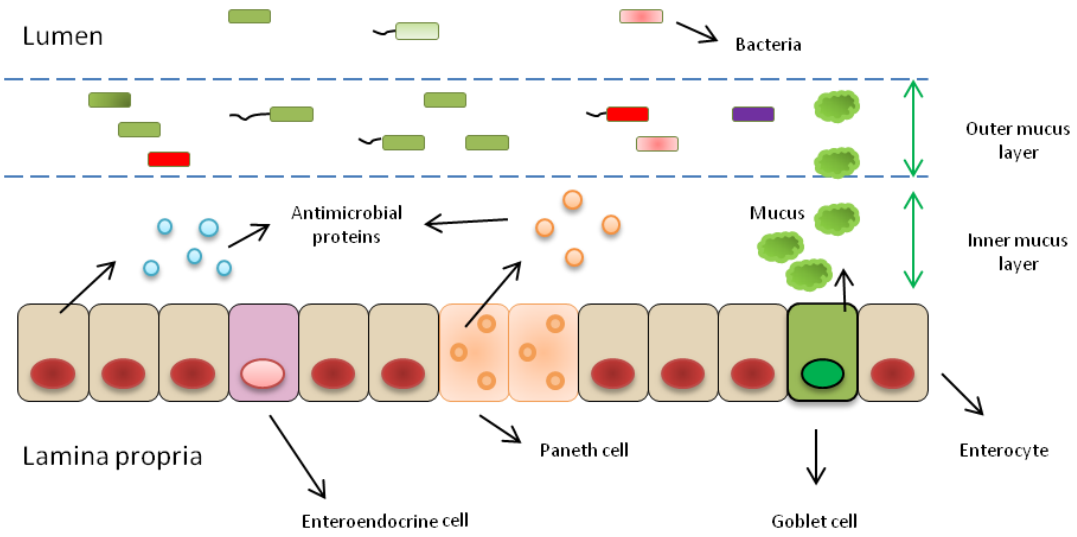

Figure 1.1 The intestinal epithelial cell barrier A single layer of intestinal epithelial cells provides a physical barrier between commensal bacteria from the intestinal lumen and lamina propria. Different intestinal epithelial cells produce antimicrobial proteins and mucus that form a protective layer.

1.1.2 Intestinal epithelial cells as the sentinels of intestinal immune system

For a long time, intestinal epithelial cells were considered to be just a physical barrier between the intestinal lumen and underlying immune cells. Tight junction complexes and the thick mucus layer were thought to be impermeable to commensal bacteria and enough to prevent an inflammatory response to these microorganisms. However it became evident that there is a crosstalk between microbes and their metabolites, epithelial cells and other cell types in the mucosa. Similarly to conventional innate immune cells, intestinal epithelial cells express pattern-recognition receptors (PRRs) to detect common microbial ligands. These are Toll-like receptors (TLRs), Nod-like receptors (NLRs) and Rig-I like receptors (RLRs) (Goto and Ivanov, 2013). As explained in the following paragraphs, these PRRs

work as a tightly regulated machinery to keep the optimal function of the epithelial barrier.

1.1.2.1 Toll-like receptors

The TLR family is the best characterised family of PRRs. It contains 10 members in humans and 13 in mice which can recognise microbes through pathogen-associated molecular patterns (PAMPs) and initiate an immune response (Akira *et al.*, 2001). For example, TLR2 recognises bacterial lipopeptides and lipoteichoic acid from the cell wall of Gram positive bacteria and cooperates with TLR1 and TLR6 (Takeuchi *et al.*, 1999). TLR3 recognises RNA from double and single stranded viruses (Alexopoulou *et al.*, 2001). TLR4 is a major receptor for lipopolysaccharide (LPS) from the outer membrane of Gram negative bacteria (Takeuchi *et al.*, 1999). TLR5 ligands are flagellin and flagellated bacteria (Hayashi *et al.*, 2001), while TLR9 recognised unmethylated CpG DNA from DNA viruses (Hemmi *et al.*, 2000) and TLR11 is activated by uropathogenic bacteria (Zhang *et al.*, 2004).

Almost all TLRs are expressed at the mRNA level in the epithelial cells of the human colon and the expression of TLR1, TLR2, TLR3, TLR4, TLR5 and TLR9 has been confirmed in the epithelial cells in the small intestine (Otte *et al.*, 2004). Activation of TLRs in the healthy intestine, however, does not initiate an immune response. Rather, signalling through TLRs is proven to be protective and crucial for the maintenance of intestinal homeostasis. TLR2 and TLR4 deficient mice have increased susceptibility to dextran sulphate sodium (DSS)-induced colitis (Rakoff-Nahoum *et al.*, 2004). Furthermore, mice deficient in MyD88, a signalling adaptor used by all TLRs showed severe susceptibility to colonic injury and severe mortality (Rakoff-Nahoum *et al.*, 2004). TLR5 knockout mice have a tendency to develop

spontaneous colitis (Wells *et al.*, 2011). On the other hand, administration of TLR4 or TLR2 ligand via the oral route completely protected intestinal microflora-depleted mice from the DSS-induced mortality (Rakoff-Nahoum *et al.*, 2004). Other TLRs also have a protective effect against DSS-induced injury. Systemic administration of flagellin (Vijay-Kumar *et al.*, 2008) and oral or systemic administration of CpG (Rachmilewitz *et al.*, 2004), both protect against DSS-induced colitis.

TLRs are also required for epithelial cell proliferation following injury. TLR4 is required for the induction of cyclooxygenase 2 (COX2) which then leads to epithelial cell production of prostaglandin E_2 (PGE_2) and induction of epidermal growth factor members (Fukata *et al.*, 2009). TLR signalling is also responsible for the movement of mesenchymal stromal cells to a position adjacent to epithelial stem cell. In the absence of MyD88 this re-positioning does not happen and stromal cells do not secrete factors responsible for the induction of epithelial cell proliferation (Brown *et al.*, 2007).

Furthermore, TLRs, especially TLR2, have been shown to be involved in the regulation of barrier function. Treatment of epithelial cells with TLR2 ligands during recovery from induced colitis resulted in the improved tight junction function and decreased epithelial cell apoptosis (Cario *et al.*, 2007).

1.1.2.2 Nod-like and RIG-1 like receptors

Although not so extensively studied as TLRs, NLRs and RLRs are also shown to be important for the intestinal epithelial cell functions.

Nucleotide-binding oligomerization domains 1 (NOD1) and 2 (NOD2) are intracellular sensors of bacterial peptidoglycan components. NOD1-deficient mice are highly susceptible to infections with *Helicobacter pylori*, a Gram-negative

bacterium found in the stomach and linked with the development of duodenal ulcer (Viala *et al.*, 2004). NOD2 deficiency results in the abnormal development and function of Peyer's patches, which are organised lymphoid nodules in the small intestine important in the immune surveillance. These mice exhibit high concentrations of pro-inflammatory cytokines, suggesting that NOD2 is important for Peyer's patches homeostasis (Frédérick *et al.*, 2007). Furthermore, both NOD1 and NOD2 gene polymorphisms are associated with susceptibility to Crohn's disease and ulcerative colitis (McGovern *et al.*, 2005).

RLRs recognise viral RNA and their expression is also connected with the function of Peyer's patches. RIG-1 deficient mice have significantly lower numbers of Peyer's patches and also severe damage and infiltration of inflammatory cells into the colonic mucosa (Wang *et al.*, 2007).

1.1.3 Intestinal epithelial cells and adaptations to the antigen-rich environment

It is obvious that a tonic level of PRR signalling is necessary to maintain intestinal homeostasis. However, it is less clear how this signalling is regulated so that it does not initiate an unnecessary immune response to commensal bacteria. A few hypotheses have been proposed over time. It was thought that the thick layer of mucus is impermeable to commensal microbes, however, it is likely that a low number of commensal bacteria cross the epithelium under steady-state conditions, as gut flora-derived microorganisms can be cultured from the spleens of mice (Abreu, 2010). Furthermore, it was though that epithelial cells serve only as a mechanical barrier and cannot sense their environment. However, it is now clear that intestinal

epithelial cells, and not just underlying immune cells, have PRRs and can therefore recognise microbial patterns (Artis, 2008). This means that there are other mechanisms in place to control the balance between homeostasis and the immune response of intestinal epithelial cells.

1.1.3.1 Spatial distribution of PRRs

The polarisation of intestinal epithelial cells seems to play a crucial role in avoiding chronic stimulation of PRRs by commensal bacteria. The epithelium is divided into an apical and basolateral domain with a distinct lipid and protein composition (Pott and Hornef, 2012). The apical membrane is exposed to the lumen and intestinal microbiota, while the basolateral side is protected from direct contact with commensals. The cellular localisation of innate immune receptors is also influenced by epithelial cell polarisation. For example, TLR5 is expressed exclusively on the basolateral side of the membrane (Gewirtz *et al.*, 2001) and because of that it can only be activated when the epithelial barrier is disrupted. TLR9 is expressed both on the apical and basolateral side of the membrane, but ligation from the apical side dampens epithelial cell activation, while ligation from the basolateral side strongly stimulates pro-inflammatory chemokine secretion (Lee *et al.*, 2006). Furthermore, TLR3, TLR7 and TLR8 are expressed in the intracellular endosomal organelles (Medzhitov, 2007) and NLRs and RLRs are found in the cytoplasm (Philpott and Girardin, 2004). These PRRs, therefore, only encounter pathogens when they invade the epithelial cell barrier.

1.1.3.2 Commensal bacteria – epithelial cell crosstalk

In addition to their role in digestion, absorption and storage of nutrients that would otherwise be inaccessible to their host, commensal bacteria also play a key role in the maintenance of gut homeostasis. Commensal bacteria have been shown to up-regulate tight junction proteins, change their expression and distribution and in that way control intestinal permeability (Ulluwishewa *et al.*, 2011). Besides that, commensals have been shown to interfere with NF-κB signalling. NF-κB is sequestered in the cytoplasm by IκB. Following cell activation, IκB is phosphorylated which targets it for ubiquitylation and degradation. Once IκB is degraded, NF-κB can move to the nucleus where it activates the transcription of many pro-inflammatory genes (Karin and Ben-Neriah, 2000). Commensal bacteria can potentially inhibit the degradation of IκB and consequently stop the nuclear translocation of NF-κB (Neish *et al.*, 2000). Furthermore, members of the *Bacteroides* species were shown to inhibit the NF-κB pathway by up-regulating the peroxisome-proliferation-activated receptor-γ (PPARγ) (Kelly *et al.*, 2004). PPARγ is a member of the nuclear hormone receptor family which binds and diverts activated NF-κB from the nucleus back to the cytoplasm (Kelly *et al.*, 2004).

Furthermore, commensal bacteria were shown to up-regulate MHCII expression by intestinal epithelial cells (Hershberg and Mayer, 2000). MHCII, together with co-stimulatory molecules CD80 and CD86 is needed for the activation of T-cells (Sharpe and Freeman, 2002). Since intestinal epithelial cells express only low levels of co-stimulatory molecules, it is speculated that MHCII up-regulation, in the absence of co-stimulation, leads to T cells tolerance, rather than activation. This way epithelial cells regulate the activation of the adaptive immune system (Hershberg and Mayer, 2000).

1.1.4 Immunomodulatory role of intestinal epithelial cells

As mentioned, intestinal epithelial cells are in a close contact with commensal microbiota from the lumen. In addition to that, they are in a close contact with immune cells in the lamina propria. Thus, epithelial cell – immune cell crosstalk is also important for the maintenance of the gut homeostasis. Increasing evidence is showing that epithelial cells can modulate the phenotype and function of various immune cells through activation of receptors or secretion of cytokines (Rimoldi *et al.*, 2005).

Several studies have implicated an immunomodulatory role for intestinal epithelial cells on antigen presenting cells, such as dendritic cells (DCs). Conditioning of monocyte-derived DCs with Caco-2 intestinal epithelial supernatants induced the production of high amounts of IL-10 from DCs and switched off the production of IL-12 (Rimoldi *et al.*, 2005). Furthermore, epithelial cell conditioned DCs were able to induce the differentiation of T-cells into more anti-inflammatory fates, such as Th2 or Treg (Rimoldi *et al.*, 2005).

The exact mechanism of this immunomodulation is still unclear; however it seems to be regulated by epithelial cell production of thymic stromal lymphopoietin (TSLP) and transforming growth factor-β (TGF-β). TSLP deletion in mice leads to over-expression of IL-12 and inability of intestinal DCs to generate protective regulatory and Th2 responses (Zaph *et al.*, 2007). TGF-β can also convert DCs into a Treg-promoting tolerogenic phenotype (Iliev *et al.*, 2009). It has been shown to act in concert with TSLP to inhibit NF-κB-dependent gene expression and production of pro-inflammatory cytokines (Zeuthen *et al.*, 2008). Mice with a DC-specific deletion of $\alpha_v\beta_8$ integrin, which is required for activation of latent TGF-β, develop severe colitis and have a reduced colonic Treg population (Travis *et al.*, 2007).

Intestinal epithelial cells can also influence B-cells. It has been shown that epithelial cells produce APRIL, a B-cell proliferation-inducing ligand and BAFF, B-cell – activating factor of the tumour necrosis factor family (He *et al.*, 2007). APRIL and BAFF give the signal for class switch recombination of IgM-positive B-cells to IgA and support IgA production *in vivo* (Mora *et al.*, 2006, He *et al.*, 2007). IgA then recognises and opsonises bacteria in the lumen, preventing their access to the lamina propria.

In addition to this, a new study has shown that semaphorin 7A, a glycoprotein expressed on the basolateral surface of intestinal epithelial cells, can stimulate IL-10 production from intestinal macrophages and suppress inflammatory responses (Kang *et al.*, 2012).

1.2 Intestinal macrophages

The intestinal macrophages constitute the largest reservoir of macrophages in the body (Lee *et al.*, 1985). They are most abundant in the colon, with slightly lower frequencies in the small intestine. Intestinal macrophages are characterised by the expression of the F4/80 antigen and the integrins CD11c and CD11b (Lee *et al.*, 1985). They also express CD64 (Tamoutounour *et al.*, 2012) and, as shown in the last few years, they express high levels of the chemokine receptor CX3CR1 (Schulz *et al.*, 2009). Although F4/80 still remains the most reliable marker of murine macrophages (Austyn and Gordon, 1981, Gordon *et al.*, 2011), recent studies have shown that eosinophils in the gut can also express this marker (Mowat and Bain, 2010). Furthermore, macrophages in the gut show significant heterogeneity (as described in details in section 1.2.2). The combination of markers such as F4/80, CX3CR1, Ly6C, MHCII, CD11b and CD11c should, therefore, be used when characterising macrophages populations in the gut to investigate these cells more precisely (Bain *et al.*, 2013).

1.2.1 The unique properties of intestinal macrophages

Unlike other macrophages in the body, intestinal macrophages express only low levels of co-stimulatory molecules, such as CD80, CD86 and CD40 (Rogler *et al.*, 1998). They express all the TLRs at mRNA and protein level (Smith *et al.*, 2011), however they are unresponsive to stimulation with TLR ligands and do not produce pro-inflammatory cytokines such as IL-12, IL-23, IL-6, IL-1 when stimulated with TLR ligands (Smith *et al.*, 2005). This unresponsiveness is not only restricted to

TLR ligation, intestinal macrophages are also unresponsive to ligands for NOD-1, NOD-2 and C-type lectins, intact bacteria, apoptotic debris, IFN-γ and phorbol 12-myristate 12-acetate (PMA) (Smith *et al.*, 2011, Hirotani *et al.*, 2005, Kamada *et al.*, 2005). They do produce anti-inflammatory IL-10 constitutively and in response to TLR ligation (Denning *et al.*, 2007) and, as shown recently, they produce pro-inflammatory TNF-α even in a steady state, but this does not lead to inflammation (Bain *et al.*, 2013). Despite this anergy, intestinal macrophages exhibit strong phagocytic and bacteriocidal activity (Smythies *et al.*, 2005). However, phagocytosis is not accompanied by cytokine release, as in other tissue, and bactericidal activity seems to be independent of the production of reactive oxygen species (ROS) (Rugtveit *et al.*, 1995). In addition to low ROS production, intestinal macrophages also produce only low levels of other pro-inflammatory mediators, such as nitric-oxide (NO) (Ikeda *et al.*, 1997). The differences between intestinal macrophages and other macrophages are summarised in **Table 1.1**

Property	**Intestinal macrophage**	**Inflammatory macrophage**
Co-stimulatory molecules (CD80, CD86, CD40)	-	+
Responsiveness to TLR stimulation	-	+
Cytokine production (IL-12, IL-6, IL-23)	-	+
Phagocytosis	++	+
NO production	-	+
ROS production	-	+
IL-10 production	+	+
TNF-α production	+	+

Table 1.1 Phenotypic comparison of macrophage populations Difference between intestinal macrophages and conventional inflammatory macrophages

1.2.2 The origin of intestinal macrophages

All tissue macrophages are derived from bone marrow stem cells through a highly regulated cascade of events. In the bone-marrow, a combination of cytokines that include IL-1, IL-3 and IL-6 together with granulocyte/macrophage colony stimulating factor (GM-CSF) and macrophage-colony stimulating factor (M-SCF) induce proliferation of a monocyte precursor into a monoblast, then a promonocyte and finally a monocyte (Smith *et al.*, 2011). After leaving the bone marrow, monocytes enter the blood, where they circulate for days before migrating into tissue (Rees, 2010). It is believed that there are two different populations of monocytes; one that migrates and replenishes macrophages in the resting tissue and one that is recruited during inflammation (Geissmann *et al.*, 2003). The first population was termed "resident" monocytes and characterised by the low expression of Ly6C glycoprotein. "Resident" monocytes are non-inflammatory and inert to stimuli (Geissmann *et al.*, 2003). The second population are termed "inflammatory" monocytes or Ly6C^{hi} and unlike "resident" monocytes they are fully responsive to stimulation and home to inflamed tissue (Geissmann *et al.*, 2003).

Because of their distinctive, non-inflammatory features, intestinal macrophages were thought to derive from "resident" monocytes. Surprisingly, experiments combining resident cell ablation with precursor cell transfer have shown that resident intestinal macrophages, actually, derive from "inflammatory" monocytes (Jung *et al.*, 2002, Varol *et al.*, 2009). Once they arrive in the gut these "inflammatory" monocytes then adapt to the gut environment by acquiring a non-inflammatory gene expression signature (Bain *et al.*, 2013). Bain *et al.* showed that the differentiation of adoptively transferred Ly6C^{hi} monocytes into resident gut macrophages happens through a number of transitional stages that they termed P1-P4 **[Figure 1.2A]**. The cells in the

P1 stage appear to be identical to "inflammatory" monocytes, with high expression of Ly6C. Moving from P1 to P4 cells gradually lose the expression of Ly6C and gain the expression of CX3CR1. They also gradually lose the expression of pro-inflammatory genes (IL-6, iNOS) which were highly expressed on cells in P1 phase, but extinguished by P4 (Bain *et al.*, 2013). In parallel, from P1 to P4, there was an increase in TGFβR2, IL-10 and other markers associated with anti-inflammatory macrophages (Bain *et al.*, 2013). This progressive development of $Ly6C^{hi}$ monocytes into $CX3CR1^{hi}Ly6C^{-}$ (P4) resident macrophages has also been proposed in a study by Tamoutounour *et al*, which they named "macrophage waterfall" (Tamoutounour *et al.*, 2012).

Interestingly, this "macrophage waterfall" was disrupted in murine model of disease. Both groups showed that inflammation disrupts full differentiation of "inflammatory" $Ly6C^{hi}$ monocytes into $CX3CR1^{hi}$ resident macrophages and causes the accumulation of cells in P1/P2 stage (Bain *et al.*, 2013, Tamoutounour *et al.*, 2012) **[Figure 1.2B]**.

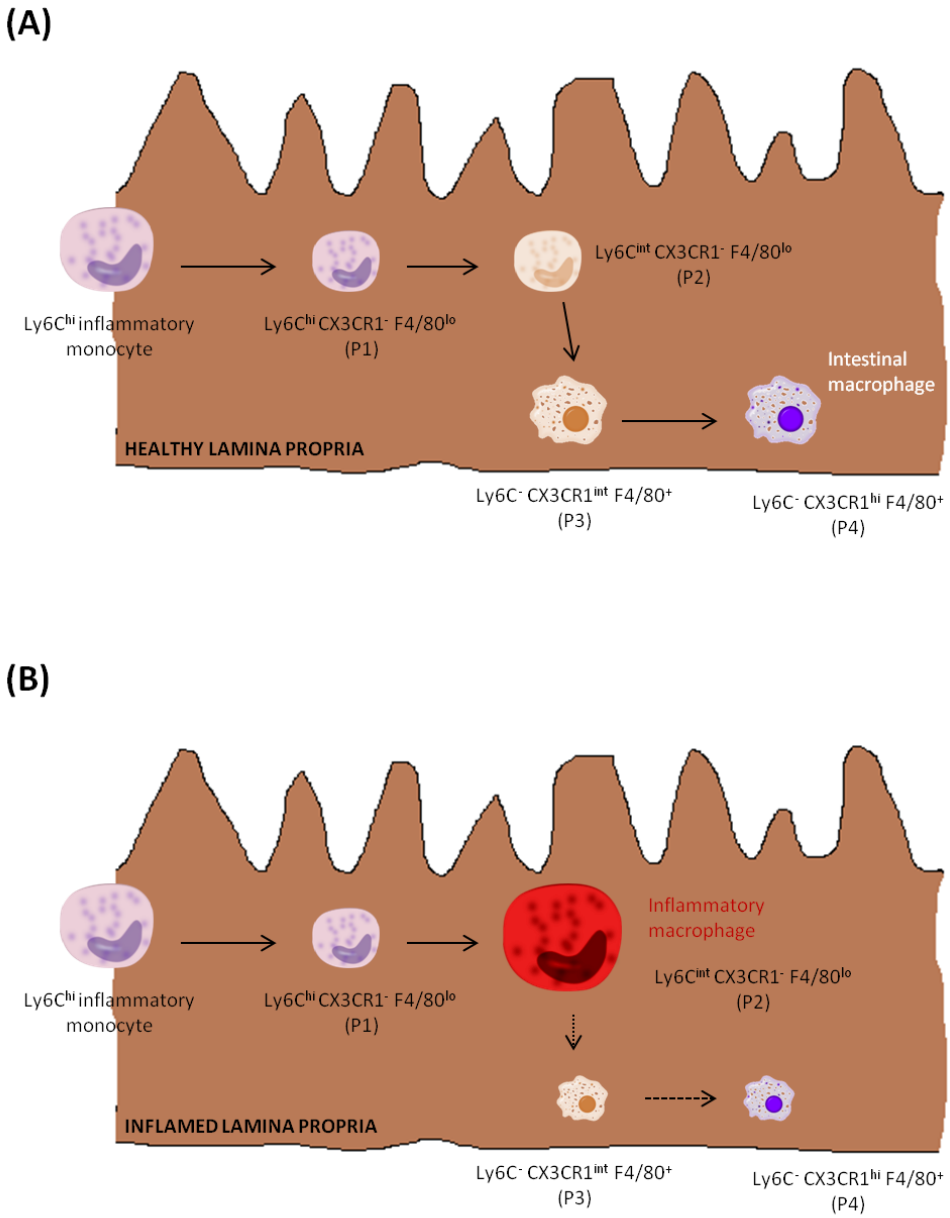

Figure 1.2 Differentiation of inflammatory monocytes into intestinal macrophages under healthy and inflammatory conditions In a healthy intestine, inflammatory monocytes differentiate into anti-inflammatory intestinal macrophages through a number of transitional stages (A). Under inflammatory conditions maturation of inflammatory monocytes is disrupted and there is an accumulation of pro-inflammatory macrophages in the lamina propria (B). Adapted from (Bain *et al.*, 2013, Tamoutounour *et al.*, 2012)

1.2.3 Mechanisms underlying the hypo-responsiveness of intestinal macrophages

While the phenotype of colonic macrophages has been extensively studied, the mechanisms that regulate their specific properties are still largely unclear. However, a number of possibilities have been proposed.

Intestinal macrophages express barely detectable levels of myeloid differentiation primary response gene 88 (MyD88) and Toll/IL-1 receptor (TIR) – domain (Smythies *et al.*, 2010). As MyD88 is crucial for NF-κB activation of all TLRs except TLR3 and TIR mediates TLR3 signalling, down-regulation of these two molecules probably results in NF-κB inactivation in intestinal macrophages (Smythies *et al.*, 2010). Consequently this stops pro-inflammatory cytokine and chemokine production. Furthermore, Hirotani *et al.* have found that colonic macrophages express IκBNS, which is a negative regulator of NF-κB signalling (Hirotani *et al.*, 2005). Another negative regulator of the NF-κB pathway was found in intestinal macrophages, IκBα (Smythies *et al.*, 2010). Intestinal macrophages do not phosphorylate IκBα or NF-κB which stops the translocation of NF-κB to the nucleus and induction of pro-inflammatory genes (Smythies *et al.*, 2010). Besides the defects in the NF-κB pathway, intestinal macrophages also lack the expression of triggering receptor expressed on myeloid cells 1 (TREM-1) (Schenk *et al.*, 2005). TREM-1 can be regarded as an amplifier of inflammation. The cross-linking of TREM-1 leads to a rapid and enhanced secretion of pro-inflammatory mediators (Schenk *et al.*, 2005).

TSLP and TGF-β, secreted by intestinal epithelial cells, have been proposed as possible candidates that suppress NF-κB and TREM-1 signalling (Artis, 2008, Schenk *et al.*, 2005, Smythies *et al.*, 2010). IL-10 is also a candidate, since the

inhibition of IL-10 production by intestinal macrophages reverses their TLR unresponsiveness *in vitro* (Denning *et al.*, 2007). Another factor could be CX3CR1-CX3CL1 interaction. While resident colonic macrophages have high expression of CX3CR1, the CX3CL1 chemokine is produced by intestinal epithelial cells in large quantities (Lucas *et al.*, 2001). Furthermore, CX3CL1 has been shown to condition macrophages in the brain (Lyons *et al.*, 2009).

1.2.4 Intestinal macrophage functions

Because of their hypo-responsiveness to stimuli and inability to mount an inflammatory response, the only role of intestinal macrophages was thought to be phagocytosis of apoptotic cells and debris. However, they have been shown to be important for intestinal homeostasis as depletion of macrophages leads to intestinal inflammation (Qualls *et al.*, 2006). One of their homeostatic-inducing roles is the regulation of epithelial cell integrity. Intestinal macrophages produce prostaglandin E2 and promote MyD88-dependent survival and proliferation of epithelial progenitor cells during colonic wound healing (Pull *et al.*, 2005). Also, they produce cyclo-oxygenase 2 (COX2) which has been linked with anti-inflammatory effects as myeloid cell specific COX2 knockout mice have increased expression of pro-inflammatory cytokines, such as IL-6, TNF-α and IFN-γ, compared to wild type (Watanabe *et al.*, 2010).

Rescigno *et al.* showed that $CX3CR1^{+}$ cells are capable of extending processes across the epithelial layer into the intestinal lumen and sample bacteria (Rescigno *et al.*, 2001). They called these cells dendritic cells, however Shulz *et al.* showed that these $CX3CR1^{+}$ cells do not migrate to mesenteric lymph nodes and are, in fact,

macrophages (Schulz *et al.*, 2009). As mentioned, these macrophages cannot migrate into the mesenteric lymph nodes and prime naïve T-cells, however one of the possibilities is that these cells pass on the antigen to the migratory population of antigen presenting cells, such as dendritic cells (Persson *et al.*, 2010). Another possibility is that by sampling the intestinal lumen, macrophages regulate adaptive immune responses within the lamina propria. Indeed, lamina propria macrophages seem to be specialised in the maintenance of regulatory T-cells (Treg). This is supported by the deficiency of CX3CR1 mutant mice to maintain their tissue Treg cells (Hadis *et al.*, 2011). $CX3CR1^{hi}$ macrophages are also shown to be crucial for the *in vivo* maintenance of Foxp3 (a master regulator of the development and function of regulatory T-cells) expression and suppressive activity of Treg cells during colitis (Murai *et al.*, 2009). *In vitro,* $CX3CR1^{hi}$ macrophages promote the differentiation of naive $CD4^{+}$ T-cells into $Foxp3^{+}$ Treg cells (Denning *et al.*, 2007).

1.3 Inflammatory bowel disease

Inflammatory bowel disease (IBD) is an inflammatory disorder of the gastrointestinal tract characterised by an abnormal immune response to antigens of the intestinal content that leads to a persistent inflammatory state (Scaldaferri and Fiocchi, 2007). Two major forms of IBD are Crohn's disease and ulcerative colitis, distinguished by the area they affect. While ulcerative colitis exclusively effects the colon, Crohn's disease can affect the whole gastrointestinal tract, but is mainly localised to the colon and ileum (Podolsky, 2002). The exact cause of IBD remains poorly understood, however different environmental factors are considered risk factors for IBD, such as smoking, diet, drugs, stress and enteric flora (Loftus, 2004).

Furthermore, advances in DNA analysis and sequencing have indentified some IBD-associated genetic mutations (Duerr, 2007). Whatever the cause may be, both ulcerative colitis and Crohn's disease are characterised by the disruption of the epithelial cell barrier and the dysfunction of the immune system.

1.3.1 The role of epithelial cells in IBD

Over the last decade, evidence has mounted that intestinal barrier disruption may be the primary driver of IBD. Increased gut permeability is most likely genetically determined. It has been shown that up to 40% of healthy first-degree relatives of patients with Crohn's disease exhibit increased intestinal permeability as measured by Cellobiosc/Mannitol test (Secondulfo *et al.*, 2001). Furthermore, the International IBD Genetics Consortium have identified multiple risk loci for Crohn's disease and ulcerative colitis, most of which are connected with epithelial barrier dysfunction (Hindryckx P, 2012).

A polymorphism in the cytoplasmic peptidoglycan receptor NOD2 is associated with Crohn's disease (Hugot *et al.*, 2001). NOD2 is highly expressed by Paneth cells which provide host defence against microbes in the ileum by secreting defensins and lyzozyme. In patients with NOD2 mutations, expression of defensins is diminished which leads to an increased number of surface associated bacteria and consequently loss of barrier function and uncontrolled inflammation (Wehkamp *et al.*, 2005). Furthermore, two other mutations of genes involved in Paneth cell and goblet cell function and development have been identified; XBP1 and Atg16L1. A Atg16L1 mutation causes impaired exocytosis of Paneth cells secretory granules. This leads to inability to release antimicrobial peptides and therefore contributes to intestinal

inflammation (Cadwell *et al.*, 2008). XBP1 is a transcriptional factor required for the normal development of Paneth cells and goblet cells (Kaser *et al.*, 2008). Mice deficient in XBP1 have reduced numbers of goblet cells and develop spontaneous intestinal inflammation (Kaser *et al.*, 2008).

Some mutation have been linked with junctional complex genes, such as HNF4A and LAMB1 (Hindryckx P, 2012) and also in genes encoding mucin proteins (Gersemann *et al.*, 2009). Mucin proteins are produced by goblet cells and mice that carry a mutation in MUC2, which is the most abundant mucin protein, develop chronic inflammation in the distal colon (Heazlewood *et al.*, 2008).

It is clear that the disruption of the intestinal cell barrier can be caused by different factors and inevitably leads to increased intestinal permeability for commensal bacteria and other antigens. This surge of antigens activates the underlying immune system which may lead to more intestinal damage.

1.3.2 The role of macrophages in IBD

As discussed previously, during IBD the intestinal epithelial barrier is disrupted which allows the invasion of commensal bacteria. This leads to influx of inflammatory cells and their constant activation. Indeed, patients with active IBD have an increased number of macrophages in the inflamed intestinal mucosa (Xavier and Podolsky, 2007) and these macrophages display a different phenotypic and functional profile than under homeostatic conditions. Macrophages in IBD patients display increased levels of co-stimulatory receptors, such as CD40, CD80 and CD86 which enables the crosstalk and activation of T-cells (Rugtveit *et al.*, 1997a). This is coupled with an increased production of pro-inflammatory cytokines, such as IL-12

and IL-23 (Kamada *et al.*, 2005). IL-12 drives IFN-γ production from T-cells, which then in turn increases macrophage activation and also increases epithelial cell permeability (Kamada *et al.*, 2005). IL-23 promotes a development of a $CD4^+$ phenotype characterised by the production of IL-17, called Th17 cells, which are involved in the pathogenesis of IBD (Kamada *et al.*, 2005).

Macrophages in IBD are also a main source of TNF-α, which is considered to be a "master regulator" of pro-inflammatory cytokine production. It has a pivotal role in orchestrating the production of a pro-inflammatory cytokine cascade and therefore drives the disease (Parameswaran and Patial, 2010). Furthermore, macrophages in the IBD show increased expression of PRRs, such as TLR2 and TLR4 and also TREM-1 which triggers the synthesis and secretion of inflammatory factors (Smith *et al.*, 2005, Schenk *et al.*, 2005). Engagement of TREM-1 leads to increased secretion of IL-1β, IL-6 and IL-8 (Schenk *et al.*, 2007). This pro-inflammatory response leads to epithelial apoptosis, necrosis, formation of granuloma and fibrosis (Heinsbroek and Gordon, 2009). Expression of tissue degrading cathepsins by intestinal macrophages has also been seen in IBD (Menzel *et al.*, 2006), together with an increased release of nitric oxide and oxygen radicals that further contribute to macrophage-dependent tissue damage (Keshavarzian *et al.*, 2003).

While macrophages in the inflamed intestine show an enhanced pro-inflammatory phenotype, their ability to eradicate intracellular pathogens is decreased as their phagocytosis is significantly reduced (Caradonna *et al.*, 2000). This probably accounts for recurrent infection in IBD patients with pathogens that directly target macrophages, such as *Mycobacterium paratuberculosis* (Weber *et al.*, 2009).

Some of the disruptions in macrophage signalling are also reported to contribute to intestinal inflammation. Selective disruption in STAT3 signalling in macrophages

leads to impaired production of anti-inflammatory IL-10 and spontaneous development of colitis in mice (Takeda *et al.*, 1999). The mutant form of NOD2, associated with Crohn's disease, is also expressed on macrophages and therefore may contribute to disease pathology (Hugot *et al.*, 2001).

1.4 TNF-α and its receptors

Tumour necrosis factor α (TNF-α) is a potent cytokine produced by many cell types, but mainly by monocytes and macrophages. It primarily occurs as a trans-membrane protein of 26 kDa, which can be cleaved by TNF-α-converting enzyme (TACE) to a 17 kDa soluble protein (Wajant *et al.*, 2003). TNF-α has an extremely complex role in the immune system. It is a regulatory cytokine that co-ordinates communication between immune cells and controls many of their functions, such as activation, apoptosis, survival, proliferation and differentiation (Parameswaran and Patial, 2010). It also has a pivotal role in orchestrating the induction of pro-inflammatory signalling cascade and it is important for the normal response to infection (Wajant *et al.*, 2003). Because of the central role in the regulation of immune system, inappropriate and excessive production of TNF-α can be harmful. Indeed, over-production of TNF-α has been associated with the pathogenesis of many diseases, including rheumatoid arthritis, Crohn's disease, atherosclerosis, psoriasis, sepsis, diabetes and obesity (Plevy *et al.*, 1997, Brennan *et al.*, 1992, Clark, 2007). Absence of TNF-α is equally detrimental. Mice lacking TNF-α show a high degree of susceptibility to infectious agents and impaired clearance of pathogens (Marino *et al.*, 1997). Furthermore, in TNF-α deficient mice colonic injury during DSS-induced colitis was significantly aggravated and their survival rate was markedly lower (Naito *et al.*, 2003). Therefore, the levels of TNF-α have to be tightly regulated in order to exhibit optimal functions in both homeostasis and disease.

Exposure of cells to TNF-α can lead to a variety of different responses. TNF signalling mainly activates NF-κB pathway leading to production of inflammatory proteins and anti-apoptotic proteins (Bradley, 2008). However, in some cases TNF

can trigger apoptosis and cell death pathway (Wang *et al.*, 2008, Micheau and Tschopp, 2003). This paradoxical role of TNF-α is mediated by two distinct receptors, TNFR1 and TNFR2 (Peschon *et al.*, 1998). While TNFR1 is expressed on almost all cell types, TNFR2 expression is restricted to endothelial cells and immune cells, especially monocytes, macrophages and T-cells (Tartaglia and Goeddel, 1992, Aggarwal, 2003). Both receptors are activated by membrane-bound (mTNF) and soluble TNF-α (sTNF), with mTNF being a stronger inducer of the TNFR2 pathway (Wajant *et al.*, 2003).

1.4.1 TNFR1 signalling

The extracellular domain of TNFR1 consists of three cysteine-rich domains that characterise the TNF receptor superfamily and a fourth which resides within a membrane. The intracellular part contains a protein-protein interaction region called the death domain (DD) (Chan *et al.*, 2000). In an unstimulated receptor the DD is pre-associated with a cytoplasmic protein designated silencer of death domain (SODD) (Jiang *et al.*, 1999). After ligand binding of TNFR1, SODD dissociates from the intracellular DD which then allows binding of different cytoplasmic proteins.

1.4.1.1 The inflammatory pathway

Intracellular DD of TNFR1 recruits a membrane-associated complex, named complex I, which comprises of the adaptor protein TNFR1-associated death domain protein (TRADD), the death domain containing protein kinase receptor – interacting protein 1 (RIP1) and several ubiquitin E3 ligases, such as TNFR-associated factor 2

(TRAF-2) and cellular inhibitor of apoptosis protein 1 and/or 2 (cIAP1, cIAP2) (Micheau and Tschopp, 2003). TRAF-2 from the TRADD-RIP-TRAF-2 complex recruits inhibitor of cellular apoptosis proteins cIAP-1 and cIAP-2, and binds to the inhibitor of κB complex (IKK). IKK then phosphorylates IκB proteins and this leads to the release of NF-κB subunits that are bound to IκB under unstimulated conditions. The free NF-κB subunits translocate into the nucleus and initiate gene transcription (Varfolomeev *et al.*, 2008) **[Figure 1.3A]**.

In complex I, RIP1 is rapidly polyubiquitylated which mediates the recruitment and activation of transforming growth factor-β (TGF-β)-activated kinase (TAK1) which, in turn, activates the IKK complex (Ea *et al.*, 2006). This leads to NF-κB activation and translocation **[Figure 1.3B]**. NF-κB is composed of dimers derived from five different subunits, p65 (RelA), RelB, cRel, p50 and p52. Signalling through TNFR1 activates the so-called classical pathway, with the p65-p50 heterodimer being a most important set of subunits for transcription. Target genes include cytokines, chemokines, receptors that regulate the adhesion and migration of cells and anti-apoptotic molecules (Vallabhapurapu and Karin, 2009).

TAK1 can also phosphorylate and activate the mitogen-activated protein kinase (MAPK) pathway (Wang *et al.*, 2001). MAPK kinase 4 and MAPK kinase 6 then activate c-Jun N-terminal kinases (JNKs) and p38 MAPK. JNK and p38 MAPK subsequently activate transcription of genes via AP-1 **[Figure 1.3C]**. AP-1 controls many processes including apoptosis, differentiation and proliferation (Nishitoh *et al.*, 1998).

1.4.1.2 The pro-apoptotic pathway

In addition to mediating cell survival and pro-inflammatory signals through NF-κB, TNFR1 can also initiate the death signalling pathway. This decision between cell survival or cell death seem to be regulated by RIP1 (O'Donnell and Ting, 2011). The activity of RIP1 is determined by its ubiquitylation status. Ubiquitylated RIP1 interacts with different ubiquitin-binding receptors that mediate cell survival in NF-κB dependent and independent manner (as explained in section 1.4.1.1) (Li *et al.*, 2006). However, when RIP1 fails to be ubiquitylated, it becomes pro-apoptotic signalling molecule by engaging caspase-8. This seems to be mediated by the negative regulators of NF-κB, such as the ubiquitin–editing enzyme A20 and the deubiquitylating enzyme cylindromatosis (CYLD). A20 and CYLD disassemble complex I by deubiquitylating RIP1 and TRAF-2. This leads to formation of the alternative cytosolic complexes, complex IIa and complex IIb (Ofengeim and Yuan, 2013). Complex IIa includes Fas-associated death domain protein (FADD), caspase 8 and RIP1 and mediates activation of caspase-8 and caspase-3 which leads to apoptosis **[Figure 1.3D]**. If caspase-8 activation is inhibited, RIP1 kinase binds to RIP3 to form complex IIb. Complex IIb mediates necroptosis (Ofengeim and Yuan, 2013).

Complex IIa and IIb can be negatively regulated by activation of NF-κB that initiate transcription of anti-apoptotic target genes, such as c-IAP1/2, TRAF-2 and FLICE-inhibitory protein (FLIP) **[Figure 1.3]**. These pro-apoptotic genes inhibit the association of RIP1 with complex II components (Naude *et al.*, 2011).

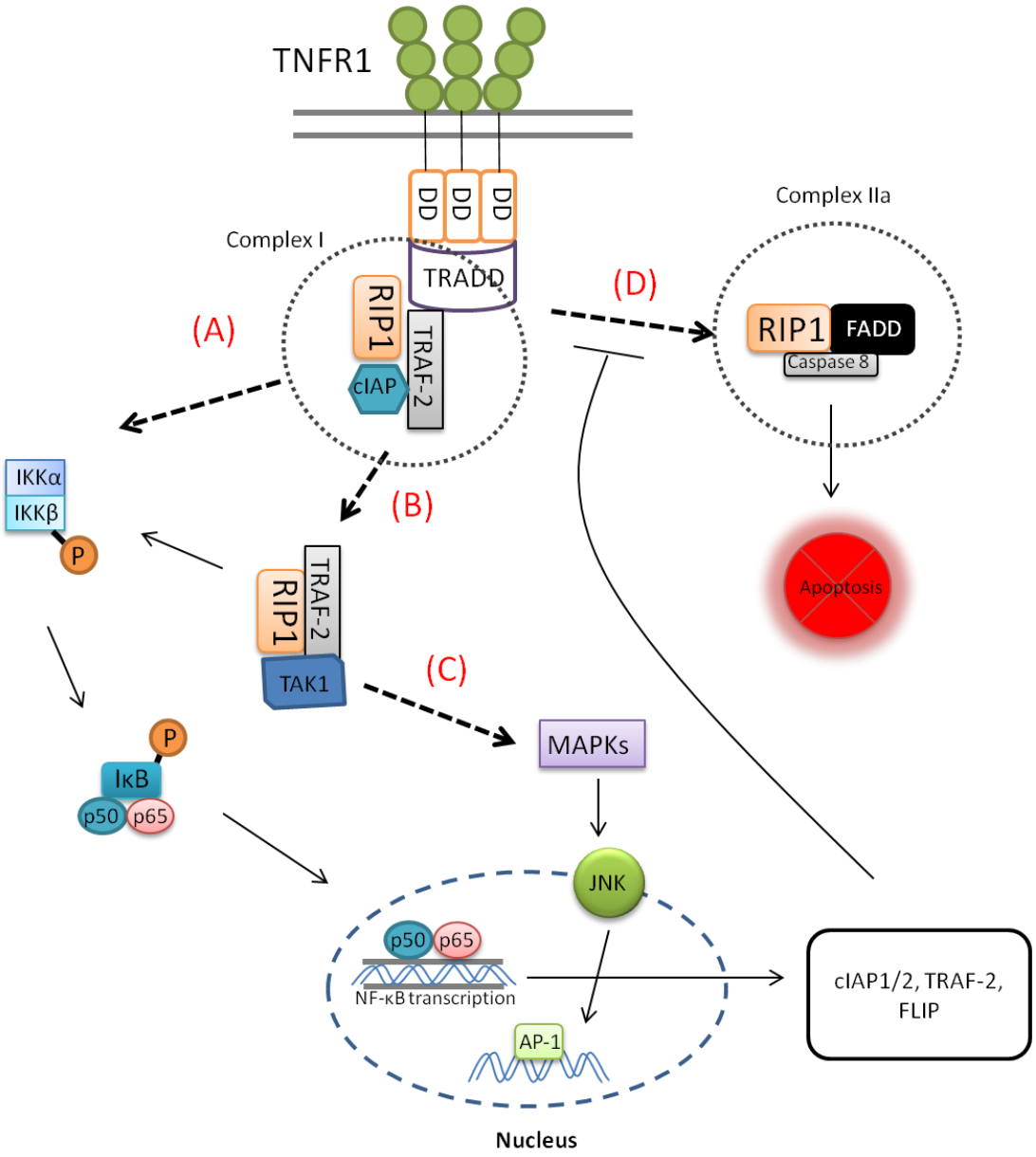

Figure 1.3 TNFR1 signalling pathway Activation of NF-κB transcription factor (A, B), activation of AP-1 transcription factor (C), activation of pro-apoptotic pathway (D); DD, death domain; TRADD, TNF receptor associated death domain; TRAF, TNF receptor associate factor; RIP, receptor interacting protein; cIAP, cellular inhibitor of apoptosis; TAK1, (TGF-β)-activated kinase; IKK, IκB kinase; IκB, inhibitor of kappa B; FADD, Fas-associated death domain protein; MAPK, mitogen-activated protein kinase; JNK, c-Jun N-terminal kinase; AP-1, transcription factor activator protein 1; NF-κB, nuclear factor kappa B; FLIP, caspase-8 homologue FLICE-inhibitory protein

1.4.2 TNFR2 signalling

The signalling pathways initiated by TNFR2 are less clearly defined. This is due to the fact that most experiments use sTNF which does not fully activate the TNFR2 pathway (Wajant *et al.,* 2003). However, it does contribute to TNFR2 signalling as only sTNF and not mTNF triggers the expression of monocyte chemoattractant protein-1 (MCP-1) in alveolar epithelial cells via TNFR2 (Liu *et al.,* 2005). This adds more complexity to the TNFR2 signalling.

TNFR2 can activate the NF-κB pathway independently of TNFR1, through classical and alternative pathways. TNF-α binding leads to trimerization of the TNFR2 receptor, binding to TRAF-2 and recruitment of TRAF-2 associated proteins, TRAF-1, cIAP1 and cIAP2. The classical pathway then activates the phosphatidylinositol 3-kinase (PI3K) and protein kinase B/serine-threonine kinase (PKB/Akt) pathway that lead to IKK activation and subsequent IκB phosphorylation and degradation **[Figure 1.4A]**. The NF-κB p50/p65 complex then translocates to the nucleus and initiates gene transcription (Al-Lamki *et al.*, 2005).

In unstimulated cells the TRAF-2-cIAP1/2 complex interacts with a complex of TRAF-3 and NF-κB inducing kinase (NIK) which leads to ubiqitination and degradation of NIK. When TNFR2 is stimulated, TRAF-3 can be degraded which leads to accumulation, rather than degradation of NIK. This leads to activation of the alternative NF-κB pathway. NIK stimulates IKKα and phosphorylates the NF-κB precursor p100, thus triggering its proteolysis to p52 (Rauert *et al.,* 2010). The p52/RelB complex then translocates into the nucleus **[Figure 1.4B]**.

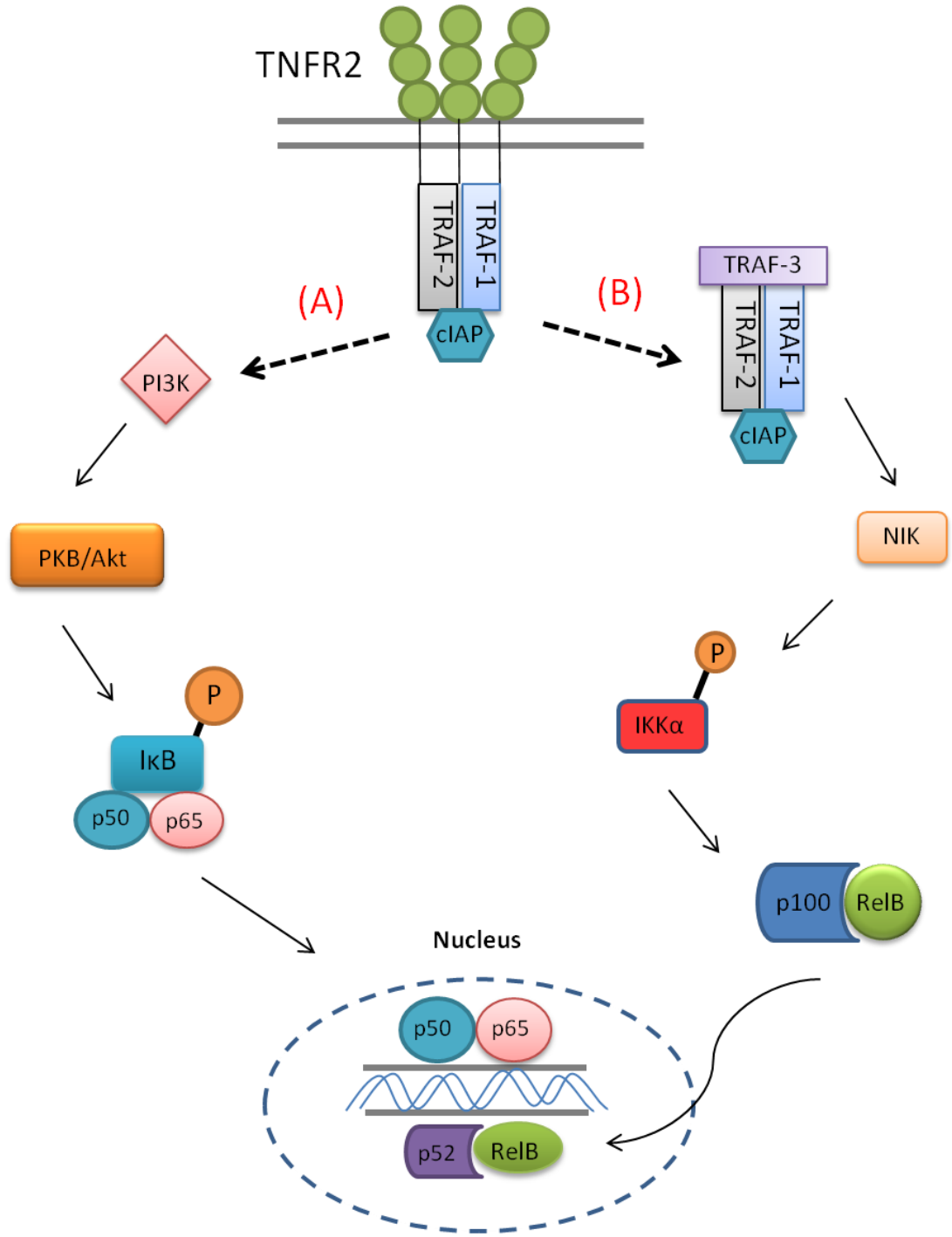

Figure 1.4 TNFR2 signalling pathway Classical NF-κB pathway (A) and alternative NF-κB pathway (B). TRAF, TNF receptor associated factor; cIAP, cellular inhibitor of apoptosis; PI3K, phosphoinositide 3-kinases; PKB/Akt, protein kinase B/serine-threonine kinase; IκB, inhibitor of kappa B; NIK, NF-κB inducing kinase; IKK, IκB kinase;

1.4.3 Crosstalk between TNFR1 and TNFR2

The intracellular part of TNFR2, unlike TNFR1, lacks a death domain and cannot bind FADD. However, it can still, in some cases, activate apoptosis, but the mechanisms behind that have not been completely elucidated. Several studies have pointed to the existence of a functional crosstalk between TNFR1 and TNFR2. It has been proposed that TNFR2 can bind and hold TNF-α and increase its concentration in the vicinity of TNFR1. TNFR1 receptor then accepts the TNF-α from TNFR2 and activates its own apoptotic signalling. This mechanism is called "ligand-passing" (Tartaglia *et al.*, 1993).

Furthermore, TNFR2 signalling can induce TRAF-2 degradation and depletion. This stops anti-apoptotic TNFR2 signalling, but also prevents the formation of TRADD-RIP-TRAF-2 complex with TNFR1. Consequently TNFR1 favours TRADD- RIP-FADD association and activation of pro-apoptotic pathway (Fotin-Mleczek *et al.*, 2002). TNFR2 can also dampen signals produced by TNFR1 activation. It has been shown that TNFR2 activation can lead to ASK-1 degradation which terminates the activation of MAPK pathway and AP-1 induced gene transcription (Zhao *et al.*, 2007). Therefore, it seems that TNFR1-TNFR2 crosstalk can serve as a feedback mechanism that either enhances or dampens signals generated by TNFR1.

1.4.4 TNFR1 and TNFR2 in disease

TNFR1 signalling usually activates pro-apoptotic and pro-inflammatory pathways, while TNFR2 is responsible for cell proliferation and pro-survival functions (Bradley, 2008). However, as mentioned previously, there is a degree of overlap between TNFR1 and TNFR2 pathways and they can both exhibit protective or

harmful effects in disease states. This seems to depend on certain factors, such as cell type, cell activation state, intracellular and extracellular environment and, in the case of infectious diseases, pathogens itself (Faustman and Davis, 2010).

1.4.4.1 Infectious diseases

TNF receptors have a strong influence on the outcome of infectious diseases. TNFR1 signalling is crucially involved in the immune response to *Listeria monocytogene* and in the absence of TNFR1, phagocytosis and breakdown of bacteria are significantly impaired, resulting in increased bacterial growth and early death due to failure of the innate immune system (Pfeffer *et al.*, 1993). The immune response to infections with mycobacteria, such as *Mycobacterium tuberculosis*, seems to be dependent on both receptors, with TNFR1 having a more important role. The TNF-mediated macrophage activation and bactericidal activity to *Mycobacterium tuberculosis* are dependent on TNFR1 and TNFR1 mutant mice die from bacterial overgrowth and necrosis (Flynn *et al.*, 1995b). Lack of TNFR2 also leads to increased sensitivity to bacteria, but it is not as extensive as in TNFR1 deficient mice (Jacobs *et al.*, 2000). TNFR2, however, proved to be protective in a model of polymicrobial sepsis with TNFR2 signalling attenuating the toxic effects of TNF-α in this model, while all the detrimental effects of TNF-α are conferred via TNFR1 (Ebach *et al.*, 2005).

TNFR2 has been shown to be more important than TNFR1 for viral control. TNFR2 seems to be crucial for the generation of antigen-specific cytotoxic T-cells for antiviral immune responses, as $CD4^+$ and $CD8^+$ T-cells were shown to depend on TNFR2 for survival during clonal expansion in response to adenovirus infections (Kim *et al.*, 2006, Kafrouni *et al.*, 2003).

TNFR1 also plays a role in protozoal infections. In murine toxoplasmosis TNFR1$^{-/-}$ mice are highly susceptible to infection and succumb to the infection within three weeks (Deckert-Schluter *et al.*, 1998). TNFR1 is also important for parasite control in infection with *Trypanosoma cruzi* and TNFR1 deficient mice have an increased parasitemia compared to wild type mice (Castanos-Velez *et al.*, 1998).

1.4.4.2 Autoimmune diseases

TNF-α has a dominant role in autoimmunity and inhibiting its biological activity substantially improves the outcome of patients suffering from autoimmune diseases, such as IBD and rheumatoid arthritis (RA) (Yapali and Hamzaoglu, 2007, Majithia and Geraci, 2007). Information about the role of TNF receptors in these diseases is limited, but they are proving to be important for the initiation and maintenance of the disease.

Rheumatoid arthritis is a chronic autoimmune inflammatory disorder characterised by inflammation of synovial tissue, leading to bone damage and erosion (Majithia and Geraci, 2007). Using animal models of inflammatory arthritis, TNFR1 has been identified as a driving force in arthritis development, enhancing the generation of osteoclasts and local bone destruction (Kobayashi *et al.*, 2000). Moreover, TNFR1 deficient mice show reduced development of collagen-induced arthritis (Tada *et al.*, 2001). On the other hand, TNFR2-deficient mice develop aggravated arthritis, joint destruction and increased osteoclastogenesis (Bluml *et al.*, 2010), indicating a protective role of TNFR2 signalling.

TNFR2 was also shown to have an anti-inflammatory role in experimental autoimmune encephalitis (EAE), which is a mouse model of multiple sclerosis (MS). MS is a chronic relapsing inflammatory disease of the central nervous system,

caused by abnormal T-cell reactivity to myelin antigens (Hafler and Weiner, 1989). TNFR1 seems to be necessary for the detrimental effects of TNF-α, which occur in the acute phase of the disease (Kassiotis and Kollias, 2001). TNFR2 signalling, however, promotes proliferation of oligodendrocyte progenitors and remyelination in the later stage (Kassiotis and Kollias, 2001).

In experimental colitis, a mouse model of IBD, TNFR2 also seems to be protective as the absence of TNFR2, especially on $CD4^+$ T-cells, leads to an accelerated onset of disease and more severe signs of inflammation (Dayer Schneider *et al.*, 2009). Furthermore, a polymorphism in TNFR2 has been found in some patients with Crohn's disease (Sashio *et al.*, 2002) and ulcerative colitis (Pierik *et al.*, 2004). The consequences of this polymorphism may be altered binding kinetics between TNF and TNFR2 and reduced activation through NF-κB, which in turn deregulates proliferative and anti-apoptotic effects of TNFR2 pathway (Till *et al.*, 2005). However, the exact role of TNFR1 and TNFR2 in colitis is still unclear as the up-regulation of TNFR2 on intestinal epithelial cells during colitis has also been connected with intestinal epithelial damage (Mizoguchi *et al.*, 2002) and some differences in TNF receptor signalling have been observed in acute and chronic stage of colitis (Chen *et al.*, 2007).

1.4.4.3 Other diseases

Circulating levels of TNF-α are independent predictors of mortality in patients with heart failure (Mann, 2002). However, anti-TNF therapy in humans failed to induce any clinical improvement (Mann, 2002). This could be due to divergent effects of TNF-α signalling through TNFR1 or TNFR2. Research has shown that ablation of the TNFR2 gene exacerbates heart failure and reduces survival, while ablation of

TNFR1 blunts heart failure and improves survival (Higuchi *et al.*, 2004, Hamid *et al.*, 2009). Therefore, TNF-α signalling through TNFR2 is cardioprotective and needed to ameliorate chamber remodelling and hypertrophy (Hamid *et al.*, 2009).

In retinal ischemia, which is a frequent complication in diabetic patients, TNFR1 and TNFR2 have also shown opposing effects. TNFR1 deficiency leads to a strong reduction in neurodegeneration, while lack of TNFR2 leads to enhancement of neurodegeneration. In this model TNF/TNFR2 signalling proved to be neuroprotective via the PKB/Akt anti-apoptotic pathway (Fontaine *et al.*, 2002).

TNF-α has also been implicated in the pathogenesis of many renal diseases, including ischaemic renal injury and glomerulonephritis. Ischaemic renal injury is acute kidney injury with an abrupt decrease in kidney function (Devarajan, 2006). Glomerulonephritis is a term for several renal diseases characterised by inflammation of the glomeruli or small blood vessels in the kidney and can lead to kidney failure (Chadban and Atkins, 2005). While TNFR2-mediated cell proliferation seems to be important for tubular regeneration in acute renal injury (Al-Lamki *et al.*, 2005), in proliferative forms of glomerulonephritis inhibition of TNFR2 proliferation may be more desirable (Vielhauer *et al.*, 2005).

Increased TNF-α levels also underlie the pathology of other inflammatory diseases, such as therapy-resistant sarcoidosis, inflammatory myopathies, inflammatory eye disease, systemic lupus erythematosus (Faustman and Davis, 2010) and the contribution of TNF/TNFR1 and TNF/TNFR2 pathways in these diseases also warrants further investigation.

1.5 AIMS AND OBJECTIVES

The intestinal immune system is exposed to more antigens than any other part of the body. In order to cope with the antigen exposure it has evolved into a highly specialised and tightly regulated system. Normal immunology "rules" often do not apply here and the immune cells of the intestine present a population of its own, distinct from their counterparts in other tissue. The mechanisms that guide their specialised roles are still unclear, mostly because the isolation of these cells presents a challenge.

Interestingly, resident intestinal macrophages have the same origin as "inflammatory" monocytes and they only lose their inflammatory properties once they arrive in the gut. With this in mind, our hypothesis was that the intestinal epithelial environment guides the phenotypic and functional changes of newly arrived monocytes in order to adapt them to an antigen-rich environment.

To test our hypothesis the aims of this thesis were:

- to isolate a viable and functional population of colonic macrophages
- to address the question of their origin and explore whether the intestinal environment, especially intestinal epithelial cells, shape their function
- to investigate the way in which intestinal macrophages contribute to homeostasis and disease and identify a potential link between epithelial cells and macrophages that regulates their function

As we have mentioned, intestinal macrophages are a major contributor in the maintenance of intestinal homeostasis. However, they are also a major driver of

disease, when homeostasis is disturbed. Better understanding of macrophage functions could reveal potential therapeutic targets which will restore their protective role and help attenuate acute and chronic intestinal diseases.

CHAPTER 2

MATERIALS AND METHODS

2.1 MATERIALS

CELL CULTURE MATERIALS/REAGENTS

Material	Source
Tissue culture flasks T-75cm^2	Nunc
Tissue culture flask T-25cm^2	Nunc
Sterile Petri dishes	Nunc
6, 26, 96-well tissue culture plates	Nunc
96-well round bottom plate	Starstedt
Trypan blue (0.4% w/v)	Sigma-Aldrich
Foetal Calf Serum	Gibco
RPMI-1640	Gibco
DMEM	Sigma-Aldrich
Penicillin Streptomycin/Glutamine	Gibco
LPS	Enzo Lifesciences
DPBS	Gibco
Sterile dH_2O	Sigma-Aldrich
PAM_3CSK_4	Invivogen
Flagellin	Invivogen
CpG	Invivogen
Trypsin/EDTA	Sigma-Aldrich
CellTiter 96™ Aqueos One Solution	Promega
Griess reagent	Promega

TNFR1 antagonist	R&D
TNFR2 antagonist	Biolegend
TNFR2 isotype control	Biolegend
TGF-β neutralising antibody	R&D
TSLP neutralising antibody	R&D
rmTGF-β	R&D

Table 2.1 Cell culture materials All cell culture materials/reagents used and corresponding sources

ELISA REAGENTS

Material	**Source**
96-well microtiter plate	Nunc
TMB	BD
Tween 20	Sigma-Aldrich
Bovine serum albumin	Sigma-Aldrich
ELISA Duoset kits	R&D Systems
DPBS	Gibco

Table 2.2 ELISA reagents All ELISA reagents used and corresponding sources

FLOW CYTOMETRY REAGENTS

Material	Source
FACS flow	BD
FACS Rinse	BD
FACS Clean	BD
Sodium azide	Sigma-Aldrich
EDTA	Sigma-Aldrich
Propidium Iodide solution	Miltenyi Biotec
Anti-F4/80 antibody	Biolegend
Anti-CD86 antibody	BD
Anti-CD80 antibody	BD
Anti-TLR2 antibody	eBioscience
Anti-TLR4 antibody	eBioscience
Anti-MHCII antibody	eBioscience
Anti-CD40 antibody	BD
Anti-TNFR1 antibody	Biolegend
Anti-TNFR2 antibody	Biolegend
DCFDA	Abcam
CellEvent™ Caspase 3/7 assay	Life Technologies

Table 2.3 Flow cytometry materials All flow cytometry materials/reagents used and corresponding sources

IMMUNOHISTOCHEMISTRY REAGENTS

Material	Source
Acetone	Sigma-Aldrich
HCl	Sigma-Aldrich
Sodium bicarbonate	Sigma-Aldrich
Ethanol	Merck
Harris Haematoxylin	Sigma-Aldrich
Eosin	Sigma-Aldrich
Histo-clear	National Diagnostics
OCT solution	TissueTek
Histobond microscope slides	RA Lamb

Table 2.4 Immunohistochemistry reagents All immunohistochemistry reagents used and corresponding sources

RNA ISOLATION AND cDNA SYNTHESIS

Material	Source
Nucleospin RNA II Columns	Macherey-Nagel
DEPC treated water	Invitrogen
High Capacity cDNA Reverse Transcription kit	Applied Biosystems
Molecular grade ethanol	Sigma-Aldrich

Table 2.5 RNA isolation materials All reagents used for RNA isolation and cDNA synthesis and corresponding sources

qRT-PCR REAGENTS

Material	Source
SYBR® Green Mastermix	Roche
Taqman® Gene Expression Mastermix	Applied Biosystems
MicroAmp® Optical 96-well plate	Applied Biosystems
MicroAmp® Optical Adhesive Film	Applied Biosystems
IL-12p40 PrimeTime qRT-PCR Primers	IDT
TNF-α PrimeTime qRT-PCR Primers	IDT
IL-6 PrimeTime qRT-PCR Primers	IDT
IL-10 PrimeTime qRT-PCR Primers	IDT
Foxp3 PrimeTime qRT-PCR Primers	IDT
TGF-β PrimeTime qRT-PCR Primers	IDT
TNFR1 PrimeTime qRT-PCR Assay	IDT
TNFR2 PrimeTime qRT-PCR Assay	IDT
Occludin PrimeTime qRT-PCR Assay	IDT
Rps18 PrimeTime qRT-PCR Primers	IDT
Rps18 PrimeTime qRT-PCR Assay	IDT

Table 2.6 Quantitative PCR reagents All qRT-PCR reagents used and corresponding sources

PRIMARY CELL ISOLATION REAGENTS

Material	Source
HBSS	Sigma-Aldrich
CMF-HBSS	Gibco
EDTA	Sigma-Aldrich
Collagenase II	Gibco
Collagenase IV	Gibco
Collagenase V	Sigma-Aldrich
Collagenase D	Roche
Dispase	Gibco
DNase	Roche
Percoll	GE Healthcare
Sodium chloride	Sigma-Aldrich
Anti-APC MicroBeads	Miltenyi Biotec
LS MACS® columns	Miltenyi Biotec
MACS® DeadCell Removal Kit	Miltenyi Biotec
M-CSF	eBioscience

Table 2.7 Primary cell isolation reagents All reagents used for primary cell isolation and corresponding sources

2.2 Flow cytometry

2.2.1 Basic principles of flow cytometry

Flow cytometry is a technology that allows the individual measurement of physical and chemical characteristics of particles as they pass one by one through a light source. A flow cytometer is made up of three main systems: fluidics, optics, and electronics. The fluidics system transports particles in a stream to the laser beam for interrogation. The optical system consists of excitation optics and collection optics. The excitation optics are lasers and lenses that shape and focus the laser beam onto a particle. The collection optics then collect the light emitted from the particle and direct that light, through optical mirrors and filters, to the appropriate detectors. The electronics system converts the detected light signals into electronic signals that can be processed by the computer **[Figure 2.1]**.

When a particle or a cell passes through a laser beam, laser light is scattered in all directions. Light that scatters axial to the laser beam is called forward scatter (FSC); light that scatters perpendicular to the laser beam is called side scatter (SSC). FSC and SSC are related to certain physical properties of cells. FSC is proportional to the cell-surface area or size, while SSC is proportional to cell granularity or internal complexity.

Fluorescent probes can also be added to the cell for detecting specific molecules in or on the cell. These probes are typically antibodies to cellular antigens with a covalently attached fluorochrome. The fluorochrome, excited by the laser light, will emit light which is collected, measured and analysed (Ormerod, 2008).

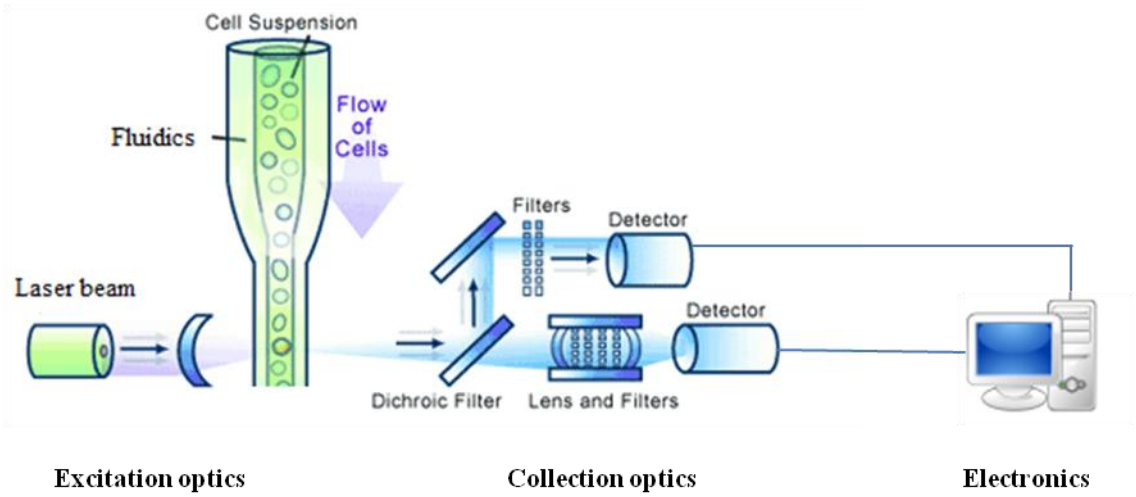

Figure 2.1 A schematic of fluorescence detection by a flow cytometer (adapted from "The Science Creative Quarterly", scq.ubc.ca, Jane Wang)

2.2.2 Cell surface marker staining

For the staining of cell surface markers in this thesis, the following protocols were used. Cells were removed from the tissue culture plates using a cell scraper and placed into a 96-well round bottom plate or 1.5ml eppendorf tubes in a concentration of 200,000-400,000 cells/well or tube. An equal amount of foetal bovine serum (FBS) was then added, to block the unspecific binding of antibodies, for 15min at RT. Cells were then washed twice with FACS buffer **[**see **Appendix A]** and incubated with appropriate fluorochrome-conjugated antibodies **[Table 2.3]** for 30min at 4ºC protected from light. Cells were then washed three times to remove the unbound antibodies and analysed using a FACSAria I (BD). Dead cells exclusion was performed by adding the propidium-iodide staining (PI; Miltenyi Biotec) at a final concentration of 1µg/ml, immediately prior to the acquisition. All the flow cytometry data was analysed using FlowJo software (Treestar).

2.2.3 Fluorescence activated cell sorting (FACS)

Fluorescence-activated cell sorting is a specialised type of flow cytometry that provides a method for the physical separation of cells of particular interest from the heterogeneous mixture, depending on their light scattering and fluorescent properties. The sample is aspirated from the reservoir and hydrodynamically focused so that cells pass one by one through the light source where they are investigated. After the signal is detected and measured, the stream that carries the cells breaks up into droplets. Individual drops, as they break away, can be charged depending on whether they contain the cell of interest or not. Drops then pass through an electrical field created by two charged plates and they are deflected into collection vessels (Davies, 2007.). In order to sort a pure population, it is important to ensure that the cell of interest is contained in a drop that does not also contain a non-target (unwanted) cell. Therefore, usually only the drop that contains the target cell is charged. However, sometimes the target cell falls near the edge of the drop and it may appear in the preceding or the following drop. In this case, to avoid cell loss, more than one drop can be charged. Thus, how the sort is going to be performed is determined by choosing the appropriate sort precision mode.

Each sort precision mode on the BD FACSAria I is made up of a set of masks: Yield mask, Purity mask and Phase mask, that are divided in 1/32-drop increments (Gautho, 2003). Mask settings determine whether a drop is going to be sorted or not, depending on the location of the target cell within a drop and the location of the non-target cell in the preceding or the following drop. For achieving the highest purity two precision modes were tested: 0-32-0 and 16-16-0. In the first mode, the Purity mask was set on maximum so a drop will only be sorted if the leading and the trailing drops do not contain unwanted cell **[Figure 2.2]**.

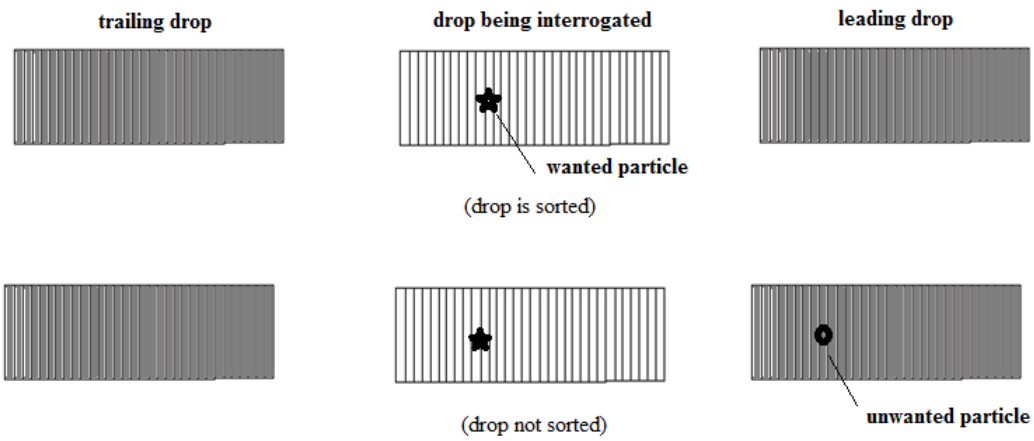

Figure 2.2 Precision mode 0-32-0 Purity mask is set on 32, which means that the drop will only be sorted if there is no unwanted particle in a trailing or a leading drop

In the second mode the Purity mask is set to 16 meaning that the drop is going to be sorted if a non-target cell falls outside the Purity mask (in other words, if the non-target cell is far enough from the target cell) **[Figure 2.3]**. The Yield mask was also set to 16 meaning that additional drop (preceding or following) will be sorted if the target cell falls within the Yield mask (additional drop will be sorted if target cell falls near the edge of the drop) **[Figure 2.4]**.

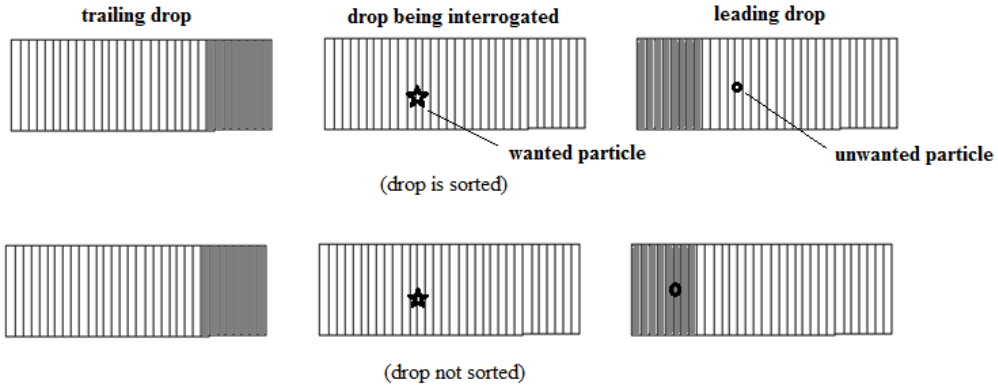

Figure 2.3 Precision mode 16-16-0 Purity is set to 16, which means that the drop will only be sorted if unwanted particle falls outside the purity mask

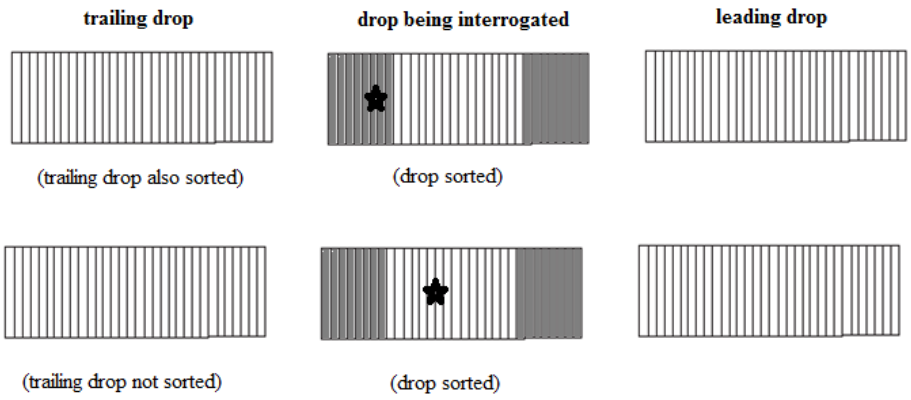

Figure 2.4 Precision mode 16-16-0 Yield is set to 16, which means that the additional drop will be sorted if a wanted particle falls within the yield mask

2.3 Cell culture

All cell culture was carried out using aseptic technique in a class II laminar airflow unit (Holten 2010 – ThermoElectron Corporation, OH, USA). Cell cultures were maintained in a 37 °C incubator with 5 % CO_2 and 95 % humidified air (Model 381 - Thermo Electron Corporation OH USA). Cells were grown in complete DMEM medium (DMEM Sigma-Aldrich, supplemented with 10% FBS and 2% penicillin - streptomycin/glutamine). FCS was heat-inactivated (56°C for 30 min) to inactivate complement and aliquoted for storage at -20 °C. Supplemented medium was stored at 4 °C for no longer than one month.

2.3.1 Murine monocyte-derived macrophage cell line, J774A.1

The J774A.1 cell line was purchased from the European Collection of Cell Cultures (ECACC) and maintained in complete DMEM in 75 cm^2 flasks. Cell monolayers were passaged at a confluency of 80% (every 3 to 4 days). Cells were detached using

a cell scraper and transferred into a 50 ml falcon. Cells were centrifuged at 250g for 5 min and resuspended in complete DMEM. For subculture, cells were plated at $1x10^6$ or $2x10^6$/25ml DMEM in a fresh $75cm^2$ flask.

2.3.2 Murine colonic epithelial cell line, CMT-93

The CMT-93 cell line was purchased from the ECACC and maintained in complete DMEM in 75 cm^2 flasks**.** Cell monolayers were passaged at a confluency of 80% (every 4 to 5 days). Cells were detached by adding 2ml of 0.25% trypsin, 0.02% EDTA solution (Sigma-Aldrich). Trypsin/EDTA solution was left on the cells at 37ºC until the cells detached (5-10min). Fresh culture medium was then added, cells centrifuged at 250g at 5min, resuspended and subcultured in a ratio 1:10, in a fresh $75cm^2$ flask.

2.4 Conditioning experiments

CMT-93 cells were grown until they were approx. 80% confluent after which fresh media was added, left on the cells for 24h and then collected, centrifuged and stored at -20ºC for conditioning experiments. This is referred to as CMT-93 conditioned media.

J774A.1 macrophages were plated in 6-wells or 24-wells tissue culture plates at a concentration of $1x10^6$ cells/ml and incubated for 2h, 6h or 24h with DMEM medium alone (unconditioned) or CMT-93 conditioned medium. After incubation, cells and supernatants were collected for further analysis. To determine the macrophage response to stimuli, macrophages were pre-conditioned for 2h, 6h or

24h in the presence or absence of CMT-93 conditioned medium before being stimulated with LPS (100ng/ml, Enzo Life Sciences), PAM_3CSK_4 (1µg/ml; InvivoGen), Flagellin (5µg/ml; InvivoGen) or CpG (2µM; InvivoGen) for 24h.

2.5 Assessment of phagocytosis

Macrophages were cultured in a 6-well plate at $5x10^5$ cells in a total volume of 2ml/well. To assess phagocytosis, macrophages were incubated with 1µm fluorescent latex beads (Sigma-Aldrich), at a concentration of 20 beads per cell, for 1h at 37ºC (Seyrantepe *et al.*, 2010). Cells were then washed with PBS/2% FCS and the uptake of beads (λ_{ex} ~470 nm; λ_{em} ~505 nm) was measured by flow cytometry. For the analysis of phagocytosis after stimulation, cells were treated with 100ng/ml LPS for 24h prior the addition of latex beads. As a negative control, the same experiment was repeated with CMT-93 cells which do not phagocytose (see **Appendix B)**. Additionally, macrophages were incubated with 10µg/ml Cytochalasin D (Sigma-Aldrich) for 30min prior to the addition of latex beads (see **Appendix B**). Phagocytosis is sensitive to treatment with cytochalasin, a drug that disrupts actin polymerization, but endocytosis is cytochalasine insensitive (DeFife *et al.*, 1999).

2.6 Enzyme-linked immunosorbent assay (ELISA)

2.6.1 Basic principles of ELISA

ELISA is a sensitive and robust method which measures the antigen concentration in an unknown sample. In all of our studies we used a sandwich ELISA to measure the amount of cytokines and chemokines in cell supernatants. In a sandwich ELISA the antigen of interest is quantified between two layers of antibodies: the capture and the detection antibody. These antibodies must bind to non-overlapping epitopes on the antigen. The detection antibody is usually conjugated with biotin which then allows for the detection reagent (streptavidin-HRP) to bind to it. The streptavidin and biotin bind with high affinity and the amount of horseradish-peroxidase (HRP) is proportional to the amount of target antigen in the sample. Substrate solution is then added (tetramethylbenzidine, TMB) and the HRP enzyme catalyses the oxidation of the TMB into a coloured product. The intensity of the colour is proportional to the concentration of antigen in the sample. Colour development is stopped by adding an acidic solution and the optical density (O.D.) of the colour is measured on a microplate reader. For each set of samples, a standard curve is generated and the values of unknown samples are calculated from the standard curve (Sandhu Premjeet1, 2012).

2.6.2 Cytokine ELISA

The concentration of cytokines IL-12p40, TNF-α, IL-6, IL-10 and IL-27 in cell supernatants was determined using ELISA Duoset kits from R&D Systems in accordance with the manufacturers' instructions. Briefly, 100µl/well of capture

antibody (diluted to the appropriate concentration in PBS) was added to an ELISA plate (Nunc) and incubated overnight at room temperature. Plates were then washed three times with Wash Buffer (PBS + 0.05% Tween-20) and blocked by adding 300µl of Blocking buffer (1% (w/v) BSA/PBS) for a minimum of 1h at room temperature. The washing step was repeated and 100µl of samples and standards (diluted to appropriate concentrations) were added per well, in triplicate. Plates were then incubated at 4ºC overnight. The next day, plates were washed again and 100µl of the biotinylated detection antibody was added to each well and incubated for 2h at RT. 100µl of Streptavidin-HRP (R&D) was then added to each well, following another wash step. Plates were incubated for 20min at RT. After the last washing step, 100µl of TMB (BD Biosciences) was added to each well and plates were left in dark for 20min or until the blue colour develops. Colour development was stopped by adding 50µl of 1M sulphuric acid (Sigma-Aldrich) to the wells. The optical density was determined at 450nm, using a VersaMax™ microplate reader (Molecular Devices).

2.6.3 Chemokine ELISA

The concentration of chemokines MIP-1α, MIP-2 and MCP-1 in cell supernatants was determined using ELISA Duoset kits from R&D Systems in accordance with the manufacturers' instructions. The protocol is as described in the last section 2.6.2.

2.7 Measurement of nitric oxide (NO) formation

NO levels were detected in the cell supernatants by measuring the production of nitrite (NO_2^-) which is a stable breakdown product of NO. The production of nitrite was measured using the Griess Reagent System (Promega). The Griess Reagent system uses sulfanilamide and N-1-napthylethylenediamine dihydrochloride (NED), under acidic (phosphoric acid) conditions, which form the coloured azo-compound in the presence of nitrite. The intensity of the colour is proportional to the concentration of nitrite in the sample. The nitrite concentration is then determined using sodium nitrite as a standard. This method was originally described by Griess (Griess, 1879).

Briefly, 50µl of samples and standards were added to the 96-well plate in triplicates. 50µl of the Sulfanilamide Solution (Promega) was then added to each well and plate was incubated for 10min at RT, protected from light. In the next step, 50µl of the NED solution (Promega) was added to all wells and incubated for another 10min at RT, protected from light. A purple/magenta colour develops and the absorbance was measured at 543nm using a VersaMax™ microplate reader (Molecular Devices).

.

2.8 Measurement of reactive oxygen species (ROS)

To measure the intracellular ROS production, $0.5x10^6$ cells/ml were incubated with 20µM of the cell permeant reagent 2',7' –dichlorofluorescein diacetate (DCFDA; Abcam) for 30 min at 37ºC in the dark, according to manufacturer's instructions. DCFDA is a fluorogenic dye that measures hydroxyl, peroxyl and other ROS activity within the cell. After diffusion into the cell, DCFDA is deacetylated by cellular esterases to a non-fluorescent compound, which is later oxidized by ROS into 2', 7'

–dichlorofluorescin (DCF) (Eruslanov and Kusmartsev, 2010). DCF is a highly fluorescent compound which can be detected by fluorescence spectroscopy with maximum excitation and emission spectra of 495nm and 529nm respectively. The fluorescence intensity of DCF was measured by flow cytometry.

2.9 MTS viability assay

To determine the number of viable cells, The CellTiter 96® AQueous One Solution Cell Proliferation Assay (Promega) was used. This assay uses the MTS tetrazolium compound (Owen's reagent) which is bioreduced by cells into a coloured formazan product that is soluble in tissue culture medium (Malich *et al.*, 1997). The quantity of formazan product is then measured by the absorbance at 490nm and it is directly proportional to the number of living cells in culture. Briefly, cells were plated on a 96-well plate at 100,000 cells/well in a total volume of 100µl. 20µl of MTS compound was added to each well and the plate was incubated at 37ºC for 1h, in a humidified, 5% CO2 atmosphere. Absorbance was then recorded at 490nm using a 96-well plate reader. Results are expressed as a percentage of untreated cells.

2.10 Caspase 3/7 assay

CellEvent® Caspase-3/7 Green Detection Reagent (Life Technologies) consist of cell permeant reagent with a four amino acid peptide (DEVD) conjugated to a nucleic acid binding dye. During apoptosis, caspase-3 and caspase-7 proteins are activated and able to cleave the DEVD sequence. Cleavage of the DEVD sequence and binding of DNA labels apoptotic cells with a bright, fluorescent signal (Belloc *et*

al., 2000). The absorption and emission wavelengths of the CellEvent® reagent are 511nm/533nm. The assay was performed according to manufacturer's instructions. Briefly, $0.5x10^6$ cells/ml were stained with 500nM CellEvent® Caspase-3/7 Green Detection Reagent for 30min at 37ºC. Samples were then analysed, without washing or fixing, on FACSAria I flow cytometer.

2.11 RNA Analysis

2.11.1 Total RNA isolation

Colonic tissue (20-30mg) was homogenised in Lysis buffer RA1 (Macherey-Nagel) using Qiagen TissueLyser LT for 5min at 50Hz. Total RNA was then isolated using a Nucleospin RNA II kit (Macherey-Nagel) according to manufacturer's instructions. Briefly, the viscosity of the lysate was first cleared by filtration through a NucleoSpin® filter and centrifuging for 1min at 11000g. 70% ethanol was added to the homogenised lysate to adjust RNA binding conditions. The NucleoSpin® RNA II column was then used to bind RNA, with the addition of Membrane Desalting Buffer to remove salt and improve the efficiency of rDNase digestion. DNA was digested using a DNase reaction mixture at RT for 15min. After 15min Buffer RA2 and RA3 were added to inactivate rDNase and wash the column. The NucleoSpin® RNA II column was then placed into a nuclease free collection tube and RNA was eluted in RNase-free H_2O. The concentration of RNA was then measured using the Nanodrop® ND-1000 (Thermo-Fisher Scientific). The purity of the RNA was determined using 260nm and 280nm absorption wavelengths. All the RNA used in this study had a A280/A260 ratio between 1.8 and 2.1 (Ralph Rapley, 1998).

2.11.2 cDNA synthesis

Complementary DNA (cDNA) is generated from mRNA using the High Capacity cDNA Reverse Transcriptase Kit (Applied Biosystems, USA). The kit contains a master mix of dNTP, random primers and the enzyme reverse transcriptase. Reverse transcriptase synthesises single strain cDNA using the mRNA strands as a template. This is then used as the template for the subsequent qRT-PCR experiments. 1µg of mRNA was used in each cDNA synthesis reaction. The settings in **Table 2.8** are used in the reaction on a PTC-200 PCR thermal cycler (MJ Research).

	Step 1	**Step 2**	**Step 3**	**Step 4**
Temperature (ºC)	25	37	85	4
Time (min)	10	120	5	∞

Table 2.8 Thermal cycling conditions

2.11.3 Basic principles of quantitative real time PCR (qRT-PCR)

The principle of polymerase chain reaction (PCR) is to specifically increase a target from an undetectable amount of starting material. This is done by using a cDNA template that we want to amplify, sequence specific oligonucleotides, heat stable DNA polymerase and thermal cycling. In classical PCR, at the end of the amplification, the product can be run on a gel for detection of the specific product. Real time PCR, however, combines the DNA amplification with the immediate detection of the product. This is done by using a fluorescent reporters and PCR instruments that are able to measure fluorescence while performing the thermal cycling needed for the PCR reaction. The amount of DNA is measured after each

cycle via fluorescent reagents that yield an increasing fluorescent signal which is proportional to the increase in target (Kolmodin and Birch, 2002).

These fluorescent reagents can be sequence specific or non-sequence specific. In this thesis both types of reagents were used, Taqman® assay and SYBR® green dye.

2.11.3.1 Taqman® assay

Taqman® assays contain two primers and a probe. A Taqman probe has a gene-specific sequence and binds the target between the two PCR primers. At the 5' end of the probe is a reporter, which is a fluorescent dye. On the 3' end of the probe is a quencher, which quenches fluorescence from the reporter in an intact probe. During PCR, the primers and probe anneal to the target and if they bind to the correct target sequence the DNA polymerase cleaves the probe, releasing the fragment with the reporter dye. Once cleaved, the reporter dye is no longer in close proximity to the quencher and therefore it can emit its full signal. Eventually, cleaved probes will accumulate and produce a signal that can be measured by the PCR instrument.

2.11.3.2 SYBR® green dye

SYBR® green is a fluorescent dye that binds to the minor groove of double-stranded DNA. During the PCR reaction, the primers will amplify the target sequence, more molecules of the dye will bind to the double-stranded product and will fluoresce. SYBR® green dye is non-sequence specific, which means it can bind to any double-stranded sequence such as primer-dimer artifacts or non-target sequence. To assess the specificity of the SYBR® green assay we, therefore, performed the dissociation analysis for each product. The dissociation step was added after the final PCR cycle.

If there is only one product present in the tube it should have one specific melting temperature, Tm. The PCR software transforms the melt profile into a peak. If there is more than one peak present that usually signals the amplification of non-target products. Presence of one pure peak shows that one target amplified, but to further evaluate this we also ran the products on the gel **[**see **Appendix C].**

2.11.4 qRT-PCR assay optimisation

Before analysis of gene expression, we first evaluated the assay performance by assessing the standard curve and PCR efficiency **[**see **Appendix C]**. A standard curve was created by carrying out a serial dilution of the PCR product. When a standard curve correlation coefficient was close to 1, the PCR efficiency was determined using the following formula:

$$E = \left(10^{-\frac{1}{slope}} - 1\right) x\ 100$$

A well performing assay will have efficiency between 90-100%, which correlates to slope values of 3.1-3.3. Non template controls (NTC) were included in all experiments. Samples with a NTC within 5 cycles of the sample Ct value were disregarded (Raymaekers *et al.*, 2009).

Premade primers and Taqman® assay primer/probes were ordered from IDT **[Table 2.6** and **Appendix C]** and used as recommended by manufacturer. Where DNA binding dye (SYBR® green) was used, the dissociation step was added, after the final PCR cycle, in order to assess primer specificity as explained in the section 2.11.3.2 **[Appendix C]**. In order to further ensure that the primers are only amplifying the product of interest, PCR product was ran on the gel (details in the

section 2.11.7) **[Appendix C]**. If assay efficiency or primer specificity was not satisfactory, new sets of primers were ordered.

2.11.5 qRT-PCR protocol

PCR was prepared in triplicate for each sample by adding cDNA, master mix and RNase free water. In experiments with Taqman® primer/probes Taqman® Gene Expression Mastermix (Applied Biosystems) was used. In other experiments we used SYBR Green Mastermix (Roche). All the primers and primer/probes were ordered from IDT and are listed in **Table 2.6** and **Appendix C**. ROX dye was used as a passive reference to normalise the well to well differences that may occur due to artefacts such as pipetting errors or instrument limitations. Samples were added to a 96-well reaction plate (Applied Biosystems) and sealed with optically clear film (Applied Biosystems). Plates were centrifuged for 1min at 1000g and run on the ABI Prism 7500 under the conditions shown in **Table 2.9**. The results were analysed using the ABI Prism sequence detection software (Applied Biosystems) and Excel Software (Microsoft).

	Step 1	**Step 2**	**Step 3a**	**Step 3b**
Temperature (ºC)	50	95	95	60
Time	2min	10min	15sec*	15sec*
			*Repeat for 40 cycles	

Table 2.9 Thermal cycling conditions

2.11.6 qRT-PCR data analysis

For gene expression analysis we used a relative quantification method in which the gene levels are expressed as a fold difference between a sample and a calibrator (such as untreated/healthy tissue). Samples were first normalised to an endogenous control which is a gene that maintains consistent expression levels despite treatment. Several endogenous controls were tested and the most suitable one (in our case 18S) was selected **[**see **Appendix C]**. Normalised samples were then compared to the calibrator (healthy control) using ΔΔCt method:

$$\Delta\Delta Ct = \Delta Ct\ sample - \ \Delta Ct\ calibrator$$

Where ΔCt sample = Ct sample – Ct endogenous control and ΔCt calibrator = Ct calibrator – Ct endogenous control.

2.11.7 DNA product analysis by gel electrophoresis

Gel electrophoresis was used to check DNA products following qRT-PCR **[**see **Appendix C]**. Samples were run on a 2% agarose gel. The gel was prepared by dissolving 2g of agarose (Termo-Fisher Scientific) in 100ml 1x TAE buffer **[**see **Appendix A]** and heating to boiling point. After cooling, 10µl of SYBR® safe DNA gel stain (Applied Biosystems) was added to the gel mix before pouring into a gel mould and setting the well comb. DNA samples were mixed with loading buffer (Fermentas) and loaded straight onto the gel, together with GeneRuler 100bp DNA ladder (Termo-Fisher Scientific). Gels were run for 1h in 1x TAE buffer at 100V and visualised using the G-box imaging system (Syngene).

2.12 Primary cell isolation

2.12.1 Mice

BALB/c mice, 6-8 weeks old, were purchased from Charles River. Mice were kept under specific pathogen-free conditions at the Bioresource Unit, Faculty of Health and Science, Dublin City University, Ireland. All mice were maintained according to the guidelines of the Irish Department of Children and Health.

2.12.2 Isolation of colonic lamina propria cells

The large intestines of mice were excised and soaked in PBS. Fat and faecal matter were removed and the tissue was washed in Hank's balanced salt solution (HBSS, Gibco) with 2% fetal bovine serum (FBS, Gibco) and cut into approx. 0.5cm sections. To remove the epithelial layer, tissue was incubated with 2mM EDTA (ethylene diamine tetraacetic acid, Sigma) in calcium, magnesium free (CMF) HBSS (Gibco), in a shaking water bath for 15min at 37°C. The supernatant was then discarded and tissue was washed with fresh CMF HBSS, following a second incubation with 2mM EDTA in CMF HBSS. The remaining tissue was washed and digested with a pre-warmed combination of enzymes in complete RPMI (Gibco) medium. Three different combinations of enzymes were used, the first contained 240U/ml Collagenase II (Gibco) and 290U/ml Collagenase IV (Gibco). The second contained 1mg/ml Collagenase D (Roche), 1mg/ml Dispase (Gibco) and 50U/ml DNase I (Roche). The third contained 1.25mg/ml Collagenase D, 0.85mg/ml Collagenase V (Sigma), 0.03mg/ml Dispase and 30U/ml DNase I. The tissue was incubated in the digestion solution, in the shaking water bath at 37°C, for either

2x20min (digestion solution was changed after 20min), 2x30min (digestion solution was changed every 30min) or 40min with or without vigorously shaking every 5-10min. Finally, the supernatant containing lamina propria cells was removed and passed through a 70µm filter (BD Bioscience). Cells were centrifuged for 5min at 300g, resuspended in complete RMPI medium, filtered again and kept on ice until used.

2.12.2.1 Separation of dead cells and debris using Percoll gradient

In this study a discontinuous (step) gradient was used. To form a discontinuous gradient, Percoll (GE Healthcare) medium was diluted to a series of different densities. First an isotonic stock solution was prepared by adding 9 parts of Percoll to one part of 1.5M NaCl. The isotonic solution was then diluted to lower densities by adding 0.15M NaCl. The solutions of different densities were then carefully layered one on top of another, starting with the most dense at the bottom of the tube. The suspension of the cells in medium was added on top of the layers and centrifuged at 300g for 30min. After centrifugation a sharp band of cells that occurred at an interface was carefully collected into a sterile 50ml tube. Dead cells and debris usually end up at the bottom of the tube or floating on the top. Collected cells were then washed in HBSS and centrifuged three times for 5min at 300g to remove Percoll.

2.12.3 Purification of colonic macrophages

2.12.3.1 Cell purification using magnetic beads

Cells isolated from mouse colons were resuspended in 90µl buffer (PBS containing 0.5% bovine serum albumin and 2mM EDTA) per 10^7 cells and incubated with 10µl of FcR Blocking Reagent (Miltenyi) for 10min at 4°C. After blocking, cells were stained with 0.2µg of allophycocyanin (APC) - conjugated anti-mouse F4/80 antibody (BioLegend) per 10^7 cells in 100µl of buffer and incubated for 30min at 4°C in the dark. Cells were then washed twice to remove unbound antibody and magnetically labelled with Anti-APC MicroBeads (Miltenyi), according to manufacturer's instructions. Briefly, the cell pellet was resuspended in 80µl of buffer and incubated with 20µl of Anti-APC Microbeads per 10^7 of total cells, for 15min in the refrigerator. Cells were then washed, resuspended in 500µl of buffer and loaded onto an LS MACS® column and placed in the magnetic field of the MACS Separator. The magnetically labelled cells were retained within the column (positive fraction) while unlabelled cells (negative fraction) ran through. To remove all unlabelled cells the column was washed three times with 3ml of buffer. After separation, the column was removed from the magnetic field and the positive fraction was eluted by firmly pushing the plunger into the column. The cell purity and viability of both fractions were measured by flow cytometry.

2.12.3.2 Removal of dead cells using MACS® Dead Cell Removal Kit (Miltenyi)

Cells were magnetically labelled with Dead Cell Removal MicroBeads (Miltenyi), according to manufacturer's instruction. Briefly, the cell pellet was resuspended in 100µl of Dead Cell Removal MicroBeads per 10^7 of total cells and incubated for

15min at room temperature. The cell suspension was then diluted with 1ml of Binding Buffer (Miltenyi) per 10^7 cells and applied onto an LS MACS® column and placed in the magnetic field of the MACS Separator. The magnetically labelled dead cells were retained in the column while the unlabelled living cells passed through. The fraction that passed through was then collected and the viability was determined by flow cytometry.

2.12.3.3 Cell purification using fluorescence-activated cell sorting (FACS)

The isolated lamina propria cells were incubated with 1:1 solution of RPMI and FBS for 15min at room temperature, to prevent non-specific binding. Cells were then washed by centrifugation at 300g for 5min and stained with 0.2µg APC-conjugated anti-mouse F4/80 antibody (BioLegend) per 10^7 cells in 100µl of sterile buffer (PBS with 2% FBS), for 30min at 4°C in the dark. After staining cells were washed two times to remove unbound antibody and resuspended in the sterile sorting buffer. Two different sorting buffers were used, the first one contained PBS with 1mM EDTA (Sigma), 25mM HEPES (Gibco) and 1% FBS (Gibco), and the second one PBS without EDTA and HEPES. Cells were kept on ice until sorting. Propidium-iodide (PI) solution (Miltenyi) was added to the cells a few minutes before sorting, at a final concentration of 1µg/ml, to enable exclusion of dead cells. Sorting was performed on the BD FACSAria I cell sorter. The day before sorting, the internal sheath path of the sorter was decontaminated with bleach or ethanol and the lines were then rinsed with DI water. Cells were sorted into polystyrene FACS tubes half filled with complete RPMI medium. Sorting was performed at two different temperatures, 4°C and room temperature and also using either slower (<10000 cells/s) or faster (>10000 cells/s)

sorting speed. In order to achieve the highest purity two precision modes were tested: 0-32-0 and 16-16-0.

After sorting cells were re-analysed on the FACS Aria I for purity and used in further experiments. Schematic of the optimised cell isolation procedure is shown in **Appendix D**.

2.12.4 Isolation and differentiation of bone marrow-derived macrophages

The bone marrow was flushed out of the femurs and tibias of adult mice. Cells were then centrifuged at 250g for 5min and resuspended in complete RPMI (Gibco) supplemented with 10% FBS (Gibco) and 2% penicillin streptomycin/glutamine (Gibco). 50ng/ml M-CSF (eBioscience) was added to generate macrophages (Sweet and Hume, 2003). Cells were plated on petri dishes (4 petri dishes/mouse; 10ml/petri dish) and placed in a CO_2 incubator at 37ºC. After 3 days, 10ml of fresh media with 50ng/ml M-CSF was added to each plate. At day 6 non-adherent cells were removed by washing with RPMI and the adherent cells were displaced using a cell scraper (Sarstedt) and collected for further experiments (Zhang *et al.*, 2008). The purity of harvested bone marrow-derived macrophages was assessed by flow cytometry and was typically >95% F4/80$^+$.

2.12.5 Isolation of peritoneal macrophages

To obtain peritoneal macrophages, euthanized mice were injected intraperitoneally with 10ml ice cold, sterile PBS (Gibco) and resident peritoneal cells were collected by harvesting the solution from the peritoneal cavity. Cells were then centrifuged at 250g for 5min, resuspended in complete RPMI and placed on a 6-well tissue culture

plates (Nunc). After 2h non-adherent cells were removed by washing with RPMI and the adherent cells were displaced using a cell scraper and collected for further experiments. Collected cells were typically >90% $F4/80^{+}$.

2.13 Mouse models of disease

2.13.1 Dextran sulfate sodium (DSS) induced model of colitis

The DSS model work was carried out in collaboration with Dr. Silvia Melgar in the Alimentary Pharmabiotic Centre, University College Cork (UCC). 25 C57BL/6 female mice, weight 18-20g at arrival, were housed in the Biological Service Unit (BSU) at UCC. DSS was administered to the mice in drinking water at a final concentration of 3% (Okayasu *et al.*, 1990b). Fresh DSS was prepared daily in normal tap water and administered *ad libitum*. Mice were split into 4 groups for the study:

1. **Control**

   No DSS was administered to the control mice

2. **Early acute**

   Mice were administered DSS for 5 days (day 0 – day 4) followed by 2 days on water and sacrificed for sample and tissue processing on day 7

3. **Late acute**

   Mice were administered DSS for 5 days (day 0 – day 4) followed by 7 days on water and sacrificed for sample and tissue processing on day 12

4. **Chronic**

   Mice were administered DSS for 5 days (day 0 – day 4) followed by 21 days on water and sacrificed for sample and tissue processing on day 26

The clinical symptoms recorded in the DSS-treated and the control mice were body weight, fur texture/posture and stool consistency on day 0 and 2 times/week from day 4. These were used to generate a daily disease activity index (DAI). At the end point of each group the length and weight of each colon were also measured and used as an indicator of colitis. 0.5cm sections of distal colon were collected for RNA purification and histology.

2.13.2 *Clostridium difficile* infection

C. difficile spores from two strains, ribotypes 001 and 027, frozen in DMEM were acquired from the Sir Patrick Dunne Laboratory at St. James's Hospital, Dublin. The *C. difficile* infection model was carried out in collaboration with Pat Casey and Colin Hill in the Alimentary Pharmabiotic Centre & Microbiology Department, University College Cork.

C57BL/6J mice were infected with *C. difficile* using an antibiotic-induced model of mouse infection (Chen *et al.*, 2008a). Mice were treated for 3 days with an antibiotic mixture of kanamycin (400 μg/ml), gentamicin (35 μg/ml), colistin (850 U/ml), metronidazole (215 μg/ml) and vancomycin (45 μg/ml) in the drinking water. Mice were subsequently given autoclaved water. On day 5, mice were injected i.p. with clindamycin (10 mg/kg). Mice were infected with 10^3 *C. difficile* spores on day 6 by oral gavage. Mice that were not treated with antibiotics were also challenged with *C.*

difficile. Animals were weighed daily and monitored for overt disease, including diarrhoea. The caecum was harvested from uninfected (day 0) and infected mice at days 3 and 7 and the contents were removed for CFU counts. 0.5cm section of distal colon was collected for tissue homogenisation and RNA purification.

The contents of the cecum were recovered from infected and uninfected mice, weighed and homogenised in 1 ml PBS by vortex mixing in a 1.5 ml microcentrifuge tube. The suspension was serially diluted (10^{-1} to 10^{-4}) and 50 µl of each dilution was spread in duplicate onto quadrants of Brazier's CCEY plates (Lab M). Plates were incubated under anaerobic conditions at 37ºC for 30h. Colonies were counted and CFU/g determined for each sample.

2.13.3 Tissue sectioning and histochemistry

Tissue sections of 0.5cm were removed from the distal part of the washed colon and embedded in optimum cutting temperature (OCT) solution (Tissue-Tek), followed by freezing in liquid nitrogen and preserved at -80ºC. The sections were cut in a controlled temperature cryostat (Leica Cryocut 1800) at -20ºC and mounted onto microscope slides (RA Lamb). Slides were left overnight at room temperature. Sections were then fixed in acetone/alcohol mix for 5min at RT and washed in PBS. Slides were stained with Harris haematoxylin (Sigma-Aldrich) for 10 minutes and washed again under running tap water for 5min. The slides were differentiated in 1% acid/alcohol for 30s 3 times and then washed under a tap for 1min. After washing slides were placed in 0.1% sodium bicarbonate (Sigma-Aldrich) for 1min followed by washing under a tap for 5min. The slides were then rinsed in 95% ethanol (Merck) for 10 dips before counterstaining with eosin (Sigma-Aldrich) for 1min by

dipping up and down. Finally the slides were dehydrated by dipping in 75% ethanol for 3min, 95% ethanol for 3min (x2), followed by 100% ethanol for 3min and 3min in Histo-clear (National Diagnostics). Slides were then mounted with mounting medium and the cover slips pushed firmly to remove bubbles.

2.14 Statistical analysis

Results are presented as mean ± standard error of the mean (SEM) and groups were compared using an unpaired Student's *t*-test or for multiple groups, a one-way ANOVA followed by a Newman-Keuls post test. All data were analysed using Prism Software (GraphPad Software, Inc.). Values of less than $p<0.05$ were considered statistically significant.

CHAPTER 3

ISOLATION AND CHARACTERISATION OF COLONIC MACROPHAGES

3.1 INTRODUCTION

The gastrointestinal mucosa is the largest reservoir of macrophages in the body (Lee *et al.*, 1985). The macrophages are found in both the small and large intestine, strategically positioned in the lamina propria which underlies the surface epithelium. The intestinal immune system is continually exposed to different environmental and dietary antigens in the presence of commensal bacteria. Furthermore, the intestinal tract is a major site of pathogen exposure. To cope with these challenges, intestinal macrophages have evolved into a specialised type of mononuclear cells that differ from other macrophage populations in the body. The most important difference is their anti-inflammatory phenotype (Smith *et al.*, 2005, Smythies *et al.*, 2005).

Unlike other tissue macrophages intestinal macrophages are in a state of hypo-responsiveness. They do not express high levels of co-stimulatory molecules such as CD80 and CD86 (Smith *et al.*, 2011). Furthermore, they do not produce pro-inflammatory cytokines or chemokines in response to stimuli; neither do they up-regulate co-stimulatory molecules or antigen-presenting receptors (Smith *et al.*, 2005, Schenk and Mueller, 2007). However, they do produce the anti-inflammatory cytokine, IL-10, in response to Toll-like receptor ligation and retain phagocytic abilities (Smith *et al.*, 2005, Hadis *et al.*, 2011). An anti-inflammatory phenotype is not the only feature of intestinal macrophages. Studies have implicated their role in the regulation of epithelial cell renewal and integrity (Pull *et al.*, 2005). Furthermore, they have been shown to support the induction and survival of T_{reg} cells in the mucosa (Denning *et al.*, 2007, Hadis *et al.*, 2011). All of these properties make them

crucial cells for maintenance of gut homeostasis. Indeed, depletion of macrophages leads to increased susceptibility to intestinal inflammation (Qualls *et al.*, 2006).

Despite the importance of this macrophage population, the molecular mechanisms underlying their specific properties still remain unclear. One of the main reasons for this is the fact that they are notoriously difficult to isolate. A typical isolation involves extensive enzymatic digestion that affects both macrophage viability and number. Also they cannot be cultured as they progressively die once removed from their natural environment.

The aim of this study was to find the best method for isolation of colonic macrophages. This involves optimising the type and amount of enzymes required for tissue digestion and optimising the time of digestion. We wanted to establish a method that would yield the highest cell number and best viability. We also wanted to purify the macrophage population from other resident cells in the lamina propria (dendritic cells, eosinophils, mast cells, T-cells, etc) using their distinguishing feature of expression of the F4/80 marker. F4/80 is a member of the epidermal growth factor – transmembrane 7 family and has been widely used as a murine macrophage marker (Austyn and Gordon, 1981, MartinezPomares *et al.*, 1996). During our optimisation studies it has become clear that colonic eosinophils can also expresses F4/80 marker (Mowat and Bain, 2010). Furthermore, the expression of chemokine receptor, CX3CR1 has proven to be a more reliable way to distinguish between colonic macrophages and other intestinal populations (Pabst and Bernhardt, 2010). Because of the inability to find a good CX3CR1 antibody, we continued using

F4/80 as a macrophage marker, but we have adapted a revised method of gating in the attempt to exclude eosinophils (as described later in the result section).

For cell purification we wanted to compare two methods, namely cell separation using magnetic beads and fluorescence activated cell sorting. Finally, we wanted to characterise the isolated colonic macrophages and compare them to other macrophage populations in order to validate our model.

3.2 RESULTS

3.2.1 Optimisation of tissue digestion

Cell isolation from tissue is a complex process that depends on many factors such as combination and concentration of enzymes and the digestion time. In order to determine the method that yields the highest viability and cell number, we tested several different variables **[Table 3.1].** The first digestion solution contained a combination of two enzymes, Collagenase II and Collagenase IV and the tissue was allowed to digest for 40min in the shaking water bath at 37°C. The cell suspension obtained after digestion contained a high amount of dead cells and debris. We then used Percoll medium to enrich the viable cell population. Percoll medium is based on colloidal silica particles that are coated with polyvinylpyrrolidone. When a solution of Percoll is centrifuged, coated silica particles begin to sediment and, since Percoll is polydisperse colloid, these particles sediment at different rates creating a gradient. This can be utilised to separate cells, viruses, organelles and other particles depending on their size and granularity. To determine the best gradient to separate viable cells from debris, we prepared a few different discontinuous gradients, 20% Percoll over 40%, 20%/50%, 30%/50% and 40%/80%. The cell suspension was layered on top of these gradients. After 30min centrifugation a thin layer of cells was collected from the interface between gradients. Cells were counted and viability was determined using Trypan blue staining. The 20%/40% gradient yielded $1x10^6$ cells, 20%/50% yielded $2.1x10^6$, 30%/50% yielded $2.3x10^6$ and 40%/80% yielded $3x10^6$ cells. Viability of those cells were 29%, 43%, 69% and 66% respectively **[Table 3.1].** Since the 40%/80% Percoll gradient yielded the highest cell number ($3x10^6$

cells) with relatively high percentage of viable cells (66%), we decided to use that gradient for further tissue digestions.

The second digestion solution that was tested contained three different enzymes, Collagenase D, Dispase and DNase I. The digestion time was split into 2x20min or 3x20min. After each 20min fresh digestion solution was added. The viable population was enriched using a 40%/80% Percoll gradient and it contained 74% viable cells; however the cell number was still low ($2x10^6$). In order to determine whether the cells were lost during digestion or during Percoll gradient separation, the Percoll step was left out. The number of cells markedly increased to $37x10^6$ cells and viability was still high (70%). Therefore Percoll gradient was not used in the further digestions.

The third digestion solution also contained Collagenase D, Dispase and DNase I with the addition of Collagenase V. The tissue was digested for 40min. After digestion, the cell suspension contained $70x10^6$ cells with 85% viability. This combination of enzymes and digestion time was then used throughout the study.

3.2.2 Optimisation of cell purification

In order to purify macrophages from the suspension of lamina propria cells we tested two different purification methods. The first method was magnetic separation using Miltenyi MACS® columns and the second method was fluorescence-activated cell sorting on BD FACSAria I. Macrophages isolated from the mouse colon were purified based on their expression of F4/80 marker which has been widely used as a murine macrophage marker (MartinezPomares *et al.*, 1996).

3.2.2.1 Cell purification using Miltenyi MACS® columns

Cells isolated from the colon were stained with allophycocyanin (APC) - conjugated anti-mouse F4/80 antibody and F4/80^{+} macrophages were purified using the Miltenyi MACS column as described in the Materials and methods section 2.12.3.1. The positive fraction obtained after purification was stained with Propidium Iodide (PI) solution to determine the cell viability. PI is a commonly used fluorescent dye for identifying dead cells as it can penetrate cell membranes of dead and dying cells and bind to DNA. Fluorescence can then be detected in the red or yellow fluorescence channel. Cell purity and viability were measured using flow cytometry.

Cells were first gated based on their size (forward scatter, FSC) and granularity (side scatter, SSC) in order to exclude debris which are smaller and less granular than the cells. Secondly, cells were gated based on their expression of F4/80 or PI. Cell purity, before and after magnetic separation, is shown by the contour plot **[Figure 3.1A]** with the F4/80 expression on the y-axis. F4/80^{+} cells shift up on the y-axis relative to the intensity of their fluorescent staining. Cell viability is shown as a dot plot **[Figure 3.1B]** with PI expression on the y-axis. Viable cells do not shift on the y-axis because they cannot take up propidium iodide dye and therefore lack fluorescence.

The lamina propria cell suspension contained 11% F4/80+ cells before magnetic separation. Following separation, purity increased to 63% F4/80+ cells **[Figure 3.1A].** On the other hand viability of the freshly isolated cells was 89% which decreased after the isolation to 54% of viable cells **[Figure 3.1B].**

One possible explanation of the decreased cell viability was unspecific binding of anti-APC beads to dead cells. To examine this, the purified sample was double-stained with PI and F4/80 antibody and analysed further. The dot plot **[Figure 3.2]**,

with F4/80 expression on the x-axis and PI expression on the y-axis, was divided into quadrants showing the percentages of dead F4/80$^-$ cells, dead F4/80$^+$ cells, unstained cells and live F4/80$^+$ cells in the sample. The sample contained 34% dead F4/80- cells (upper right quadrant) indicating that anti-APC beads un-specifically bind dead non-macrophage cells, decreasing the purity of the sample.

To remove dead cells from the sample we used MACS® Dead Cell Removal Kit (Miltenyi) as described in Materials and methods section 2.12.3.2. The percentage of viable cells was then determined by flow cytometry using PI staining. Viability of the sample is shown as a dot plot **[Figure 3.3]** with PI fluorescence on the y-axis. Following the use of Dead Cell Removal Kit, dead cells were enriched instead of removed from the sample (97% dead cells after the use of kit). This technique was not used any further.

3.2.2.2 Cell purification using fluorescence-activated cell sorting

Cells isolated from the colonic lamina propria were sorted on the FACS Aria I cell sorter as described in Material and methods section 2.12.3.3.

In order to achieve the highest purity and viability of sorted cells, a number of parameters that can affect sorting efficiency, were tested **[Table 3.2]**. Firstly, cells for sorting were kept in two different sorting buffers, one containing EDTA (Sigma) and HEPES buffer (Gibco), and one without EDTA/HEPES. The first buffer increased the cell viability and it was used for further sorting experiments **[Table 3.2]**. Secondly, cell sorting was performed at different temperatures, which also had an effect on cell viability. Viability of the cells sorted at 4°C was higher than of those sorted at room temperature. Also higher viability and purity was achieved if the speed of sorting was slower (less than 10000 events per second).

In order to sort a pure population, it is important to ensure that the cell of interest is contained in a drop that does not also contain a non-target (contaminating) cell. Therefore, usually only the drop that contains target cell is charged. However, sometimes the target cell falls near the edge of the drop and it may appear in the preceding or the following drop. In this case, to avoid the cell loss, more than one drop can be charged. Thus, how the sort is going to be performed is determined by choosing the appropriate sort precision mode (sort precision mode is described in more details in Material and methods section 2.2.3).

For achieving the highest purity, two precision modes were tested: 0-32-0 and 16-16-0. Although sort precision in the first mode is stricter, the second mode yielded higher cell number and purity and it was used throughout the study.

Figure 3.4 shows the gating strategy that was used for all the sorting experiments. The sample was first gated based on the size (FSC) and granularity (SSC) to exclude debris **[Figure 3.4A**]. The acquired population was then further gated based on the FSC-area vs. FSC-height to remove single cells from doublets. Doublets occur when two cells are stuck together and are seen by the flow cytometer as a single, larger particle. They appear differently in a graphical display and can therefore be gated out since they fall off the primary axis of population **[Figure 3.4B]**. It was important to sort only live cells that can be put into culture following sorting; therefore dead cells were gated out using PI staining **[Figure 3.4C].** Finally, live cells were gated based on their F4/80 expression **[Figure 3.4D]**. Only live, F4/80^{+} cells were sorted.

To confirm that the required population was collected, sorted cells were re-analysed on the flow cytometer. Contour plots and dot plots **[Figure 3.5]** show purity and viability of cells before and after sorting. Before sorting lamina propria cells contained 12% F4/80^{+} cells which were 81% viable **[Figure 3.5A]**. Sorted cells were

93% F4/80^{+} and viability was 96% **[Figure 3.5B]**. To check for the actual purity, since some of the cells can lose the antibody during sorting, sorted cells were re-stained with F4/80 antibody which increased the purity to 96% **[Figure 3.5C**].

Fluorescence-activated cell sorting was shown to be a more efficient method for purification of colonic macrophages when compared to magnetic separation **[Table 3.3]**; therefore this method was used throughout the study.

3.2.3 Isolation and differentiation of bone marrow-derived macrophages

In order to assess the phenotypic and functional characteristics of colonic macrophages and compare them with another macrophage population, bone marrow-derived macrophages (BMMØ) were generated. Bone marrow cells were isolated from the femurs and tibias of BALB/c mice and differentiated into BMMØ *in vitro* in the presence of the macrophage colony-stimulating factor (eBioscience) for 6 days. The macrophage colony-stimulating factor (M-CSF) is a lineage-specific growth factor responsible for differentiation and proliferation of myeloid progenitors into cells of macrophage lineage (Sweet and Hume, 2003). Purity of the differentiated macrophages was determined by flow cytometry using the F4/80 macrophage marker and it was regularly higher than 95%. The histogram in **Figure 3.6** shows the percentage of BMMØ that express F4/80 marker.

3.2.4 Colonic macrophages are hypo-responsive to Toll-like receptor stimulation

Both colonic macrophages (colonic MØ) and bone marrow-derived macrophages (BMMØ) were cultured in the presence of LPS (100ng/ml; Enzo Life Sciences) or

PAM_3CSK_4 (1µg/ml; InvivoGen) for 24h. Unstimulated cells were used as a control. After 24h supernatants were harvested and stored at -20°C, while cells were analysed for the expression of CD80, CD86, MHC class II and CD14 by flow cytometry. Expression of surface markers, before and after LPS or PAM stimulation, is shown as histograms and compares BMMØ and colonic MØ.

Unstimulated BMMØ expressed basal levels of CD80, CD86, MHC class II and CD14 and as expected they were all up-regulated following LPS stimulation **[Figure 3.7].** However, that was not the case for the colonic MØ. Expression of CD80 and CD86 on colonic MØ was low or almost absent, however there was expression of CD14 and MHC class II but it was lower compared to BMMØ. More importantly there was no up-regulation of these markers following LPS stimulation **[Figure 3.7]**. The same trend was observed after PAM_3CSK_4 stimulation **[Figure 3.9]**.

We also assessed expression of the Toll-like receptors, TLR2 and TLR4 on both macrophage populations using flow cytometry. Untreated BMMØ expressed both TLR2 and TLR4 receptors and they were both up-regulated after LPS stimulation **[Figure 3.8].** However, expression of TLR2 and TLR4 on colonic MØ was very low and did not change following LPS stimulation **[Figure 3.8]**. Similar expression profiles were observed after PAM_3CSK_4 stimulation **[Figure 3.10]**.

Another hallmark of macrophage activation is the production of a wide range of cytokines following encounters with pathogens. After stimulation with LPS and PAM_3CSK_4, for 24h, supernatants were collected from the BMMØ and colonic MØ and cytokine levels were measured by ELISA, including IL-12p40, TNF-α, IL-6, IL-10 and IL-27. LPS stimulation of BMMØ resulted in increased production of all cytokines measured. However, while colonic MØ secreted low levels of TNF-α, IL-6, IL-10 and IL-27, these levels did not change in response to LPS **[Figure 3.11]**. A

similar profile was observed following PAM_3CSK_4 stimulation, although production of IL-10 was slightly higher in PAM-stimulated colonic MØ than unstimulated colonic MØ **[Figure 3.12]**.

3.2.5 Colonic MØ retain phagocytic abilities

So far in this study we have shown that colonic macrophages fail to up-regulate co-stimulatory molecules when stimulated with TLR ligands and also fail to produce pro-inflammatory cytokines which are characteristics of colonic macrophages. We next wanted to measure their ability to phagocytose and compare it to BMMØ, as colonic macrophages have been reported to maintain phagocytic ability.

Both BMMØ and colonic MØ were cultured with 1µm fluorescent latex beads (Sigma) at 37°C. After 1h cells were washed and analysed by flow cytometry for the uptake of beads. Beads show green fluorescence which can be measured in the FITC channel (475-700nm). Cells that took up the beads show fluorescence, which is then seen on the histogram as a shift to the right **[Figure 3.13**]. Colonic MØ showed high uptake of beads (32.9% phagocytosing cells) without prior activation indicating that their phagocytic ability is retained. Phagocytosis of BMMØ was lower with 23.2% phagoytosing cells.

3.2.6 Colonic macrophages become pro-inflammatory in the disease

While colonic macrophages seem unresponsive to inflammatory stimuli, it has been shown that during intestinal inflammation phenotype of colonic macrophages becomes pro-inflammatory, with the up-regulation of co-stimulatory molecules, such as CD80 and Toll-like receptors (TLR), such as TLR4 (Rugtveit *et al.*, 1997a,

Hausmann *et al.*, 2002). They also produce pro-inflammatory cytokines (Rugtveit *et al.*, 1997b). In order to confirm this phenotype switch, we isolated colonic MØ from the colons of mice following induction of colitis using dextran sodium sulfate (DSS), as described in Materials and methods section 2.13.1. Colonic MØ from healthy controls and DSS mice were sorted, as previously described, and left in culture for 24h. After 24h supernatants were collected and stored at -20ºC and cells were stained with fluorescently labelled antibodies against CD86 and TLR4 and analysed by flow cytometry. The revised method of colonic macrophage gating was used in this experiment. Live, single cells were gated based on their high expression of F4/80 ($F4/80^{low}$ cells were not gated) and then subgated based on their FSC and SSC properties **[Appendix E].** Eosinophils have the forward and side scatter properties of granulocytes (Mowat and Bain, 2010) and can be distinguished from macrophages. Colonic MØ from the diseased mouse show much higher expression of CD86 and TLR4 when compared to healthy controls **[Figure 3.14A]**. Secretion of pro-inflammatory cytokines was measured in the collected supernatants by ELISA and colonic MØ from the DSS mice produced significantly higher amounts of IL-12p40 ($p<0.001$), TNF-α ($p<0.05$) and IL-6 ($p<0.001$) **[Figure 3.14B]**.

3.3 FIGURES

Digestion solutions	Digestion time	Percoll gradient	Cell count	Cell viability	Isolation time
Solution 1 **240 U/ml Collagenase II** **290 U/ml Collagenase IV**	40min	20%/40%	$1x10^6$	29%	6-8h
		20%/50%	$2.1x10^6$	43%	
		30%/50%	$2.3x10^6$	69%	
		40%/80%	$3x10^6$	66%	
Solution 2 **1 mg/ml Collagenase D** **1 mg/ml Dispase** **50 U/ml DNase I**	2x20min	40%/80%	$2x10^6$	74%	
	3x20min	Not used	$37x10^6$	70%	4h
Solution 3 **1.25 mg/ml Collagenase D** **0.85 mg/ml Collagenase V** **0.03 mg/ml Dispase** **30 U/ml DNase I**	40min (tube was shaken vigorously every 5-10 min)	Not used	$70x10^6$	85%	

Table 3.1 Optimisation of tissue digestion. Different combinations and concentrations of enzymes in the digestion solution, Percoll gradients and times of digestion were tested in order to achieve the highest number and viability of cells in the single cell suspension.

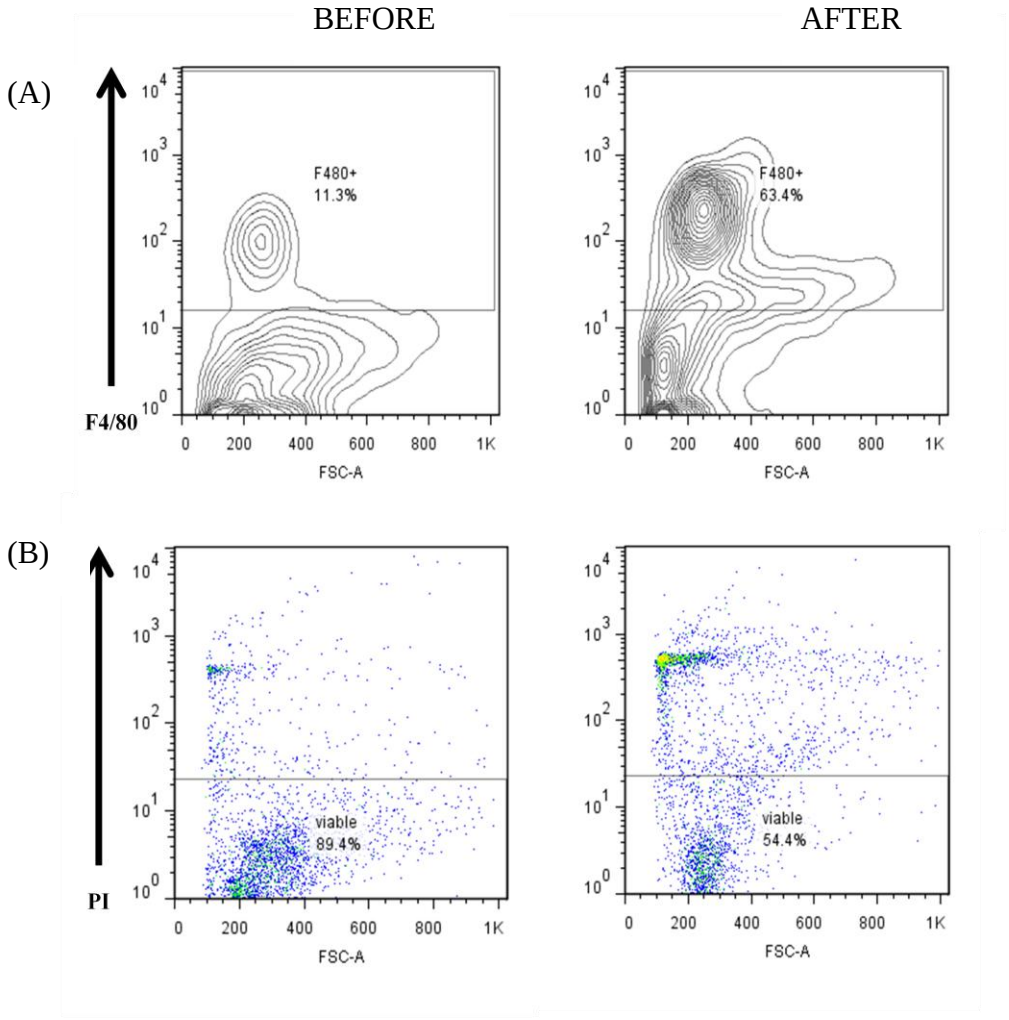

Figure 3.1 Cell purity and viability before and after magnetic separation using Miltenyi MACS® columns After tissue digestion cells were stained with APC anti-mouse F4/80 antibody (BioLegend), magnetically labelled with Anti-APC Microbeads (Miltenyi Biotec) and the cell suspension was loaded onto a MACS® column, according to manufacturer's instructions. Cells were then analysed using a BD FACSAria I cytometer. Contour plot and dot plot represent cells stained with APC F4/80 antibody (BioLegend) and Propidium Iodide stain (Miltenyi), respectively. Cell purity **(A)** and viability **(B)** was measured before and after magnetic separation. Data are representative of three independent experiments.

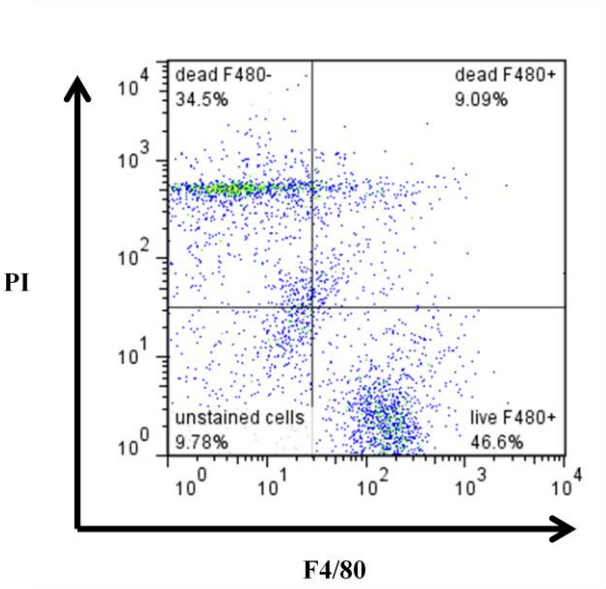

Figure 3.2 Magnetic beads bind the cells in an unspecific manner After magnetic separation, the positive fraction was analysed based on the expression of F4/80 vs. Propidium Iodide fluorescence. The dot plot is divided into quadrants showing the percentages of dead F4/80$^-$ cells, dead F4/80$^+$ cells, unstained cells and live F4/80$^+$ cells in the sample. Sample contains 34 % dead F4/80$^-$ cells. Data are representative of three independent experiments.

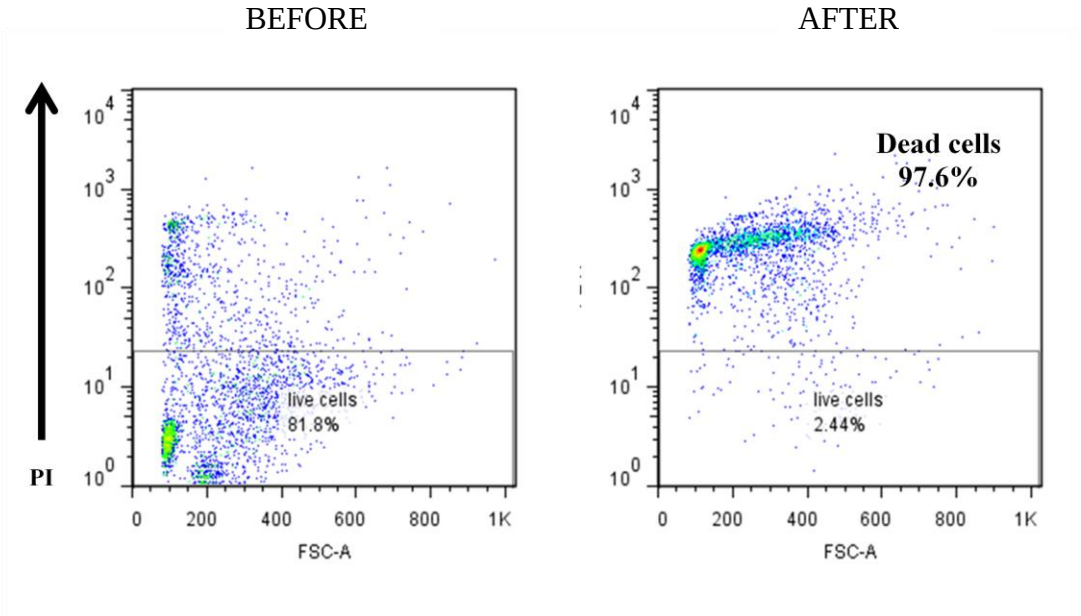

Figure 3.3 Dead cells are enriched instead of removed using Dead Cell Removal Kit (Miltenyi). After tissue digestion, the Dead Cell Removal Kit was used according to manufacturer's instruction to eliminate dead cells from the sample. Cells were then analysed on FACSAria I based on their Propidium Iodide fluorescence. Dot plots show the percentage of viable cells before and after the use of the kit. Data are representative of three independent experiments.

Parameters tested		Effect on cell viability	Effect on cell purity
Sorting buffer (PBS + 1% FCS)	+ EDTA, HEPES	↑	-
	- EDTA, HEPES	↓	-
Temperature of sorting	+4°C	↑	-
	RT	↓	-
Sort precision mode	0-32-0	-	↓
	16-16-0	-	↑
Speed of sorting	<10000 events/s	↑	↑
	>10000 events/s	↓	↓

Table 3.2 Optimisation of fluorescence-activated cell sorting Different parameters were tested in order to find optimal conditions for sorting of colonic macrophages on a BD FACSAria I cells sorter.

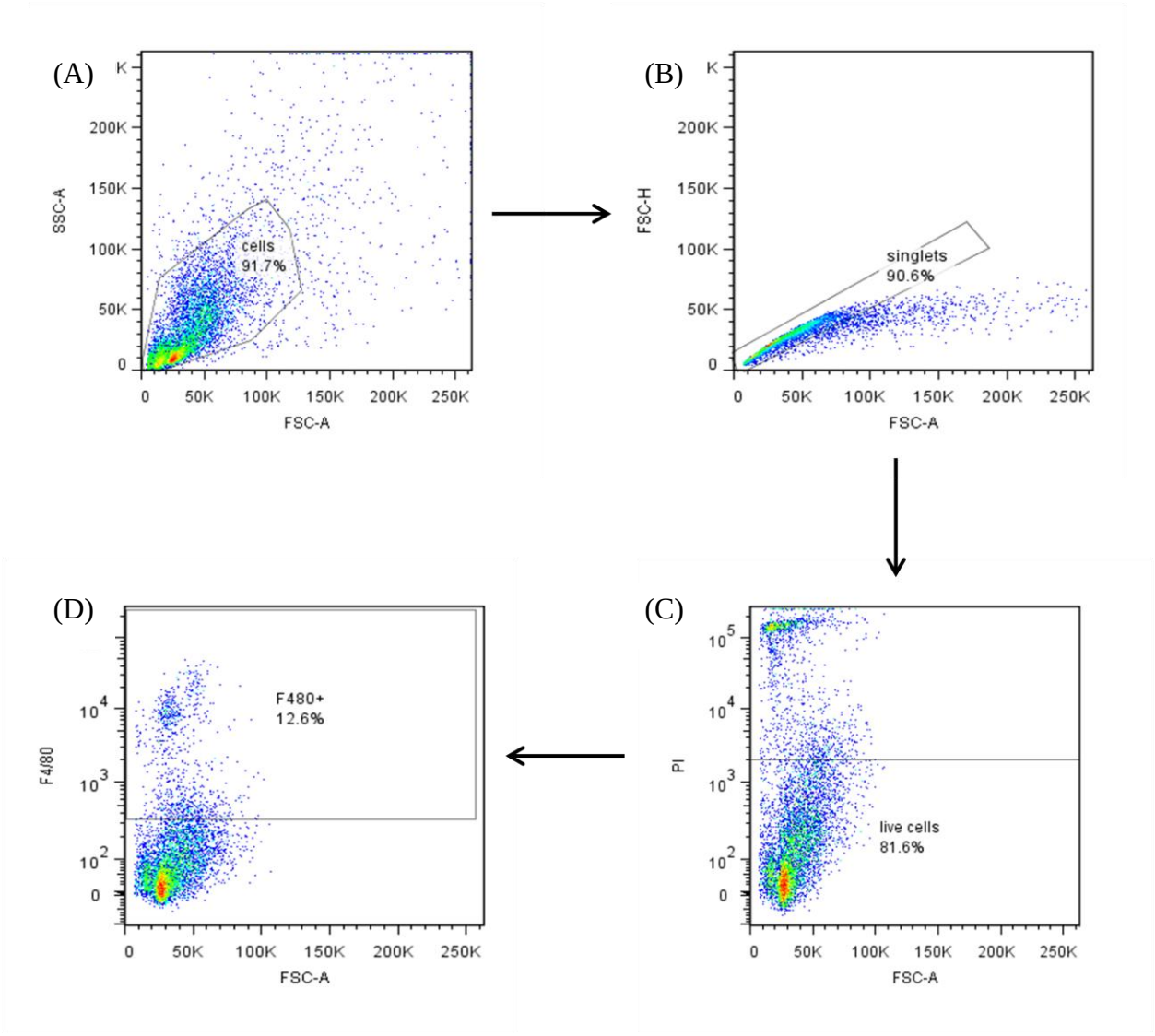

Figure 3.4 Gating strategies for sorting Cells were gated according to their size (FSC) and granularity (SSC) **(A)**, doublets were excluded **(B)** and to assess viability dead cells were gated out based on the Propidium Iodide stain **(C)**. Live-gated singe cells were then further gated based on their F4/80 expression **(D)**. Data are representative of three independent experiments.

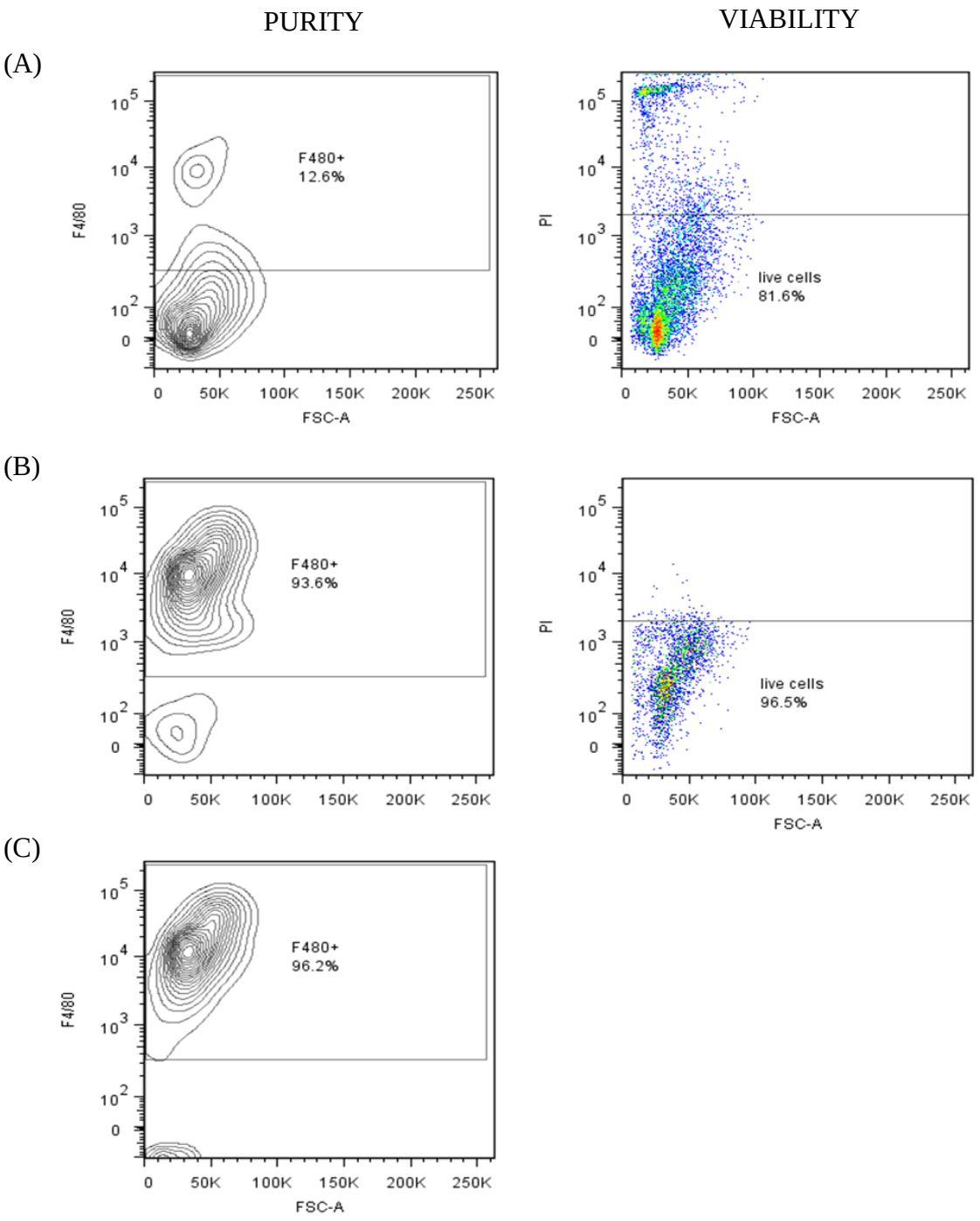

Figure 3.5 Cell purity and viability after fluorescence-activated cell sorting After tissue digestion, cells were stained with APC F4/80 antibody (BioLegend) and Propidium Iodide (Miltenyi) and sorted using BD FACSAria I cell sorter. Cells were gated based on their size (FSC) and granularity (SSC) and doublets were excluded. Furthermore cells were gated based on their expression of F4/80 and Propidium Iodide. Only live F4/80^{+} cells were sorted. Purity and viability of cells is shown before **(A)** and after sorting **(B).** Some of the cells lose the antibody during sorting; therefore cells were re-stained with F4/80 antibody following sorting to show the actual purity **(C)**. Data are representative of three independent experiments.

Method used	Purity	% viable cells after purification	Number of cells after purification
MACS® column	60-70%	50-60	$2.2\pm0.5x10^6$
Cell sorting	93-97%	95-97	$1\pm0.5x10^6$

Table 3.3 Summary of the tested purification methods Purity, viability and number of colonic macrophages following two different purification methods

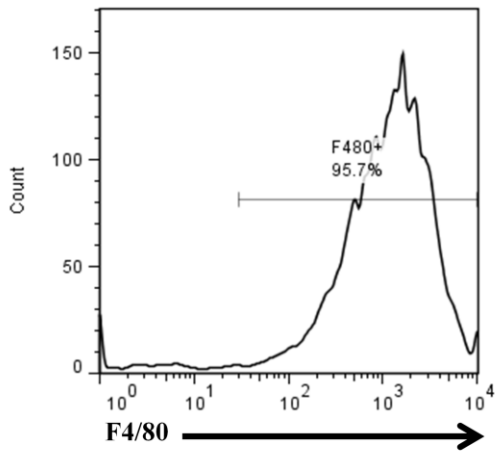

Figure 3.6 Purity of bone marrow - derived macrophages Macrophages derived from mouse bone marrow were stained with an F4/80 marker and purity was analysed on FACSAria I. The histogram shows the percentage of cells that express the F4/80 macrophage marker. Data are representative of three independent experiments.

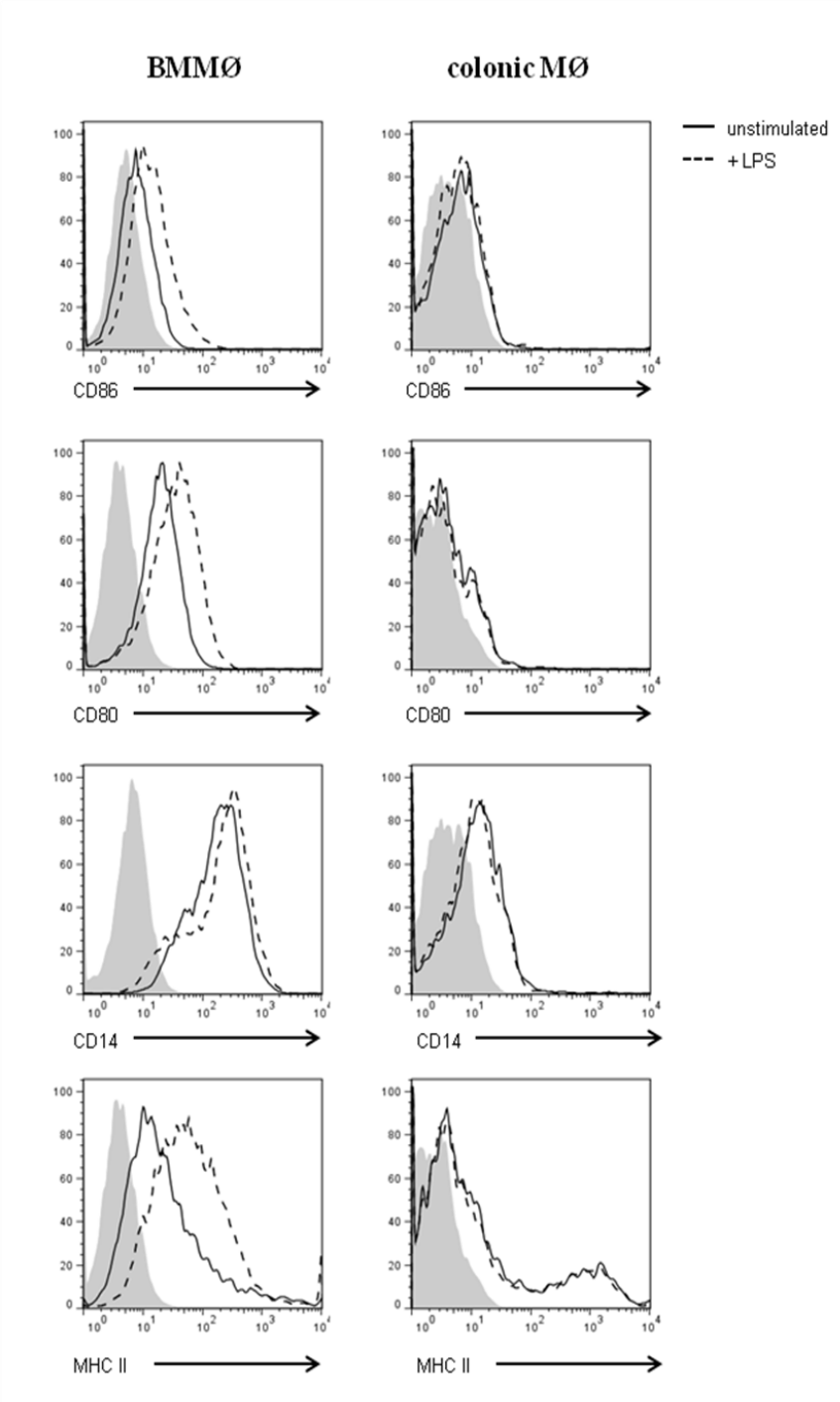

Figure 3.7 Expression of cell surface markers following LPS stimulation, comparing colonic and bone marrow-derived macrophages Bone marrow-derived macrophages (BMMØ) and colonic macrophages (colonic MØ) were stained with fluorescently labelled antibodies after 24h stimulation with LPS (100ng/ml) and surface expression was analysed on FACSAria I. Cells were gated on F4/80 positive population. The histograms show marker expression on unstimulated cells (black line) compared to LPS-stimulated cells (dashed line). Filled histograms represent unstained cells. Data are representative of three independent experiments.

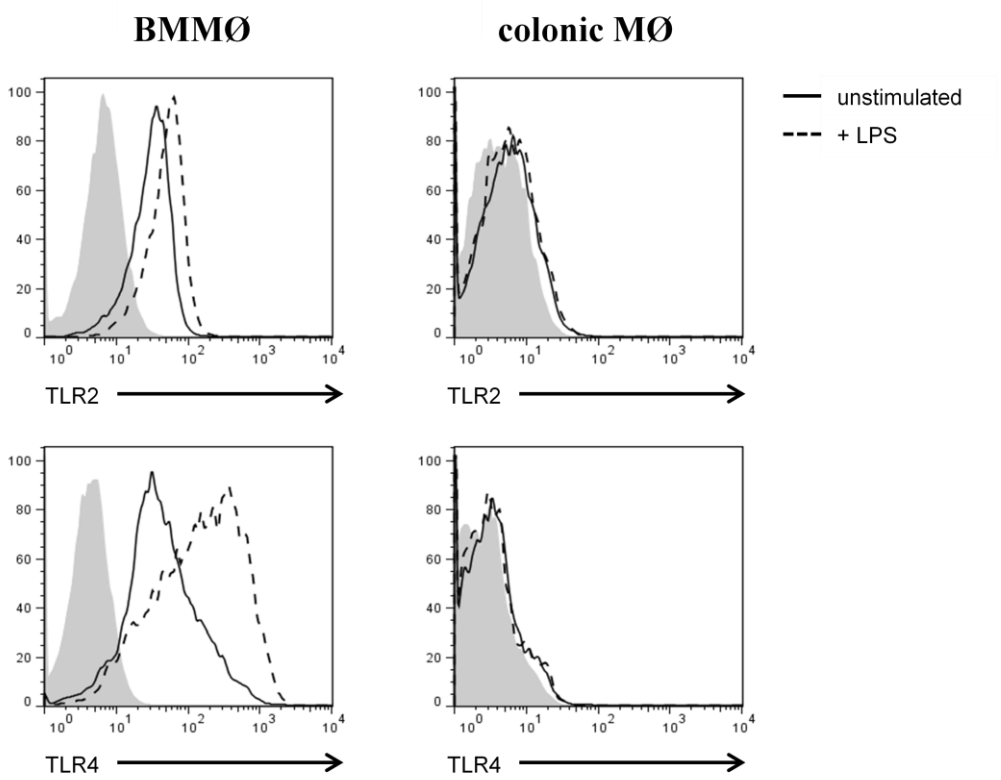

Figure 3.8 Expression of Toll-like receptors following LPS stimulation, comparing colonic and bone marrow-derived macrophages Bone marrow-derived macrophages (BMMØ) and colonic macrophages (colonic MØ) were stained with fluorescently labelled antibodies after 24h stimulation with LPS (100ng/ml) and surface expression was analysed on FACSAria I. Cells were gated on F4/80 positive population. The histograms show marker expression on unstimulated cells (black line) compared to LPS-stimulated cells (dashed line). Filled histograms represent unstained cells. Data are representative of three independent experiments.

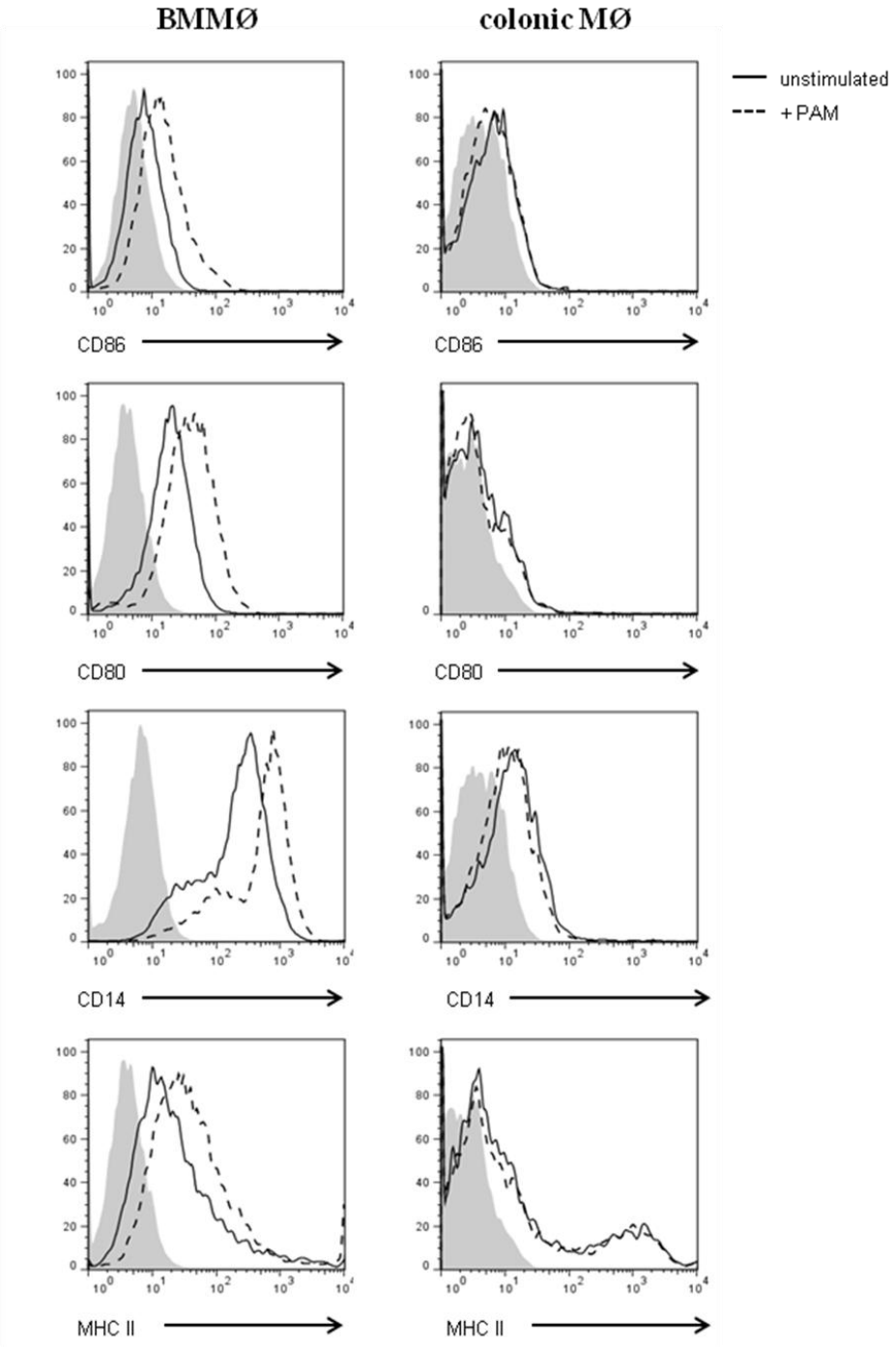

Figure 3.9 Expression of cell surface markers following PAM_3CSK_4 stimulation, comparing colonic and bone marrow-derived macrophages Bone marrow-derived macrophages (BMMØ) and colonic macrophages (colonic MØ) were stained with fluorescently labelled antibodies after 24h stimulation with PAM_3CSK_4 (1µg/ml) and surface expression was analysed on FACSAria I. Cells were gated on F4/80 positive population. The histograms show marker expression of unstimulated cells (black line) compared to PAM_3CSK_4- stimulated cells (dashed line). Filled histograms represent unstained cells. Data are representative of three independent experiments.

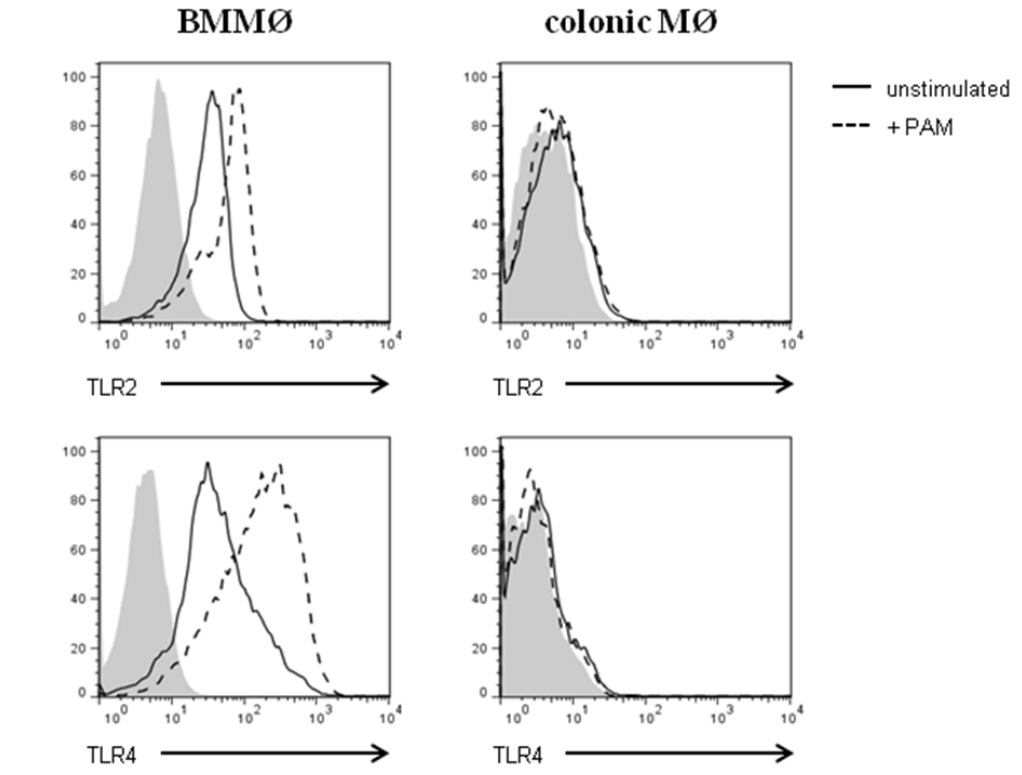

Figure 3.10 Expression of Toll-like receptors following PAM_3CSK_4 stimulation, comparing colonic and bone marrow-derived macrophages Bone marrow-derived macrophages (BMMØ) and colonic macrophages (colonic MØ) were stained with fluorescently labelled antibodies after 24h stimulation with PAM_3CSK_4 (1µg/ml) and surface expression was analysed on FACSAria I. Cells were gated on F4/80 positive population. The histograms show marker expression of unstimulated cells (black line) compared to PAM_3CSK_4- stimulated cells (dashed line). Filled histograms represent unstained cells. Data are representative of three independent experiments.

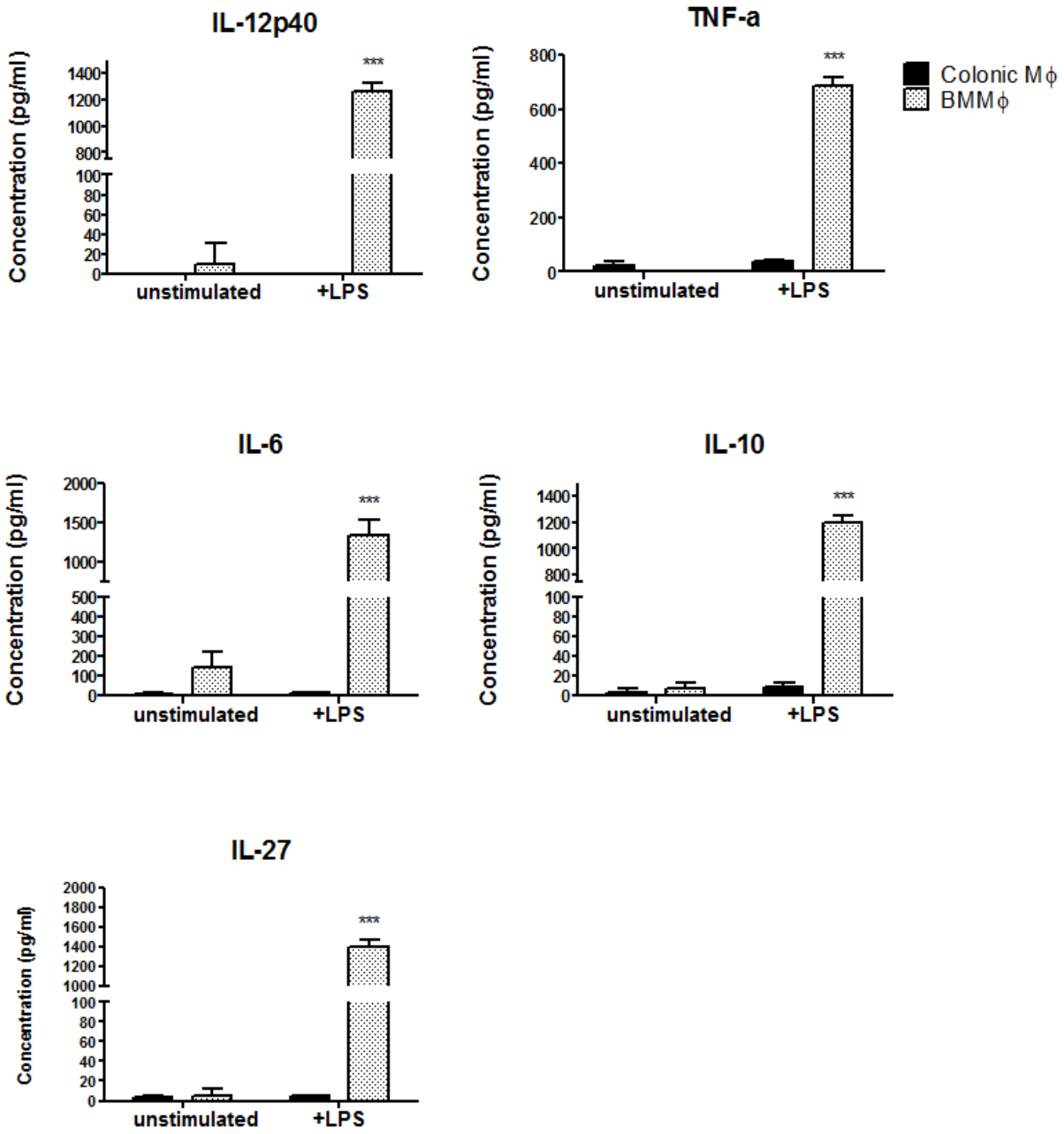

Figure 3.11 Cytokine secretion by colonic and bone marrow-derived macrophages following LPS stimulation Bone marrow-derived (BMMØ) and colonic macrophages (colonic MØ) were stimulated with LPS (100ng/ml) and after 24h supernatants were collected. Secretion of cytokines was measured by ELISA (R&D), according to manufacturer's instruction. Data are presented as mean ± SEM of three replicates and are representative of three independent experiments. ***P<0.001 vs. unstimulated BMMØ by unpaired *t*-test

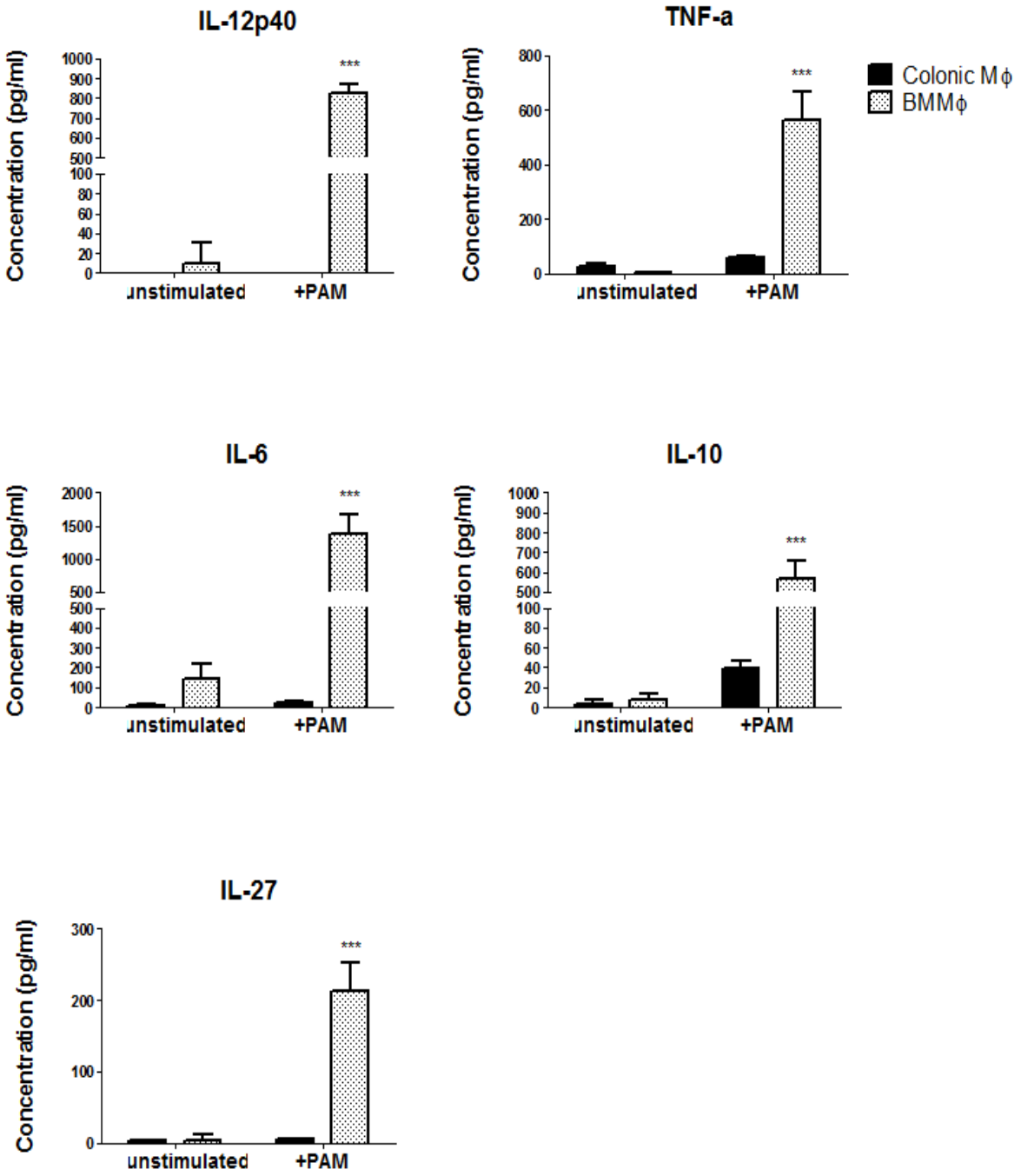

Figure 3.12 Cytokine secretion by colonic and bone marrow-derived macrophages following PAM_3CSK_4 stimulation Bone marrow-derived (BMMØ) and colonic macrophages (colonic MØ) were stimulated with PAM_3CSK_4 (1µg/ml) and after 24h supernatants were collected. Secretion of cytokines was measured by ELISA (R&D), according to manufacturer's instruction. Data are presented as mean ± SEM of three replicates and are representative of three independent experiments. ***P<0.001 vs. unstimulated BMMØ by unpaired *t*-test

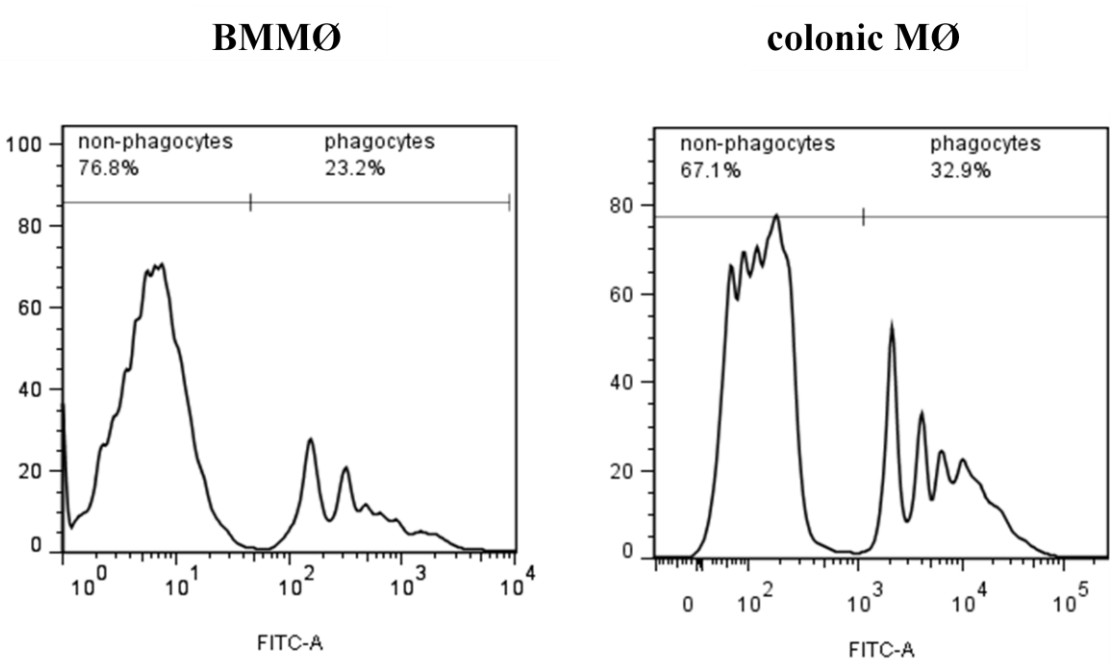

Figure 3.13 Phagocytosis of colonic and bone marrow-derived macrophages Bone marrow-derived (BMMØ) and colonic macrophages (colonic MØ) were cultured with 1µm fluorescent latex beads (Sigma) for 1h. Cells were washed and analysed by flow cytometry for uptake of beads. Gates on histograms show percentage of cells that contain beads (phagocytes) or do not contain beads (non-phagocytes). Data are representative of three independent experiments.

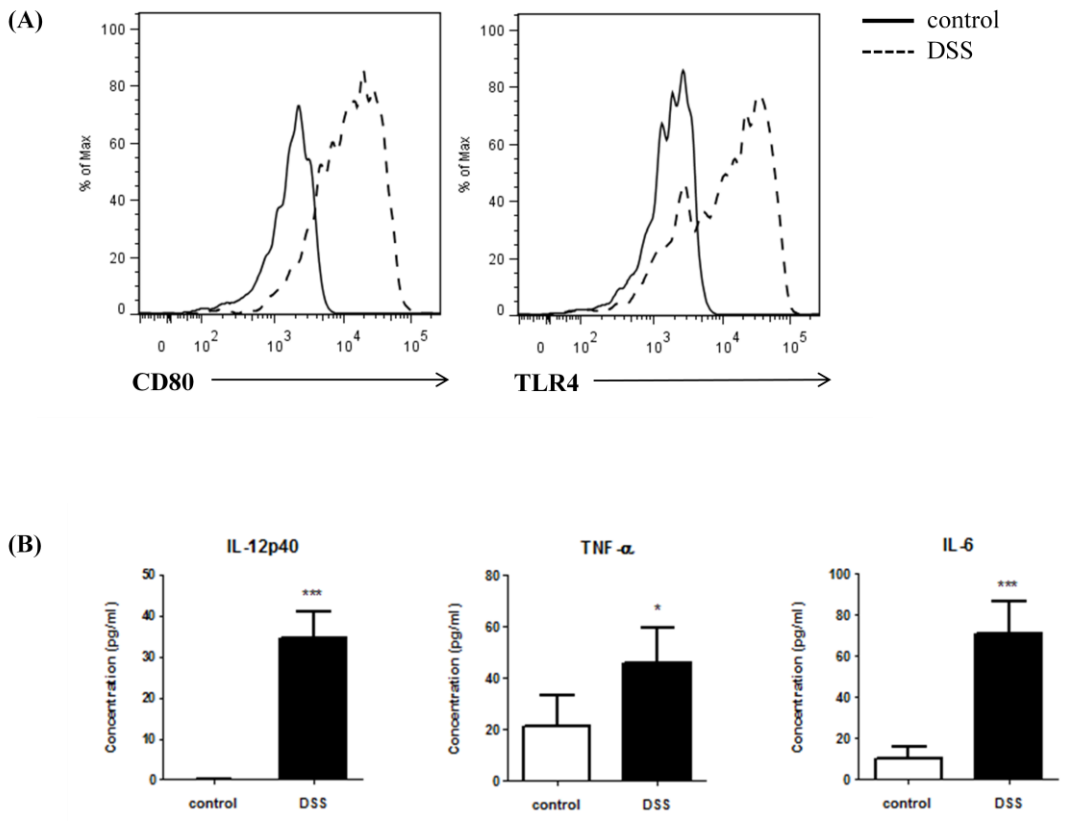

Figure 3.14 Colonic MØ have altered phenotype in inflammatory disease Mice were administered 3% DSS in drinking water for 5 days, followed by two days of water only. On day 7 mice were sacrificed and lamina propria cells were isolated from the colon. Expression of surface markers was measured on live, F4/80$^+$ cells and compared between a healthy control (black histogram) and diseased mouse (dashed histogram) **(A)**. Live, F4/80$^+$ cells were sorted using FACSAria I cell sorter (BD) and the production of cytokines was measured by ELISA (R&D) following 24h in the culture. Data are presented as mean ± SEM **(B)**. n=2 mice/control and 5 mice/DSS group. Statistical analysis was performed using unpaired *t*-test. *P<0.05, ***P<0.001 vs. control.

3.4 DISCUSSION

The aim of this study was to optimise a method for the isolation and purification of colonic macrophages. Firstly, we wanted to establish a method for the digestion of tissue that would give us a single cell suspension with the highest cell number and viability. Secondly, we wanted to find the best way to purify the cells of interest from the obtained suspension with no risk to the achieved viability. Lastly, we wanted to characterise the purified cells to confirm that we have the appropriate population and that the cell phenotype and function was not affected during the harsh isolation procedure.

The intestinal immune system is comprised of three main lymphoid areas: the lamina propria which is located just underneath the epithelium, the intraepithelial compartment and the lymphoid nodules. The majority of macrophages are located in the lamina propria (Mahida *et al.*, 1989a). There are a variety of protocols published in the literature for the isolation of intestinal cells. The first protocols that were established attempted to isolate lymphoid cells with particular interest in lymphocytes (Bull and Bookman, 1977, Vanderheijden and Stok, 1987). While all the protocols vary in terms of the type and concentration of enzymes used and the time of the incubation and temperature, they all use collagenases as the main enzymes. Collagenases are enzymes that break down the native collagen that holds the animal tissue together. They are used for the isolation of a wide variety of cell types, mostly because they generally have little effect on the cell function and phenotype (Gibson *et al.*, 1985, Holt *et al.*, 1986). The first enzyme solution we used contained a mixture of collagenase type II and collagenase type IV. Although

Lefrancois and Lycke reported that the use of collagenases, without other additional enzymes, gives the best final yield of live lamina propria lymphocytes (Lefrancois and Lycke, 2001), our sample which was digested in just collagenases contained the highest number of dead cells and undigested tissue. This indicated that the enzyme concentration was not high enough to digest all the tissue and also that the enzyme combination was toxic to the cells. Other researchers (Pavli, 2001, Weigmann *et al.*, 2007) suggested the use of collagenase D as an enzyme of choice, together with dispase and DNase. Collagenase D has high collagenase activity and very low tryptic activity while dispase is a neutral protease suitable for a gentle dissociation of tissue while preventing unwanted cell clumping. DNase is also reported to reduce cell clumping. In our hands this enzyme combination reduced the number of dead cells; however the digestion was still incomplete with the highest amount of undigested tissue. This may be due to the low concentration of enzymes used or the short incubation time. Since our cell viability increased using this combination we did not want to increase the concentration of enzymes and therefore risk the viability. Instead, we incubated the tissue for 40min or 60min and replaced the digestion solution with a fresh one every 20min. This, however, did not improve tissue digestion. Platt *et al.* used a similar combination of enzymes with the addition of collagenase V and were able to obtain a higher cell number than with the use of only dispase and DNase. Addition of the collagenase V to our digestion solution also improved the tissue digestion without a decrease in the cell viability. Therefore the digestion solution which contained collagenase D, dispase and Dnase, with the addition of collagenase V was used throughout the study.

In order to improve the removal of dead cell and debris we utilised the property of Percoll medium to form a gradient during centrifugation and separate cells based on their size and granularity. In agreement with others (Weigmann *et al.*, 2007) we found a 40% over 80% Percoll gradient to be the best in the enrichment of a viable population, however it was at the expense of cell numbers. When we left out the Percoll step the cell number markedly increased. Lefrancois and Lycke also reported that a Percoll gradient purification usually resulted in the loss of approx 50% cells (Lefrancois and Lycke, 2001). This may be due to cell clumping in the Percoll medium resulting in the sedimentation of cells at the bottom of the tube where they are mistaken for debris. Also, in some cases, thin layer of cells between gradients were almost invisible making it difficult to extract all the cells from the layer. Although the Percoll step had a benefit in the early stages of the optimisation, when our sample contained high amount of cell debris and undigested tissue, the improved digestion solution resulted in a single cell suspension with the highest viability and the Percoll gradient centrifugation could be left out. Furthermore leaving out the Percoll step shortened the isolation procedure which, in turn, also increased the cell viability.

Once we optimised the digestion procedure, we next assessed two different techniques for cell purification; magnetic separation and fluorescence-activated cell sorting. Both techniques are widely used and rely on the labelling of cells of interest with antibodies in order for them to be purified. In the first method the appropriate cells are magnetically labelled and retained in the magnetic field to be separated from the rest of the population. The second method is separation of cells based on their fluorescent marker using a specialised flow cytometer. We experienced

difficulties using the magnetic separation method as the separated fraction consistently had low purity and viability. Flow cytometric analysis showed high numbers of dead, non-macrophage cells present in the sample after the purification. We demonstrated that this was most likely due to unspecific binding of the magnetic beads to dead cells since they tend to be quite sticky. In order to remove the dead cells from the sample we used the Miltenyi Dead Cell Removal MicroBeads which recognise the antigen in the plasma membrane of apoptotic and dead cells and bind to it. Although magnetically labelled dead cells were supposed to be retained in the magnetic column and depleted in that way, we found that after the use of the kit the purified sampled contained only dead cells. It is possible that the amount of dead cells after the tissue digestion was too high and quickly saturated the column, resulting in the majority of dead cells passing through instead of being retained in the column. However, our sample contained only 10-15% dead cells after the digestion. It is more likely that the Miltenyi beads were not appropriate for use in the intestinal cell preparations since those cells tend to be much stickier than the cells obtained after the digestion of other tissue such as spleen, increasing the potential for unspecific binding of the beads. Other research groups we consulted experienced the same problem (personal communication). A cheaper and more user friendly method would be negative selection using magnetic beads, where everything but the cells of interest would be magnetically labelled and depleted from the sample; however there were currently no negative selection kits for the intestine on the market at the time of this study.

The fluorescence-activated cell sorting proved to be a better method to purify intestinal macrophages, although the technique was more difficult to optimise. Our

initial problem was low cell viability which we improved by using a specialised sorting solution with the addition of EDTA and HEPES. This decreased cell clumping and increased cell viability by keeping the pH in the optimal range. Based on the fluorescent properties and light scatter, we were able to visualise the population of interest on the flow cytometer, which was not an option while using magnetic separation. Also, we were able to distinguish between dead and live cells. Although the cell sorting was time consuming, better control of a population we wanted to collect, yielded samples with high cell purity and viability.

Following the optimisation of the method for isolation and purification of colonic macrophages, we next characterised their phenotype and function. In agreement with previous studies (Rogler *et al.*, 1998, Hirotani *et al.*, 2005, Smith *et al.*, 2011) our colonic macrophages showed low expression of the co-stimulatory molecules CD80 and CD86, but high expression of MHC class II. Furthermore, we were able to detect low expression of TLR2 and TLR4, which concurs with findings from Platt *et al.* (Platt *et al.*, 2010). Although it has been widely accepted that human intestinal macrophages do not express CD14 (Smith *et al.*, 2001), it has been shown that CD14 may be expressed at low levels intracellularly in murine colonic macrophages (Nakata *et al.*, 2006b). We however observed relatively high surface expression of CD14 on the colonic macrophages we isolated which is supported by a recent study of Mowat *et al*. who also reported that most mouse intestinal macrophages express high levels of this molecule (Bain and Mowat, 2011). We also examined the response of the colonic macrophages to stimulation with TLR ligands and showed that they do not respond to the TLR stimuli by producing pro-inflammatory cytokines or by up-regulating the expression of co-stimulatory molecules and other

innate immune receptors which are characteristics of these cells (Rogler *et al.*, 1998, Hirotani *et al.*, 2005, Smith *et al.*, 2011). Furthermore, our colonic macrophages maintained avid phagocytic ability which has been previously reported (Smythies *et al.*, 2005).

During the study presented in this chapter, it has become obvious that F4/80 marker does not stain only macrophages in the colon, but also eosinophils (Mowat and Bain, 2010). Since we did not include eosinophil marker, Siglec-F, or other newly described colonic macrophage markers (Bain *et al.*, 2013) in our experiments, we adapted a new gating strategy in the attempt to define macrophage population more precisely. In our lamina propria suspension, F4/80^{+} cells were further gated based on their FSC and SSC properties to exclude eosinophils that have the forward and side scatter properties of granulocytes (Mowat and Bain, 2010). Although our samples still might contain some non-macrophage cells, we believe that the revised gating strategy improves the authenticity of our colonic macrophage population. This revised gating strategy was also employed later in the chapter 5.

While colonic macrophages do not appear to respond to inflammatory stimuli their phenotype is significantly altered during the intestinal inflammation. It is not clear whether this is due to the loss of homeostatic factors that are usually present in the healthy intestine or due to the effects of newly produced inflammatory factors (Bain *et al.*, 2013, Tamoutounour *et al.*, 2012). However, during inflammation, intestinal macrophages display a pro-inflammatory phenotype with higher expression of co-stimulatory molecules (Rugtveit *et al.*, 1997a) and Toll-like receptors (Hausmann *et al.*, 2002) as well as higher production of IL-12, TNF-α, IL-6 and other pro-

inflammatory cytokines (Rugtveit *et al.*, 1997b, Platt *et al.*, 2010). To confirm that we also see these changes as well as to confirm again that we are isolating the correct population, we sorted and characterised colonic macrophages from mice from a dextran sulphate sodium (DSS) induced colitis model. DSS-induced colitis is a well-established animal model of mucosal inflammation with similarities to human inflammatory bowel disease (Wirtz and Neurath, 2007). It is induced by the addition of DSS to drinking water and it is characterised by the weight loss, diarrhea, blood in stools, epithelial cell degeneration and infiltiration of immune cells into lamina propria and submucosa (Kullmann *et al.*, 2001). As anticipated, colonic macrophages that we isolated from mice with DSS colitis showed higher expression of CD80 and TLR4 as well as increased production of pro-inflammatory cytokines.

Taken together, the results from our phenotypic analysis demonstrate that we have isolated the cells from a mouse colon that resemble colonic macrophage population in phenotypic and functional characteristics as reported by other groups. The optimised isolation procedure can, therefore, be used to obtain colonic macrophages for future experiments.

CHAPTER 4

CROSSTALK BETWEEN INTESTINAL EPITHELIAL CELLS AND MACROPHAGES

4.1 INTRODUCTION

It is clear that macrophages in the intestine represent a unique population distinct from their counterparts in other tissues. All of their properties have developed in order to keep the balance between protective immunity and tolerance in the antigen-rich environment of the gut. Although we now know that macrophages are critical for the maintenance of gut homeostasis (Qualls *et al.*, 2006), it is still unclear how and when they acquire these homeostatic abilities.

It has been speculated that intestinal macrophages originate from a special lineage of blood monocytes termed "resident" monocytes, which have homeostatic properties and home to noninflamed tissue, unlike "inflammatory" monocytes that home to inflamed tissue (Geissmann *et al.*, 2003). However Varol et al showed that, in a mouse depleted of mononuclear phagocytes, adoptively transferred "resident" monocytes fail to replenish intestinal macrophages (Varol *et al.*, 2009). On the contrary, they showed that intestinal macrophages are replenished by "inflammatory" monocytes. This was confirmed in the recent study by Bain et al. where they demonstrate that inflammatory blood monocytes migrate to the intestine, where they then differentiate into anti-inflammatory macrophages through a number of transitional stages (Bain *et al.*, 2013). Since this plasticity happens only in the intestine, it is probable that the intestinal environment itself is responsible for altering the phenotype of inflammatory monocytes upon their arrival in the gut.

Intestinal epithelial cells were once thought to be just a physical barrier that separates the luminal contents from the lamina propria. However, in addition to this

barrier function, there is increasing evidence to show that the intestinal epithelium has an immunomodulatory role, influencing underlying immune cells and shaping their function (Shale and Ghosh, 2009). This led to the characterisation of many pattern recognition receptors that are expressed by intestinal epithelium. Almost all Toll-like receptors (TLR) have been shown to be expressed at the mRNA level in the colon and small intestine (Wells *et al.*, 2011). However signalling through these TLR in the healthy intestine does not promote inflammation. Rather TLR signalling in epithelial cells seems to be necessary for maintaining the intestinal homeostasis (Rakoff-Nahoum *et al.*, 2004). In addition to that, epithelial cells also secrete various factors that can modulate the immune response in the intestine, such as antimicrobial peptides and chemokines (Wells *et al.*, 2011). Furthermore, intestinal epithelial cells are capable of processing and presenting antigens through major histocompatibility complex (MHC) which enables their interactions with T cells, even in the healthy gut (Shale and Ghosh, 2009).

Considering the above mentioned properties of intestinal epithelial cells and a strategic position of intestinal macrophages, just underneath the epithelium (Hume *et al.*, 1984), we hypothesised that epithelial cells may play an important role in monocyte differentiation into intestinal macrophages. It has been shown already that the mucosal environment can change the ability of dendritic cells to mount an immune response. Culture of human monocyte-derived dendritic cells with epithelial cell supernatants resulted in the induction of non-inflammatory dendritic cells that favour the generation of a Th2 response (Rimoldi *et al.*, 2005). Furthermore, co-culture of monocyte-derived dendritic cells with Caco-2 intestinal epithelial monolayers resulted in dendritic cells with reduced expression of MHC class II,

CD86 and CD80 and reduced levels of inflammatory cytokine production (Butler *et al.*, 2006).

To test our hypothesis we wanted to establish a model which would partially mimic the environment to which monocytes are exposed, once they arrive in the gut. Since mouse epithelial cells are difficult to obtain and culture *in vitro,* we used a colonic epithelial cell line, CMT-93, which has an epithelial morphology and form junctional complexes and microvilli with attached glycoproteins (Franks and Hemmings, 1978). We then exposed monocyte-derived macrophages J774A.1 to CMT-93 supernatants in order to investigate whether the soluble factors secreted by colonic epithelial cells can induce differentiation of monocyte-derived macrophage into a tolerogenic phenotype resembling intestinal macrophages.

4.2 RESULTS

4.2.1 Characterisation of a mouse colonic epithelial cell line, CMT-93

In the *in vitro* system we established, we wanted to expose J774A.1 monocyte-derived macrophages to soluble factors secreted by CMT-93 colonic epithelial cells. After this conditioning, we wanted to measure cytokine and chemokine production from those conditioned macrophages and compare them to the unconditioned macrophages. To ensure that any cytokine and chemokine levels detected are not present in CMT-93 supernatants itself, we measured the levels of cytokines and chemokines produced by this cell line in response to a panel of TLR ligands.

4.2.1.1 CMT-93 cells do not produce cytokines in response to stimuli

CMT-93 cells were plated on a 6-well plate, at $0.25x10^6$ cells/2ml, and left until they were confluent. Media was then discarded, fresh media added and the cells were stimulated with PAM_3CSK_4 (1 μg/ml), LPS (100ng/ml), Flagellin (5μg/ml), CpG (2μM) or medium alone as a control. After 24h supernatants were collected and the production of cytokines was measured by ELISA.

We did not detect any TNF-α or IL-10 production from the control cells and the levels of other cytokines were low (<40pg/ml). There was no significant up-regulation of cytokine production even after stimulation with a range of TLR ligands **[Figure 4.1]**.

4.2.1.2 CMT-93 cells secrete MIP-2 and MCP-1

The supernatants from the previous experiments were also used to measure the production of chemokines by CMT-93 cells. Production of MIP-1 was low and did not change following TLR stimulation, however there was a significant up-regulation in the production of MIP-2 ($p<0.001$) and MCP-1 ($p<0.001$) in response to TLR2 (PAM) and TLR4 (LPS) ligation, but not in a response to TLR5 (Flagellin) or TLR9 (CpG) **[Figure 4.2]**.

4.2.1.3 CMT-93 cells express MHCII, TLR2 and TLR4 but do not up-regulate their expression following stimulation

Epithelial cells throughout the intestine constitutively express major histocompatibility complex (MHC) class II (Hershberg *et al.*, 1998) and TLRs (Abreu, 2010). We used flow cytometry in order to confirm the expression of these receptors on the CMT-93 cell line.

CMT-93 cells were plated on a 6-well plate, at $0.25x10^6$ cells/2ml, and left until they were confluent. Media was then discarded, fresh media added and the cells were stimulated with PAM_3CSK_4 (1 μg/ml), LPS (100ng/ml), Flagellin (5μg/ml), CpG (2μM) or medium alone as a control. After 24h cells were collected and stained with fluorescently labelled antibodies against MHC class II, TLR2 and TLR4 and the expression of these markers was measured by flow cytometry.

CMT-93 cells do express MHCII, TLR2 and TLR4, however the expression of these markers was unaffected by stimulation with a range of TLR ligands **[Figure 4.3]**.

4.2.2 Conditioning with epithelial cell supernatants does not have a strong effect on surface marker expression, but modulates the production of TNF-α, MIP-1α and MIP-2

In order to assess the effect of epithelial cell conditioning on macrophages, we started with a short 2h exposure of J774A.1 macrophages to CMT-93 supernatants.

For flow cytometry studies macrophages were cultured for 2h in the unconditioned medium or CMT-93 conditioned medium. After 2 hours cells were stained with fluorescent antibodies against CD80, CD86, CD40, MHC class II, TLR2 and TLR4 and their expression was measured on FACS Aria I flow cytometer. The histograms in **Figure 4.4** show surface expression of each marker comparing macrophages in unconditioned and CMT-93 conditioned media. Conditioning for 2h did not have a strong effect on surface marker expression. There was only a slight down-regulation of MHC class II and TLR4 and no change in the expression of other surface markers we investigated.

Supernatants from the same experiment were used to measure the production of cytokines and chemokines by J774A.1 macrophages. Conditioned macrophages produced significantly higher levels of TNF-α ($p<0.01$) with no change in production of IL-12p40, IL-6, IL-10 and IL-27 **[Figure 4.5]**. Conditioning also resulted in increased production of MIP-1α ($p<0.01$) and a decrease in MIP-2 ($p<0.01$) **[Figure 4.6]**.

4.2.3 CMT-93 conditioning alters the macrophage ability to mount the immune response to LPS

When exposed to stimuli, such as lipopolysaccharide (LPS) from the outer membrane of Gram negative bacteria, macrophages elicit a strong inflammatory response (Adams and Hamilton, 1984). To explore whether the exposure to epithelial cell media has an effect on the ability of macrophages to mount such a response, we pre-conditioned J774A.1 macrophages with CMT-93 conditioned media for 2h before stimulating with LPS (100ng/ml). After 24h supernatants were collected to measure the production of cytokines and chemokines and the cells were stained with fluorescently labelled antibodies to measure the expression of surface markers by flow cytometry.

In **Figure 4.7** we demonstrate that the expression of CD86, CD80, CD40, MHCII, TLR2 and TLR4 surface markers is up-regulated following LPS activation, as expected. However, pre-conditioning of macrophages with epithelial cell media, resulted in a marked down-regulation of CD40, MHCII and TLR4 (dashed histograms). There was also a slight down-regulation of CD80 expression. Additional controls showing histograms of conditioned vs. conditioned LPS-stimulated cells are added in **Appendix F**.

The epithelial cell pre-conditioning also had an effect on the production of cytokines and chemokines by macrophages. LPS up-regulated the production of IL-12p40, TNF-α, IL-6, IL-10 and IL-27 cytokines **[Figure 4.8]** and MIP-1α, MIP-2 and MCP-1 chemokines **[Figure 4.9]** from unconditioned cells, as expected. The conditioned macrophages, however, produced significantly lower amounts of IL-12p40 ($p<0.01$), IL-6 ($p<0.001$), IL-10 ($p<0.001$) and IL-27 ($p<0.01$), when exposed to LPS, but higher amounts of TNF-α ($p<0.001$) **[Figure 4.8]**. The production of MCP-1 was

also significantly down-regulated ($p<0.01$), however conditioning did not have any effect on the production of MIP-1α or MIP-2 **[Figure 4.9]**.

4.2.4 CMT-93 conditioning alters the macrophage ability to mount the immune response to different TLR ligands

We have shown so far that epithelial cell conditioning alters the macrophage response to LPS, which is a TLR4 ligand. The strongest effect was the decrease in CD40, MHCII and TLR4 expression and the decrease in the production of pro-inflammatory cytokines, except TNF-α which was increased **[Figure 4.7 and Figure 4.8]**. We next wanted to investigate whether these effects are restricted solely to TLR4 ligation or if conditioning also affects the macrophage response to other TLR ligands. J774A.1 macrophages were, therefore, exposed to CMT-93 supernatants for 2h before being stimulated with PAM_3CSK_4 (PAM; TLR2 ligand), Flagellin (TLR5 ligand) or CpG (TLR9) ligand. After 24h, expression of surface markers and cytokine production were measured by flow cytometry and ELISA respectively.

As shown in **Figure 4.10** stimulation with PAM, Flagellin and CpG up-regulated the expression of CD40, CD80 and MHCII on unconditioned cells, as expected. This up-regulation was suppressed on conditioned macrophages (dashed histograms), similar to the effects observed on conditioned LPS-stimulated macrophages **[Figure 4.7]**.

The effects of conditioning on cytokine production were also similar to that observed from conditioned LPS-stimulated macrophages. Pre-conditioning with epithelial cell media significantly down-regulated the production of IL-12p40 ($p<0.001$) in response to PAM, Flagellin and Cpg and IL-6 ($p<0.001$) in response to PAM and

CpG. Pre-conditioning also significantly up-regulated the production of TNF-α ($p<0.001$) in response to PAM, Flagellin and CpG **[Figure 4.11]**.

4.2.5 Longer conditioning has a more potent effect on macrophage phenotype

In order to investigate whether the length of time of conditioning further affects macrophage phenotype, we cultured J774A.1 macrophages with CMT-93 supernatants for 2h, 6h and 24h. While 2h conditioning did not have a strong effect on the expression of CD80, CD40, MHCII and TLR4, these surface markers were markedly down-regulated following 24h conditioning **[Figure 4.12]**. Down-regulation of CD40 was observed as early as the 6h time point. The longer conditioning time did not change the expression of CD86 and TLR2 **[Figure 4.12]**.

2h conditioning up-regulated the production of TNF-α and this effect was maintained after 6h and 24h conditioning ($p<0.001$) **[Figure 4.13]**. After 24h, conditioned macrophages showed reduced secretion of IL-12p40 ($p<0.01$), IL-6 ($p<0.05$) and IL-27 ($p<0.05$), while the secretion of IL-10 was unaffected **[Figure 4.13]**.

The effect of conditioning on chemokine secretion was the same after 2h and 24h, with conditioned macrophages secreting more MIP-1α ($p<0.01$) and less MIP-2 ($p<0.01$) **[Figure 4.14]**.

4.2.6 Longer conditioning affects macrophage response to stimuli

Since the longer conditioning time resulted in a more potent effect on macrophage phenotype in a steady state, we next examined its effect on the macrophage response

to LPS. The LPS-induced expression of MHCII and TLR4 was decreased even after 2h pre-conditioning and this was maintained after 24h. The LPS-induced increase of CD80 was decreased at 2h and more pronounced after 6h and 24h pre-conditioning. The LPS-induced CD40, however, was down-regulated after 2h pre-conditioning, but at the 6h and 24h time point it expression was similar to that of unconditioned cells **[Figure 4.15]**. Longer pre-conditioning did not affect the expression of CD86 and TLR2 in response to LPS. Furthermore, a longer pre-conditioning time did not have a stronger effect on cytokine and chemokine production and profiles remained the same after 2h, 6h or 24h pre-conditioning, except for the production of IL-27 and MCP-1 **[Figure 4.16 and 4.17]**. IL-27 production, in response to LPS, was the same as that of unconditioned cells after 24h pre-conditioning **[Figure 4.16]**. On the other hand, cells that were pre-conditioned for 24h secreted more MCP-1 in response to LPS ($p<0.05$) **[Figure 4.17]**.

4.2.7 Conditioned macrophages display enhanced phagocytic activity

Phagocytosis and clearance of pathogens is a hallmark of macrophage function and while colonic macrophages are hypo-responsive, they maintain a strong phagocytic capacity (Smythies *et al.*, 2005). Therefore we investigated the effect of CMT-93 conditioning on macrophages' ability to phagocytose.

J774A.1 macrophages were cultured in the presence of conditioned or unconditioned media for 24h before we assessed their ability to phagocytose. When the phagocytosis was measured in response to stimuli, LPS was added for 24h following 24h pre-conditioning. To measure phagocytosis fluorescent latex beads were added to the culture and macrophages were left to phagocytose for 2h. Cells were then

washed and the uptake of beads was measured by flow cytometry. Cells that took up the beads showed green fluorescence which can be measured in the FITC channel of the flow cytometer and expressed as a percentage of phagocytosing cells. Conditioned macrophages show higher uptake rate than unconditioned macrophages, both in a steady state (49.2% phagocytes vs. 65.6% phagocytes after 2h conditioning, 49.2% vs. 61.5% after 6h conditioning and 49.2% vs. 59.5% after 24h conditioning) **[Figure 4.18A]** and in a response to LPS stimulation (58.8% phagocytes vs. 78.9% phagocytes after 2h pre-conditioning, 58.8% vs. 78.5% after 6h pre-conditioning and 58.8% vs. 80.1% after 24h pre-conditioning **[Figure 4.18B]**. The rate of phagocytosis did not depend on the time of conditioning.

4.2.8 Conditioned macrophages produce lower amounts of nitrite and reactive oxygen species

Classically activated macrophages produce large quantities of inflammatory mediators such as nitric oxide (NO) and reactive oxygen species (ROS) in response to bacterial endotoxins. However, colonic macrophages do not generate a significant respiratory burst and nitric oxide production under the same conditions (Ikeda *et al.*, 1997, Mahida *et al.*, 1989b). Therefore we measured the levels of NO and ROS on conditioned macrophages to investigate whether epithelial cell soluble factor also affect these parameters.

To measure the NO levels, J774A.1 macrophages were cultured with conditioned or unconditioned media for 24h before being stimulated with LPS for another 24h. NO levels were then detected in the supernatants by measuring the production of nitrite (NO_2^-) which is a stable breakdown product of NO. Levels of nitrite from

unstimulated macrophages were undetectable, but following stimulation with LPS, macrophages produced high amounts of nitrite, as expected **[Figure 4.19]**. Conditioned macrophages produced significantly lower levels of nitrite in response to LPS, both after 6h ($p<0.01$) and 24h pre-conditioning ($p<0.05$) **[Figure 4.19]**.

ROS levels were measured using the cell permeant reagent 2',7' – dichlorofluorescein diacetate (DCFDA), a fluorogenic dye that measures hydroxyl, peroxyl and other ROS activity within the cell. J774A.1 macrophages were conditioned as previously described and the fluorescent signal relative to intracellular ROS generation was then measured by flow cytometry and compared between unconditioned (black histograms) and conditioned cells (dashed histograms). Conditioning for 2h, 6h and 24h decreased the basal levels of ROS in unstimulated macrophages **[Figure 4.20A]**. The levels of ROS were also down-regulated in conditioned macrophages in response to LPS **[Figure 4.20B]**, however, while 6h conditioning was enough to decrease the ROS production from unstimulated macrophages, 24h pre-conditioning was necessary to detect the decrease of ROS in LPS-stimulated conditioned macrophages **[Figure 4.20B]**.

4.2.9 CMT-93 conditioning does not affect macrophage viability

In order to show that conditioning with CMT-93 cell supernatants is not affecting macrophage viability and consequently their response to stimuli, J774A.1 macrophages were incubated with either unconditioned media or CMT-93 conditioned media for 24h. After 24h cells were stained with PI viability stain and the percentage of viable cells was determined by flow cytometry. Macrophages

conditioned with CMT-93 media showed the same viability as unconditioned macrophages **[Figure 4.21A]**.

Cell viability was also determined by the MTS assay that measures the bioreduction of MTS tetrazolium compound into a coloured formazan product. This reduction will happen only in the metabolically active cells and the quantity of formazan is directly proportional to the number of living cells in the culture. As shown in **Figure 4.21B**, conditioned macrophages did not exhibit reduced viability when compared to unconditioned macrophages.

4.2.10 Conditioned macrophages do not exhibit increased caspase activity in response to TNF-α

So far we have shown that macrophages conditioned with colonic epithelial cells media exhibit an anti-inflammatory phenotype. However, these macrophages produced significantly higher amounts of TNF-α than unconditioned controls, both in a steady state and in a response to TLR ligation **[Figure 4.11, 4.13, 4.16]**. The treatment of cells with TNF-α can lead to activation of caspase cascade involving caspase-8 and caspase-3, which can then induce apoptosis (Bradley, 2008) . To determine whether TNF-α has a same effect on conditioned and unconditioned cells, we incubated these cells with recombinant TNF-α (10ng/ml) for 24h and measured the activity of caspase-3. Caspase-3 activity was measured using the CellEvent Caspase-3/7 Green Detection reagent (Invitrogen) as described in Materials and methods section 2.10. The percentage of cells positive for active caspase-3/7 was determined by flow cytometry and expressed relative to control (unstimulated cells). Incubation of unconditioned cells with TNF-α led to an increased caspase-3/7

activity, as expected ($p<0.05$) **[Figure 4.22]**. Conditioning of cells protected against this with the activity of caspase-3/7 in conditioned cells similar to the control cells **[Figure 4.22]**.

4.2.11 Conditioned macrophages show higher expression of TNFR2

The activities of TNF-α are mediated by two receptors, TNFR1 (p55) and TNFR2 (p75) (Peschon *et al.*, 1998). While signalling through TNFR1 usually activates pro-inflammatory and apoptotic pathways, TNFR2 signalling is associated with more anti-inflammatory and immunoprotective effects of TNF-α (Bradley, 2008). Considering that TNF-α stimulation did not induce caspase-3 activation in conditioned cells, we wanted to investigate and compare the expression of TNF receptors on unconditioned and conditioned macrophages.

J774A.1 macrophages were incubated with either unconditioned media or CMT-93 conditioned media for 24h. After 24h macrophages were labelled with fluorescent antibodies against TNFR1 and TNFR2 and their expression was investigated by flow cytometry. Macrophages conditioned with CMT-93 cell media showed higher expression of TNFR2, but not TNFR1 (dashed histograms), compared to unconditioned control (black histograms) **[Figure 4.23]**.

4.3 FIGURES

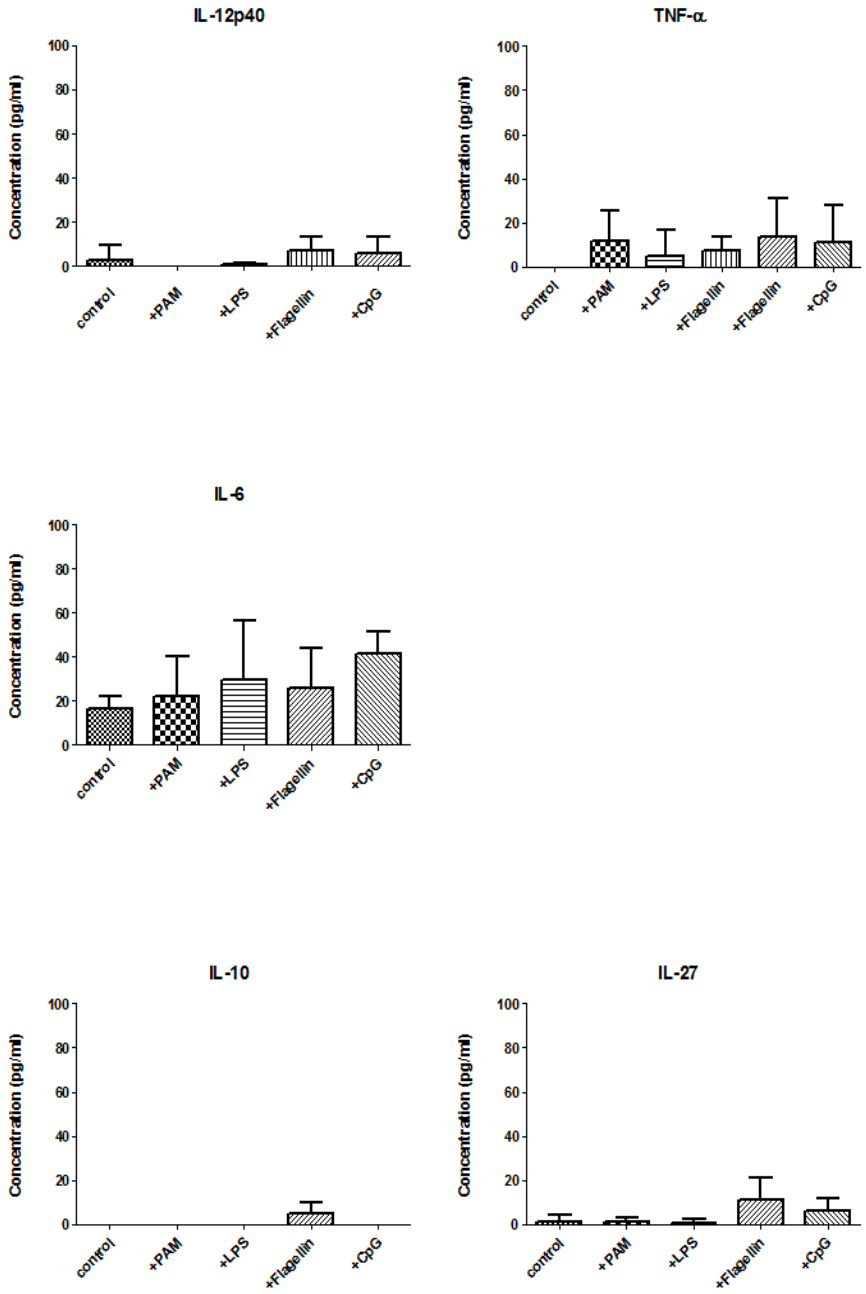

Figure 4.1 Cytokine production from CMT-93 cells in response to stimulation with different TLR ligands CMT-93 cells were stimulated with PAM_3CSK_4 (1 µg/ml), LPS (100ng/ml), Flagellin (5µg/ml), CpG (2µM) or medium alone as a control. After 24h supernatants were collected and cytokine secretion was measured by ELISA (R&D) according to manufacturer's instruction. Data are representative of three independent experiments. Statistical significance for multiple comparisons was determined by one-way ANOVA followed by Newman-Keuls analysis.

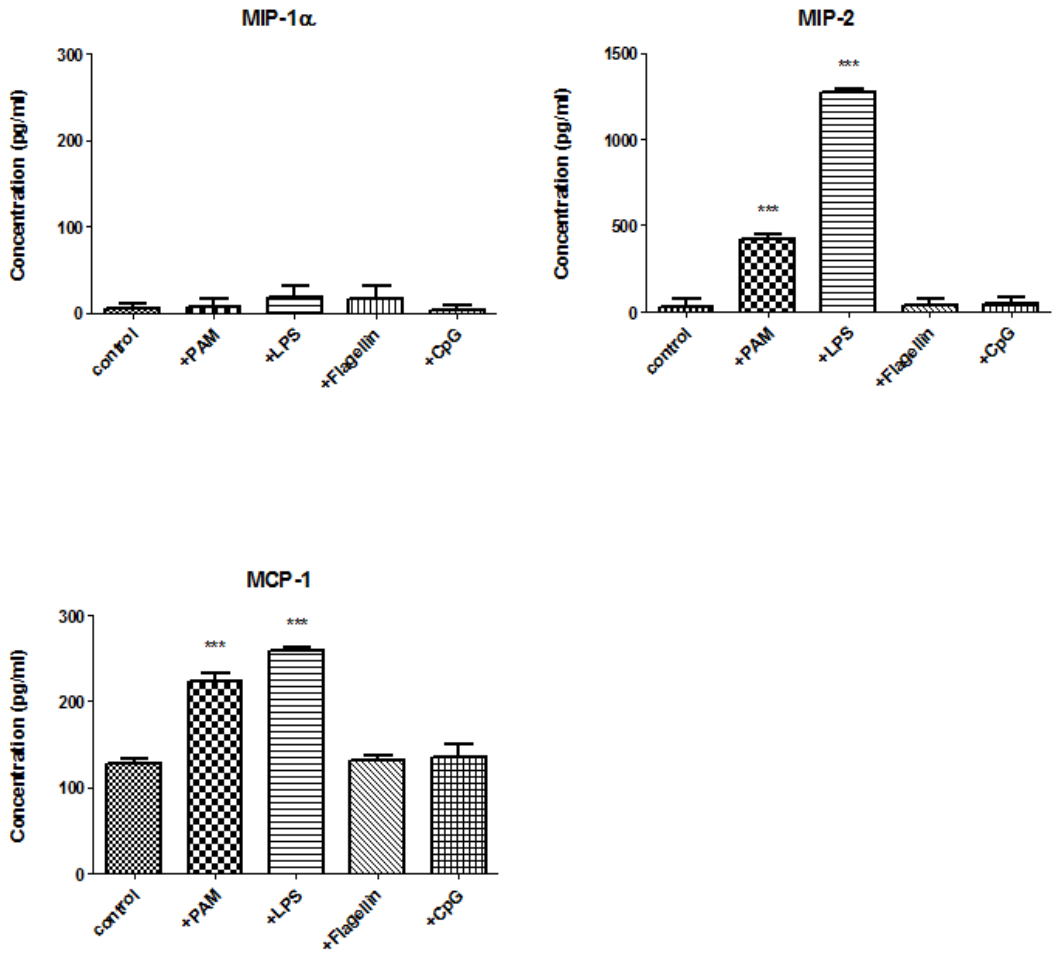

Figure 4.2 Chemokine production from CMT-93 cells in response to stimulation with different TLR ligands CMT-93 cells were stimulated with PAM_3CSK_4 (1 µg/ml), LPS (100ng/ml), Flagellin (5µg/ml), CpG (2µM) or medium alone as a control. After 24h supernatants were collected and chemokine secretion was measured by ELISA (R&D) according to manufacturer's instruction. Data are presented as mean ± SEM of three replicates and are representative of three independent experiments. Statistical significance for multiple comparisons was determined by one-way ANOVA followed by Newman-Keuls analysis. ***P<0.001 vs. control

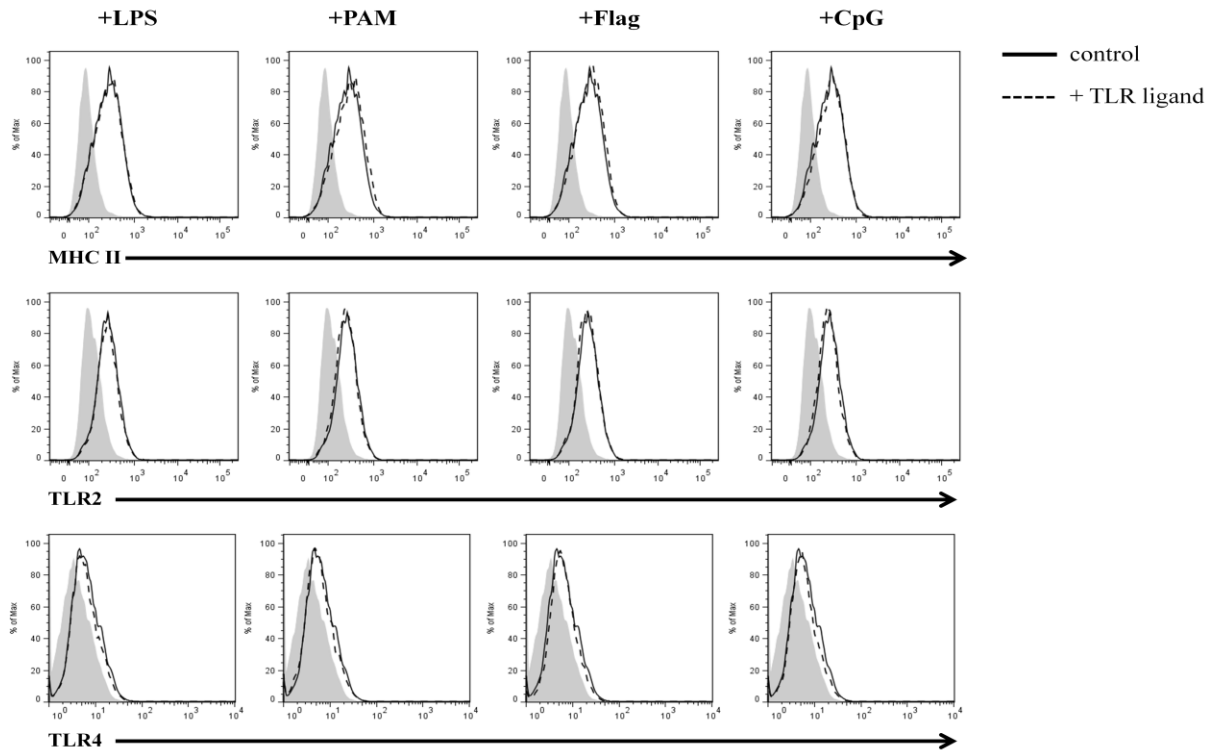

Figure 4.3 Expression of surface markers on CMT-93 cells in response to stimulation with different TLR ligands CMT-93 cells were stimulated with PAM3CSK4 (1µg/ml), LPS (100ng/ml), Flagellin (5µg/ml), CpG (2µM) or medium alone as a control. After 24h cells were stained with fluorescently labelled antibodies and the expression of surface markers was measured by flow cytometry. Histograms show surface marker expression of unstimulated control cells (black line) compared to TLR-ligand stimulated cells (dashed line). Filled histograms represent fluorescence of unstained cells. Data are representative of three independent experiments.

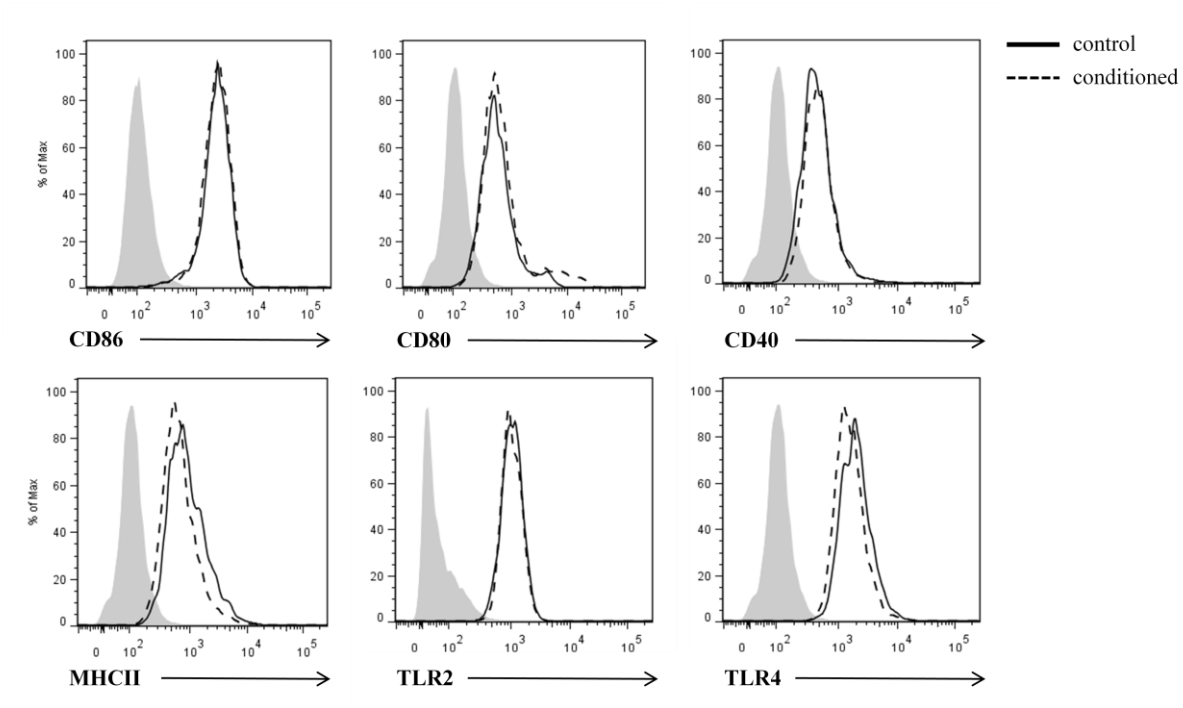

Figure 4.4 Expression of surface markers on CMT-93 conditioned macrophages. J774A.1 macrophages were incubated with unconditioned medium or CMT-93 conditioned medium for 2h. After 2h conditioning cells were stained with fluorescently labelled antibodies for CD86, CD80, CD40, MHCII, TLR2 and TLR4 and expression was measured by flow cytometry. Histograms show surface marker expression of conditioned cells (dashed line) compared to unconditioned control cells (black line). Filled histograms represent fluorescence of unstained cells. Data are representative of three independent experiments.

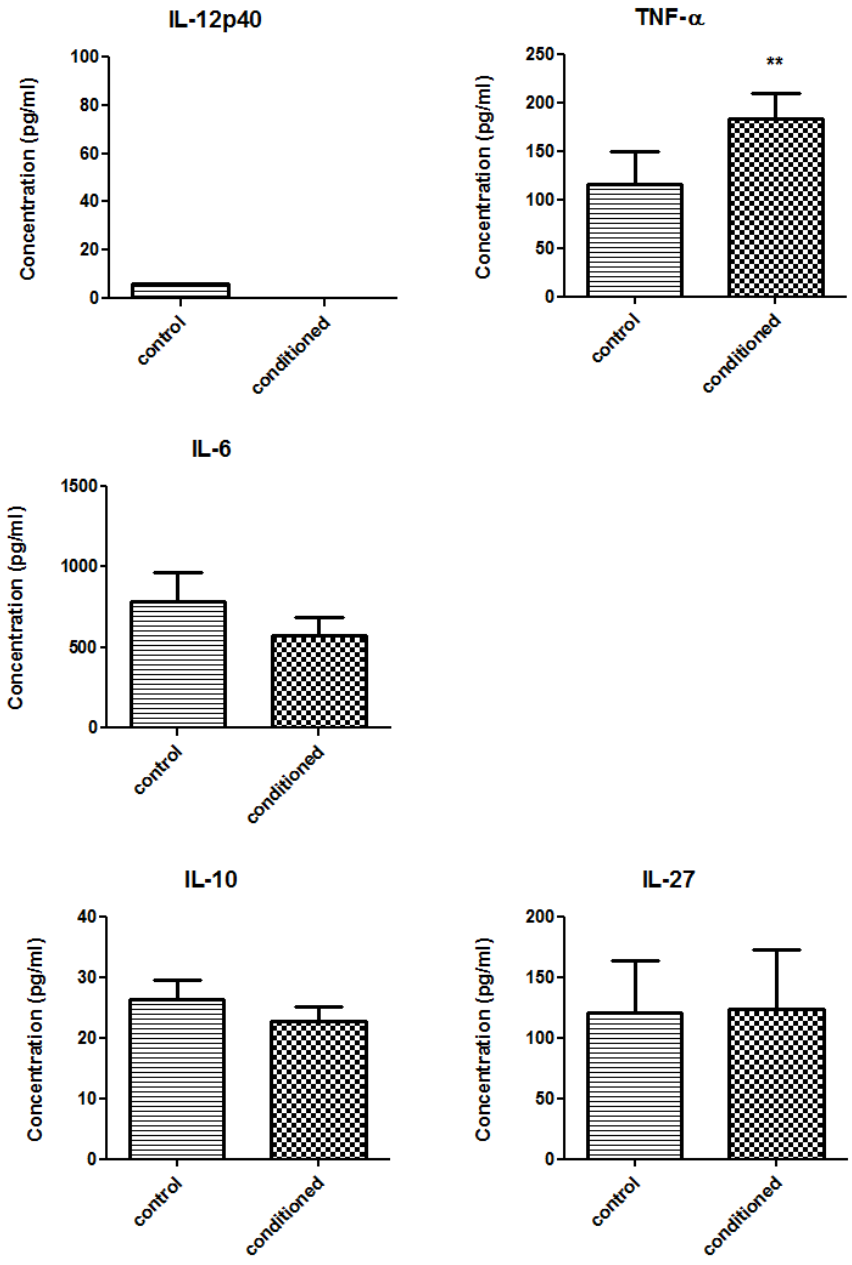

Figure 4.5 Cytokine secretion from CMT-93-conditioned macrophages. J774A.1 macrophages were incubated with unconditioned medium or CMT-93 conditioned medium for 2h. After 2h supernatants were collected and cytokine secretion was measured by ELISA (R&D) according to manufacturer's instruction. Data are presented as mean ± SEM of three replicates and are representative of three independent experiments. **P<0.01 vs. control, by unpaired *t*-test.

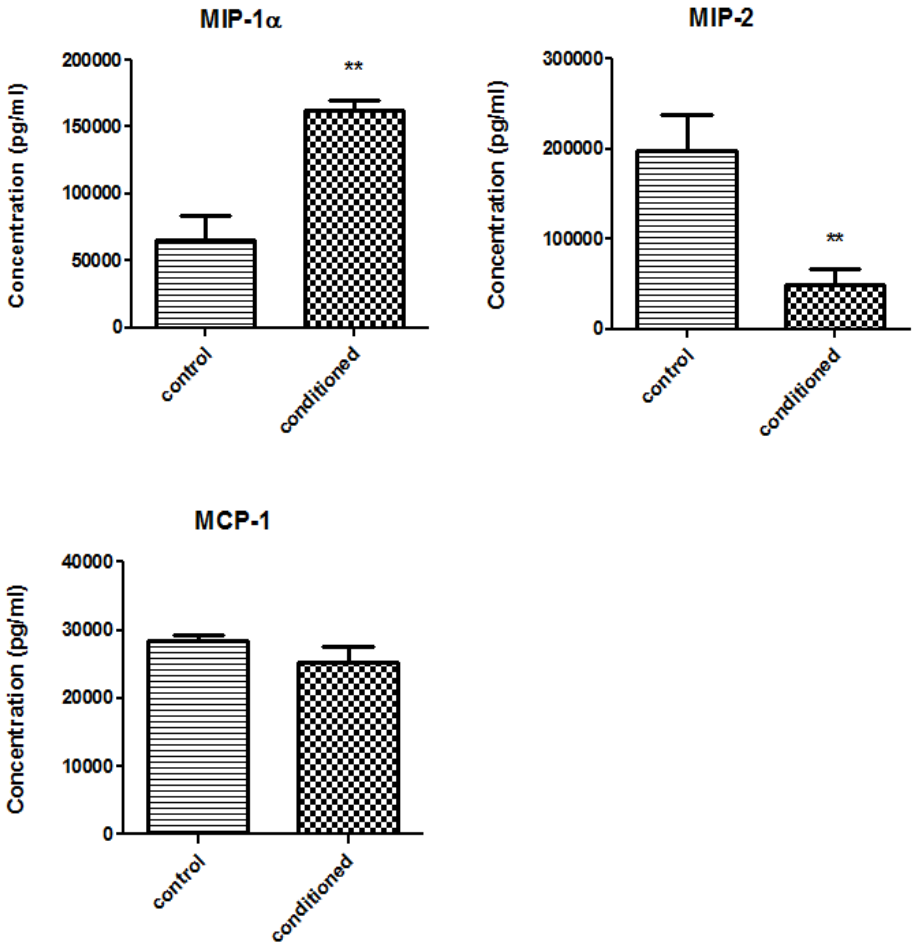

Figure 4.6 Chemokine secretion from CMT-93-conditioned macrophages. J774A.1 macrophages were incubated with unconditioned medium or CMT-93 conditioned medium for 2h. After 2h supernatants were collected and chemokine secretion was measured by ELISA (R&D) according to manufacturer's instruction. Data are presented as mean ± SEM of three replicates and are representative of three independent experiments. **P<0.01 vs. control, by unpaired *t*-test.

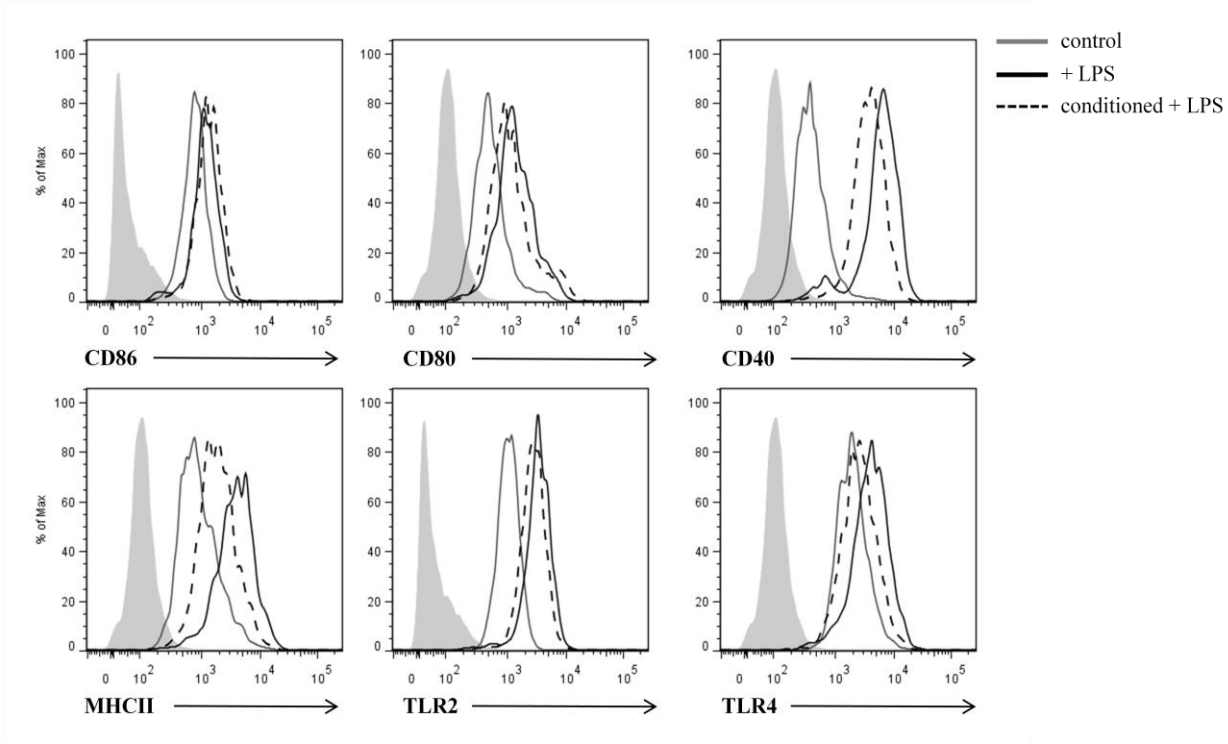

Figure 4.7 Expression of surface markers on CMT-93-conditioned macrophages following TLR4 ligation. J774A.1 macrophages were incubated with unconditioned medium or CMT-93 conditioned medium for 2h before adding LPS (100ng/ml). After 24h cells were stained with fluorescently labelled antibodies for CD86, CD80, CD40, MHCII, TLR2 and TLR4 and the expression was measured by flow cytometry. Histograms show the expression of a particular surface marker on unconditioned LPS-stimulated cells (black line) compared to conditioned LPS-stimulated cells (dashed line). Unconditioned, unstimulated cells were used as a control (gray line) and filled histograms represent fluorescence of unstained cells. Data are representative of three independent experiments.

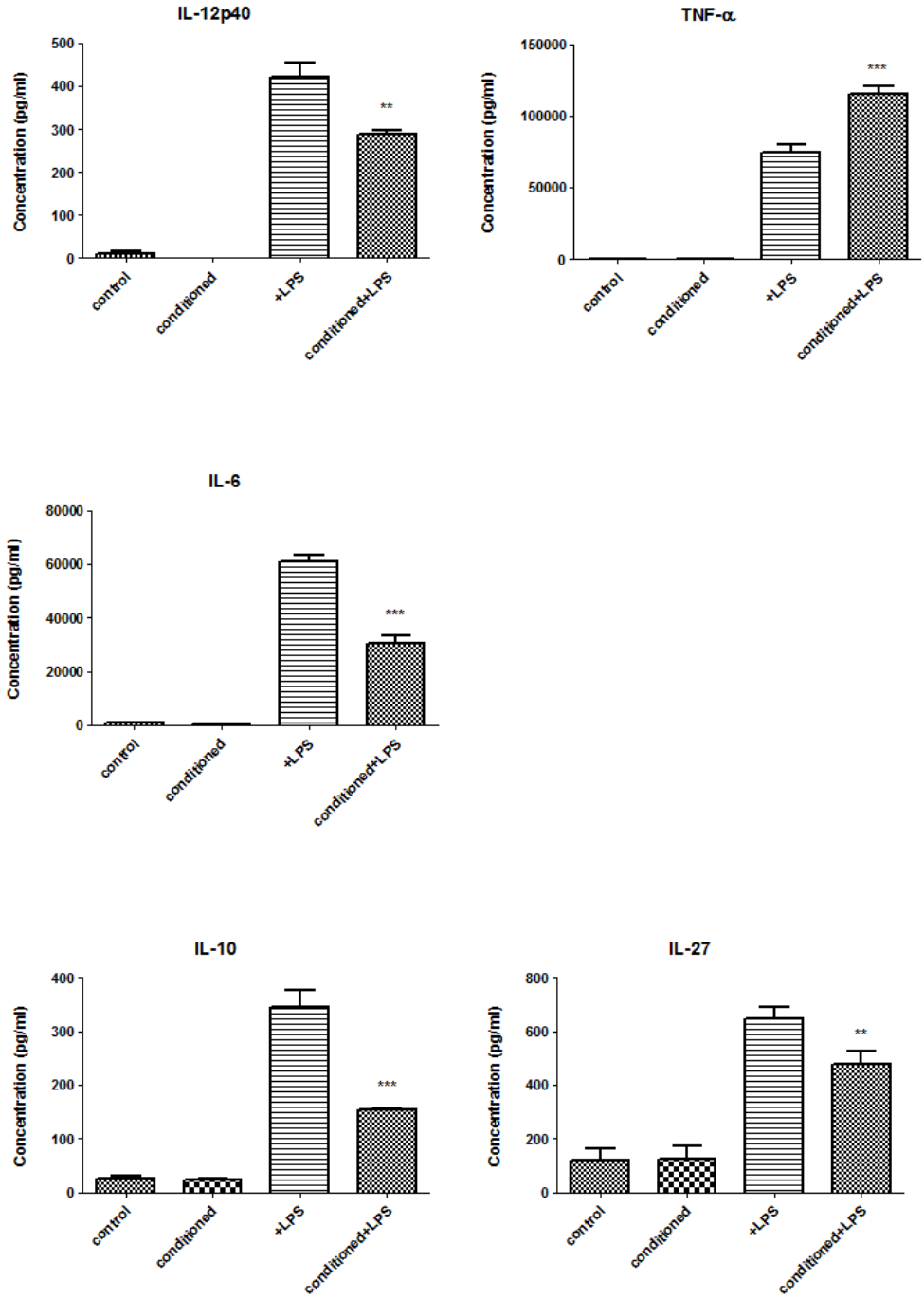

Figure 4.8 Cytokine secretion from CMT-93-conditioned macrophages following TLR4 ligation. J774A.1 macrophages were incubated with unconditioned medium or CMT-93 conditioned medium for 2h before adding LPS (100ng/ml). Unconditioned and conditioned, unstimulated cells were used as a control. After 24h supernatants were collected and cytokine secretion was measured by ELISA (R&D) according to manufacturer's instruction. Data are presented as mean ± SEM of three replicates and are representative of three independent experiments. Statistical significance for multiple comparisons was determined by one-way ANOVA followed by Newman-Keuls analysis. ***P<0.001, **P<0.01 vs. unconditioned+LPS

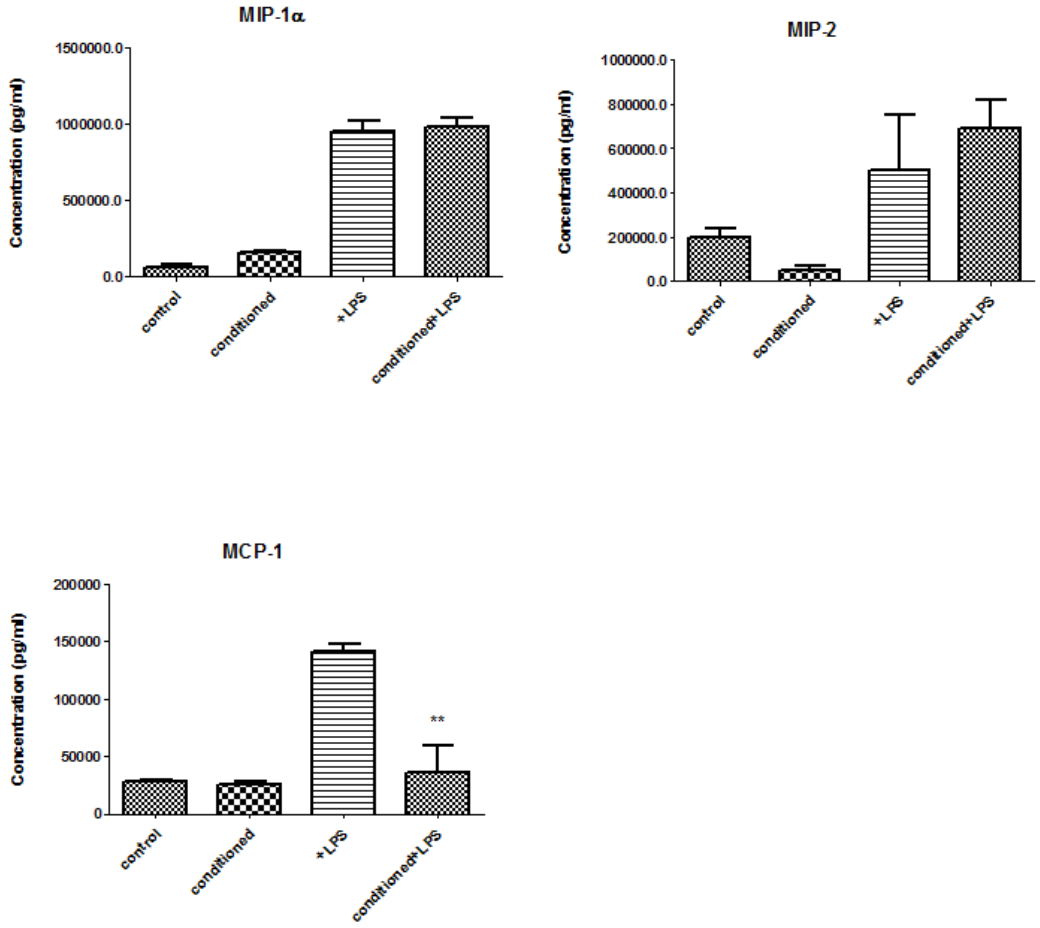

Figure 4.9 Chemokine secretion from CMT-93-conditioned macrophages following TLR4 ligation. J774A.1 macrophages were incubated with unconditioned medium or CMT-93 conditioned medium for 2h before adding LPS (100ng/ml). Unconditioned, unstimulated cells were used as a control. After 24h supernatants were collected and chemokine secretion was measured by ELISA (R&D) according to manufacturer's instruction. Data are presented as mean ± SEM of three replicates and are representative of three independent experiments. Statistical significance for multiple comparisons was determined by one-way ANOVA followed by Newman-Keuls analysis. **P<0.01 vs. unconditioned+LPS

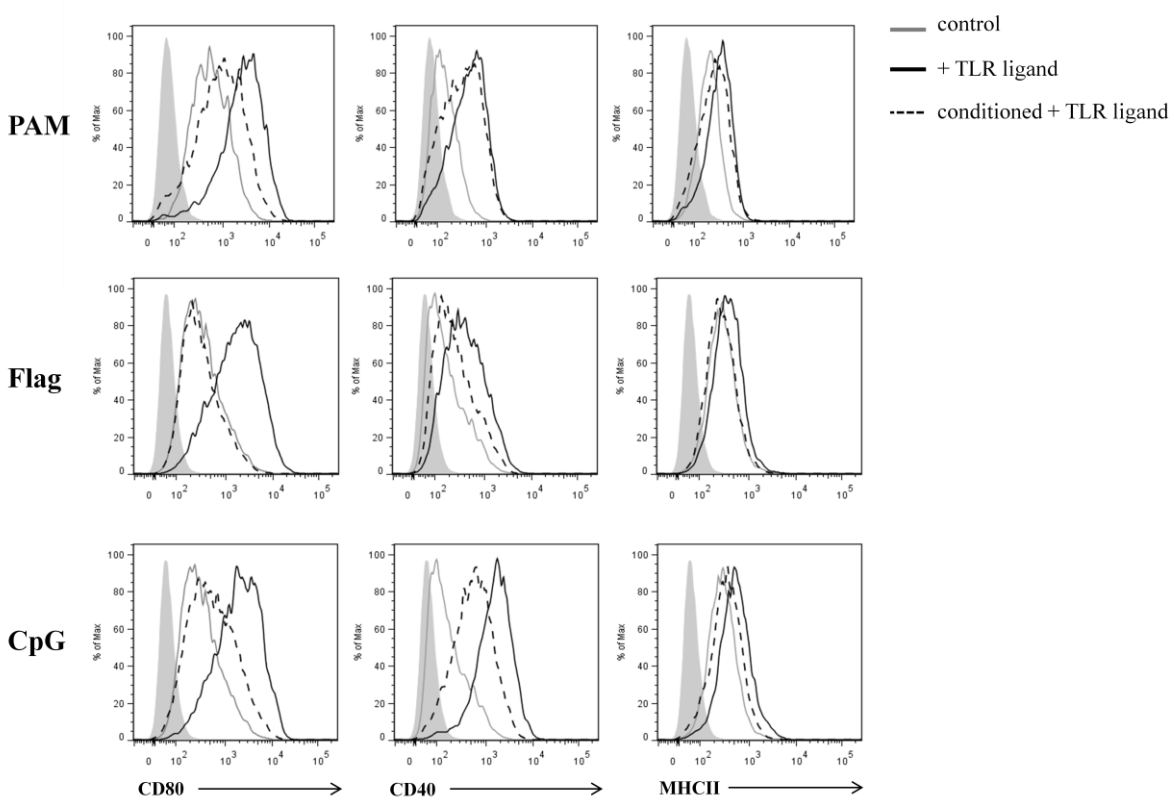

Figure 4.10 CMT-93 conditioning impairs up-regulation of surface markers on macrophages in response to different TLR ligands J774A.1 macrophages were incubated with unconditioned medium or CMT-93 conditioned medium for 2h before adding PAM_3CSK_4 (1µg/ml), Flagellin (5µg/ml) or CpG (2µM) for 24h. Cells were then stained with fluorescently labelled antibodies for CD80, CD40 and MHCII and the expression was measured by flow cytometry. Histograms show the expression of surface marker on unconditioned cells stimulated with the appropriate TLR ligand (black line) compared to conditioned TLR ligand-stimulated cells (dashed line). Unconditioned, unstimulated cells were used as a control (gray line) and filled histograms represent fluorescence of unstained cells. Data are representative of three independent experiments.

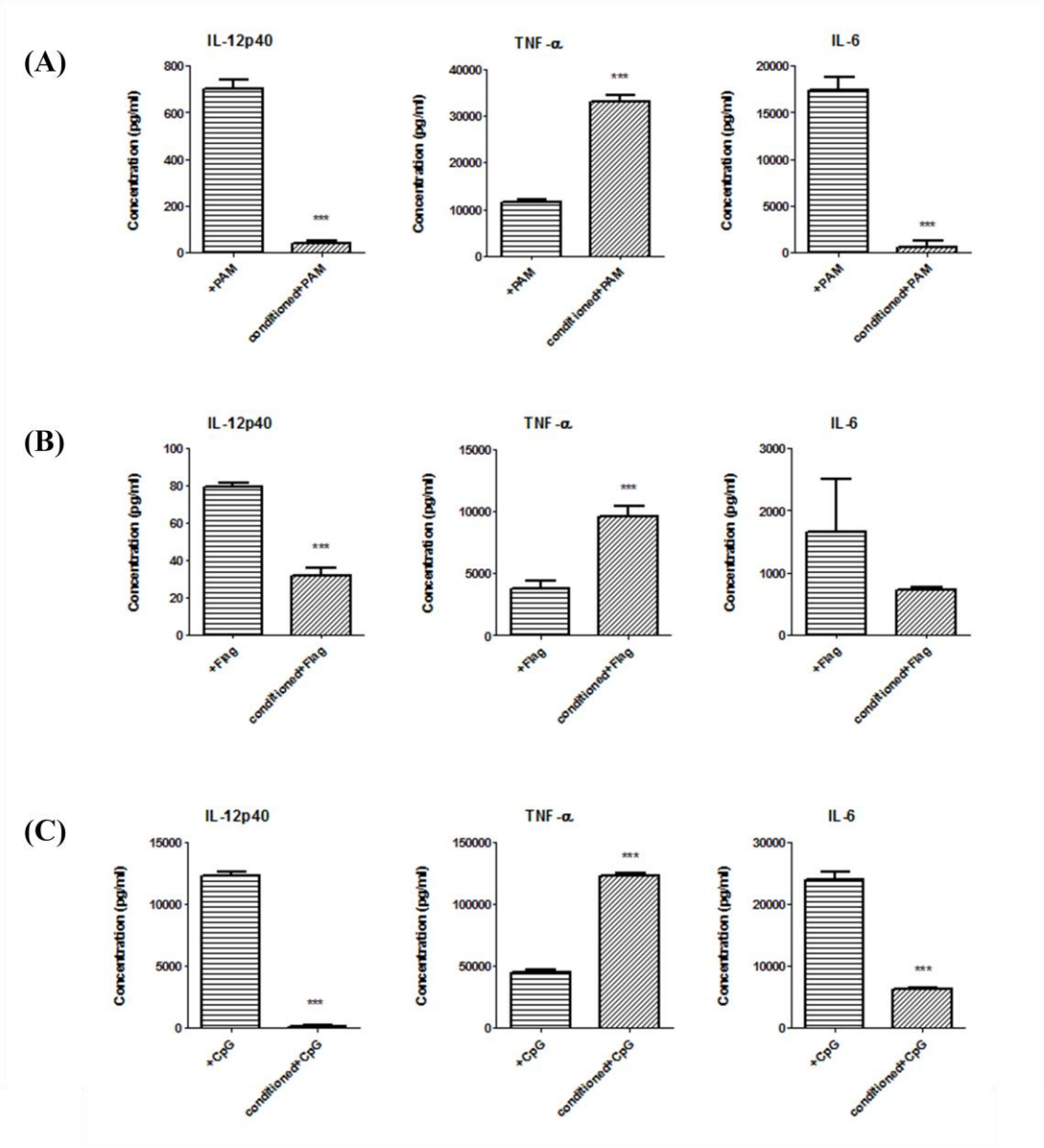

Figure 4.11 CMT-93 conditioned macrophages have similar cytokine profile following ligation with different TLR ligands J774A.1 macrophages were incubated with unconditioned medium or CMT-93 conditioned medium for 2h before adding PAM_3CSK_4 (1µg/ml) **(A)**, Flagellin (5µg/ml) **(B)** or CpG (2µM) **(C)** for 24h. 24h supernatants were collected and cytokine secretion was measured by ELISA (R&D) according to manufacturer's instruction. Data are presented as mean ± SEM of three replicates and are representative of three independent experiments. Statistical significance was determined by unpaired *t*-test. ***P<0.001 vs. unconditioned TLR ligand-stimulated cells.

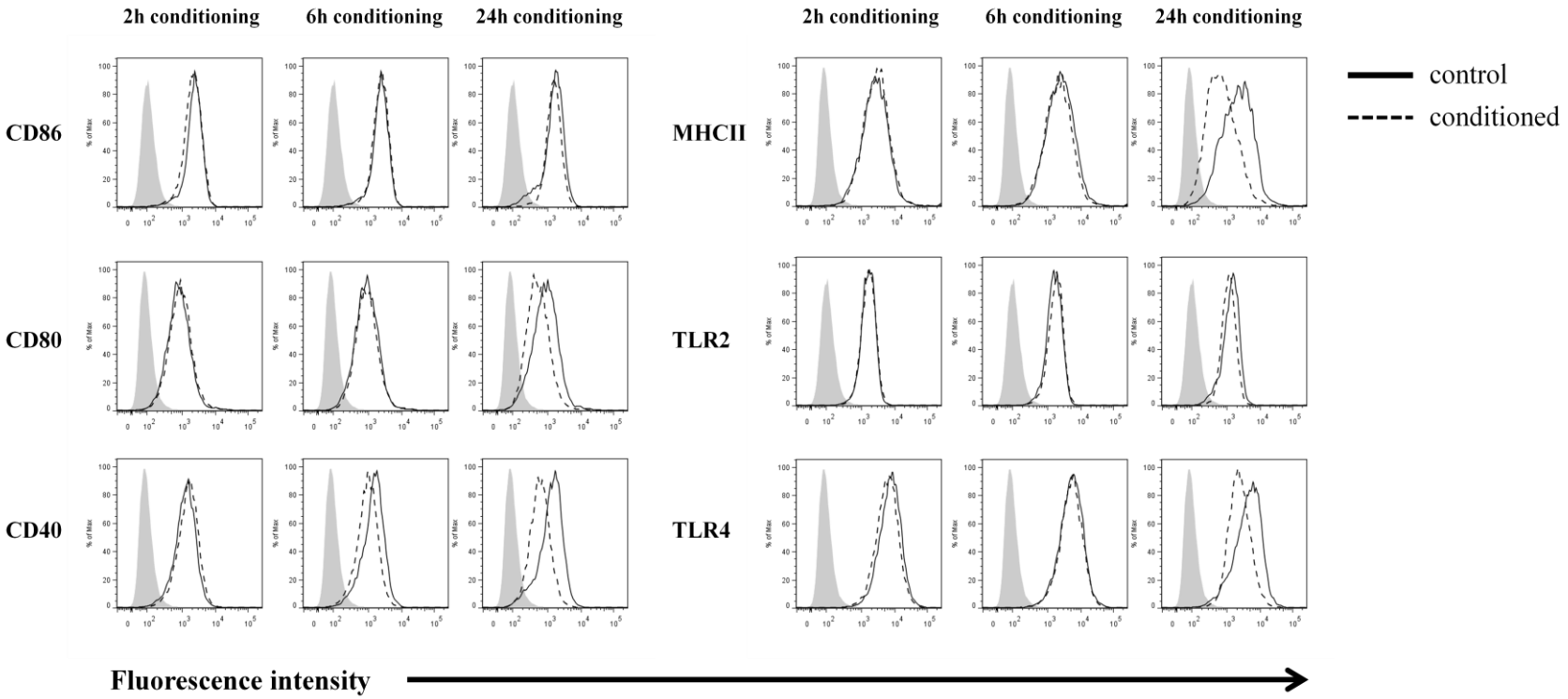

Figure 4.12 Effects of longer conditioning on macrophage phenotype. J774A.1 macrophages were incubated for 2h, 6h or 24h with unconditioned media as a control or CMT-93 supernatants (conditioned) and analysed for the expression of surface markers by flow cytometry. Histograms show surface marker expression on unconditioned cells (black line) and conditioned cells (dashed line). Filled histograms represent fluorescence of unstained cells. Data are representative of three independent experiments.

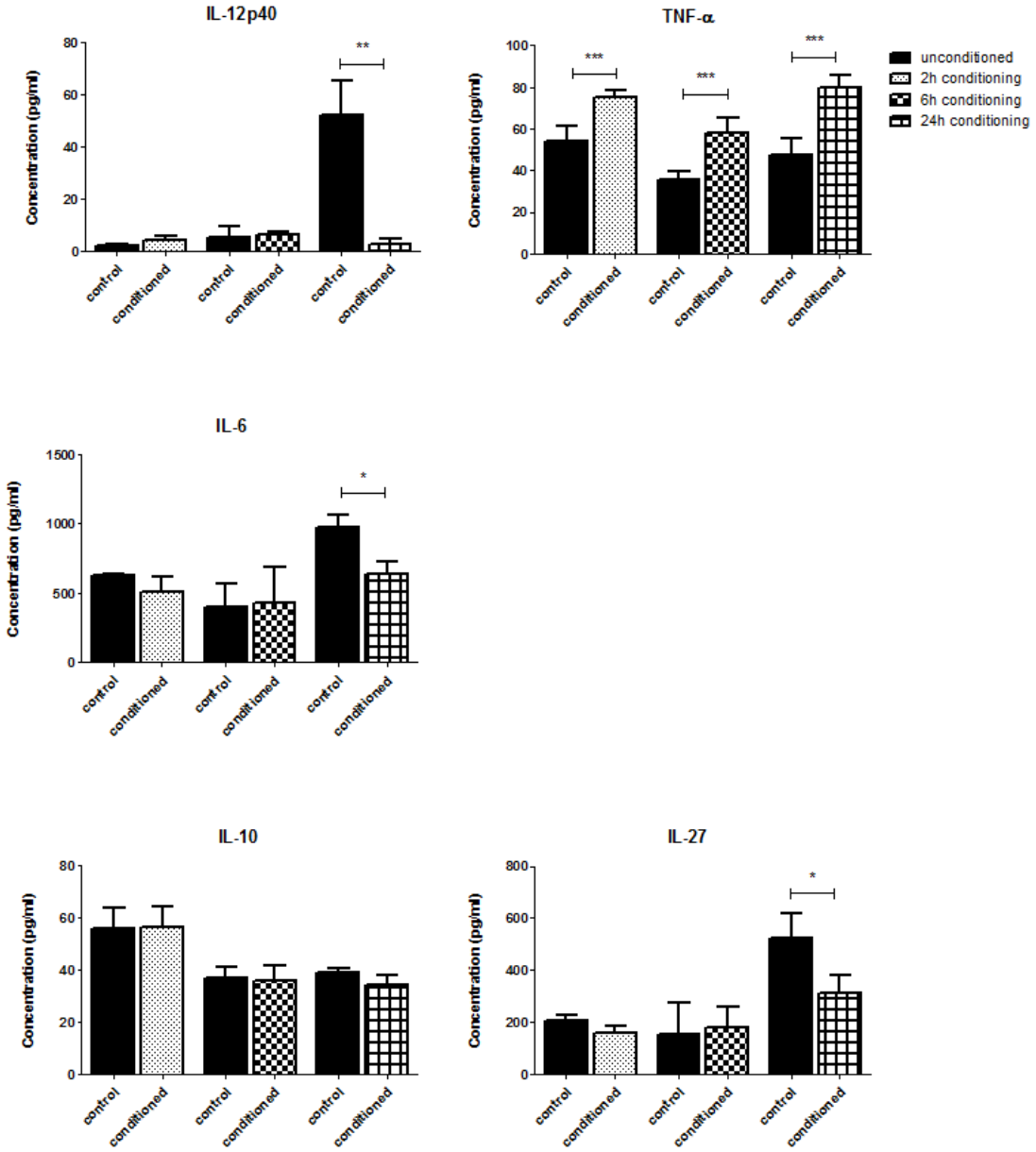

Figure 4.13 Effects of longer conditioning on cytokine production J774A.1 macrophages were incubated with unconditioned medium or CMT-93 conditioned medium for 2h, 6h or 24h. At the end of each time point supernatants were collected and cytokine secretion was measured by ELISA (R&D) according to manufacturer's instruction. Data are presented as mean ± SEM of three replicates and are representative of three independent experiments. *P<0.05, **P<0.01, ***P<0.001control vs. conditioned, determined by unpaired *t*-test.

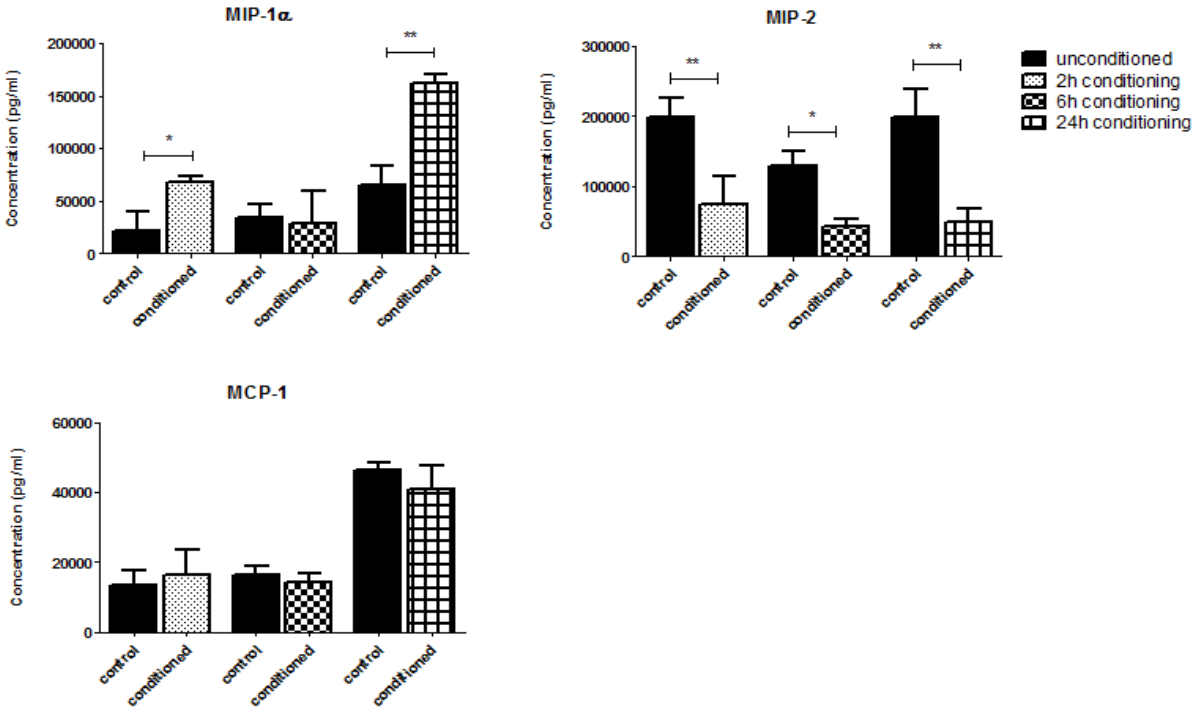

Figure 4.14 Effects of longer conditioning on chemokine production J774A.1 macrophages were incubated with unconditioned medium or CMT-93 conditioned medium for 2h, 6h or 24h. At the end of each time point supernatants were collected and chemokine production was measured by ELISA (R&D) according to manufacturer's instruction. Data are presented as mean ± SEM of three replicates and are representative of three independent experiments. *P<0.05, **P<0.01 control vs. conditioned, determined by unpaired *t*-test.

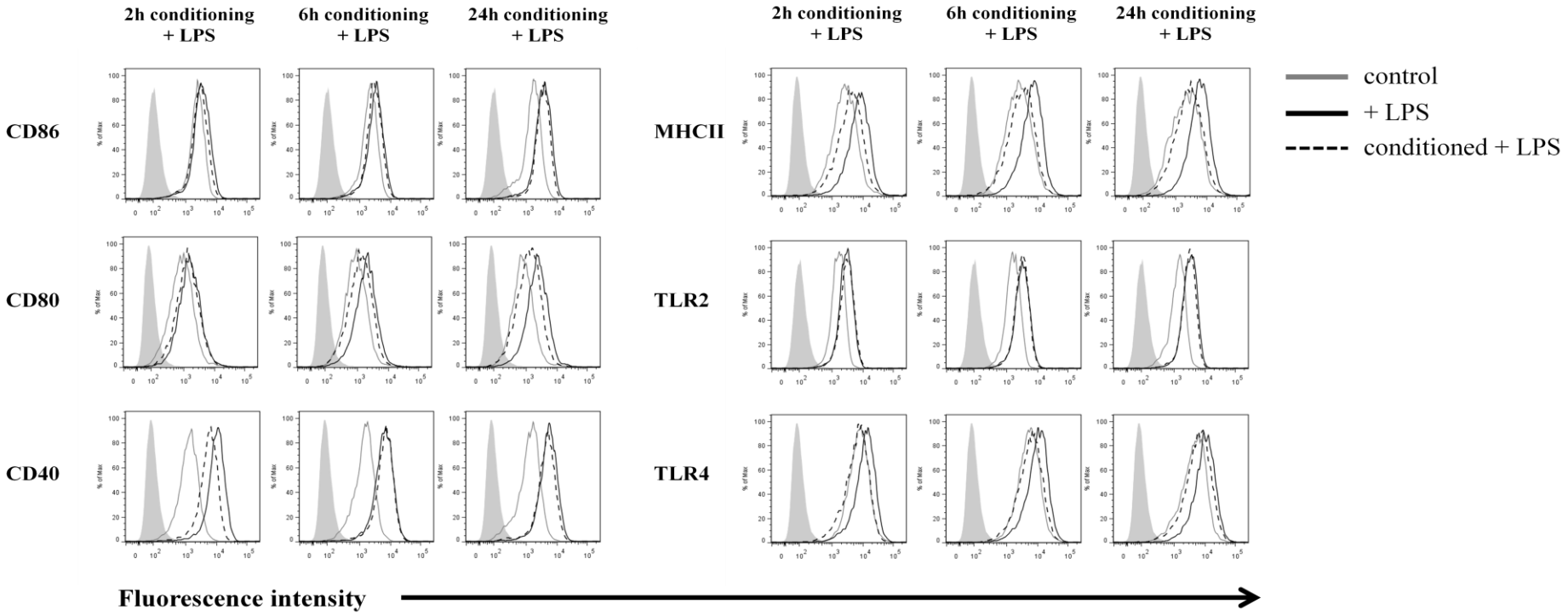

Figure 4.15 Effects of longer conditioning on macrophage response to stimuli J774A.1 macrophages were incubated for 2h, 6h or 24h with unconditioned media or CMT-93 supernatants before being stimulated with LPS (100ng/ml) for 24h. Expression of surface markers was analysed by flow cytometry. Histograms show surface marker expression on unconditioned cells (black line) compared to conditioned cells (dashed line) following LPS stimulation. Grey line represents the expression on unstimulated controls. Filled histograms represent fluorescence of unstained cells. Data are representative of three independent experiments.

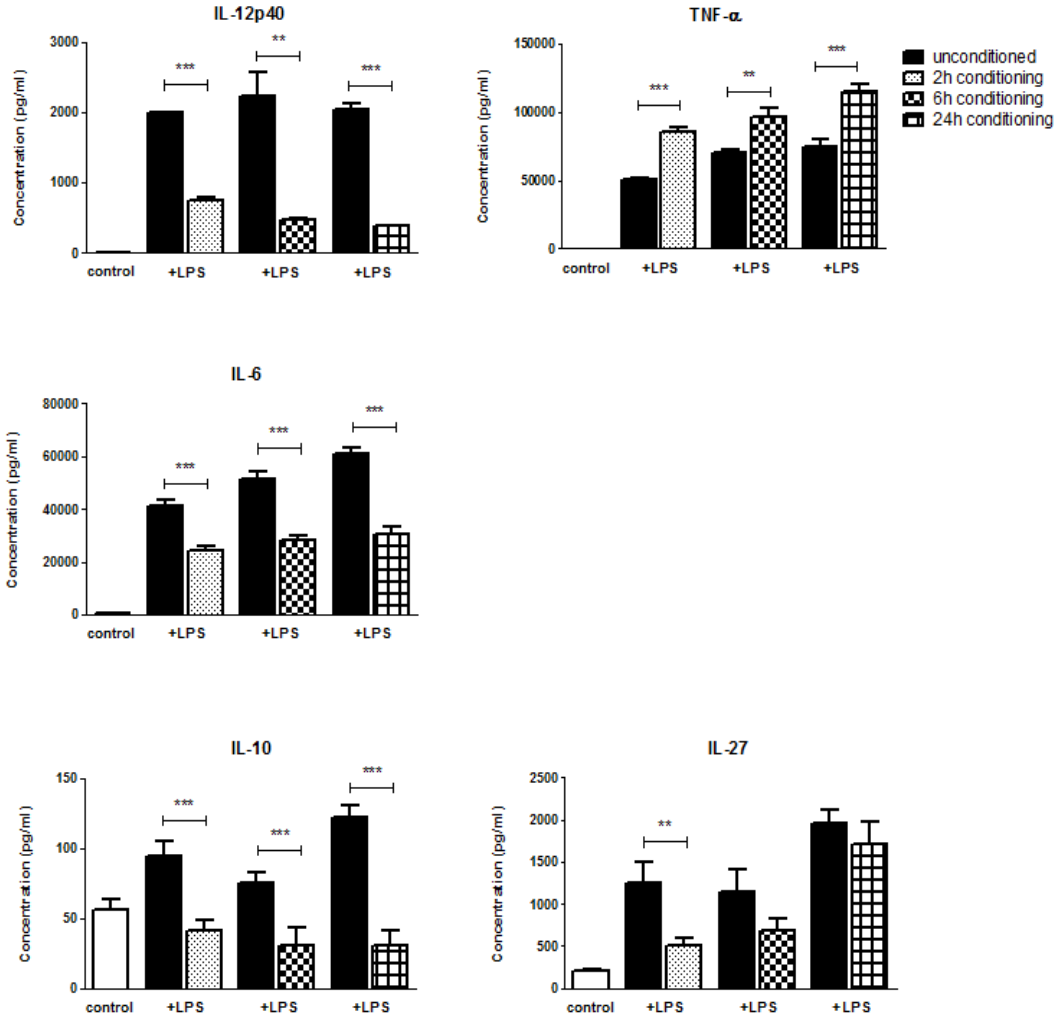

Figure 4.16 Effects of longer conditioning on cytokine production following TLR4 ligation J774A.1 macrophages were incubated for 2h, 6h or 24h with unconditioned media or CMT-93 supernatants before being stimulated with LPS (100ng/ml) for 24h. Supernatants were then collected and cytokine production was measured by ELISA (R&D) according to manufacturer's instruction. Data are presented as mean ± SEM of three replicates and are representative of three independent experiments. **P<0.01, ***P<0.001 determined by unpaired *t*-test.

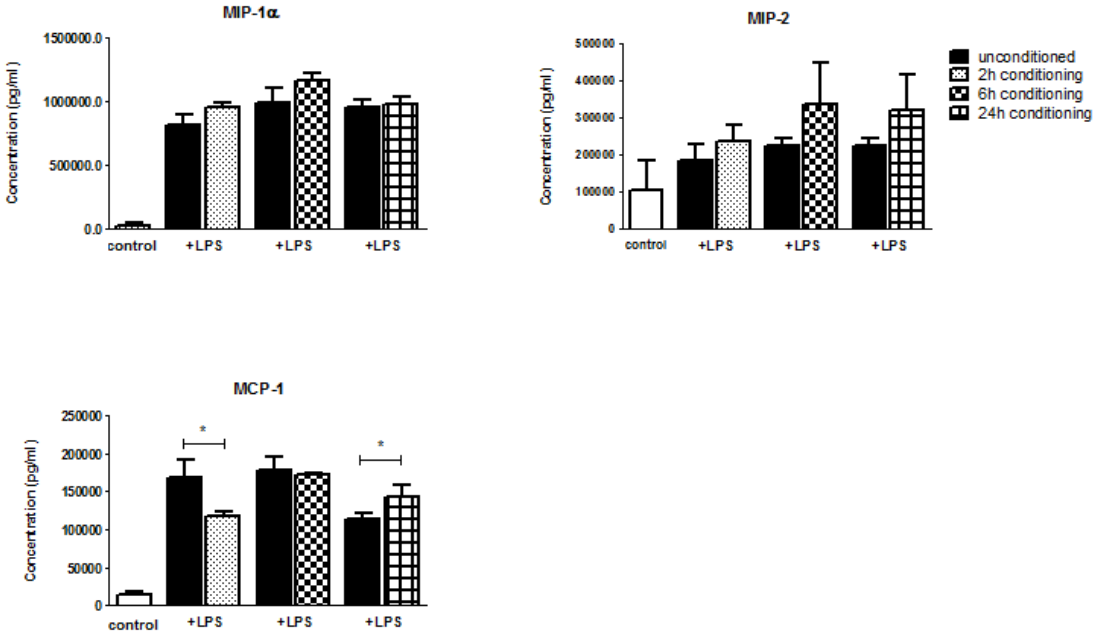

Figure 4.17 Effects of longer conditioning on chemokine production following TLR4 ligation J774A.1 macrophages were incubated for 2h, 6h or 24h with unconditioned media or CMT-93 supernatants before being stimulated with LPS (100ng/ml) for 24h. Supernatants were then collected and chemokine production was measured by ELISA (R&D) according to manufacturer's instruction. Data are presented as mean ± SEM of three replicates and are representative of three independent experiments. *P<0.05 determined by unpaired *t*-test.

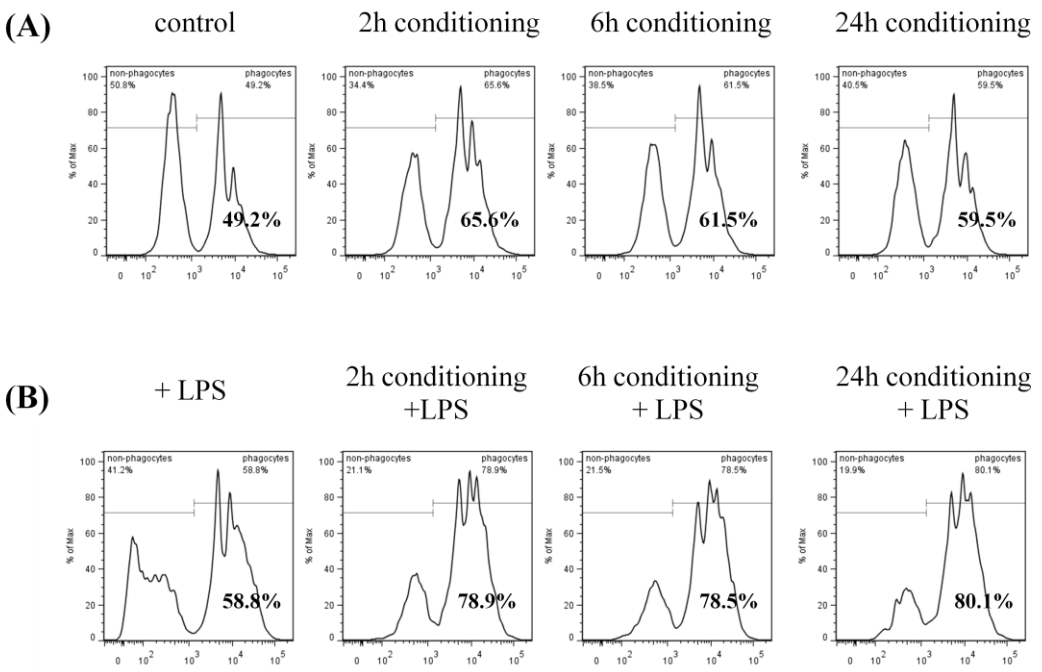

Figure 4.18 Conditioned macrophages display enhanced phagocytic activity. J774A.1 macrophages were incubated with unconditioned media or colonic epithelial cell supernatants for 2h, 6h or 24h **(A)**. Pre-conditioned cells were stimulated with LPS (100ng/ml) for 24h **(B)**. To assess phagocytic ability of cells, 1µm fluorescent latex beads (Sigma) were added to the culture and macrophages were left to phagocytose for 2h. Cells were then washed and analysed by flow cytometry for the uptake of beads. Histograms show the percentages of cells that contain beads (phagocytes) or do not contain beads (non-phagocytes). Percentage of cells containing beads is additionally highlighted on each histogram. Data are representative of three independent experiments.

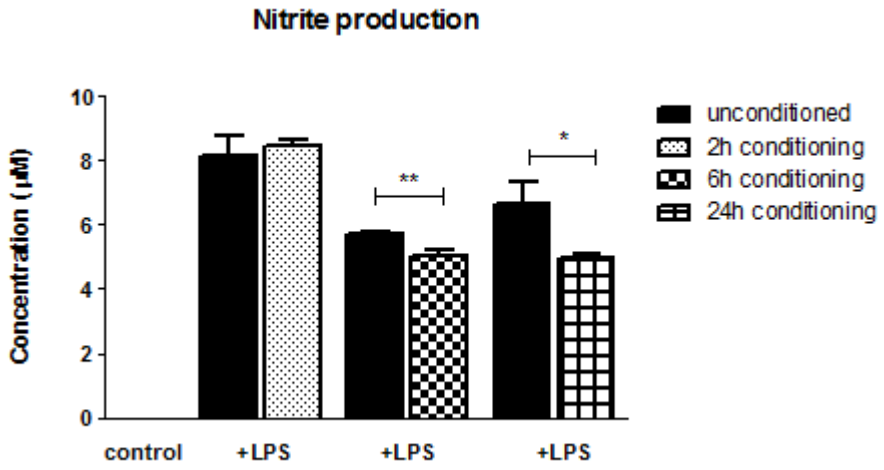

Figure 4.19 Conditioned macrophages produce lower amounts of nitrite in response to LPS stimulation J774A.1 macrophages were pre-conditioned with colonic epithelial cell media for 2h, 6h or 24h before being stimulated with LPS (100ng/ml) for 24h. The concentration of nitrite in supernatants was determined spectrophotometrically using Griess reagent. Data are presented as mean ± SEM of three replicates and are representative of three independent experiments. *$p<0.05$, **$p<0.01$ determined by unpaired t-test.

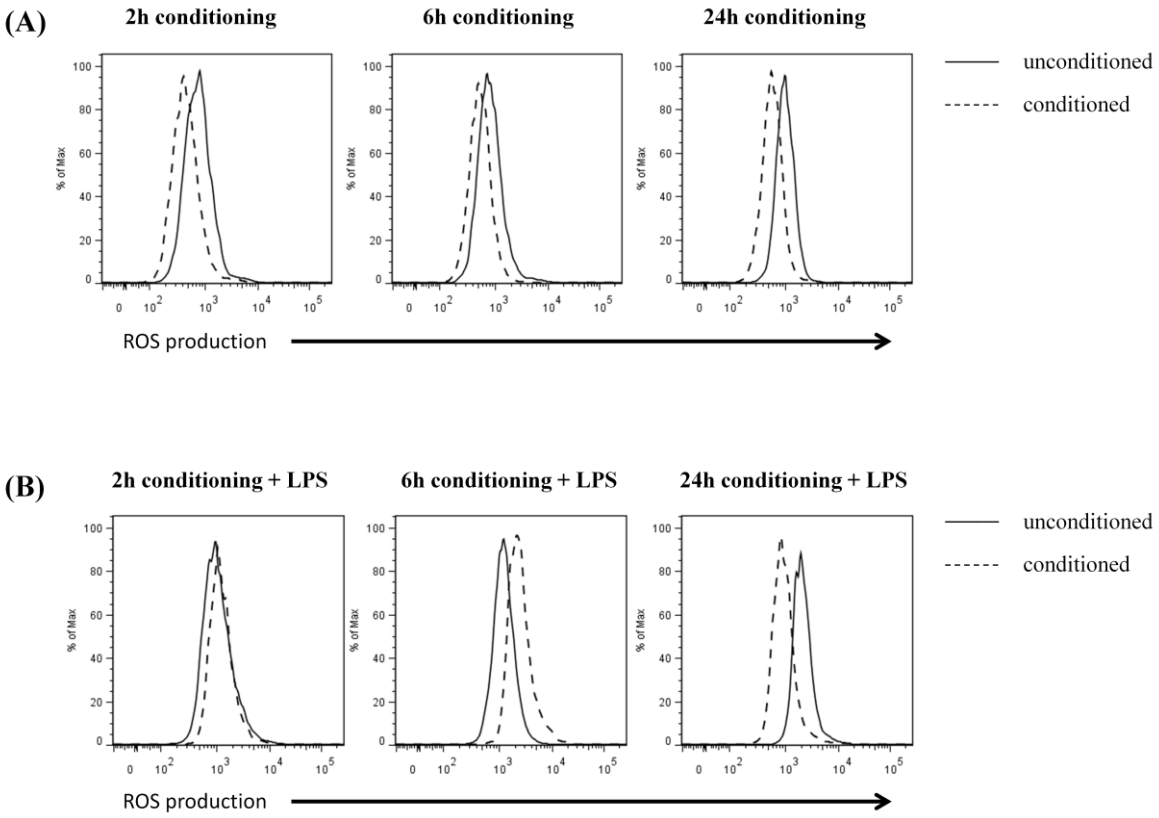

Figure 4.20 Conditioned macrophages produce lower levels of reactive oxygen species (ROS) in a steady state and in response to LPS stimulation. J774A.1 macrophages were incubated with unconditioned media or CMT-93 supernatants for 2h, 6h or 24h **(A)**. After pre-conditioning, cells were stimulated with LPS (100ng/ml) for 24h **(B)**. To measure the production of reactive oxygen species, cell were labelled with DCFDA (Abcam), acording to manufacturer's instructions, and the fluorescent signal relative to intracellular ROS generation was then measured by flow cytometry and compared between unconditioned cells (black line) and conditioned cells (dashed line). Data are representative of three independent experiments.

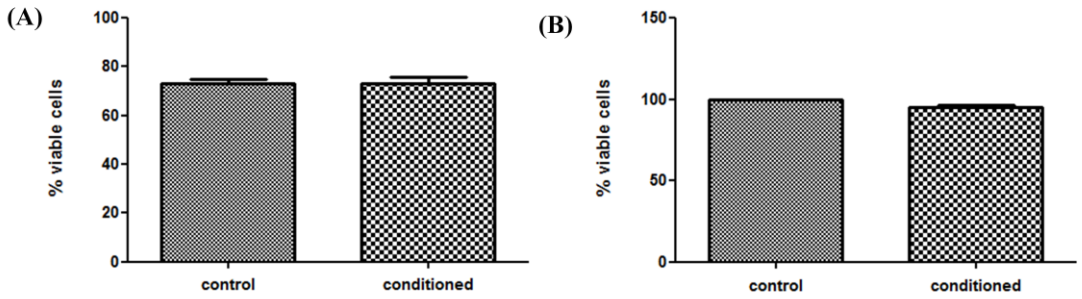

Figure 4.21 CMT-93 conditioning does not affect macrophage viability J774A.1 macrophages were incubated with unconditioned or CMT-93 conditioned media. After 24h cells were labelled with Propidium-iodide (Miltenyi) staining and the percentage of viable cells was determined by flow cytometry **(A)**. Cell viability was also measured using the MTS assay (Promega) and is expressed as a percentage of the control (unconditioned) cells **(B)**. Data are representative of three independent experiments.

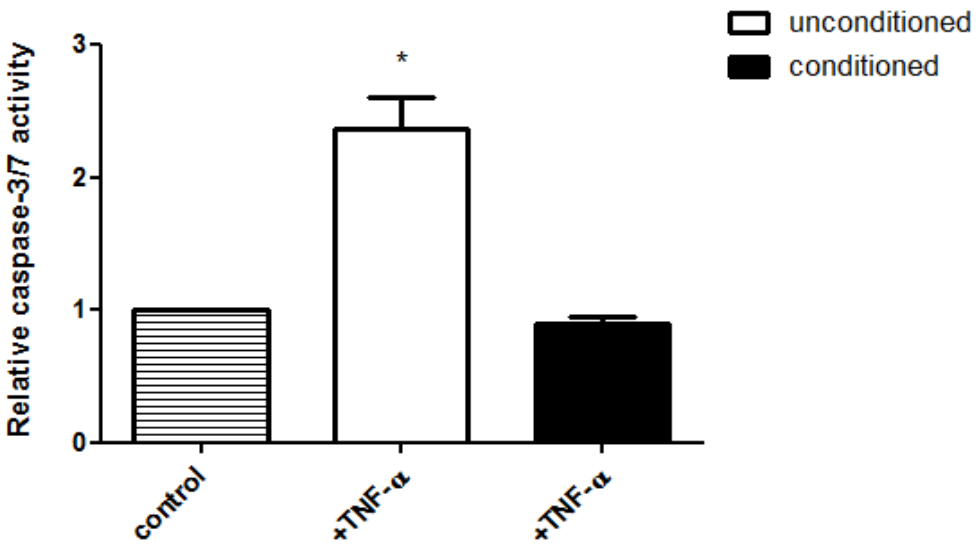

Figure 4.22 Conditioned macrophages do not exhibit increased caspase activity in response to TNF-α. J774A.1 macrophages were incubated with conditioned or unconditioned media for 24h and then stimulated with the recombinant TNF-α (10ng/ml) for another 24h. Cells were then labelled with CellEvent Caspase-3/7 Green Detection Reagent (Invitrogen), according to manufacturer's instructions. The percentage of cells positive for active caspase-3/7 was determined by flow cytometry and expressed relative to control (unstimulated cells). Data are presented as mean ± SEM of three replicates and are representative of two independent experiments. *$p<0.05$ vs. control, determined by unpaired t-test.

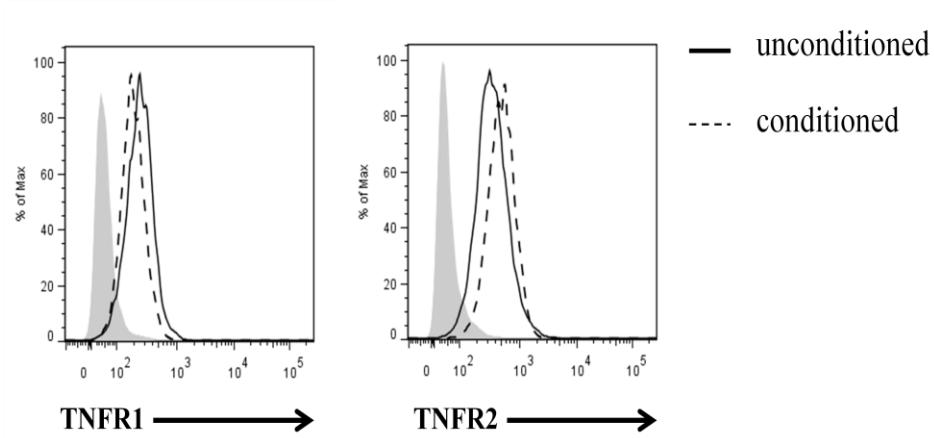

Figure 4.23 Epithelial cell conditioning is increasing the expression of TNFR2. J774A.1 macrophages were incubated with conditioned or unconditioned media for 24h. After 24h the cell were stained with fluorescent antibodies against TNF-receptor 1 (TNFR1) and TNF-receptor 2 (TNFR2) and their expression was analysed by flow cytometry. Histograms show the expression of receptors on unconditioned cells (black line) compared to conditioned macrophages (dashed line). Data are representative of three independent experiments.

4.4 DISCUSSION

Macrophages in the intestine are continuously replenished from inflammatory blood monocytes which change their phenotype upon the arrival in the gut (Varol *et al.*, 2009, Bogunovic *et al.*, 2009). Through a number of differentiation stages, inflammatory monocytes lose their pro-inflammatory features and develop into a non-inflammatory subset that helps to maintain gut homeostasis (Bain *et al.*, 2013)**.** It is still unclear what is driving these changes; however, given its importance as a first line of defence between the gut microbiota and immune cells, it is most likely that the epithelium has a major role in this process. The main goal of this chapter was, therefore, to investigate whether the soluble factor secreted from colonic epithelial cells can alter macrophage phenotype into a phenotype resembling colonic macrophages.

Macrophages conditioned with epithelial cell media showed altered expression of cell surface receptors involved in the immune response. We observed decreased expression of CD40 and CD80 co-stimulatory molecules, as well as MHCII and TLR4, on steady-state macrophages following conditioning. Conditioned macrophages also showed impaired sensitivity to LPS with a decrease in expression of TLR4 in response to this ligand. Furthermore, they almost completely switched off the TLR-induced up-regulation of CD80 and MHC class II. Development of a hypo-responsive phenotype following conditioning was also observed when we examined the production of cytokines. Conditioned macrophages, in a steady-state and in response to LPS, showed significantly lower production of pro-inflammatory IL-12p40 and IL-6. Low expression of co-stimulatory molecules, low cytokine

secretion, as well as the inability to mount an immune response to bacterial ligand, are all characteristics of colonic macrophages as we discussed and demonstrated in chapter 3. Interestingly, although some changes occurred even after a short 2h exposure to epithelial cell supernatants, longer conditioning had a more potent modulatory effect and macrophages developed a more pronounced anti-inflammatory phenotype when exposed to the epithelial cell media for longer. This gradual transition into an anti-inflammatory macrophage is also observed *in vivo*. Bain et al. showed that inflammatory monocytes, once they arrive in the gut, slowly lose their inflammatory characteristics and become TLR hypo-responsive resident macrophages over a period of 24-48h (Bain *et al.*, 2013).

Reduced production of IL-12p40 has also been observed by other groups after they exposed monocyte-derived dendritic cells to human intestinal epithelial cell line, Caco-2, supernatants (Rimoldi *et al.*, 2005, Butler *et al.*, 2006). The same groups reported down-regulation of co-stimulatory molecules on dendritic cells following conditioning, which correlates with our findings. However, while other groups concentrated only on these parameters, we also investigated the effects of epithelial cells on chemokine production and macrophage function, such as phagocytosis. Conditioning with epithelial cell media significantly increased the production of MIP-1α chemokine from unstimulated macrophages and MCP-1 from LPS-stimulated macrophages. Intestinal macrophages also produce MCP-1 as has been shown by Takada et al. The same study showed that intestinal macrophages from $MCP^{-/-}$ mice produce lower amounts of IL-10 compared to WT mice (Takada *et al.*, 2010) which supports the homeostatic role of this chemoattractant in the intestinal environment. MIP-1α is important for the recruitment of eosinophils and neutrophils

(Cook, 1996), but also regulates various aspects of tissue homeostasis, such as stem cell development and angiogenesis (Menten *et al.*, 2002). Contrary to our previous understanding that eosinophils appear in the intestine only in a rare parasitic infections, recent studies show unexpectedly large amounts of eosinophils in preparations from healthy small intestine and colon (Mowat and Bain, 2010). It is speculated that they may contribute to epithelial renewal and barrier integrity in the gut or may even be a source of the conditioning factors that maintain local macrophage hypo-responsiveness (Blanchard and Rothenberg, 2009, Mowat and Bain, 2010). If that is the case, the up-regulated production of eosinophil-recruiting chemokines that we report after epithelial cell conditioning may suggest a mechanism that supports intestinal homeostasis.

Phagocytosis is the hallmark of macrophage function. It is vital for the clearance of infectious pathogens as well as apoptotic cells (Aderem and Underhill, 1999). Colonic macrophages have been shown to be highly phagocytic even though they do not activate an immune response following phagocytosis (Smythies *et al.*, 2005). Here we show that the phagocytic ability of macrophages is enhanced following conditioning with epithelial cell supernatant. Macrophages cultured in the presence of epithelial cell media increased their intake of fluorescent beads, both in a steady-state and after LPS stimulation. However, although our conditioned macrophages became highly phagocytic they did not demonstrate any increase in their respiratory burst capacity and nitric oxide production, which would typically accompany phagocytic activity. This further suggests that conditioning the macrophages with epithelial cell media induces a similar phenotype to that of a colonic macrophage, as intestinal macrophages isolated from normal, non-inflamed human colonic mucosa

do not show significant respiratory burst (Mahida *et al.*, 1989b) neither do they express inducible nitric-oxide synthase (Ikeda *et al.*, 1997).

It has been shown in several studies that intestinal macrophages produce the anti-inflammatory cytokine IL-10 (Denning *et al.*, 2007, Hadis *et al.*, 2011). However, we failed to observe induction of IL-10 following conditioning. Increased IL-10 production was also not observed in the study by Rimoldi *et al*. where they conditioned dendritic cells with Caco-2 supernatants (Rimoldi *et al.*, 2005), therefore it is possible that IL-10 production depends on different factors and it is not induced by epithelial cell priming. A study by Ueda *et al*. showed that IL-10 production is dependent on the presence of commensal microbiota and that colonic macrophages isolated from germ-free mice produce lower levels of IL-10 (Ueda *et al.*, 2010). Zeuthen *et al*. also investigated the effects of Gram positive (G+) and Gram negative (G-) commensals on Caco-2 conditioned dendritic cells and showed that IL-10 is increased following encounter will G+ bacteria, but decreased upon encountering G- bacteria (Zeuthen *et al.*, 2008). Use of LPS in our study, which is a major component of the outer membrane of G- bacteria, may therefore explain a decrease of IL-10 following conditioning. This is supported by our finding that epithelial cell conditioning did not alter IL-10 expression from unstimulated macrophages.

Considering that conditioned macrophages exhibited primarily anti-inflammatory properties, we were surprised with the finding that both unstimulated and LPS-stimulated conditioned macrophages had significantly increased production of TNF-α. TNF-α is usually seen as a potent pro-inflammatory cytokine implicated in various autoimmune and inflammatory diseases, such as rheumatoid arthritis, psoriasis,

Crohn's disease, sepsis, diabetes and obesity (Plevy *et al.*, 1997, Brennan *et al.*, 1992, Clark, 2007). Binding of TNF-α to its receptors can, in some conditions, initiate a caspase cascade, involving caspase-8 and caspase-3 activation, which leads to apoptosis and cell death (Bradley, 2008, Rath and Aggarwal, 1999). Interestingly, while activation of unconditioned macrophages with recombinant TNF-α did induce caspase-3 activation, our conditioned cells had the same levels of active caspase-3 as unstimulated controls. Additional controls are needed to investigate whether this protects the cell against apoptosis. Pro-survival effects of TNF-α have been documented before. TNF-α actually shows a remarkable functional duality, being engaged both in tissue regeneration and destruction (Wajant *et al.*, 2003). For example, in tuberculosis TNF-α is responsible for the extensive tissue destruction, fibrosis and the formation of cavities (Mootoo *et al.*, 2009). On the other hand, TNF-α has been found to stimulate proliferation of gastric epithelial cells during ulcer repair (Luo *et al.*, 2005). A dual role for TNF-α has also been implicated during experimental autoimmune encephalomyelitis (EAE), a murine model of multiple sclerosis. In the acute phase of the disease TNF-α has a detrimental activity, while in the later phase it is actually responsible for a spontaneous regression of EAE (Kassiotis and Kollias, 2001).

This dual role of TNF-α seems to be dependent on the specific TNF receptor signalling. The activities of TNF-α are mediated by two receptors, TNF-R1 (p55) and TNF-R2 (p75) (Peschon *et al.*, 1998). TNFR1 is constitutively expressed in most tissue, whereas TNFR2 is usually found in cells of the immune system (Wajant *et al.*, 2003). Although their mechanisms have not been completely elucidated, it seems that they have opposing effects. The pro-inflammatory and apoptotic pathways of

TNF-α are largely mediated through TNFR1, while TNFR2 has been shown to mediate signals that promote proliferation and tissue repair (Bradley, 2008). In a mouse model of retinal ischemia TNFR2 protected against ischemic tissue destruction (Fontaine *et al.*, 2002) and it also proved to be cardioprotective in an *in vivo* heart failure model in mice (Hamid *et al.*, 2009). In the same studies, signalling through the TNF-R1 showed opposite effects, supporting the disease progression. With this in mind, we hypothesised that TNF-α does not activate caspase in conditioned macrophages because it somehow favours the protective TNFR2 pathway. In order to explore that, we investigated the expression of TNF receptors on unconditioned and conditioned cells. Indeed, macrophages conditioned with colonic epithelial cell media showed higher expression of TNFR2.

Recent studies show that, contrary to popular belief, colonic macrophages do produce TNF-α in a steady-state (Bain *et al.*, 2013, Mowat, 2011). This production, however, does not lead to inflammation. It has been speculated that it is counteracted by the secretion of IL-10 from the same macrophages or maybe it is "extinguished" by some other anti-inflammatory products secreted from the surrounding cells (Mowat, 2011). So far, our data show that exposure to epithelial cell-derived factors results in the development of an anti-inflammatory macrophage that resembles the intestinal macrophage phenotype. Also, conditioning up-regulates the expression of TNFR2. Taken this into account, we hypothesise that maybe there is a high expression of TNFR2 on colonic macrophages, which has a role in limiting the pro-inflammatory effect of TNF-α while potentiating its homeostatic function, such as organogenesis of secondary lymphoid tissue of the intestine (Kuprash *et al.*, 1999)

or/and macrophage proliferation and differentiation (Guilbert *et al.*, 1993, Witsell and Schook, 1992).

Taken together, our data suggests that colonic epithelial cell-derived factors play a key role in monocyte differentiation into intestinal macrophages. It also implicates the role of TNFR2 as a possible mechanism by which macrophages maintain gut homeostasis. It is important to note that intestinal epithelial cells *in vivo* exist in a polarised state, divided into an apical and basolateral domain with a distinct protein and lipid composition (Pott and Hornef, 2012). The secretion of soluble factors produced by epithelial cells can vary between the apical and the basolateral side, with some factors being predominantly trafficked just to the one side (Yakovich *et al.*, 2010). In our model we have not grown CMT-93 cells in polarising conditions, therefore this vectorial nature of soluble factor release was not taken into account. In order to fully elucidate the effect of epithelial cell soluble factors on macrophage phenotype CMT-93 cells should be grown on transwell plates, as described by Iliev *et al*, and conditioning experiments should be repeated with apical and basolateral secretions separately (Iliev *et al.*, 2009).

In the next chapter we move into the *in vivo* models of gut inflammation and infection, in order to confirm the hypothesis of the importance of TNFR2 on colonic macrophages and to attempt to elucidate the role of TNFR2 on colonic macrophages in homeostasis and disease.

CHAPTER 5

THE ROLE OF MACROPHAGE TNFR2 IN THE GUT

5.1 INTRODUCTION

In the previous chapter we show the development of an anti-inflammatory phenotype in macrophages, induced by colonic epithelial cell soluble factors. With low production of pro-inflammatory cytokines and other pro-inflammatory mediators, inertia when exposed to stimuli, but with high phagocytosis, these macrophages resemble colonic macrophages. However, even though they display an anti-inflammatory phenotype, conditioned macrophages still produce TNF-α. This was confusing as TNF-α is usually seen as a pro-inflammatory cytokine involved in disease induction (Clark, 2007). Furthermore, these macrophages also seem to have decreased caspase-3 activity following TNF stimulation and have higher expression of TNFR2 than control macrophages. This data, together with the fact that colonic macrophages also produce TNF-α (which was speculated before (Nakata *et al.*, 2006a), and confirmed recently (Bain *et al.*, 2013)) lead us to believe that there might be a non-inflammatory role for TNF-α in intestinal homeostasis and that it might be regulated by TNFR2.

TNF-α is a pleiotropic cytokine produced by many different cell types, but mostly monocytes and macrophages (Parameswaran and Patial, 2010). It exerts a broad range of biological effects, including cell activation and migration, cell proliferation, differentiation and apoptosis (Tracey and Cerami, 1993) and it has a well-characterised role in the pathogenesis of various inflammatory diseases (Plevy *et al.*, 1997, Brennan *et al.*, 1992). However, apart from the pro-inflammatory role, increasing evidence points to anti-inflammatory properties of TNF-α. In the mouse model of multiple sclerosis, TNF-α has been shown to be involved in resolution of

disease (Kassiotis and Kollias, 2001). Furthermore, TNF-α treatment also significantly increased epithelial cell proliferation and repair during ulcer healing (Luo *et al.*, 2005).

All known responses to TNF are triggered by binding to two different receptors, TNFR1 and TNFR2. These receptors are differentially expressed within the body with TNFR1 being expressed on almost all cell types while TNFR2 expression is restricted to endothelial cells and immune cells, especially monocytes and macrophages (Tartaglia and Goeddel, 1992, Aggarwal, 2003). Both TNFR1 and TNFR2 possess sequences that bind to intracellular adaptor proteins and in that way link stimulation of receptor to activation of various signalling processes. It has been shown that TNFR1 is primarily responsible for initiating inflammatory responses (vanderPoll *et al.*, 1996). However, the intracellular region of TNFR1 can also interact with a complex of apoptosis-related proteins giving TNFR1 the ability to induce cell death (Van Herreweghe *et al.*, 2010). Activation of TNFR2, on the other hand, has been shown to be needed for clonal expansion of T-cells in response to intracellular bacterial pathogens (Kim *et al.*, 2006) and for the resolution of pulmonary inflammation after bacterial challenge (Peschon *et al.*, 1998). However, opposite roles were also reported for both receptors with TNFR1 being essential to protect mice against tuberculosis and *Toxoplasma gondii* (Flynn *et al.*, 1995a, Deckert-Schluter *et al.*, 1998) while TNFR2 signalling induced the development of renal injury in a model of glomerulonephritis (Vielhauer *et al.*, 2005). This is further complicated by the fact that both receptors share part of their pathway and TNFR2 can actually pass the TNF ligand to TNFR1 (Tartaglia *et al.*, 1993).

In this chapter we, therefore, sought to investigate the role of TNFR2 on colonic macrophages. Firstly we wanted to determine whether TNF receptors are expressed on colonic macrophages in homeostasis and then investigate the role of TNFR2 *in vivo* using animal models of disease and *in vitro* using specific antagonistic antibodies to TNFR1 and TNFR2.

5.2 RESULTS

5.2.1 Colonic MØ have higher expression of TNFR2 than peritoneal MØ

In order to investigate if colonic macrophages express TNFR2 and whether this expression is higher than on macrophages from other tissue, we isolated and compared macrophage population from the colonic lamina propria and from the peritoneal cavity. The peritoneal cavity provides an easily accessible site for the harvesting of moderate numbers of resident, non-manipulated macrophages. Unlike colonic macrophages, peritoneal macrophages respond to stimulation, produce pro-inflammatory cytokines and have high expression of co-stimulatory receptors (Marcinkiewicz, 1991, Wang *et al.*, 2013a).

Lamina propria cells and resident peritoneal cells were isolated as described in Materials and methods (section 2.12) and stained for the F4/80 macrophage marker and two TNF-α receptors, TNFR1 and TNFR2. Cells were gated based on their size and granularity (FSC; SSC) and doublets and dead cells were excluded from the analysis. Expression of TNFR1 and TNFR2 was then analysed on live F4/80^{+} cells. As we can see in **Figure 5.1** colonic macrophages show much higher expression of TNFR2 than peritoneal macrophages.

5.2.2 Mouse models of disease

In order to investigate the potential role of TNFR2 in disease we used two different mouse models; DSS-induced colitis which is a model of intestinal inflammation and *Clostridium difficile* -associated model of intestinal infection.

5.2.2.1 Clinical assessment of DSS-induced colitis

The DSS model was carried out in collaboration with Dr. Silvia Melgar in the Alimentary Pharmabiotic Centre, University College Cork, as described in Materials and methods (section 2.13). To assess the development of the disease, mice were weighed and scored (every 3-4 days) for disease activity index (DAI) based on stool composition, fur texture and posture. As expected, control mice maintained a healthy weight gain during study **[Figure 5.2A]**. DSS treated groups immediately started to lose weight, with the biggest weight loss at day 7. Following this, mice started to recover and the chronic group returned to their normal weight by the day 26 **[Figure 5.2A]**. The DAI showed a similar pattern of a disease progression. No disease activity was observed in the control mice, while there was a rapid increase in the disease activity scores in all DSS treated groups, with mild recovery in chronic group by the end of the study **[Figure 5.2B]**. At each end point, colons were removed, measured and weighed. The weight and length of the colon are useful indicators of disease progression as the cell infiltration and inflammation increase the weight of the colon and also shrink the colon length (Okayasu *et al.*, 1990a). As we can see in **Figure 5.2C and D** colons from the early ($p<0.01$) and late ($p<0.05$) acute group were significantly shorter than control, with a recovery in the chronic group. Also, there was an increase in colon weight in all the DSS treated groups ($p<0.05$) **[Figure 5.2E]**.

Small sections of distal colon (0.5cm) were removed for histology and stained with hematoxylin and eosin (H&E), as described in Materials and methods section 2.13.3. The H&E staining of control shows a healthy colon with crypts and goblet cells present **[Figure 5.3]**. In the early and late acute phase we can see a visible reduction

in goblet cells, together with loss of crypts and infiltration of inflammatory cells to the mucosa **[Figure 5.3]**. The chronic group shows recovery with the regeneration of crypts and re-epithelisation, consistent with the rest of the data **[Figure 5.3]**.

5.2.2.2 Expression of TNF receptors on colonic MØ at different stages of DSS colitis

Lamina propria cells were isolated from the colons of healthy mice and mice treated with DSS in early acute (day 7), late acute (day 12) and chronic phase (day 26) of disease. Cells were then stained with fluorescent antibodies to determine the expression of TNF-receptors by flow cytometry. Cells were first gated based on their size (FSC) and granularity (SSC) and doublets and dead cells were excluded. Expression of TNF receptors was analysed on live $F4/80^+$ cells. As shown in **Figure 5.4A** colonic macrophages had decreased expression of TNFR1 in the early and acute phase of DSS colitis, which then returned to normal in the chronic phase. On the other hand, expression of TNFR2 was similar to control in the early and acute phase, while macrophages in the chronic phase had increased expression of TNFR2 **[Figure 5.4A]**.

Colonic macrophages were sorted and mRNA was isolated using Nucleospin RNA II columns (Macherey-Nagel). The gene expression levels of TNFR1 and TNFR2 were quantified using qRT-PCR. The expression levels were normalised to 18S levels and the gene expression is shown as a fold change relative to the control. qRT-PCR data correlates with the protein expression with an increase in TNFR2 mRNA expression in the chronic phase ($p<0.05$) **[Figure 5.4B]**. Due to a low quality of mRNA isolated from the early acute phase, gene expression of TNF receptors in that phase could not be determined.

5.2.2.3 Expression of TNF receptors and TNF-α in the colonic tissue of DSS-treated mice

Small sections of distal colon from each mouse were removed and homogenised in order to extract mRNA. The levels of TNFR1, TNFR2 and TNF-α mRNA were quantified using qRT-PCR. The expression levels were normalised to 18S levels and the gene expression is shown as a fold change relative to the control. TNF-α was significantly up-regulated in the early acute stage of disease, with a 20-fold increase in the expression compared to control ($p<0.001$) **[Figure 5.5]**. Levels of TNF-α then decreased in the late and chronic phase, but they stayed higher than in the control ($p<0.01$ and $p<0.05$, respectively). A similar pattern was seen in the expression of TNFR1 and TNFR2, with the highest fold increase observed in the early acute phase ($p<0.001$) **[Figure 5.5]**. The expression of TNFR2 mRNA did not correlate with the expression of TNFR2 on colonic macrophages; however increase in the chronic phase is consistent **[Figure 5.4]**. This was not surprising as mRNA was isolated from the whole tissue and therefore represents the levels of TNFR2 from all the cells present in that tissue. TNFR2 is reported to be highly expressed on regulatory T-cells (Treg) (Chen *et al.*, 2008b). Treg can be distinguished by the expression of transcription factor Foxp3, which is a key control gene in their development and function (Sakaguchi, 2005). To determine whether Treg contribute to the high TNFR2 expression in the acute phase of DSS colitis, we analysed the levels of Foxp3 mRNA in the colonic tissue. There was a 40-fold increase in the levels of Foxp3 during the early and acute phase of colitis, compared to control ($p<0.01$) **[Figure 5.6]**. In the chronic phase, however, the expression of Foxp3 was not significantly different than in the control. This indicates that the increase in TNFR2

mRNA in the chronic phase is not due to Treg and may be coming from macrophages.

5.2.2.4 Clinical assessment of a mouse model of Clostridium difficile infection

The *C. difficile* infection model was carried out in collaboration with Pat Casey in Alimentary Pharmabiotic Centre & Microbiology Department, University College Cork, as described in Materials and methods section 2.13. Two ribotypes (RT) of *C. difficile* were used, 001 and 027, as they differ in the severity of infection. RT 027 has been described as a more virulent ribotype with higher toxin production and increased mortality (McDonald *et al.*, 2005). To assess the development of a disease, mice were weighed daily and body weight change was monitored. As expected, control mice maintained a healthy weight gain during the study, while mice infected with both ribotypes showed a weight loss which peaked on day 3 post-infection **[Figure 5.7A]**. After day 3 mice started to recover with the group infected with RT 001 recovering quicker than a group infected with RT 027. At day 3 and 7 caeca were harvested and the contents were removed for colony forming unit (CFU) counts. As expected, the RT 027 infected group had significantly higher numbers of *C. difficile* spores compared to the RT 001 group at day 3 ($p<0.01$) **[Figure 5.7B]**. Furthermore, at day 7, the RT 027 group still had high counts of *C. difficile* spores, unlike the RT 001 group ($p<0.05$).

Small sections of distal colon (0.5cm) were removed for histology and stained with hematoxylin and eosin (H&E), as described in Materials and methods section 2.13.3. The H&E staining of the control shows a healthy colon, while there is a loss of crypts and infiltration of inflammatory cells present on day 3 in both ribotypes

[Figure 5.7C]. On day 7, recovery was seen in the RT 001 infected mice but not in the RT 027 infected mice, consistent with the rest of the data.

5.2.2.5 Mice infected with 027 ribotype have slower recovery

To investigate the progression of *C. difficile* infection, small sections of colonic tissue collected from RT 001 and RT 027 infected mice were homogenised in order to extract mRNA. The levels of the pro-inflammatory cytokines IL-12p40, IL-6 and TNF-α and the anti-inflammatory cytokine IL-10 were quantified using qRT-PCR. The levels of TNF-α peaked on day 3 in both groups, with 4 fold increase compared to control, and then returned to normal levels by the day 7 **[Figure 5.8]**. The levels of IL-6 appeared to be higher in mice infected with RT 001 on day 3, although this did not reach statistical significance between the two ribotypes. On day 7 IL-6 was significantly higher in the RT 027 group than in the RT 001 group ($p<0.05$) **[Figure 5.8]**. The levels of IL-12p40 were low on day 3 in both groups, however by day 7 production of IL-12p40 was significantly increased in the RT 027 group compared to the RT 001 group ($p<0.05$) **[Figure 5.8]**. Levels of the anti-inflammatory cytokine IL-10 peaked on day 7 and were significantly higher in mice infected with RT 001 ($p<0.05$) **[Figure 5.8]**.

5.2.2.6 TNFR2 is up-regulated only in mice infected with 001 ribotype

The levels of TNFR1 and TNFR2 mRNA were also quantified using qRT-PCR in both RT 001 and RT 027 infected mice. While the levels of TNFR1 did not change during 7 days of infection, TNFR2 was significantly up-regulated in the tissue of RT

001 infected mice on day 3, with a 3 fold difference in the expression compared to control ($p<0.01$) **[Figure 5.9]**. In the tissue of DSS infected mice the levels of Foxp3 cells were high **[Figure 5.6]** and probably contributed to the high levels of TNFR2 observed. To determine whether the TNFR2 levels in RT 001 infected mice were also due to Treg cells, we analysed the expression of Foxp3 mRNA. Foxp3, however, could not be detected in the tissue of *C. difficile* infected mice, indicating that TNFR2 comes from the innate immune cells.

5.2.2.7 Colonic epithelial cells contribute to TNFR2 expression in vitro and in vivo

In chapter 4 we showed that conditioning with colonic epithelial cells media modulates macrophage phenotype into an anti-inflammatory phenotype that resembles colonic macrophages. The conditioned macrophages also had an increased expression of TNFR2, but not TNFR1, which led us to believe that TNFR2 may be contributing to an anti-inflammatory role of colonic macrophages. To determine whether conditioned macrophages lose their anti-inflammatory phenotype when removed from epithelial cell environment, we conditioned cells for 24h and then split them into two groups. Group 1 was conditioned with fresh epithelial cell media for another 24h, while the group 2 was removed from conditioned media and cultured in unconditioned media for 24h. In **Figure 5.10A** we can see that conditioned macrophages (Group 1) showed an increase in TNF-α and MIP-1α production and a decrease in IL-6 production, as observed in chapter 4. They also showed decreased expression of CD80, MHCII and TLR4 and increased expression of TNFR2 **[Figure 5.10B]**. Interestingly, when removed from colonic epithelial cell media for 24h (Group 2), macrophages lost their anti-inflammatory phenotype and

started reverting into their unconditioned phenotype **[Figure 5.10A and B]**. Importantly, the high expression of TNFR2 was also lost **[Figure 5.10B]**. This suggests the importance of epithelial cell soluble factors in the regulation of TNFR2 expression.

If macrophages require "signals" from epithelial cells in order to up-regulate TNFR2, as we have seen *in vitro*, then in the case of intestinal inflammation when epithelial cell barrier is disrupted, those "signals" would be lost, hence TNFR2 up-regulation would be disabled. The loss of epithelial barrier function is associated with the loss of the tight junction proteins, such as occludin (Mennigen *et al.*, 2009). We, therefore, investigated the occludin levels in our animal disease models, to determine the level of epithelial cell disruption.

As shown in **Figure 5.11A** mRNA expression of occludin in the tissue of DSS-treated mice is down-regulated in the acute phase of colitis, with gradual recovery towards the chronic phase. Importantly, the recovery of epithelial cells correlates with the up-regulation of TNFR2 on colonic macrophages **[Figure 5.4]**.

In the *C. difficile* model of infection occludin mRNA is significantly down-regulated in mice infected with RT 027 on day 3 ($p<0.01$), but not in mice infected with RT 001 **[Figure 5.11B]**. This may explain why mice infected with RT 027 do not show up-regulation of TNFR2, while RT 001 infected mice do **[Figure 5.9]**. This further supports the requirement of epithelial cell "signals" for TNFR2 up-regulation which is lost during the acute phase of DSS-colitis and during RT 027 infection, because of the epithelial cell disruption.

5.2.3 The effects of TNF receptor antagonists on cytokine secretion from unconditioned and conditioned macrophages

In order to further examine the role of TNF receptor on macrophages, we used receptor blocking antibodies for TNFR1 and TNFR2, on both unconditioned and conditioned macrophages, and investigated their cytokine response in a steady state and after LPS stimulation.

J774A.1 macrophages were cultured with conditioned or unconditioned media for 24h before the addition of TNFR1 antagonist (5µg/ml; R&D) or TNFR2 antagonist (5µg/ml; Biolegend) for another 24h. Supernatants were then collected and the levels of cytokines were determined by ELISA (R&D). The isotype control antibody for TNFR2 antagonist (5µg/ml; Biolegend) was also added to a culture of macrophages to determine the specificity of the inhibitory effect (see **Appendix G**). Both TNFR1 and TNFR2 blocking antibodies slightly decreased basal levels of anti-inflammatory IL-10, from unconditioned and conditioned macrophages **[Figure 5.12 and 5.14]**. TNF-α secretion was significantly up-regulated in response to TNFR1 ($p<0.001$) or TNFR2 ($p<0.001$) antagonist on unconditioned macrophages, with TNFR2 blocking antibody having a much stronger effect **[Figure 5.12]**. TNFR2 antagonist had the same effect on conditioned macrophages, significantly increasing TNF-α levels ($p<0.001$). TNFR1 antagonist however did not have an effect on conditioned macrophages **[Figure 5.14]**. TNF receptor antagonists did not have an effect on IL-27 secretion from unconditioned macrophages **[Figure 5.12]**; however blocking TNFR2 signalling significantly down-regulated secretion of IL-27 from conditioned macrophages ($p<0.05$) **[Figure 5.14]**. Levels of IL-12p40 and IL-6 were also measured but they could not be detected.

To investigate the macrophage response to LPS in the presence of TNFR1 or TNFR2 blocking antibodies, conditioned and unconditioned macrophages were pre-exposed to TNFR1 or TNFR2 antagonist for 1h before the addition of LPS (100ng/ml; Enzo Lifesciences). After 24h supernatants were harvested and cytokine levels were measured by ELISA (R&D). Both TNFR1 and TNFR2 blocking antibodies significantly down-regulated the LPS-induced production of IL-12p40 from unconditioned macrophages ($p<0.001$), with anti-TNFR2 having a slightly stronger effect **[Figure 5.13]**. The production of IL-12p40 on conditioned macrophages was however down-regulated only in a response to TNFR2 antagonist ($p<0.001$) **[Figure 5.15]**. TNF-α levels significantly increased when TNFR2, but not TNFR1 signalling was blocked, in both unconditioned and conditioned macrophages ($p<0.001$) **[Figure 5.13 and 5.15]**. LPS-induced secretion of IL-6 was down-regulated ($p<0.001$) and IL-10 up-regulated ($p<0.001$) in response to anti-TNFR1 on unconditioned macrophages **[Figure 5.13]**. LPS-induced IL-6 was also down-regulated in conditioned macrophages but in response to both TNFR1 and TNFR2 blocking antibodies ($p<0.05$ and $p<0.01$, respectively), not only TNFR1 **[Figure 5.15]**. While the TNFR1 and TNFR2 receptor antagonists did not have an effect on IL-27 production from unconditioned macrophages **[Figure 5.13]**, they significantly decreased IL-27 production from conditioned macrophages ($p<0.05$ and $p<0.01$, respectively) **[Figure 5.15]**.

5.2.4 TNF receptor antagonists do not have an effect on surface marker expression

Since the TNFR antagonists showed a strong effect on cytokine production from macrophages, we wanted to investigate whether they also affected the expression of macrophage surface markers.

J774A.1 macrophages were incubated with unconditioned or conditioned media for 24h before the addition of TNFR1 (5µg/ml; R&D) or TNFR2 (5µg/ml; Biolegend) blocking antibodies. After 24h cells were collected and stained with appropriate fluorescently labelled antibodies. The expression of CD86, CD80, CD40, MHCII, TLR2 and TLR4 was then analysed by flow cytometry. There was no change in the cell surface marker expression after the addition of the TNF receptor blocking antibodies **[Figure 5.16 and 5.17]**.

5.2.5 Phagocytosis is down-regulated in response to TNF receptor blocking antibodies

To determine whether phagocytosis is affected if TNFR1 or TNFR2 receptors are blocked, conditioned and unconditioned macrophages were incubated with TNFR1 (5µg/ml; R&D) or TNFR2 (5µg/ml; Biolegend) blocking antibodies for 24h. After 24h fluorescent latex beads (20beads/cell; Sigma-Aldrich) were added to the culture and macrophages were left to phagocytose for 1h. The up-take of beads was then measured by flow cytometry. Phagocytosis was significantly down-regulated from both unconditioned ($p<0.05$) and conditioned ($p<0.01$) macrophages after the addition of TNFR2 blocking antibody **[Figure 5.18]**. Phagocytosis of conditioned macrophages was also affected if we blocked TNFR1 ($p<0.01$) **[Figure 5.18]**.

5.2.6 TGF-β regulates the expression of TNFR2

Intestinal epithelial cells produce different factors that can regulate intestinal environment, such as antimicrobial peptides, cytokines and chemokines. Two of the cytokines that have been reported to have immunosuppressive role on underlying dendritic cells and T-cells are thymic stromal lymphopoietin (TSLP) and transforming growth factor β (TGF-β) (Rimoldi *et al.*, 2005, Das *et al.*, 2013). We, therefore, sought to examine whether the presence of these cytokines in conditioned media have an effect on the expression of macrophage TNFR2.

Neutralising antibodies against TSLP (10μg/ml; R&D) or TGF-β (10μg/ml; R&D) were added to conditioned media for 2h at 4ºC. Conditioned media with neutralised TSLP or TGF-β was then added to J774A.1 macrophages and left for 24h. After 24h macrophages were collected and stained with fluorescently labelled antibodies to TNFR1 and TNFR2. In parallel, macrophages were grown in conditioned or unconditioned media without neutralising antibodies, as a control. As shown in **Figure 5.19A and B**, conditioned macrophages (black histogram) have up-regulated TNFR2 expression when compared to unconditioned macrophages (gray histogram). However, if we block TGF-β in conditioned media, this up-regulation is lost **[Figure 5.19A]**. Neutralisation of TSLP, on the other hand, did not have an effect of TNFR2 expression on conditioned macrophages **[Figure 5.19B]**. Additional controls showing histograms of control vs. control + anti-TGF-β are added in **Appendix F**.

To further examine whether the presence of TGF-β has an effect on TNFR2, we incubated J774A.1 macrophages with recombinant TGF-β (10ng/ml; R&D) for 24h. Indeed, addition of TGF-β up-regulated the expression of TNFR2, but not TNFR1 **[Figure 5.20A]**.

Our *in vitro* data indicates a role for TGF-β in the regulation of TNFR2 expression. Therefore, we wanted to investigate whether the levels of TGF-β correlate with the up-regulation of TNFR2 expression *in vivo*. As shown in **Figure 5.20B** the expression of TGF-β mRNA is up-regulated in all three phases of DSS-induced colitis, similar to TNFR2 **[Figure 5.5]**. Furthermore, TGF-β is up-regulated in the tissue of RT 001 infected mice ($p<0.01$), but not RT 027 infected mice on day 3 **[Figure 5.20C]**, correlating with the up-regulated expression of TNFR2 in RT 001, but not RT 027 infected mice **[Figure 5.9]**.

5.3 FIGURES

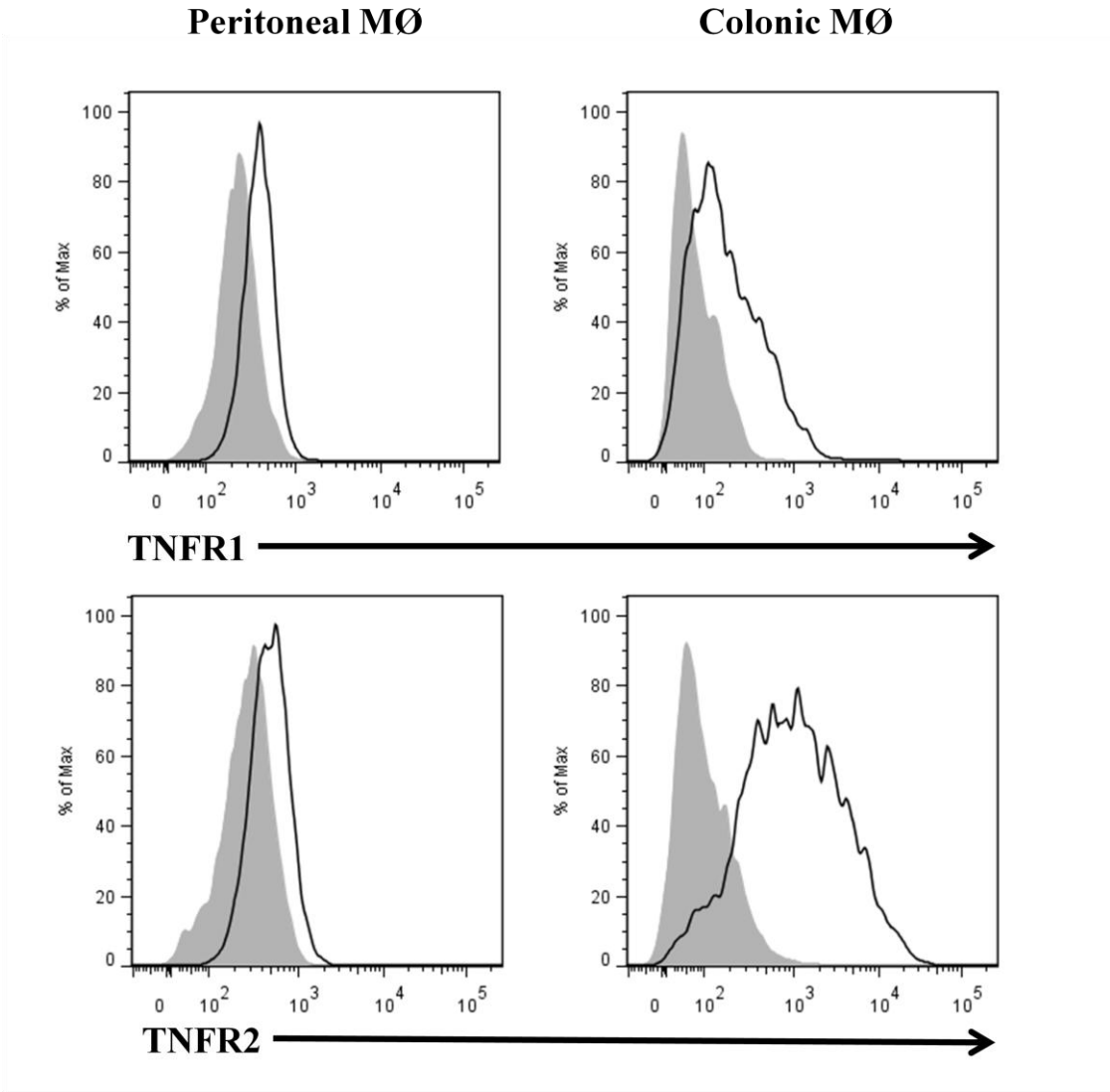

Figure 5.1 Colonic MØ have higher expression of TNFR2 than peritoneal MØ. Cells were isolated from the peritoneal cavity and colonic tissue of BALB/c mice, stained with fluorescent antibodies against TNFR1 and TNFR2 and analysed by flow cytometry. Histograms from a representative mouse show the expression of TNF receptors on F4/80$^+$ live cells. Filled histograms represent a background fluorescence of unstained cells.

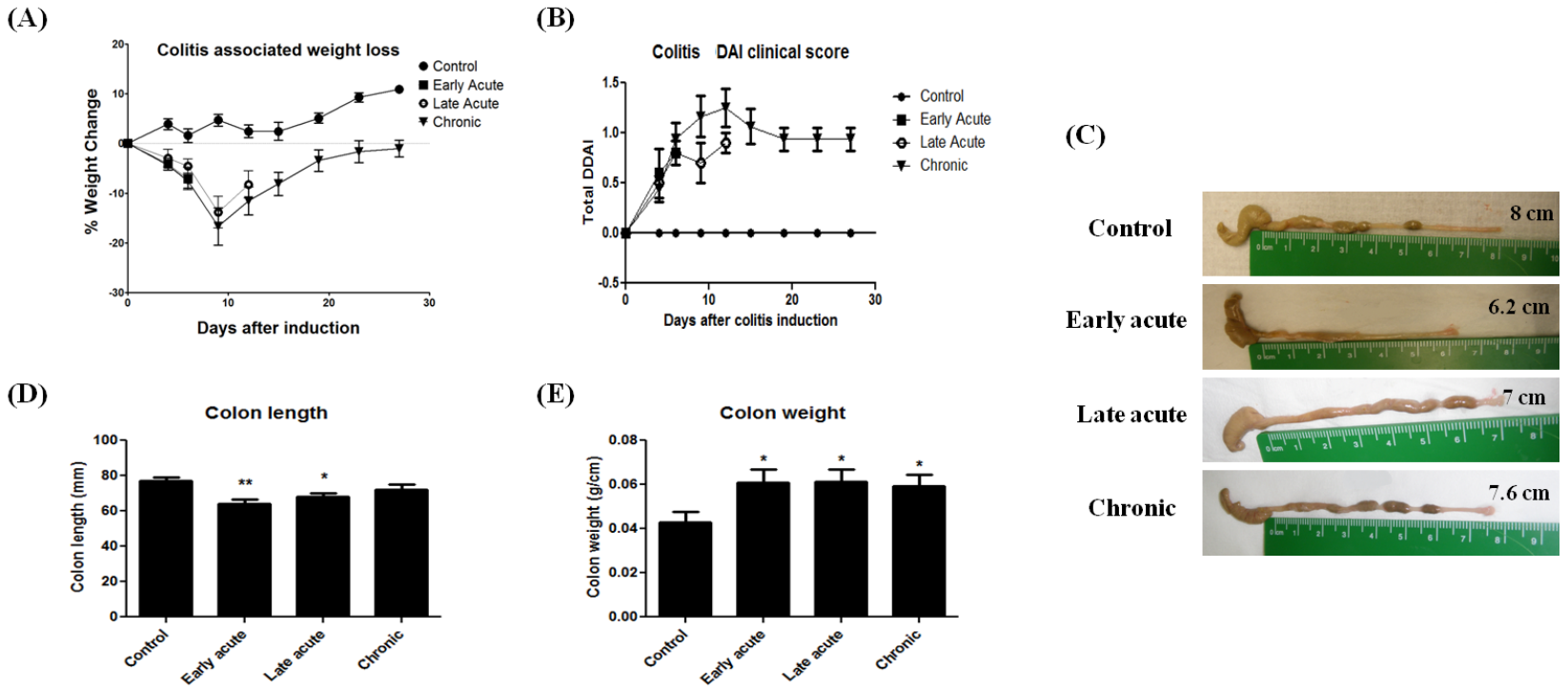

Figure 5.2 Clinical assessment of DSS-induced colitis. Mice were given 3% DSS in drinking water for 5 days, followed by water only. Mice were then sacrificed on day 7 (early acute), day 12 (late acute) and day 26 (chronic) to study the progression from the acute phase to chronic inflammation/recovery. Body weight change was calculated by dividing body weight on the specified day by starting body weight and expressed in percentage **(A)**. Daily disease activity index (DAI) scores (a combine measure of weight change, stool consistency and fur texture/posture) are reported for each experimental group. A higher score depicts a sicker animal **(B)**. Colons were removed and length **(C and D)** and weight **(E)** measured. Data presented are mean ± SEM of n=5/early acute; 5/late acute; 8/chronic and 6/control group. *P<0.05, **P<0.01 by unpaired *t*-test, compared to control.

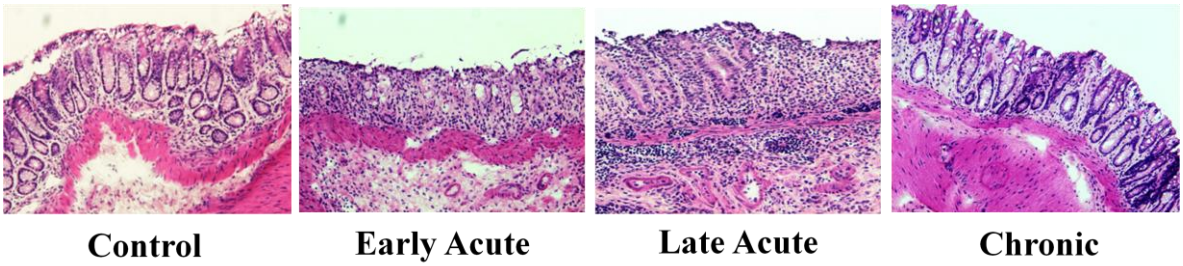

Figure 5.3 Histology of DSS-induced colitis. Sections of a distal colon were removed and stained with hematoxylin and eosin. The control is showing a healthy colon, while loss of crypts, the reduction of goblet cells and infiltration of inflammatory cells to the mucosa are visible in the early acute and the late acute phase. Regeneration of crypts and re-epithelisation is observed in the chronic phase.

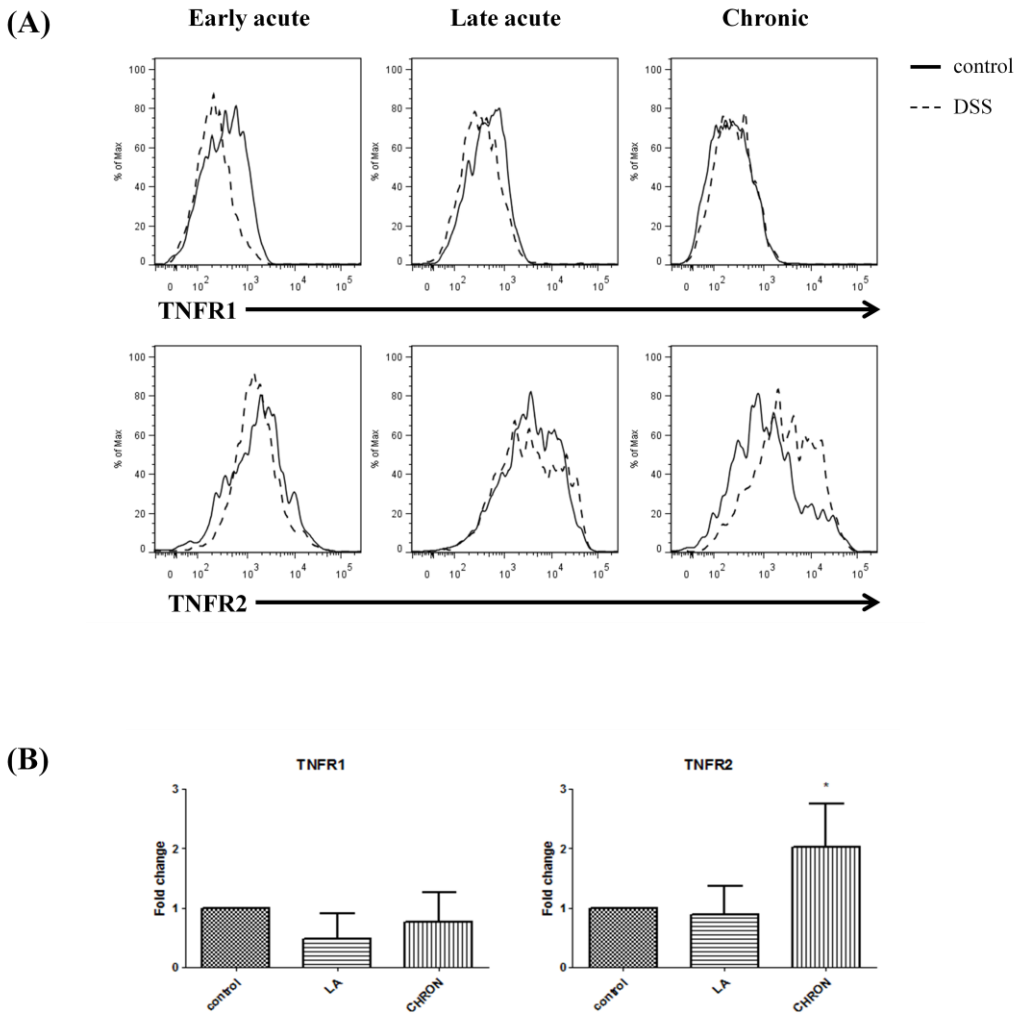

Figure 5.4 Expression of TNF receptors on colonic MØ throughout different stages of DSS colitis. Colonic lamina propria cells were isolated from the healthy controls and diseased mice in different stages of DSS colitis. Cells were stained with fluorescently labelled antibodies against TNFR1, TNFR2 and F4/80 and analysed by flow cytometry. Histograms from a representative mouse show an expression of TNFR1 and TNFR2 on F4/80^{+} live cells, compared between healthy controls (black histogram) and DSS-treated mice (dashed histogram) **(A)**. mRNA was isolated from sorted F4/80^{+} macrophages and the expression levels of TNFR1 and TNFR2 were determined by qRT-PCR. The gene expression levels were normalised to endogenous control 18S. The mean relative gene expression was calculated using the $2^{-\Delta\Delta Ct}$ method **(B)**. *P<0.05 vs. control, determined by unpaired *t*-test

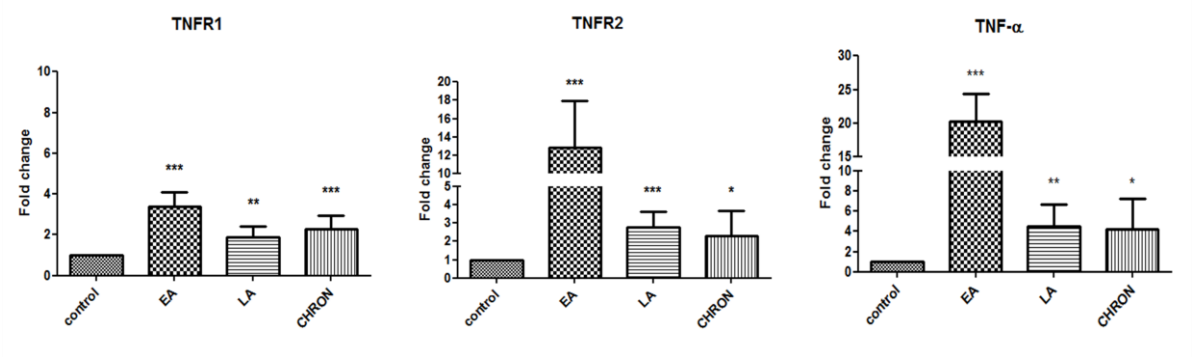

Figure 5.5 Expression of TNF receptors and TNF-α in the colonic tissue of DSS-treated mice. Tissue from each sample was homogenised using the Qiagen TissueLyser LT with stainless steel beads. Following homogenisation, mRNA was extracted using Nucleospin RNA II kit (Macherey-Nagel) and quantified on the nanodrop. Equalised ammounts of mRNA were converted into cDNA using a High Capacity cDNA Mastermix (Roche). The cDNA was mixed with primers for TNFR1, TNFR2 and TNF-α (all IDT) and analysed on the ABI Prism 7500. cDNA samples were assayed in triplicate and gene expression levels were normalised to endogenous control, 18S. The mean relative gene expression was calculated using the $2^{-\Delta\Delta Ct}$ method. Results are mean ± SEM of 6mice/control, 5mice/early acute phase (EA), 5mice/late acute phase (LA) and 8mice/chronic phase (CHRON). *P<0.05, **P<0.01, ***P<0.001 vs. control, determined by unpaired *t*-test

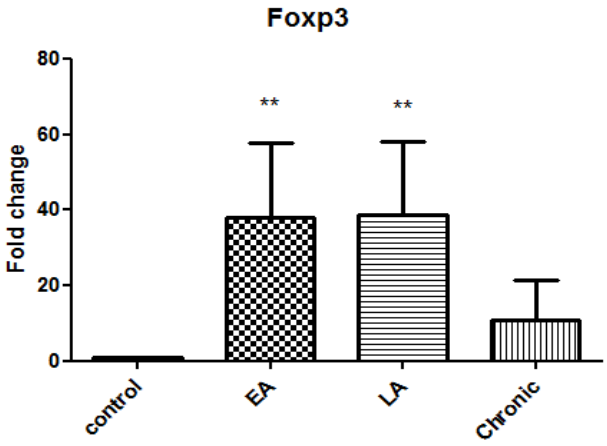

Figure 5.6 Expression of Treg transcription factor in the colonic tissue of DSS-treated mice. Tissue from each sample was homogenised using the Qiagen TissueLyser LT with stainless steel beads. Following homogenisation, mRNA was extracted using Nucleospin RNA II kit (Macherey-Nagel) and quantified on the nanodrop. Equalised ammounts of mRNA were converted into cDNA using a High Capacity cDNA Mastermix (Roche). The cDNA was mixed with primers for Foxp3 (IDT) and analysed on the ABI Prism 7500. cDNA samples were assayed in triplicate and gene expression levels were normalised to endogenous control, 18S. The mean relative gene expression was calculated using the $2^{-\Delta\Delta Ct}$ method. Results are mean ± SEM of 6mice/control, 5mice/early acute phase (EA), 5mice/late acute phase (LA) and 8mice/chronic phase. **P<0.01 vs. control, determined by unpaired *t*-test

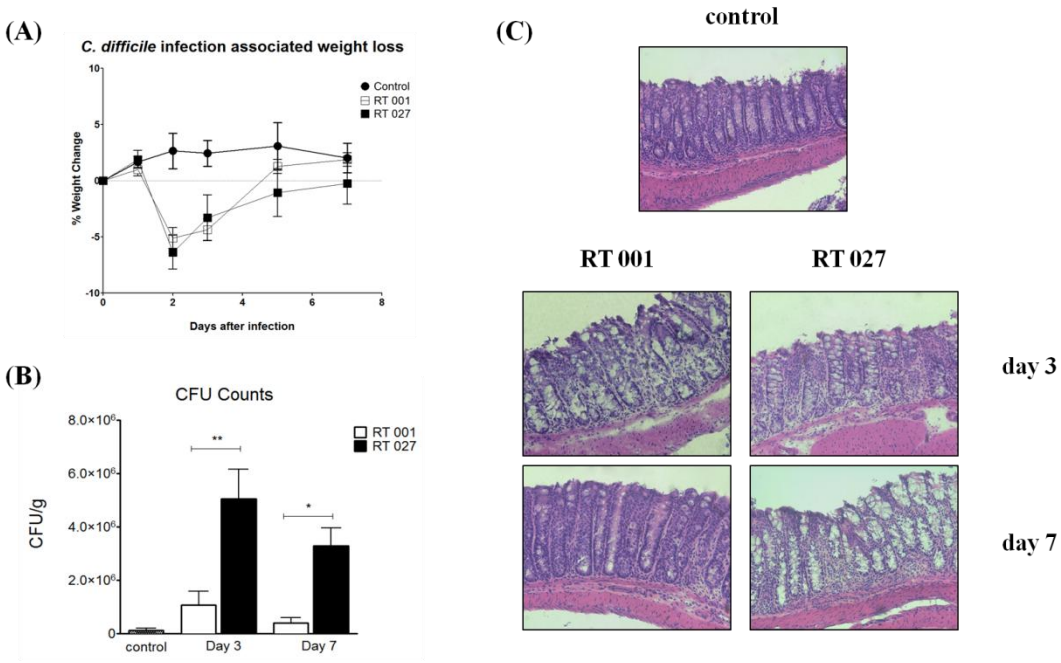

Figure 5.7 Clinical assessment of a mouse model of *Clostridium difficile* infection, using two different ribotypes. Mice were treated for 3 days with an antibiotic mixture of kanamycin (400µg/ml), gentamicin (35 µg/ml), colistin (850 U/ml), metronidazole (215 µg/ml) and vancomycin (45 µg/ml) in the drinking water. On day 5, mice were injected i.p. with clindamycin (10mg/kg). Mice were infected with 10^3 *C. difficile* spores on day 6 by oral gavage and sacrificed on day 3 and day 7 post-infection. Body weight change was calculated by dividing body weight on the specified day by starting body weight and expressed in percentage **(A)**. CFU counts in the caecum were determined for each sample **(B)**. Sections of a distal colon were removed and stained with hematoxylin and eosin. The control is showing a healthy colon. There is a loss of crypts and infiltration of inflammatory cells present on day 3 in both ribotypes, with recovery on day 7 in RT 001 infected mice, but not RT 027 infected mice **(C)**. Results are mean ± SEM of 6mice/group. *P<0.05, **P<0.01 determined by unpaired *t*-test

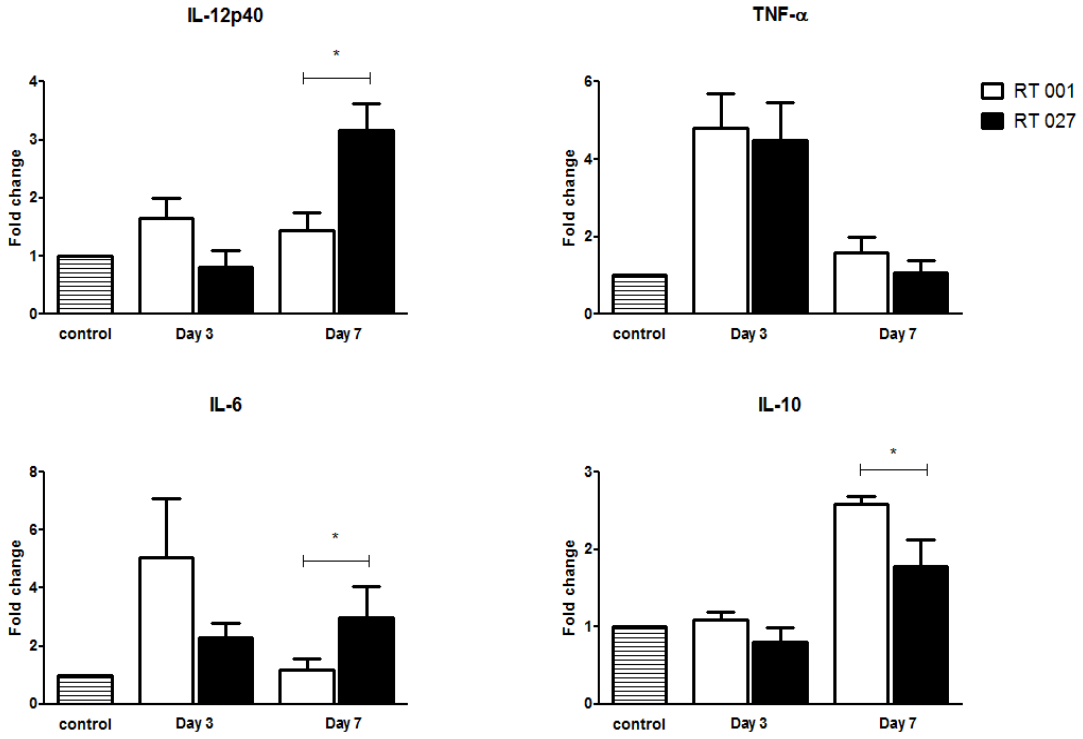

Figure 5.8 Differences in a severity of infection between 001 and 027 *C. difficile* ribotypes. Tissue from each sample was homogenised using the Qiagen TissueLyser LT with stainless steel beads. Following homogenisation, mRNA was extracted using Nucleospin RNA II kit (Macherey-Nagel) and quantified on the nanodrop. Equalised ammounts of mRNA were converted into cDNA using a High Capacity cDNA Mastermix (Roche). The cDNA was mixed with primers for IL-12p40, TNF-α, IL-6 and IL-10 (all IDT) and analysed on the ABI Prism 7500. cDNA samples were assayed in triplicate and gene expression levels were normalised to endogenous control, 18S. The mean relative gene expression was calculated using the $2^{-\Delta\Delta Ct}$ method. Results are mean ± SEM of 6 mice per group. *P<0.05 determined by unpaired *t*-test.

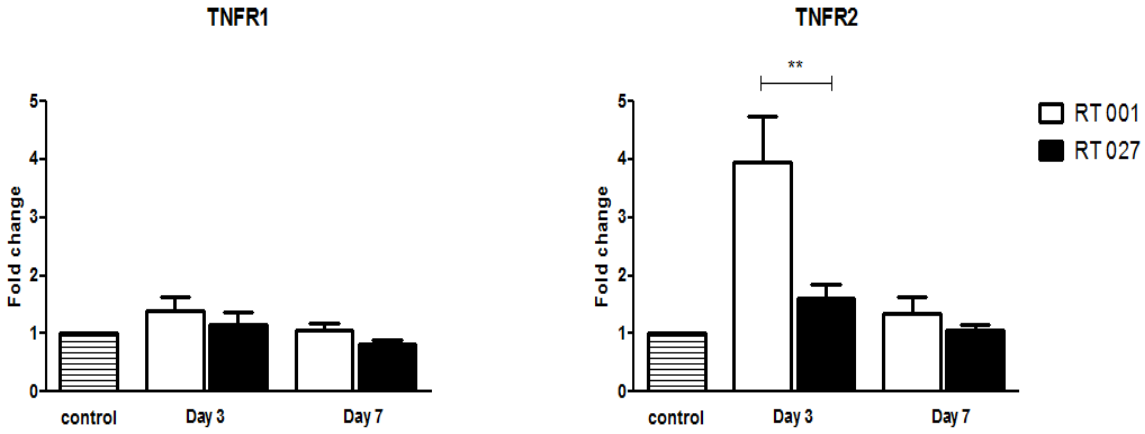

5.9 Expression of TNF receptors in the colonic tissue of *C. difficile* infected mice. Tissue from each sample was homogenised using the Qiagen TissueLyser LT with stainless steel beads. Following homogenisation, mRNA was extracted using Nucleospin RNA II kit (Macherey-Nagel) and quantified on the nanodrop. Equalised ammounts of mRNA were converted into cDNA using a High Capacity cDNA Mastermix (Roche). The cDNA was mixed with primers for TNFR1, TNFR2 (all IDT) and analysed on the ABI Prism 7500. cDNA samples were assayed in triplicate and gene expression levels were normalised to endogenous control, 18S. The mean relative gene expression was calculated using the $2^{-\Delta\Delta Ct}$ method. Results are mean ± SEM of 6 mice per group. **P<0.01 determined by unpaired *t*-test.

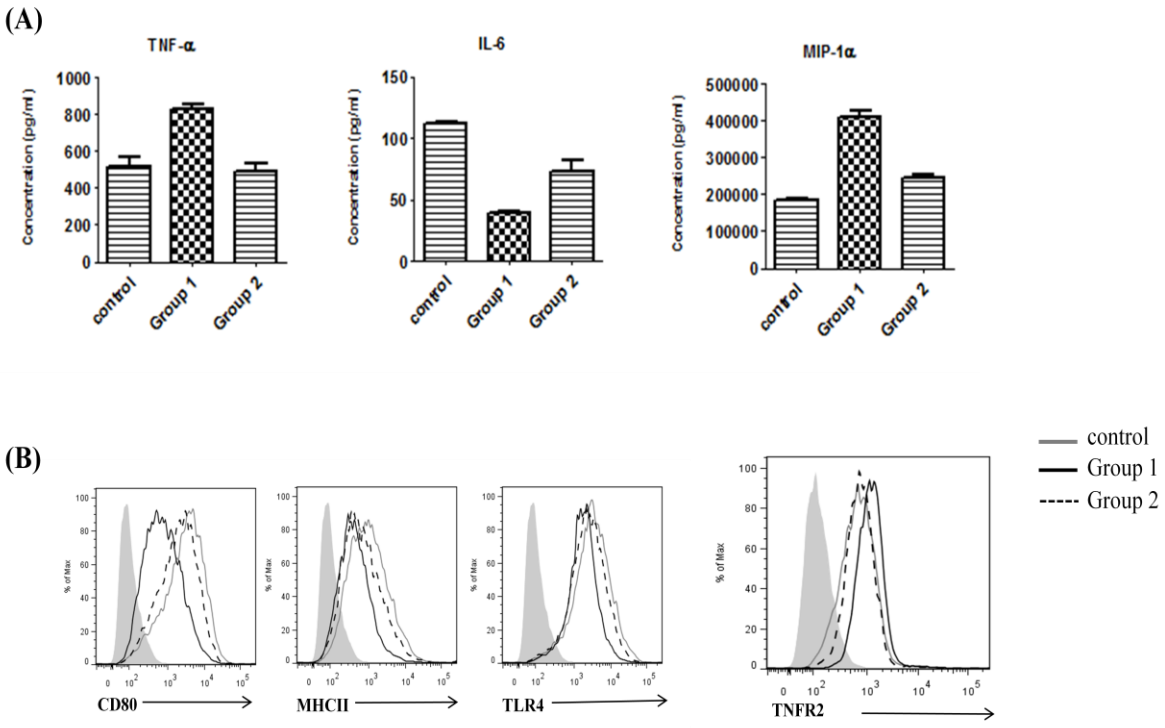

5.10 Conditioned macrophages lose their hypo-responsive phenotype when removed from epithelial cell media J774A.1 macrophages were incubated with unconditioned media (control) or CMT-93 conditioned media. After 24h, CMT-93 conditioned macrophages were split in two groups – Group 1 was incubated with fresh conditioned media for another 24h while in the Group 2 conditioned media was removed and changed with unconditioned media. Cytokine and chemokine production was measured in the collected supernatants, using ELISA (R&D) **(A)** Histograms show the expression of surface markers compared between Group 1 (black line) and Group 2 (dashed line). Grey histograms represent control cells, while the filled histograms represent the fluorescence of unstained cells **(B)**. Data are presented as mean ± SEM of three replicates and are representative of two independent experiments.

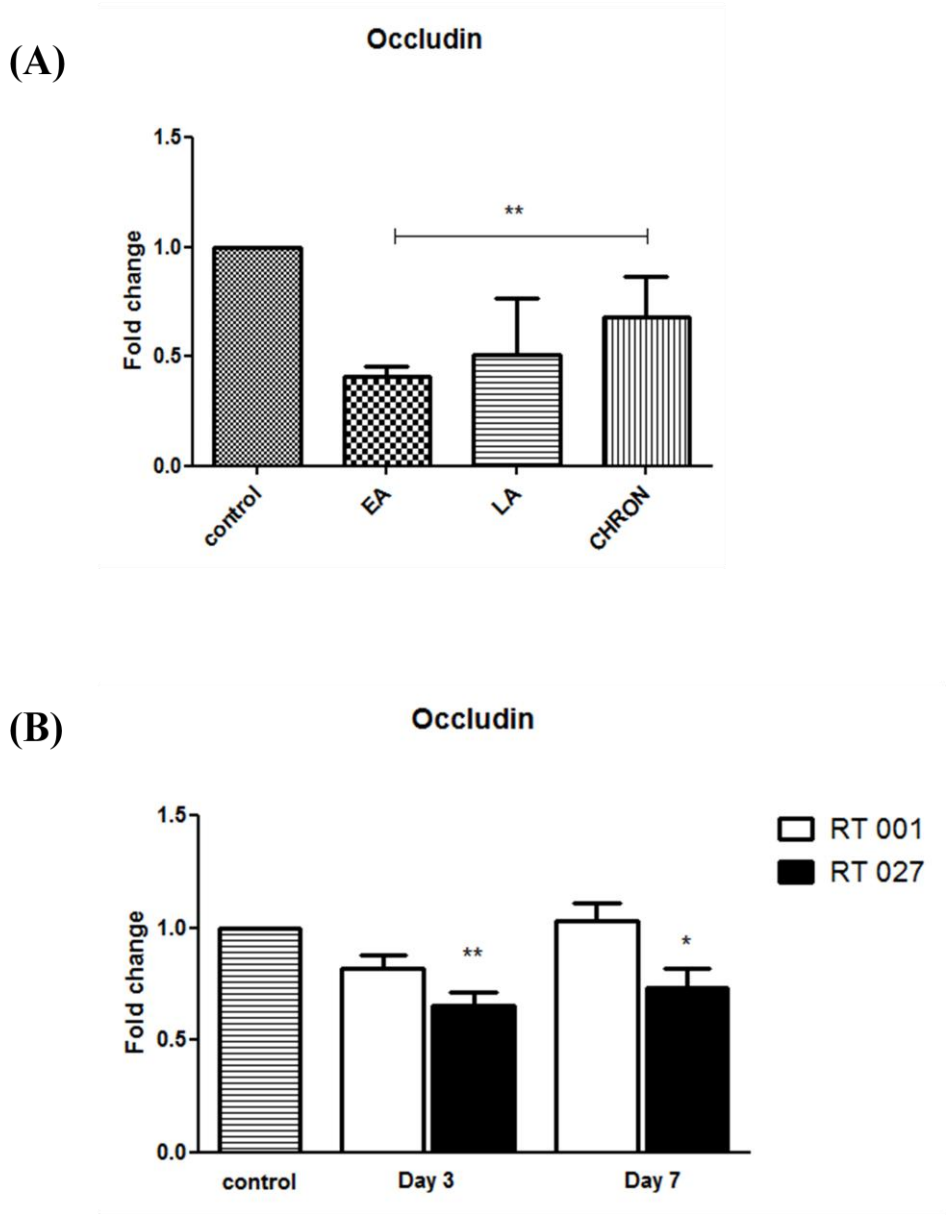

Figure 5.11 Expression of tight junction protein in the colonic tissue of DSS treated mice (A) and *C. difficile* infected mice (B). Tissue from each sample was homogenised using the Qiagen TissueLyser LT with stainless steel beads. Following homogenisation, mRNA was extracted using Nucleospin RNA II kit (Macherey-Nagel) and quantified on the nanodrop. Equalised ammounts of mRNA were converted into cDNA using a High Capacity cDNA Mastermix (Roche). The cDNA was mixed with primers for Occludin (IDT) and analysed on the ABI Prism 7500. cDNA samples were assayed in triplicate and gene expression levels were normalised to endogenous control, 18S. The mean relative gene expression was calculated using the $2^{-\Delta\Delta Ct}$ method. Results are mean ± SEM. *P<0.05, **P<0.01 EA vs. Chron, determined by unpaired *t*-test. Figure (B) shows statistical significance of sample vs. control

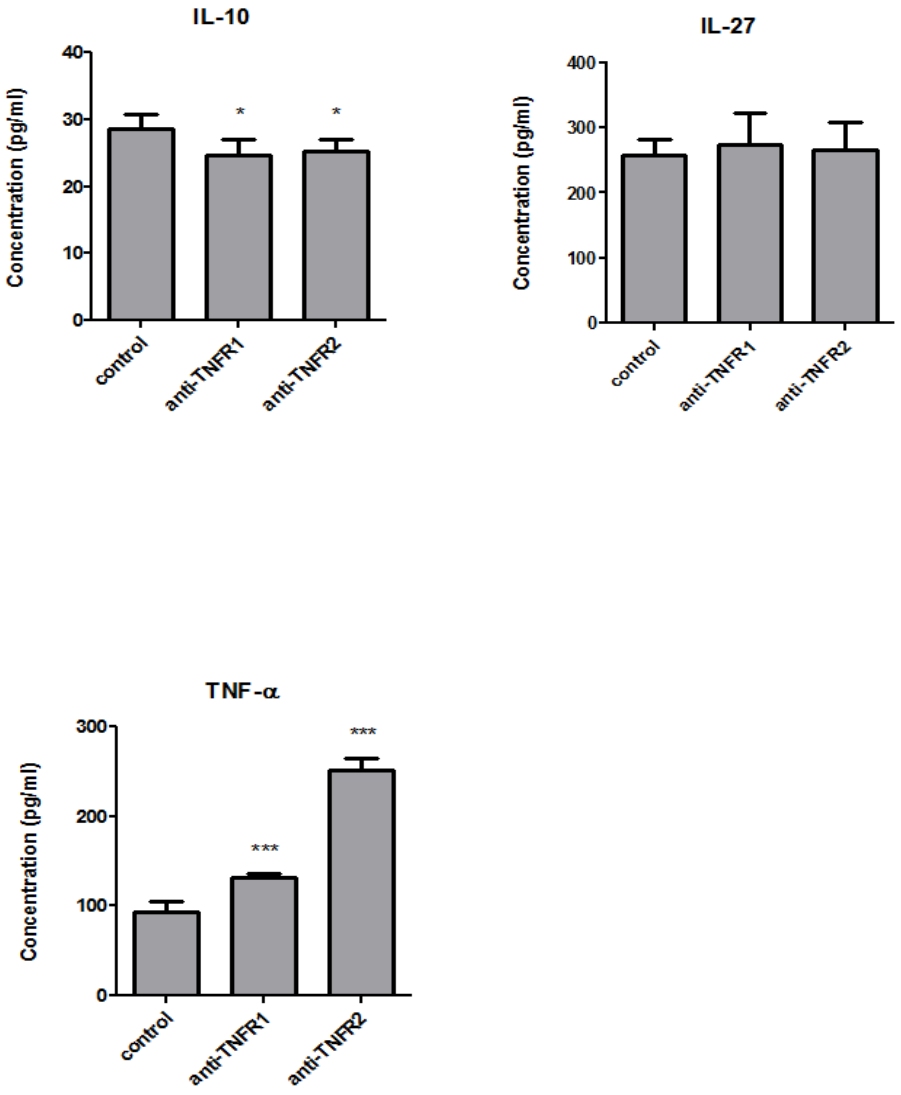

5.12 Effect of TNF receptor antagonists on cytokine secretion from steady-state macrophages J774A.1 macrophages were incubated with TNFR1 (5μg/ml; R&D) or TNFR2 (5μg/ml; Biolegend) blocking antibodies for 24h. After 24h cell supernatants were collected and cytokine secretion was measured using ELISA (R&D). Levels of IL-12p40 and IL-6 were also measured but they could not be detected. Results are mean ± SEM of three replicates and are representative of three independent experiments. Statistical significance for multiple comparisons was determined by one-way ANOVA followed by Newman-Keuls analysis.*P<0.05, ***P<0.001 vs. control (untreated cells).

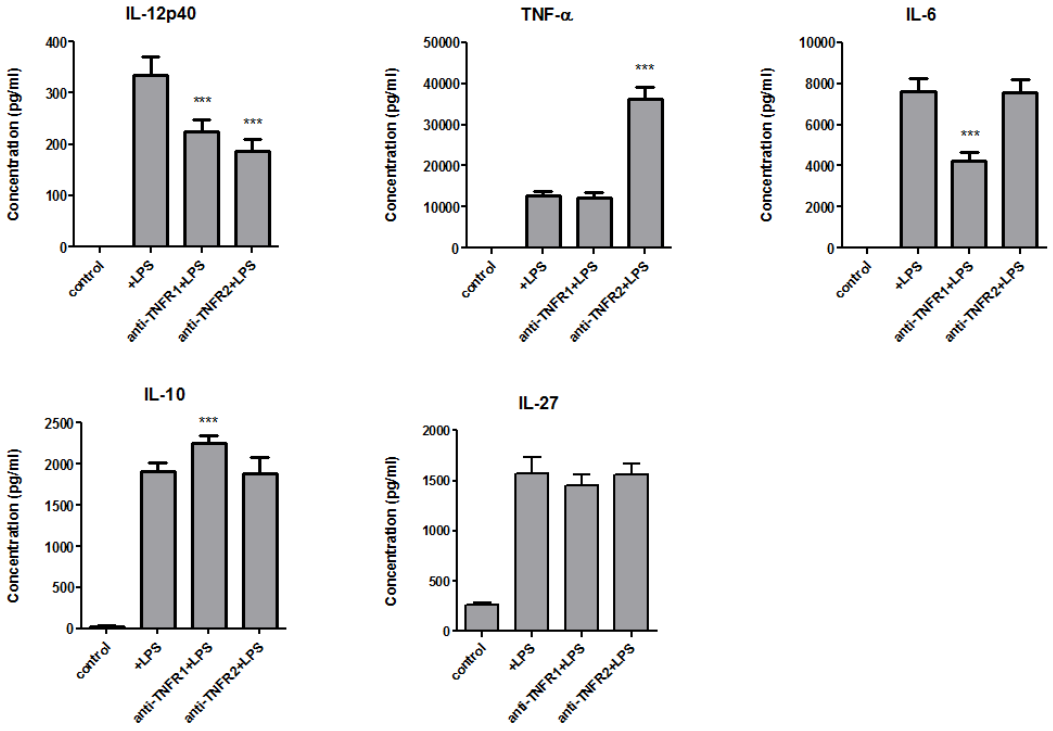

5.13 Effect of TNF receptor antagonists on cytokine secretion from LPS stimulated macrophages J774A.1 macrophages were pre-incubated with TNFR1 (5µg/ml; R&D) or TNFR2 (5µg/ml; Biolegend) blocking antibodies for 1h before being stimulated with LPS (100ng/ml). After 24h cytokine secretion was measured in the cell supernatants using ELISA (R&D). Results are mean ± SEM of three replicates and are representative of three independent experiments. Statistical significance for multiple comparisons was determined by one-way ANOVA followed by Newman-Keuls analysis. ***P<0.001 vs. LPS-treated cells

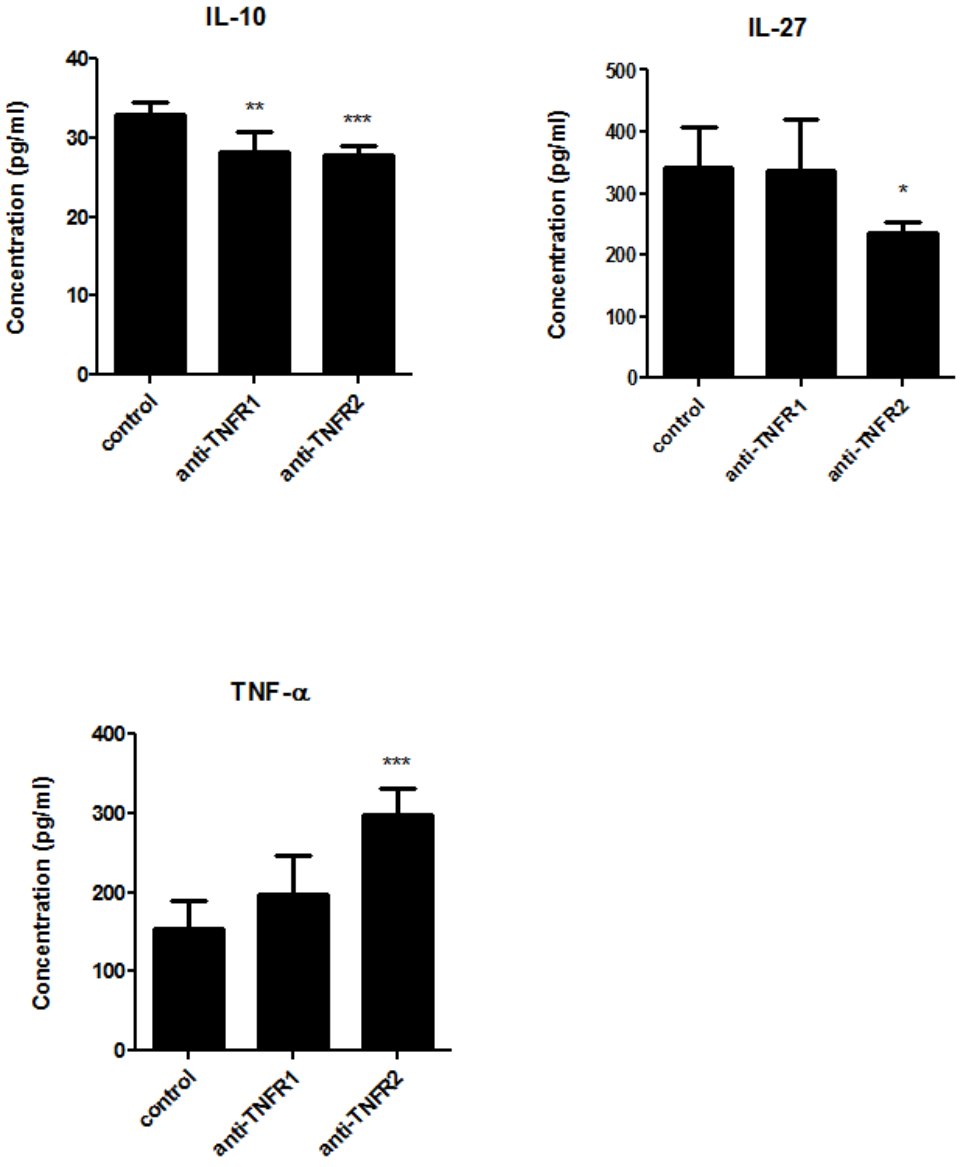

5.14 Effect of TNF receptor antagonists on cytokine secretion from conditioned macrophages J774A.1 macrophages were conditioned with colonic epithelial cell media for 24h before being treated with TNFR1 (5µg/ml; R&D) or TNFR2 (5µg/ml; Biolegend) blocking antibodies. After 24h cell supernatants were collected and cytokine secretion was measured using ELISA (R&D). Levels of IL-12p40 and IL-6 were also measured but they could not be detected. Results are mean ± SEM of three replicates and are representative of three independent experiments. Statistical significance for multiple comparisons was determined by one-way ANOVA followed by Newman-Keuls analysis.*P<0.05, **P<0.01, ***P<0.001 vs. control (untreated cells).

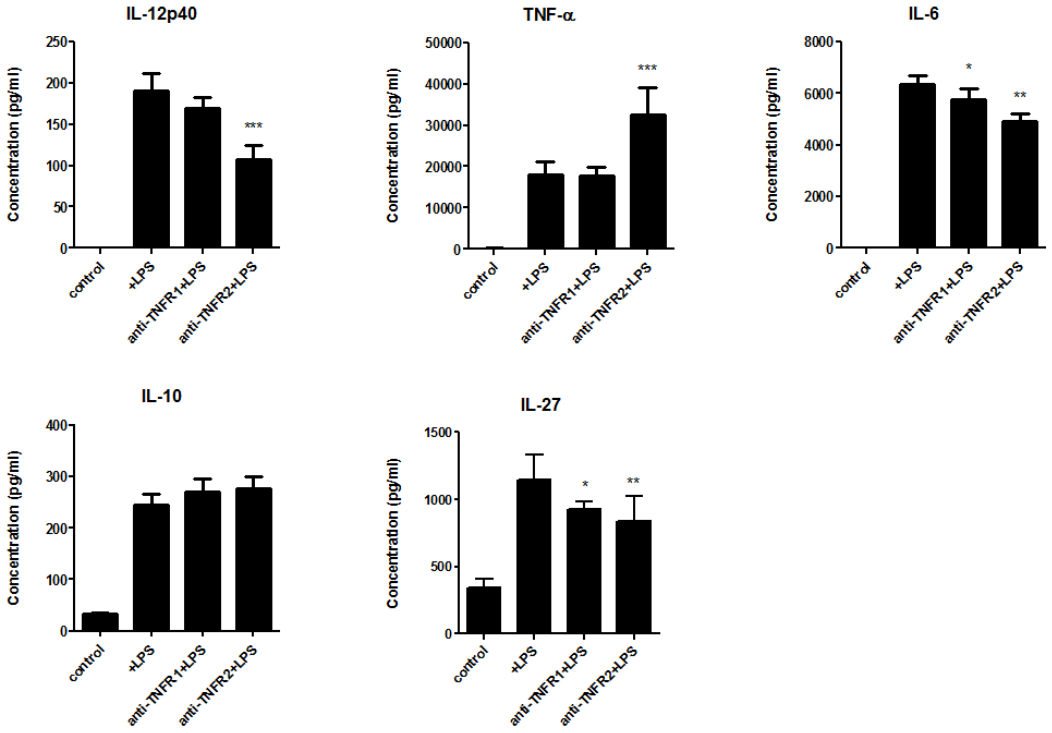

5.15 Effect of TNF receptors antagonists on cytokine secretion from conditioned LPS-stimulated macrophages J774A.1 macrophages were conditioned with colonic epithelial cell media for 24h. After 24hh cells were pre-incubated with TNFR1 (5µg/ml; R&D) or TNFR2 (5µg/ml; Biolegend) blocking antibodies for 1h and then stimulated with LPS (100ng/ml). After 24h cell supernatants were collected and cytokine secretion was measured using ELISA (R&D). Results are mean ± SEM of three replicates and are representative of three independent experiments. Statistical significance for multiple comparisons was determined by one-way ANOVA followed by Newman-Keuls analysis.*P<0.05, **P<0.01, ***P<0.001 vs. LPS stimulated cells

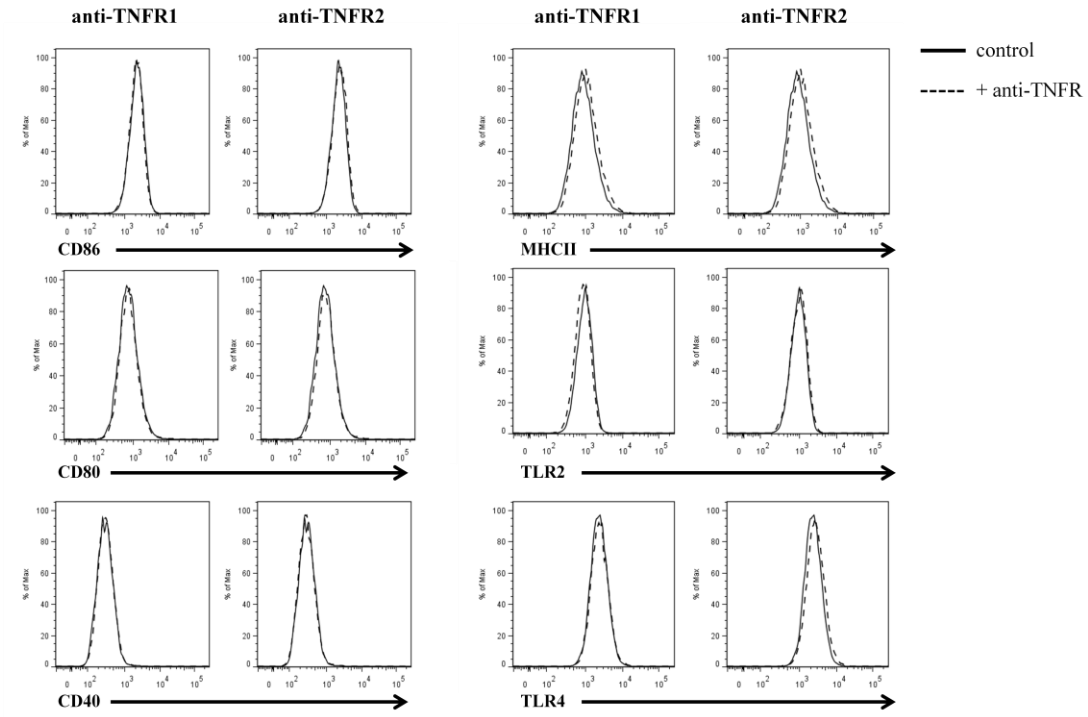

5.16 TNF receptor antagonists do not have an effect on the expression of surface markers on unconditioned macrophages J774A.1 macrophages were incubated with TNFR1 (5μg/ml; R&D) or TNFR2 (5μg/ml; Biolegend) blocking antibodies for 24h. Macrophages were then stained with appropriate antibodies and the expression of surface markers was measured by flow cytometry. Data are representative of three independent experiments.

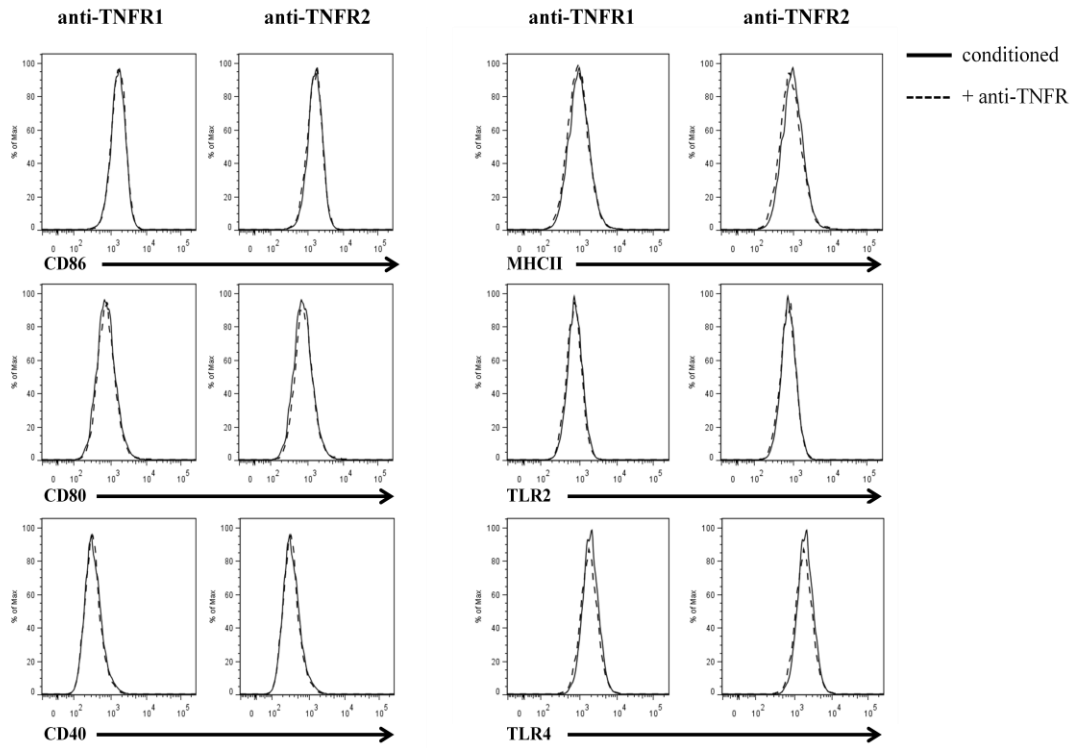

5.17 TNF receptor antagonists do not have an effect on the expression of surface markers on conditioned macrophages J774A.1 macrophages were conditioned with colonic epithelial cell media for 24h before being incubated with TNFR1 (5µg/ml; R&D) or TNFR2 (5µg/ml; Biolegend) blocking antibodies for 24h. Macrophages were then stained with appropriate antibodies and the expression of surface markers was measured by flow cytometry. Data are representative of three independent experiments.

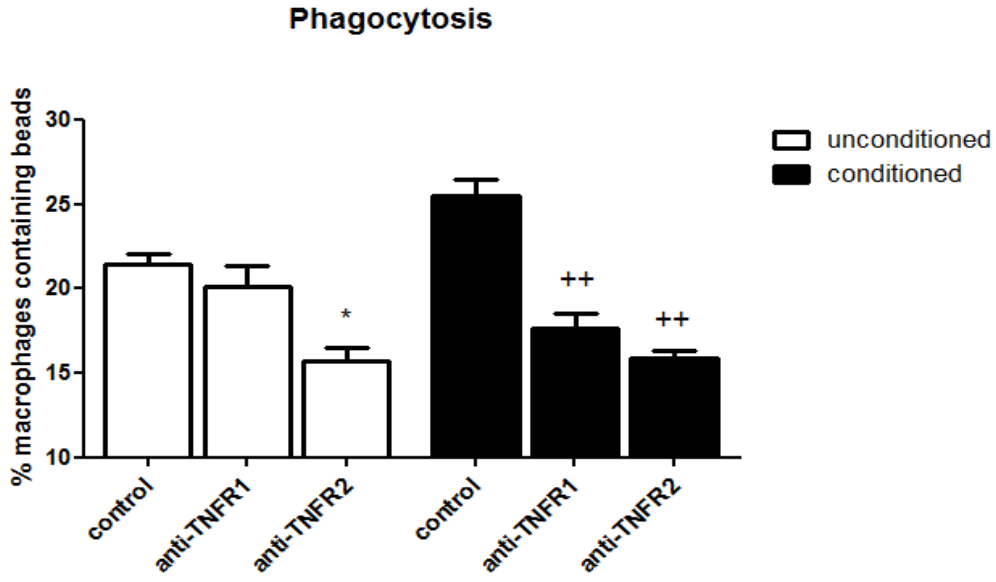

5.18 Phagocytosis is down-regulated in response to TNF receptor blocking antibodies J774A.1 macrophages were incubated with conditioned or unconditioned medium for 24h, before being treated with TNFR1 (5µg/ml; R&D) or TNFR2 (5µg/ml; Biolegend) blocking antibodies. After 24h fluorescent latex beads (Sigma-Aldrich) were added to the culture and macrophages were left to phagocytose for 1h. The uptake of beads was then measured by flow cytometry. Results are shown as mean ± SEM of three replicates and are representative of three independent experiments. Statistical significance for multiple comparisons was determined by one-way ANOVA followed by Newman-Keuls analysis. *$P<0.05$ vs. unconditioned control and $^{++}P<0.01$ vs. conditioned control

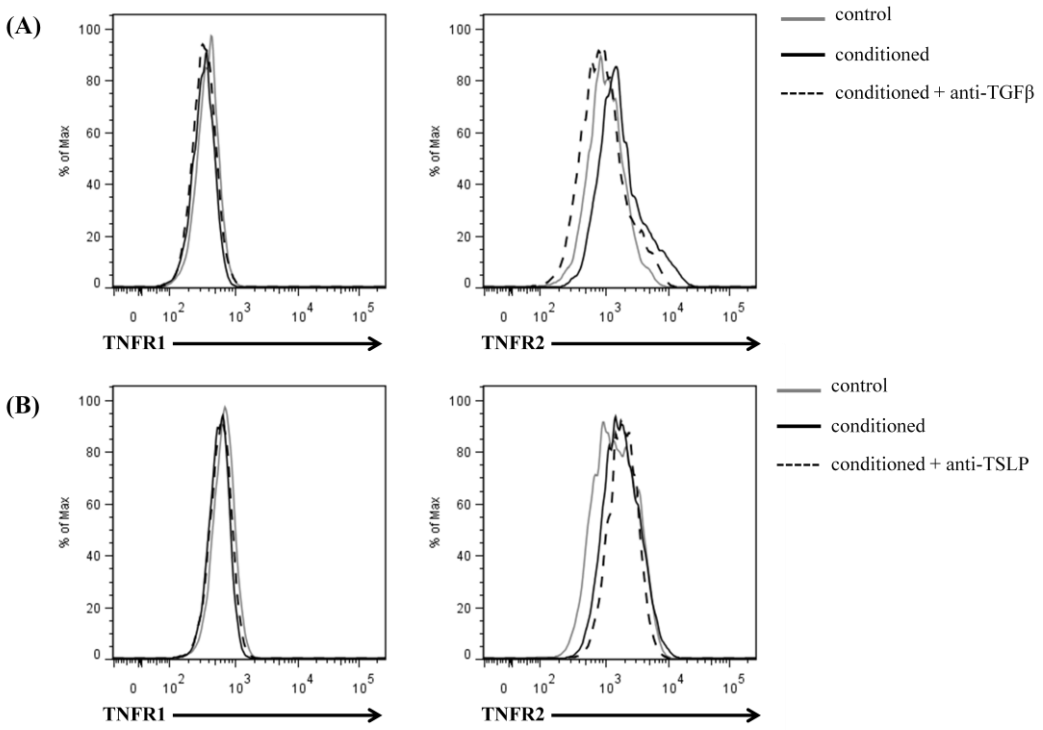

5.19. Neutralisation of TGF-β, but not TSLP, in conditioned media down-regulates macrophage TNFR2 expression J774A.1 macrophages were cultured with unconditioned media or CMT-93 supernatants that contained TGF-β neutralising antibody (10μg/ml; R&D) **(A)** or TSLP neutralising antibody (10μg/ml; R&D) **(B)**. After 24h cells were stained with fluorescently labelled antibodies against TNFR1 and TNFR2 and the expression of receptors was determined by flow cytometry. Data are representative of three independent experiments.

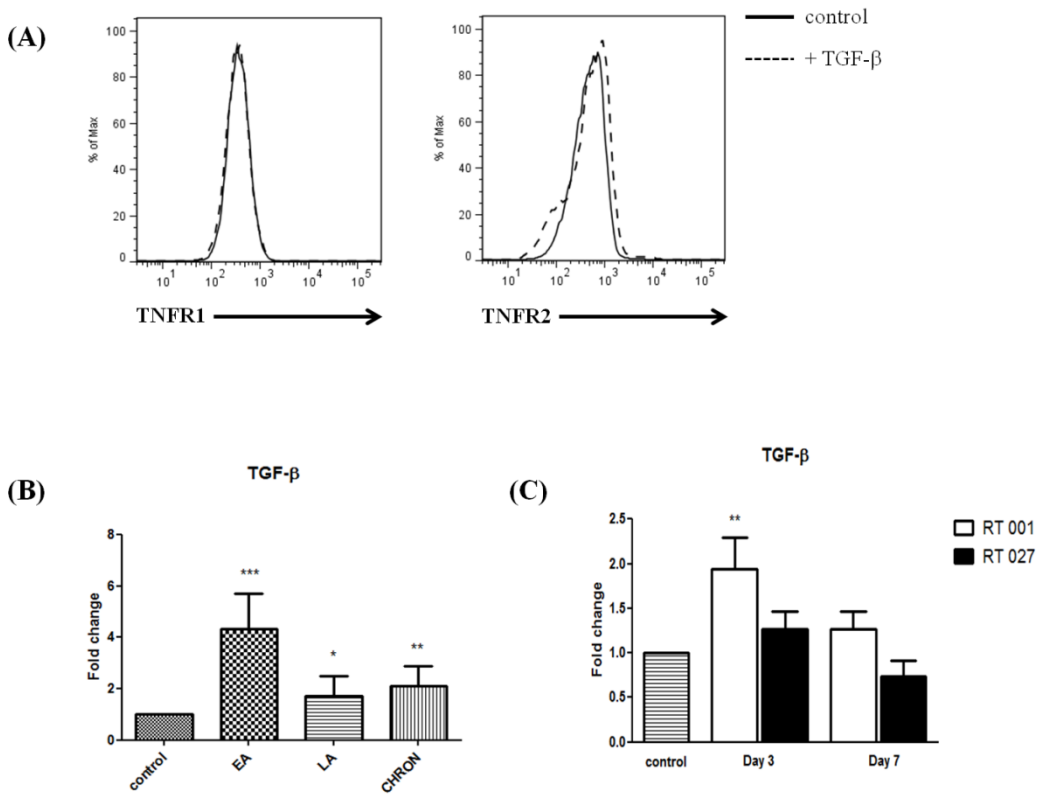

5.20 TGF-β induces TNFR2 expression *in vitro* and correlates with TNFR2 expression *in vivo* J774A.1 macrophages were cultured with recombinant TGF-β (10ng/ml; R&D) or media alone as a control. After 24h hours cells were labelled with fluorescent antibodies against TNFR1 and TNF2 and the expression of receptors was measured by flow cytometry **(A)**. The expression of TGF-β in the colonic tissue of DSS treated mice **(B)** or *C. difficile* infected mice **(C)** was measured by qRT-PCR. cDNA samples were assayed in triplicate and gene expression levels were normalised to endogenous control, 18S. The mean relative gene expression was calculated using the $2^{-\Delta\Delta Ct}$ method. Results are mean ± SEM. *P<0.05, **P<0.01, ***P<0.001 vs. control, determined by unpaired *t*-test

5.4 DISCUSSION

In chapter 4 we showed that soluble factors secreted by colonic epithelial cells can induce anti-inflammatory, colonic macrophage-like phenotype in monocyte-derived macrophages. This was accompanied by an increase of TNFR2, but not TNFR1 on conditioned macrophages. In this chapter, therefore, we sought to investigate the importance of macrophage TNFR2 *in vivo* and the role of TNFR2 in homeostasis and disease.

Firstly, we wanted to investigate the expression of TNFR2 on colonic macrophages in a healthy mouse. Peritoneal macrophages, as another example of tissue macrophages, were used as a comparison. Peritoneal macrophages are extensively studied as they can be easily obtained from a peritoneal cavity. Unlike colonic macrophages they respond to stimulation, produce pro-inflammatory cytokines and have high expression of co-stimulatory receptors (Marcinkiewicz, 1991, Wang *et al.*, 2013a). Here we show that the expression of TNFR2 is much higher on colonic macrophages than on peritoneal macrophages. Considering the homeostatic role of colonic macrophages in the intestine and increasing evidence of TNFR2 in immunosuppressive signalling (Kassiotis and Kollias, 2001, Fontaine *et al.*, 2002, Hamid *et al.*, 2009), we hypothesised that TNFR2 on macrophages contributes to the regulation of gut homeostasis.

To examine this idea further we investigated the role of TNFR2 in disease. We used two different mouse models, DSS-induced colitis and *C. difficile* associated intestinal infection, both of which affect the lower intestinal tract, especially the

colon. Dextran sulfate sodium induced colitis is a well appreciated and widely used model of inflammatory bowel disease. Colitis is induced by addition of DSS to drinking water. DSS is toxic to colonic epithelial cells and induces the break-down of the epithelial barrier function (Poritz *et al.*, 2007). This allows the entry of microorganisms and antigens from the lumen which then results in activation of immune cells and inflammation. It is characterised by weight loss, blood in the stool, diarrhea and infiltration of immune cells into the lamina propria and submucosa (Kullmann *et al.*, 2001). Depending on the concentration, duration and frequency of DSS administration, mice can develop acute or chronic colitis (Okayasu *et al.*, 1990a). In our study, DSS was administered for 5 days, followed by 21 days of water. The first group of mice was sacrificed on day 7 which correlates with the early acute phase, the second group was sacrificed on day 12 corresponding to late acute phase and finally the chronic phase group was sacrificed on day 26. Although by day 26 mice did not completely recover, we could observe regeneration of crypts and re-epithelisation, the length of the colon returning to control levels, a gain in weight and improvement in the DAI scores. This recovery correlated with the increased expression of TNFR2 on colonic macrophages, both at the protein and mRNA levels, indicating that TNFR2 may be supporting the recovery process. An anti-inflammatory role for TNFR2 in disease has been reported previously. Kontoyiannis *et al.* showed that in the mouse model of rheumatoid arthritis (RA), TNFR2-deficient mice showed much more aggressive and destructive type of arthritis with enhanced swelling of the joints and enhanced destruction of bone and cartilage, compared to wild-type (Kontoyiannis *et al.*, 1999). In addition another group showed that transplantation of bone-marrow cells lacking TNFR2 into human TNF-transgenic mice, which spontaneously develop arthritis, leads to the

development of a more severe inflammation with increased levels of joint destruction and an increase in bone erosion and osteoclast numbers (Bluml *et al.*, 2010). Interestingly, both groups reported that deficiency in TNFR1 leads to reduced disease pathology.

With this in mind, we expected that the mRNA levels of TNFR2 in colonic tissue would also increase with recovery. However, we observed significantly higher levels of TNFR2 in all stages of DSS colitis, but the peak of expression was in the early acute stage at day 7. Another cell type that preferentially expresses TNFR2 is regulatory T-cells (Treg). TNFR2 plays an important role in Treg biology by promoting their expansion and function (Chen *et al.*, 2007). Indeed, TNFR2-deficient Treg have reduced ability to prevent experimental colitis *in vivo* (Housley *et al.*, 2011). Using a distinct marker for Treg, Foxp3 (Sakaguchi, 2005), we showed that there is a high expression (40-fold increase in mRNA) of $Foxp3^+$ cells in the acute phase of DSS colitis, but not in the chronic phase. This could contribute to the peak of TNFR2 we are seeing in the acute phase. Furthermore, TNFR2 is up-regulated on colonic epithelial cells in patients with inflammatory bowel disease (IBD) and mice with experimental colitis (Mizoguchi *et al.*, 2002). However unlike on Treg, epithelial cell TNFR2 may be involved in the perpetuation of inflammatory processes and altered epithelial cells functions (Mizoguchi *et al.*, 2002). It is possible that high TNFR2 expression in the early acute phase, when the disease is in full force, is therefore coming from both Treg and epithelial cells, but with a different role. In the late acute phase, anti-inflammatory TNFR2 on Treg might slowly start to tip the balance towards recovery and then in the chronic phase macrophage TNFR2 might serve as a mechanism to restore the homeostasis.

To further examine this potential role of TNFR2 in resolution or/and homeostasis, we used another animal model of disease; *C. difficile* associated infection. *Clostridium difficile* is a Gram-positive, anaerobic, spore-forming intestinal pathogen. It is the leading source of hospital-acquired infections causing antibiotic-associated diarrhea and pseudomembranous colitis (Bartlett *et al.*, 1978, McDonald *et al.*, 2006). The use of almost any antibiotic can lead to *C. difficile* infection (Owens *et al.*, 2008) and the epidemiology of the disease is constantly changing due to the emergence of new virulent strains (McDonald *et al.*, 2005). We used two different ribotypes of *C. difficile,* 001 and 027, with 027 being a more virulent strain (McDonald *et al.,* 2005). This gave as an opportunity to investigate the difference in immune response towards this pathogen. As expected, while both infections peaked at day 2 and 3, mice infected with RT 001 recovered more quickly. Mice infected with RT 027 had a significantly higher number of *C. difficile* spores in the ceacum on day 3 compared to RT 001 mice and the spore count remained high even on day 7. This correlated with the cytokine data, with mice infected with RT 027 having high expression of pro-inflammatory IL-12p40 and IL-6 mRNA on day 7, while the expression of these cytokines in RT 001 infected mice returned to control levels. Furthermore, expression of anti-inflammatory IL-10 was lower in RT 027 infected mice than RT 001 on day 7. Since IL-10 is an immunoregulatory cytokine which ameliorates the excessive Th1 and $CD8^+$ T cell response during infection (Couper *et al.*, 2008), this further supports slower disease resolution in RT 027 infected mice. Interestingly, when we investigated the expression of TNFR2 in these mice, up-regulated TNFR2 was seen in RT 001 infected mice on day 3. Considering that mice infected with RT 001 have a milder disease profile and recover more quickly, it is

possible that TNFR2 aids in recovery. Unfortunately, since the mice had to be sacrificed in Cork and only snap-frozen tissue was collected and brought to our lab, we were not able to isolate colonic macrophages to confirm this high TNFR2 expression. However, we did show that Foxp3 expression could not be detected in the tissue; therefore TNFR2 is most likely coming from the cells of innate immunity. It would be interesting to isolate colonic macrophages and evaluate the expression of TNFR2 during infection with these two strains. The importance of colonic macrophages in the resolution of *C. difficile* infection is further highlighted in the work by Inui *et al.* showing that mice deficient in CX3CR1, which is a newly identified marker for colonic macrophages (Pabst and Bernhardt, 2010, Medina-Contreras *et al.*, 2011), had increased inflammation following *C. difficile* challenge (Inui *et al.*, 2011). It is possible that more virulent RT 027 somehow stops the up-regulation of TNFR2 disabling it from exhibiting anti-inflammatory properties, while this is not the case in RT 001 infection, which then can be resolved. Our group has shown that *C. difficile* surface layer proteins (SLPs) are recognised by antigen-presenting cells through TLR4 (Ryan *et al.*, 2011). Sequences of SLPs are highly variable between strains which can then potentially affect how they are recognised by the innate immune system and therefore may explain why some strains cause more severe infections (Ryan *et al.*, 2011). SLPs from RT 027 might escape the host defence by not activating the immunosuppressive TNFR2 which may then enable pathogen dissemination and more severe pathology. This however needs further investigation.

Since we have shown in chapter 4 that colonic epithelial cell conditioning is needed to induce TNFR2 up-regulation, we were interested to see what would happen if

macrophage – epithelial cell crosstalk was deregulated. *In vitro,* when conditioned macrophages were removed from epithelial cell media, they lost their anti-inflammatory properties and TNFR2 expression returned to normal (lower) levels. In DSS-induced colitis, dextran sulphate sodium induces epithelial cell degeneration and necrosis, leading to the break-down in epithelial barrier function (Araki *et al.*, 2010). The loss of epithelial barrier function is associated with the loss of the tight junction proteins, such as occludin (Mennigen *et al.*, 2009) and we have shown that occludin mRNA levels are down-regulated in the early acute colitis, with the recovery towards the chronic phase. It is, therefore, possible that the recovery of epithelial cells in the chronic phase is responsible for "sending a signal" for the up-regulation of TNFR2 on macrophages. Epithelial disruption in the acute phase would then explain the inability of macrophages to up-regulate TNFR2 earlier in order to resolve the inflammation and return to homeostasis. This epithelial cell-macrophage crosstalk is further supported in the *C. difficile* model, when on day 3 occludin mRNA levels are significantly down-regulated in RT 027 infected mice, but not RT 001. Consequently TNFR2 is up-regulated in RT 001 infection, but the epithelial cell "signal" for TNFR up-regulation is lost in RT 027 infection.

To get further insight into the role of TNFR2 on macrophages, we decided to specifically block TNFR1 or TNFR2 signalling *in vitro* and analyse macrophage response in steady-state and after LPS stimulation. Blocking of either of the TNF receptor induced a decrease in IL-10 in unstimulated macrophages, although this change was really small and we cannot be sure how physiologically relevant it is. While the TNFR1 antagonist marginally induced the production of TNF-α from steady state macrophages, TNFR2 antagonist, to our surprise, caused complete over-

production of TNF-α (levels of TNF-α doubled). This was mimicked when the cells were incubated with TNFR2 antagonist for 1h before stimulation with LPS (levels of TNF-α in the cell supernatant increased from 10ng/ml to 35ng/ml). TNFR1 antagonist, on the other hand, did not have an effect on LPS-induced TNF-α production. Blocking of TNFR1, however, seemed to induce an anti-inflammatory response to LPS, with decreased IL-6 levels and increased IL-10 levels. The response of conditioned cells was similar and again we observed marked over-production of TNF-α when TNFR2 was blocked. This data suggests that the role of TNFR2 might be in limiting TNF-α production or in controlling the levels of TNF-α. If we look at our mRNA data from colonic tissue in both disease models, we can see that TNF-α is up-regulated at the same time as TNFR2, therefore it is possible that TNFR2 is trying to "mop up" the excessive TNF production or direct it towards immunosuppressive effects. Interestingly, in the *C. difficile* model RT 027 infected mice have up-regulated TNF-α expression on day 3, but do not up-regulate TNFR2 which then correlates with more severe infection in these mice. TNF-α has also been shown to selectively inhibits IL-12p40 transcription in human monocyte-derived macrophages (Ma *et al.*, 2000). Our data also shows that by blocking TNFR2 TNF-α levels go up while IL-12p40 levels go down. Furthermore, in chapter 4 we showed that while conditioned macrophages produce TNF-α, their IL-12p40 levels are always down-regulated. This indicates a regulatory mechanism between these two cytokines which might be regulated by TNFR2 as suggested by a new study by Martin *et al.* (Martin *et al.*, 2013).

Another interesting observation was that while TNFR1 and TNFR2 antagonists did not have an effect on IL-27 production from unconditioned macrophages, IL-27

secretion from conditioned macrophages was down-regulated if TNFR2 was blocked. This was interesting because IL-27 has been shown to be important for limiting intestinal inflammation in a murine model of colitis (Troy *et al.*, 2009). In this model, IL-27-IL27R interactions controlled the balance of pro-inflammatory cytokine production by intestinal $CD4^+$ T cells, decreased the accumulation of neutrophils and monocytes and decreased pro-inflammatory cytokine production by neutrophils (Troy *et al.*, 2009). Furthermore, recombinant human IL-27 inhibited differentiation of both human and mouse Th17 cells and significantly reduced the severity of the 2,4,6-trinitrobenzene sulfonic acid (TNBS)-induced acute colitis in mice (Sasaoka *et al.*, 2011). TNFR2 signalling might therefore contribute to IL-27 production in the intestine, potentiating the immunosuppressive effect. This immunosuppressive effect of TNFR2 was further supported by our finding that functional TNFR2 is needed for phagocytosis. Blocking of TNFR2 signalling decreased the number of phagocytic macrophages. Interestingly, phagocytosis is also down-regulated in patients with IBD (Caradonna *et al.*, 2000).

Intestinal epithelial cells constitutively secrete a broad range of antimicrobial peptides that are needed for the neutralisation of luminal bacteria (Artis, 2008). They also secrete different chemokines and cytokines that have an effect on antigen-presenting cells and lymphocytes in the mucosa (Artis, 2008). Two of these cytokines have been implicated in the induction of a tolerogenic phenotype of intestinal immune cells; thymic stromal lymphopoietin (TSLP) and transforming growth factor β (TGF-β). TSLP is produced mainly by non-hematopoietic cells and it is important for the activation of myeloid dendritic cells in the thymus and for the positive selection of regulatory T-cells (Watanabe *et al.*, 2004). In *in vitro* studies

Rimoldi *et al.* demonstrated that TSLP secreted from intestinal epithelial cells can limit the expression of IL-12 by dendritic cells and their capacity to promote Th1 cell differentiation (Rimoldi *et al.*, 2005). Furthermore, these dendritic cells produced IL-10 and promoted Treg responses in a TSLP-dependent manner (Rimoldi *et al.*, 2005). Together with TSLP, TGF-β has been shown to induce a tolerogenic phenotype in monocyte-derived dendritic cells *in vitro* (Zeuthen *et al.*, 2008). TGF-β can inhibit NF-κB dependent gene expression and limit the expression of pro-inflammatory cytokines by dendritic cells and macrophages (Smythies *et al.*, 2005). Furthermore, TGF-β modulates T-cells responses in the gut (Das *et al.*, 2013). TGF-β and TSLP, therefore, were possible candidates to regulate macrophage TNFR2 expression in our experiments. In order to investigate this, we neutralised TGF-β or TSLP in CMT-93 conditioned media and investigated the expression of TNFR2 in the absence of these cytokines. While the absence of TSLP did not have an effect on TNFR2 expression, lack of TGF-β in conditioned media decreased the expression of TNFR2. This was further supported by the increase of TNFR2 when macrophages were cultured in the presence of recombinant TGF-β. Furthermore, the expression of TGF-β in colonic tissue of DSS-treated and *C. difficile* infected mice correlated with the up-regulated expression of TNFR2.

Taken together our data implicates TGF-β as a possible signal from intestinal epithelial cells, involved in the regulation of macrophage TNFR2 expression. However, TGF-β most likely is not the only signal for TNFR2 up-regulation. Even though its expression was high in early and late acute phase of DSS-colitis, macrophages did not exhibit TNFR2 up-regulation in these stages. Presence of other soluble mediators from epithelial cells might also be involved in this mechanism.

Another possibility is that TNFR2 regulation depends on a certain isoform of TGF-β. TGF-β exists in at least three isoforms, TGF-β1, TGF-β2 and TGF-β3 (Cheifetz *et al.*, 1987). Interestingly, TGF-β2 has been shown to suppress macrophage inflammatory responses in the developing intestine and protects against inflammatory mucosal injury (Maheshwari *et al.*, 2011). Therefore, more in-depth analysis of the TNFR2 - TGF-β mechanism is needed.

Thus far, TNFR2 has been implicated in deregulation of epithelial cells functions in acute colitis (Mizoguchi *et al.*, 2002), but also in expansion and function of regulatory T-cells (Chen *et al.*, 2007). Here we show that macrophage TNFR2 might have a function in disease resolution and recovery. Furthermore, its role seems to be partially driven by TGF-β production from intestinal epithelial cells, indicating the importance of crosstalk between different cells in the intestinal environment. This crosstalk gets disrupted during intestinal inflammation and finding a way to restore it might prove beneficial for the attenuation of acute and chronic intestinal inflammation.

CHAPTER 6

GENERAL DISCUSSION

6.1 GENERAL DISCUSSION

Macrophages are cells of innate immunity that play a central role in inflammation, wound healing, tissue homeostasis and tissue remodelling. They are professional phagocytes, able to clear pathogens and dying cells. They recognise pathogens through their pattern recognition receptors (such as TLRs) and initiate the immune response by presenting the antigens to surrounding lymphocytes, while secreting a variety of cytokines and chemokines to attract and activate other immune and non-immune cells (Gordon, 2007). The largest pool of macrophages in the body is the intestine (Hume, 2006). Macrophage numbers in different parts of the intestine seem to correlate with the relative bacterial load and are, therefore, highest in the colon, where the number of commensals is 10^{13} organisms/g luminal content (Lee *et al.*, 1985). However, despite their large number and exposure to commensal bacteria, macrophages in the colon do not initiate an inflammatory cascade in response to bacterial overload. Intestinal macrophages have evolved into a specialised population of macrophages, distinct from their counterparts in other tissue, with a main goal to maintain intestinal homeostasis (Schenk and Mueller, 2007).

Intestinal macrophages are anti-inflammatory and inert to stimuli, which is surprising considering that they originate from inflammatory monocytes (Varol *et al.*, 2009). Thus, the intestinal environment must be changing and shaping the phenotype of monocytes, once they arrive in the gut, so they adapt to the antigen-rich environment. Indeed, Bain *et al.* along with Tamoutounour *et al.* proved that inflammatory blood monocytes change their phenotype and function and become anti-inflammatory intestinal macrophages, once they home to the gut (Tamoutounour

et al., 2012, Bain *et al.*, 2013). In this thesis, we show that intestinal epithelial cells play a major role in this process and provide signals that induce and support macrophage differentiation.

Monocyte-derived macrophages conditioned with intestinal epithelial cell media showed a gradual, time dependent transition into a colonic macrophage-like phenotype. We show that while short 2h conditioning time did induce change in some of the parameters, such as decrease in NO and ROS production and increase in phagocytosis, the shift towards the anti-inflammatory phenotype was more pronounced with longer conditioning. Interestingly, this correlates with *in vivo* observations by a few other groups. Using 5-bromo-2-deoxyuridine (BrdU) labelling, to track Ly6C^{hi} inflammatory monocytes, Bain *et al.* showed that these monocytes, once they arrive in the gut, differentiate into resident macrophages through a number of transitional stages, which they named P1-P4. The P1 population, which is similar to inflammatory monocytes, gradually acquires tolerogenic properties, and evolves through P2 and P3 stage into the P4 anti-inflammatory resident macrophages (Tamoutounour *et al.*, 2012, Bain *et al.*, 2013). During the first 12h from their arrival into the gut, cells went through P1 and P2 stage and after 24h they were detectable in P3 and P4 stages (Bain *et al.*, 2013). Similar to an early decrease in NO production observed in our experiments, these macrophages also show down-regulated iNOS expression (enzyme that catalyses the production of NO) early, in the P2 stage. Furthermore, correlating with our observation, a decrease in IL-6 was only visible later in P4 stage. Transition from P1-P4 was also accompanied by an increase in phagocytosis and hypo-responsiveness to TLR stimulation, which correlate with our findings (Bain *et al.*,

2013). Weber *et al.* published similar observations. They characterised two distinct macrophage populations in the colon, GFP^{lo} and GFP^{hi}, which correlate to P1 and P4 respectively, and showed that GFP^{hi} macrophages secrete significantly lower levels of IL-6, but also IL-12, the same as our conditioned macrophages (Weber *et al.*, 2011).

Both groups also reported an increase in IL-10 mRNA and protein levels from P1-P4. However, we did not see a change in IL-10 production following conditioning. The presence of local microbiota might be needed in order to induce the production of IL-10 by colonic macrophages as shown by Ueda *et al.* and Rivollier *et al.* Both groups showed that IL-10 production from colonic macrophages was severely reduced in germ free mice, compared with normal specific-pathogen-free animals (Ueda *et al.*, 2010, Rivollier *et al.*, 2012). Our closed *in vitro* system does not take into account the effect of microbiota which can therefore account for the inability of our conditioned macrophages to up-regulate IL-10. This is not the only limitation of our model. The influence of other cell types present in the gut was also not taken into consideration. Furthermore, the vectorial nature of soluble factor secretion is not assessed since CMT-93 cells were not grown in polarised state. Addressing these limitations could improve our model and give a clearer picture of epithelial cell – macrophage crosstalk.

Interestingly, macrophages from P1-P4 maintained their production of TNF-α and there was no significant difference in TNF-α mRNA levels between these populations (Bain *et al.*, 2013). Also there was no significant difference in TNF-α secretion between GFP^{lo} and GFP^{hi} populations (Weber *et al.*, 2011). This correlates

with our data showing that while soluble factor from epithelial cells decrease the production of other pro-inflammatory mediators, TNF-α is left intact. The reason for this is probably that there is an important role for TNF-α in multiple processes, such as cell differentiation, proliferation, survival and response to pathogens, and not just in tissue damage and disease progression. In fact, TNF-deficient mice have an enhanced immune and inflammatory response to DSS, compared to wild type mice, which leads to exacerbation of colitis (Naito *et al.*, 2003, Noti *et al.*, 2010). However, the question remains about the way in which TNF-α levels are controlled so that they do not lead to inflammation, but still exert other homeostatic properties. We show, for the first time, that TNF receptors, particularly TNFR2, might play a role in regulating TNF-α in the intestine and balancing its homeostatic and disease resolution properties.

As mentioned throughout this study, TNFR1 and TNFR2 mostly play opposing roles in disease, however they do share a part of the pathway and can enhance or inhibit each other's functions (Fotin-Mleczek *et al.*, 2002, Zhao *et al.*, 2007). TNFR1 pathway is one of the most studied, while the TNFR2 pathway is less clear due to its inability to be properly activated in the laboratory settings (Wajant *et al.*, 2003). Also, information about their role in diseases is often contradictory, probably because it is based on studies with TNFR1 or TNFR2 deficient animals, while in a physiological environment these two receptors exist on the same cell at the same time and their ratio could play a critical role in particular settings.

During this study we observed that, together with increased TNF-α levels, conditioned macrophages have increased expression of TNFR2 and decreased

caspase-3 activity. This led us to believe that TNFR2 plays a regulatory role, favouring the protective effects of TNF-α. The much higher expression of TNFR2 on colonic macrophages than peritoneal macrophages further supported our idea of the importance of TNFR2 in the intestinal environment. The role of TNF receptors in intestinal disease, such as DSS-induced colitis has been studied before, however, not at a cellular level. Wang *et al.* showed an opposing role of TNF receptors in DSS-induced colitis. Ablation of TNFR1 accelerated the onset and enhanced the disease, while TNFR2 ablation attenuated the severity of the colitis (Wang *et al.*, 2012). While this does not support our data indicating a protective role of TNFR2, it is interesting to mention that the authors observed an increase in apoptotic lamina propria cells in TNFR2 deficient mice (Wang *et al.*, 2012). Although they do not provide details of which particular lamina propria cells underwent increased apoptosis, this observation correlates with our data showing that increased expression of TNFR2 on conditioned macrophages protects from apoptosis. Furthermore, the authors only investigated the early acute phase of colitis, and mice were sacrificed on day 8. The early acute phase is characterised by an infiltration of many inflammatory cells into the lamina propria, with macrophages and neutrophils being amongst the first. Therefore, without the anti-apoptotic effects of TNFR2 in TNFR2-deficient mice, these cells probably undergo apoptosis, which reduces their number and consequently reduces the inflammation. This would explain the attenuated colitis seen in TNFR2 deficient mice. However, this would not be beneficial in the later stages of disease when macrophages are needed to clear the inflammation. Indeed, we show that macrophage TNFR2 is important in the later phase of colitis, probably to aid the recovery. Recently, the same group investigated the role of TNF receptors in chronic colitis and showed that TNF-α signalling via

TNFR1 and TNFR2 actually has a protective role in chronic intestinal inflammation (Wang *et al.*, 2013b). Both TNFR1 and TNFR2 deficient mice had exacerbated disease progression with increased production of pro-inflammatory cytokines and increased apoptosis of intestinal epithelial cells. The authors conclude that a distinct effect of TNF-α signalling via TNFR2 in the acute and chronic phase of colitis might be attributed to a different cell type in charge of delivering TNFR2-mediated signals at different stages of inflammation (Wang *et al.*, 2013b). It is possible that macrophages contribute to the exacerbation of chronic colitis in TNFR2-deficient mice as we have shown that TNF-α levels are significantly up-regulated when TNFR2 signalling is blocked, while their ability to phagocytose is down-regulated. Thus, while in the acute phase TNFR2 deficiency leads to apoptosis, decreases macrophage number and attenuates the disease, later in the disease the inability of macrophages to up-regulate TNFR2 and consequently control TNF-α levels and clear dead cells and debris probably supports and drives the disease. Therefore, lack of TNFR2 most likely impairs the resolution of intestinal inflammation.

The role of TNFR2 is resolution is further supported by our finding that mice infected with a less virulent 001 strain of *C. difficile*, unlike mice infected with highly virulent 027 strain, up-regulate TNFR2 and successfully clear the infection. To our knowledge the role of TNF receptors in *C. difficile* infection has not been investigated yet. However, the importance of macrophage in the clearance of *C. difficile* is demonstrated in the study by Inui *et al.* showing that mice deficient in $CX3CR1^{+}$ cells have increased inflammation following *C. difficile* challenge (Inui *et al.*, 2011). Furthermore, work in our lab has also highlighted the importance of macrophages in the clearance of *C. difficile* infection. Macrophages exposed to *C.*

difficile surface layer proteins (SLPs) from 001 strain increase their phagocytic abilities, probably as an attempt to clear the pathogen (Collins *et al*, submitted to Microbes and infection). It would be interesting to see whether SLPs from RT 027 inhibit phagocytosis and in that way cause more severe infection. That would correlate with our observation that TNFR2 expression positively regulates phagocytosis. Inability of RT 027 infected mice to up-regulate TNFR2 on day 3 of infection might, therefore, lead to inability to increase phagocytosis in response to bacteria.

TNF-α is considered to be a driving force of many inflammatory diseases, including IBD (Yapali and Hamzaoglu, 2007). Consistent with this, TNF-neutralising antibodies have been shown to successfully improve the outcome of IBD patients (Yapali and Hamzaoglu, 2007). Currently there are five different drugs targeting TNF, licensed for the treatment of various autoimmune diseases; 4 antibodies directed against TNF, infliximab, adalimumab, certolizumab, golimumab and one recombinant fusion protein of soluble TNFR2, etanercept (MacDonald *et al.*, 2012). However, only 50% of patients respond to anti-TNF therapy and the response weakens with time (Colombel *et al.*, 2010). Furthermore, therapy with anti-TNF antibodies is associated with the development of other immune-mediated diseases, such as lupus, psoriasis and increased risk of infections (Colombel *et al.*, 2010). With these adverse effects aside, infliximab and the other three TNF antibodies are still effective in maintaining long-term remission in a large number of IBD patients. However, other anti-TNF therapies, such as etanercept, a soluble TNFR2 that was design to neutralise TNF-α, or LMP-420, an inhibitor of TNF synthesis, show no effect in IBD (Sandborn *et al.*, 2001, Hale and Cianciolo, 2008). This poses a

question as to whether anti-TNF therapies do indeed work via neutralisation of TNF-α or they exhibit some other mechanisms.

Recent studies showed a few different mechanisms of action between infliximab which is effective in IBD and etanercept which is ineffective. In addition to its role in binding and neutralising TNF-α, infliximab is shown to induce apoptosis of inflammatory cells, such as T-cells and monocytes (Shen *et al.*, 2005). Etanercept, on the other hand, failed to induce apoptosis (Shen *et al.*, 2005). This could account for a better prognosis of patients treated with infliximab, because treatment with infliximab decreases the number of inflammatory cells which consequently attenuates inflammation, but it is also probably responsible for the adverse effects, such as recurrent infections. The second difference was surprising as it was shown that infliximab, but not etanercept induces the development of regulatory T-cells and regulatory macrophages (Ricciardelli *et al.*, 2008, Vos *et al.*, 2011). Infliximab binds to membrane TNF-α (mTNF) and soluble TNF-α (sTNF), unlike etanercept that only binds to sTNF (Vos *et al.*, 2011). Furthermore, infliximab can induce reverse signalling of TNF-α by ligation to mTNF (Waetzig *et al.*, 2002). It is interesting to speculate that maybe infliximab, in a way, mimics the effect of TNF receptors or induces the TNF receptor pathway upon binding to mTNF. Several groups have demonstrated that macrophages in the intestine exist in a continuum, differentiating from P1 to P4 phase, probably guided by the epithelial cells as we have shown in our study (Weber *et al.*, 2011, Tamoutounour *et al.*, 2012, Bain *et al.*, 2013). In disease, cells are arrested in P1 and P2 phase, however there is still a small number of P3 and P4 cells present in the intestine (Bain *et al.*, 2013). It would be interesting to characterise the expression of TNF receptors on these macrophage populations in

health and disease. It is possible that P1 and P2 macrophages have lower TNFR2 expression than P3 and P4. Indeed, we show that TNFR2 is more highly expressed on conditioned macrophages that resemble the P3/P4 phenotype. Binding of infliximab to P1 and P2 could then favour TNFR1 pathway and induce apoptosis as seen by Shen *et al.* (Shen et al., 2005). However, binding of infliximab to P3 and P4 macrophages could induce TNFR2 ligation and therefore induce the development of regulatory macrophages. Induction of regulatory T-cells following infliximab therapy could also be the effect of infliximab on TNFR2, since it has been shown that signalling of mTNF through TNFR2 promotes the expansion and function of mouse regulatory T-cells (Chen *et al.*, 2007, Chen *et al.*, 2008b). Rapid elimination of inflammatory cells through apoptosis can explain a rapid beneficial response to TNF antibodies in the early stages of IBD treatment. The potential effect of infliximab on TNFR2 and expansion of regulatory T-cells and macrophages could then account for the maintenance of remission. However, since infliximab does not selectively target TNFR1 or TNFR2 and can bind to mTNF on any cell, it cannot lead to full resolution of disease since its effects are uncontrolled and can, at any point, tip TNFR1-TNFR2 signalling to less favourable functions.

Macrophages in the intestine, therefore, exist in a continuum, rather than one separate population and we provide evidence that intestinal epithelial cells play a role in macrophage adaptation to the unique intestinal environment. Interestingly, as mentioned, during inflammation this transition is interrupted and macrophages accumulate in P1 and P2 phase (Tamoutounour *et al.*, 2012, Rivollier *et al.*, 2012, Bain *et al.*, 2013). This is partially beneficial as P1 and P2 macrophages are able to initiate an immune response, but leads to detrimental effects when left uncontrolled.

It is still unclear what stops the differentiation of inflammatory macrophages during disease, but the loss of immunomodulatory signals from epithelial cells could be one of the factors. In the last few years, evidence is accumulating that the disruption of epithelial cell barrier could be a driving force behind IBD (Hindryckx P, 2012) and we also show that once removed from the epithelial cell media macrophages lose their anti-inflammatory properties which supports the importance of epithelial cell – macrophage crosstalk. Our main research findings are summarised in **Figure 6.1**.

Our study also implicates an important role for TNFR2 in the maintenance and restoration of intestinal homeostasis. Studies of DSS-induced model of colitis, together with the studies of anti-TNF therapy also suggest an important role of TNF receptors in the disease progression. Rather than just blocking TNF-α, which is needed for a variety of functions, selective blocking or activation of TNF receptors could be more beneficial. However, more in-depth understanding of the TNF receptor pathway, distribution and the crosstalk is needed, because, as we have shown, TNFR1:TNFR2 ratio on a particular cell, stage of disease and a cell type itself can contribute to different activity of these receptors. Targeting TNFR2 could be a more effective therapy than targeting TNFR1, since TNFR2 is not expressed on all the cells, but confined to endothelial and immune cells (Tartaglia and Goeddel, 1992). However, induction of TNFR2 will have to be cell specific and introduced at the right stage of disease. Nevertheless, the potential for "highjacking" the protective pathway of TNFR2 as a way of controlling intestinal disease is a promising solution that would enhance a physiological mechanism of disease resolution, rather than just dealing with the symptoms, as do the currently available therapies.

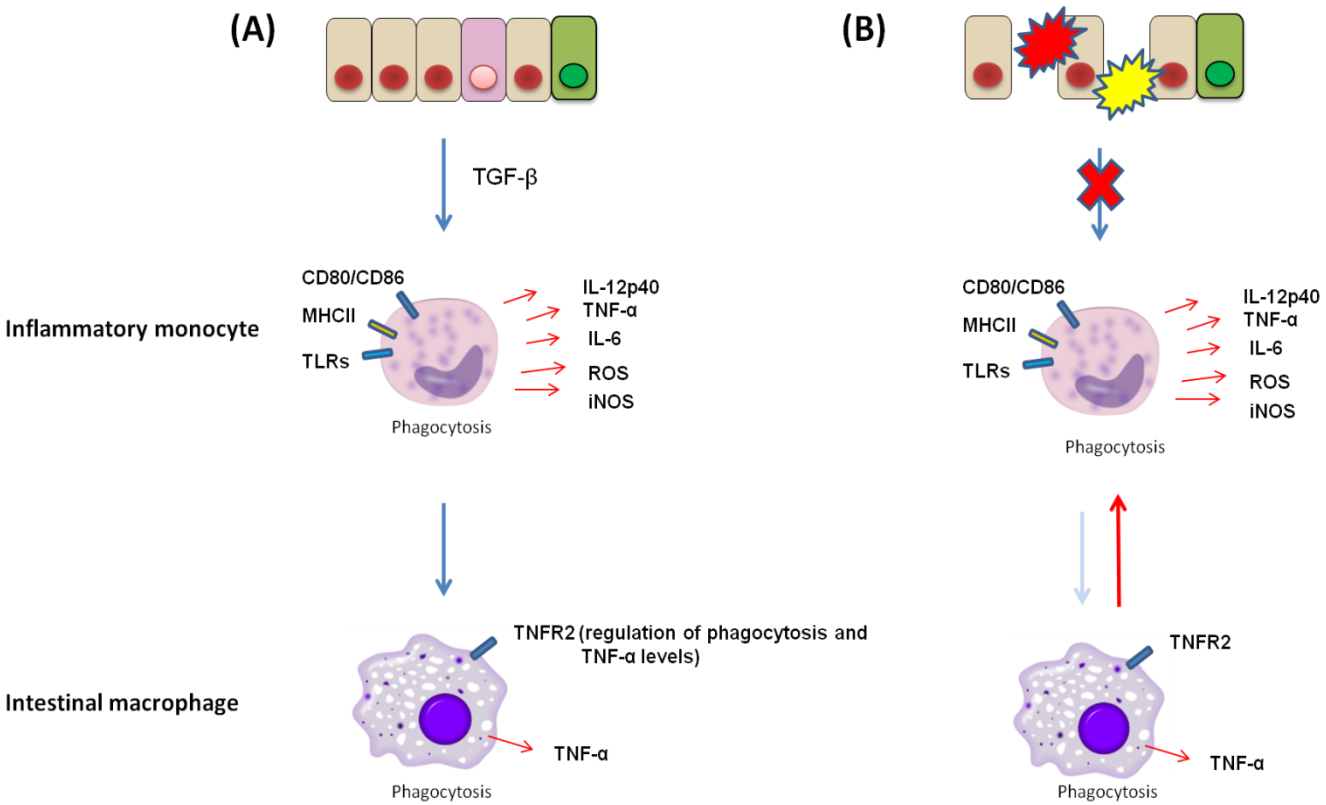

Figure 6.1 Summary of the main research findings Soluble factors produced by intestinal epithelial cells guide the phenotypic and functional changes of newly arrived inflammatory monocytes into hypo-responsive, TNFR2^{high} intestinal macrophages. TNFR2 is important for the regulation of phagocytosis and TNF-α levels **(A)**. In disease, when epithelial cell barrier is compromised, conditioning factors are lost causing the accumulation of inflammatory monocytes and inflammation **(B)**.

CHAPTER 7

APPENDICES

APPENDIX A

BUFFERS

FACS buffer

FCS	2%
NaN_3	0.05%

Dissolve in PBS

Phosphate buffered saline (PBS)

Na_2HPO_4 x $2H_2O$	8.0 mM
KH_2PO_4	1.5 mM
NaCl	137 mM
KCl	2.7 mM

Dissolve in H_2O and pH to 7.4

TAE buffer

Tris	40 mM
Acetic acid	20 mM
EDTA	1 mM

Dissolve in H_2O

Sorting buffer

FCS	1%
EDTA	1 mM
HEPES	25 mM

Dissolve in PBS

APPENDIX B

PHAGOCYTOSIS (controls)

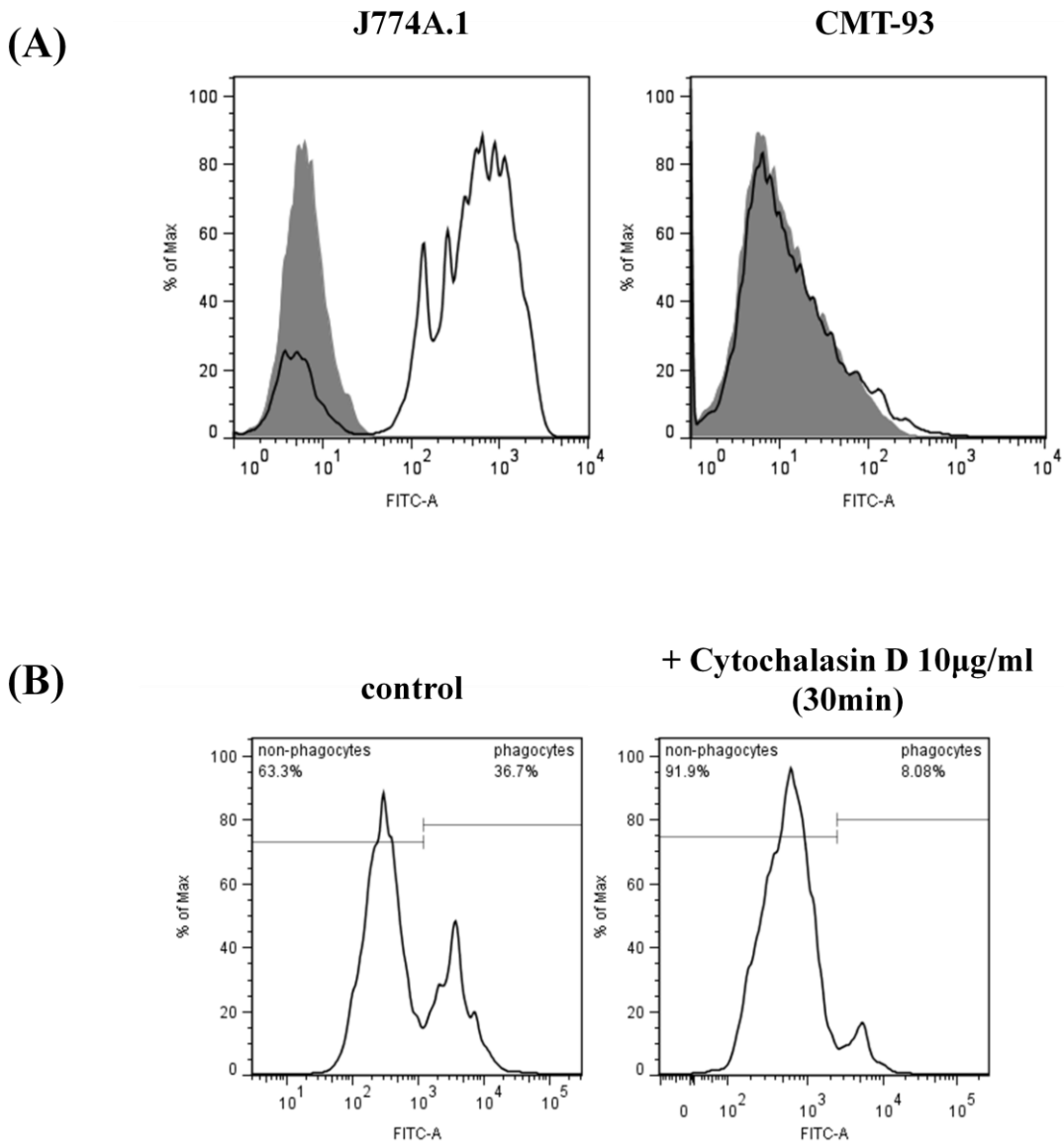

Figure 7.1 Controls used in the phagocytosis assay J774A.1 macrophages and CMT-93 colonic epithelial cells were incubated with fluorescent latex beads (Sigma-Aldrich) in a concentration of 20beads/cell for 6h (A) or 1h (B) at 37ºC. J774A.1 macrophages were pre-incubated with cytochalasin D (10µg/ml; Sigma-Aldrich) for 30min before the addition of fluorescent latex beads (B). Uptake of beads was then measured by flow cytometry.

APPENDIX C

PRIMER SEQUENCES

Foxp3

Primer 1 5’- CTG TCT TCC AAG TCT CGT CTG – 3’

Primer 2 5’- CTG GTC TCT GCA GGT TTA GTG– 3’

IL-6

Primer 1 5’- TCC TTA GCC ACT CCT TCT GT– 3’

Primer 2 5’- AGC CAG AGT CCT TCA GAG A– 3’

IL-10

Primer 1 5’- GGC ATC ACT TCT ACC AGG TAA– 3’

Primer 2 5’- TCA GCC AGG TGA AGA CTT TC– 3’

IL-12p40

Primer 1 5’- AAG TCC TCA TAG ATG CTA CCA AG– 3’

Primer 2 5’- CAC TGG AAC TAC ACA AGA ACG A– 3’

Occludin

Primer 1 5’- GTT GAT CTG AAG TGA TAG GTG GA– 3’

Primer 2 5’- CAC TAT GAA ACA GAC TAC ACG ACA– 3’

Rps18

Primer 1 5’- ACA CCA CAT GAG CAT ATC TCC– 3’

Primer 2 5’- CCT GAG AAG TTC CAG CAC AT– 3’

TGF-β

Primer 1 5’- CCG AAT GTC TGA CGT ATT GAA GA– 3’

Primer 2 5’- GCG GAC TAC TAT GCT AAA GAG G– 3’

TNF-α

Primer 1 5’- TCT TTG AGA TCC ATG CCG TTG– 3’

Primer 2 5’- AGA CCC TCA CAC TCA GAT CA– 3’

TNFR1

Primer 1 5’- GCA AAG ACC TAG CAA GAT AAC CA– 3’

Primer 2 5’- GCC ACT GCA AGA AAA ATG AGG– 3’

TNFR2

Primer 1 5’- CTT GGC ATC TCT TTG TAG GCA– 3’

Primer 2 5’- TTG GTC TGA TTG TTG GAG TGA– 3’

EFFICIENCY AND DISSOCIATION CURVES

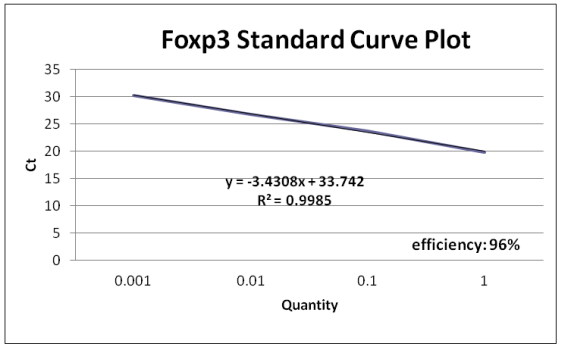

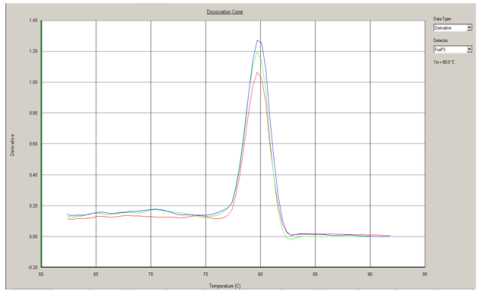

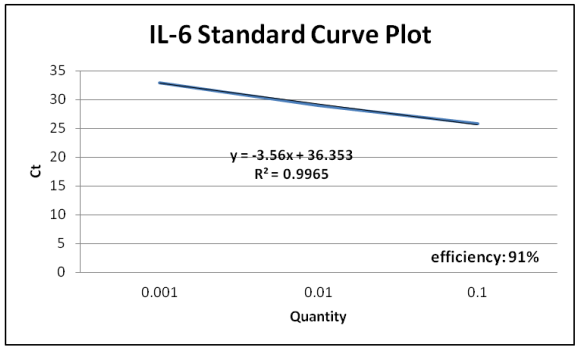

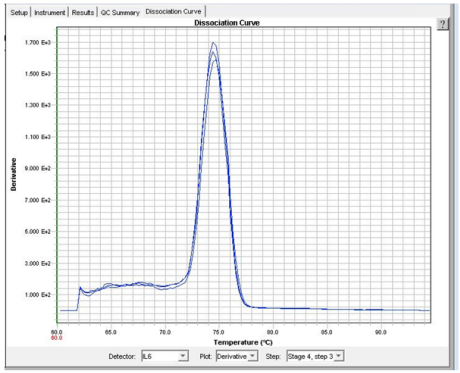

Figure 7.2A Evaluation of the IDT PrimeTime qRT-PCR primers A standard curve was created by carrying out a serial dilution of the PCR product. When a standard curve correlation coefficient was close to 1, the PCR efficiency was determined using the following formula:

$$E = \left(10^{-\frac{1}{slope}} - 1\right) x\ 100$$

To assess the specificity of the SYBR® green assay the dissociation analysis was performed for each product. The dissociation step was added after the final PCR cycle.

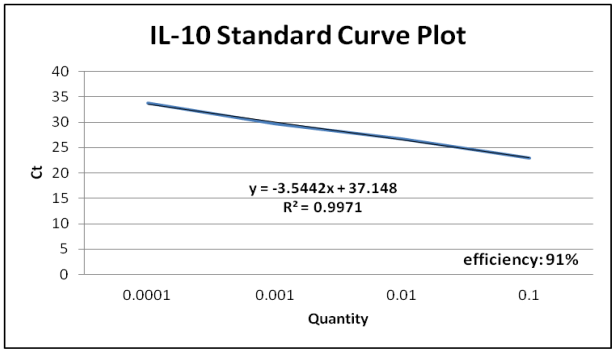

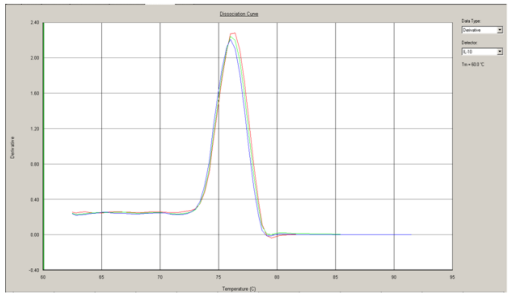

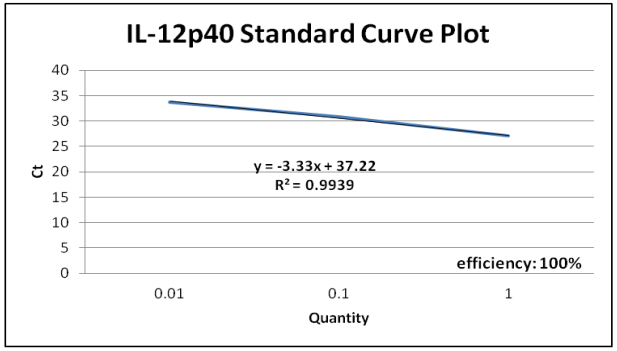

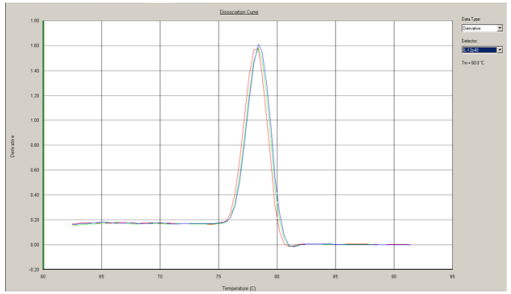

Figure 7.2B Evaluation of the IDT PrimeTime qRT-PCR primers A standard curve was created by carrying out a serial dilution of the PCR product. When a standard curve correlation coefficient was close to 1, the PCR efficiency was determined using the following formula:

$$E = \left(10^{-\frac{1}{slope}} - 1\right) x\ 100$$

To assess the specificity of the SYBR® green assay the dissociation analysis was performed for each product. The dissociation step was added after the final PCR cycle.

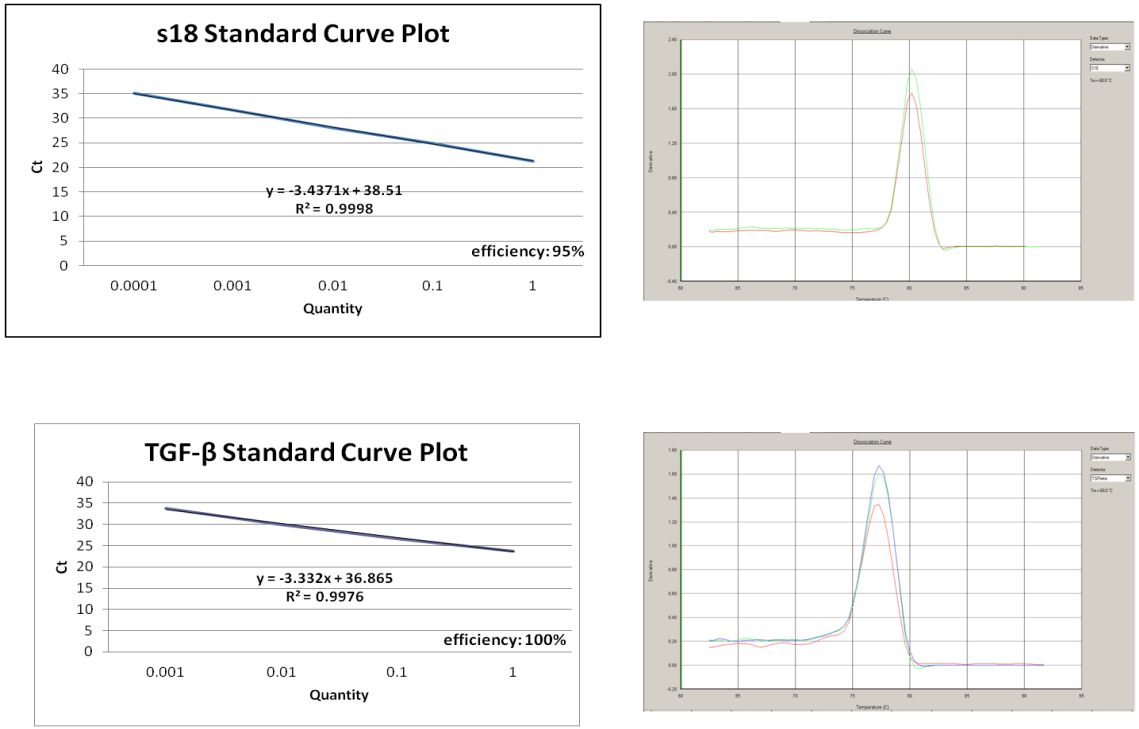

Figure 7.2C Evaluation of the IDT PrimeTime qRT-PCR primers A standard curve was created by carrying out a serial dilution of the PCR product. When a standard curve correlation coefficient was close to 1, the PCR efficiency was determined using the following formula:

$$E = \left(10^{-\frac{1}{slope}} - 1\right) x\ 100$$

To assess the specificity of the SYBR® green assay the dissociation analysis was performed for each product. The dissociation step was added after the final PCR cycle.

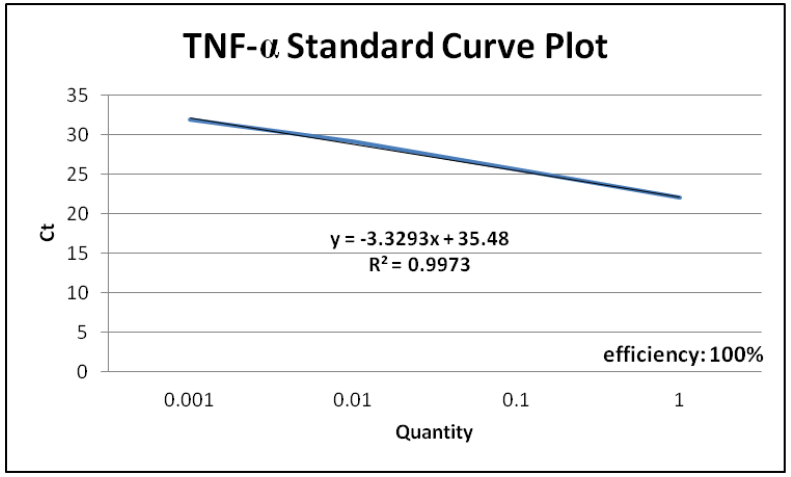

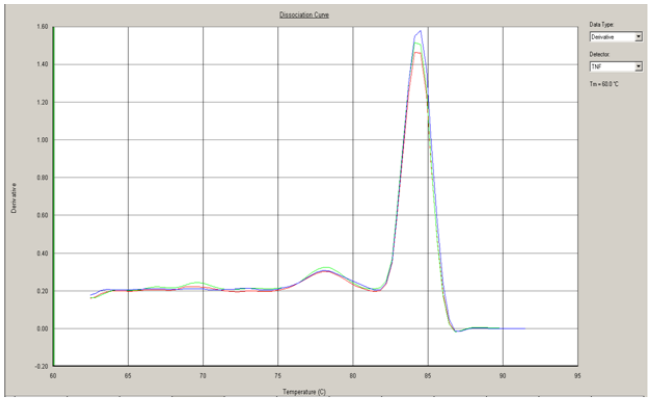

Figure 7.2D Evaluation of the IDT PrimeTime qRT-PCR primers A standard curve was created by carrying out a serial dilution of the PCR product. When a standard curve correlation coefficient was close to 1, the PCR efficiency was determined using the following formula:

$$E = \left(10^{-\frac{1}{slope}} - 1\right) x\ 100$$

To assess the specificity of the SYBR® green assay the dissociation analysis was performed for each product. The dissociation step was added after the final PCR cycle.

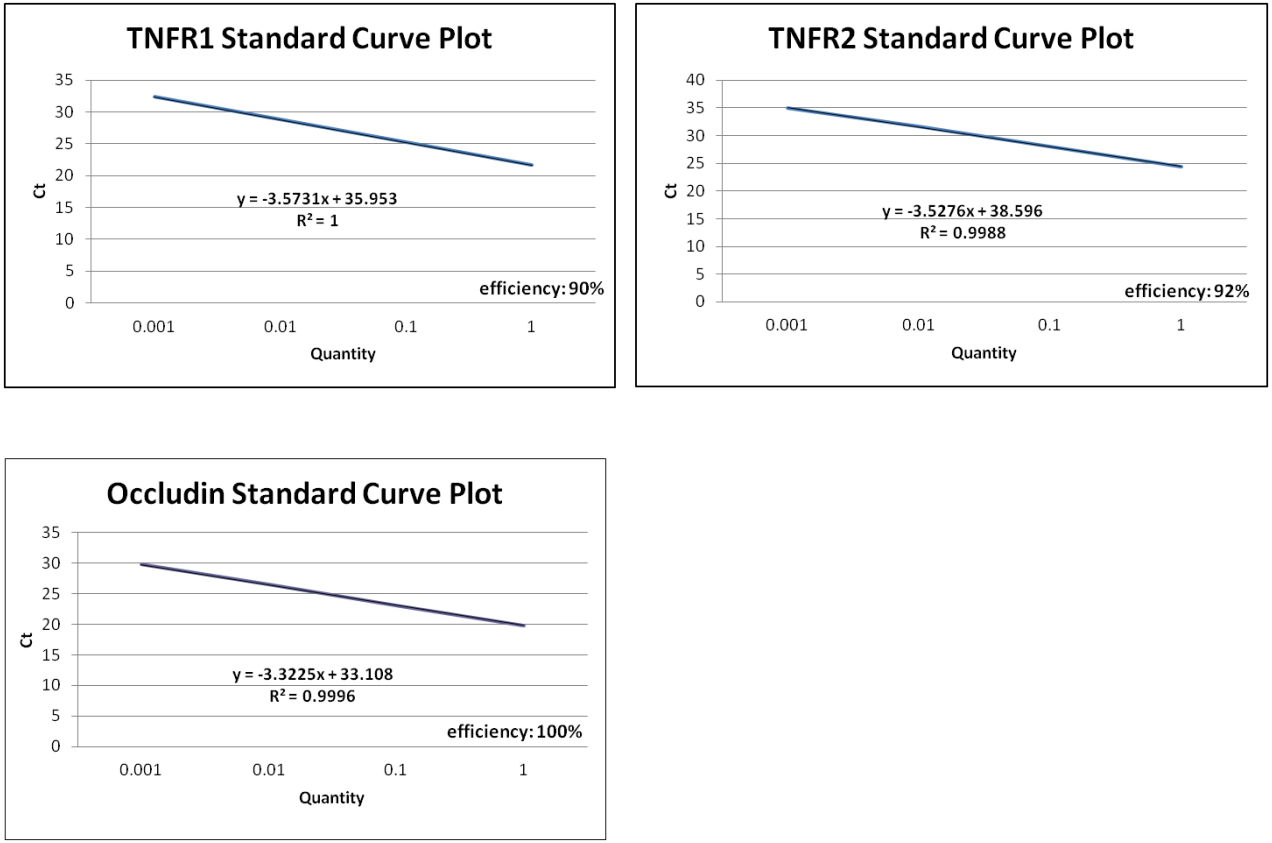

Figure 7.3 Evaluation of the IDT PrimeTime qRT-PCR Taqman assay A standard curve was created by carrying out a serial dilution of the PCR product. When a standard curve correlation coefficient was close to 1, the PCR efficiency was determined using the following formula:

$$E = \left(10^{-\frac{1}{slope}} - 1\right) x\ 100$$

PCR GEL

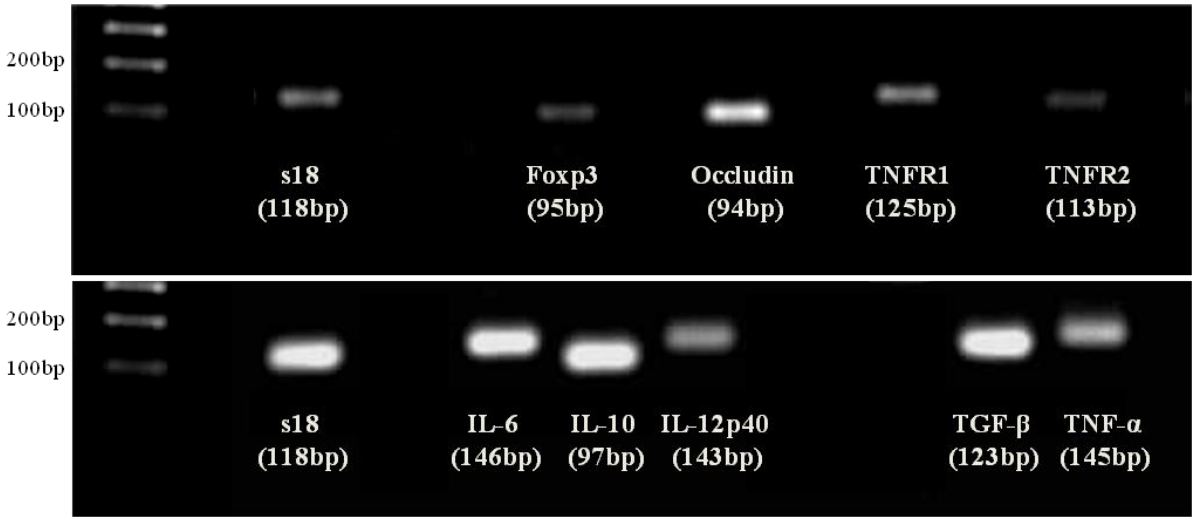

Figure 7.4 DNA product analysis by gel electrophoresis DNA samples were mixed with loading buffer (Fermentas) and loaded onto the 2% agarose gel, together with GeneRuler 100bp DNA ladder (Termo-Fisher Scientific). Gels were run for 1h in 1x TAE buffer at 100V and visualised using the G-box imaging system (Syngene).

ENDOGENOUS CONTROLS

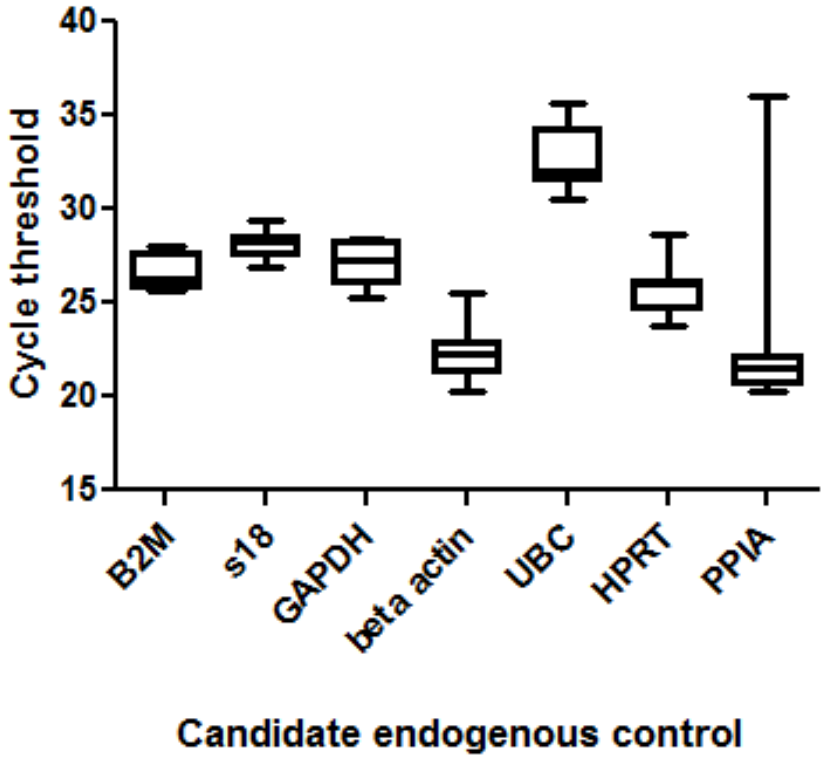

Figure 7.5 Endogenous controls tested on a colonic tissue B2M, Beta-2-microglobulin; s18, ribosomal protein s18; GAPDH, Glyceraldehyde 3-phosphate dehydrogenase; UBC, ubiquitin C; HPRT, Hypoxanthine Phosphoribosyltransferase; PPIA, Peptidylprolyl Isomerase A

APPENDIX D

Primary cell isolation procedure

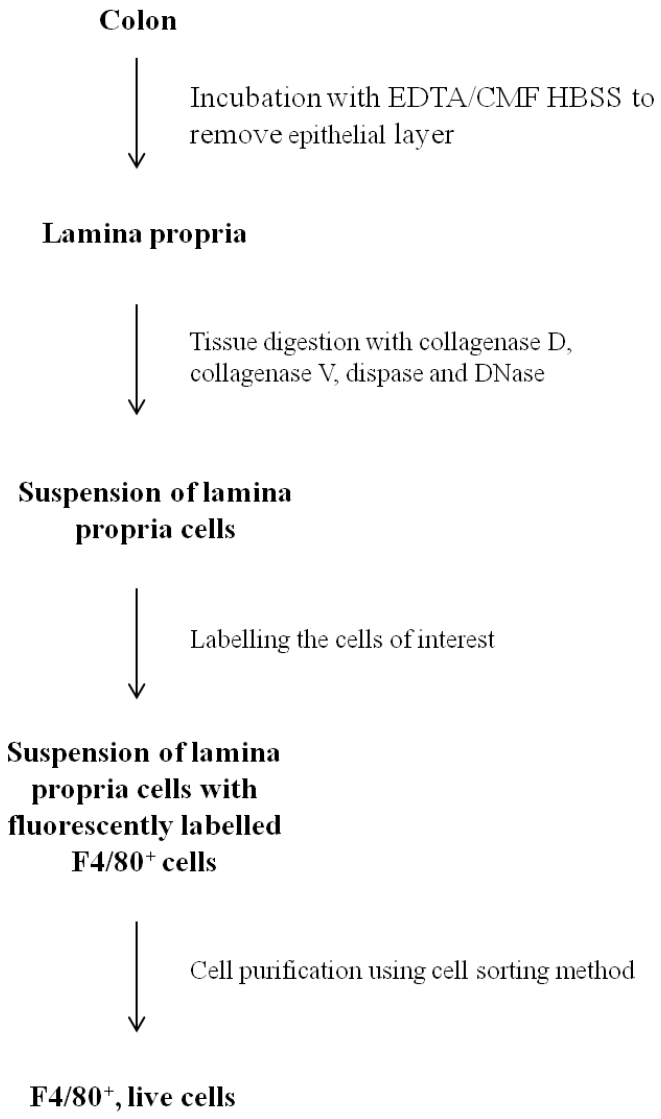

Figure 7.6 Schematic of the procedure for isolation of lamina propria macrophages Flow diagram depicting a tissue digestion and cell purification method, optimised to obtain live, F4/80$^+$ lamina propria macrophages

APPENDIX E

Revised gating strategy

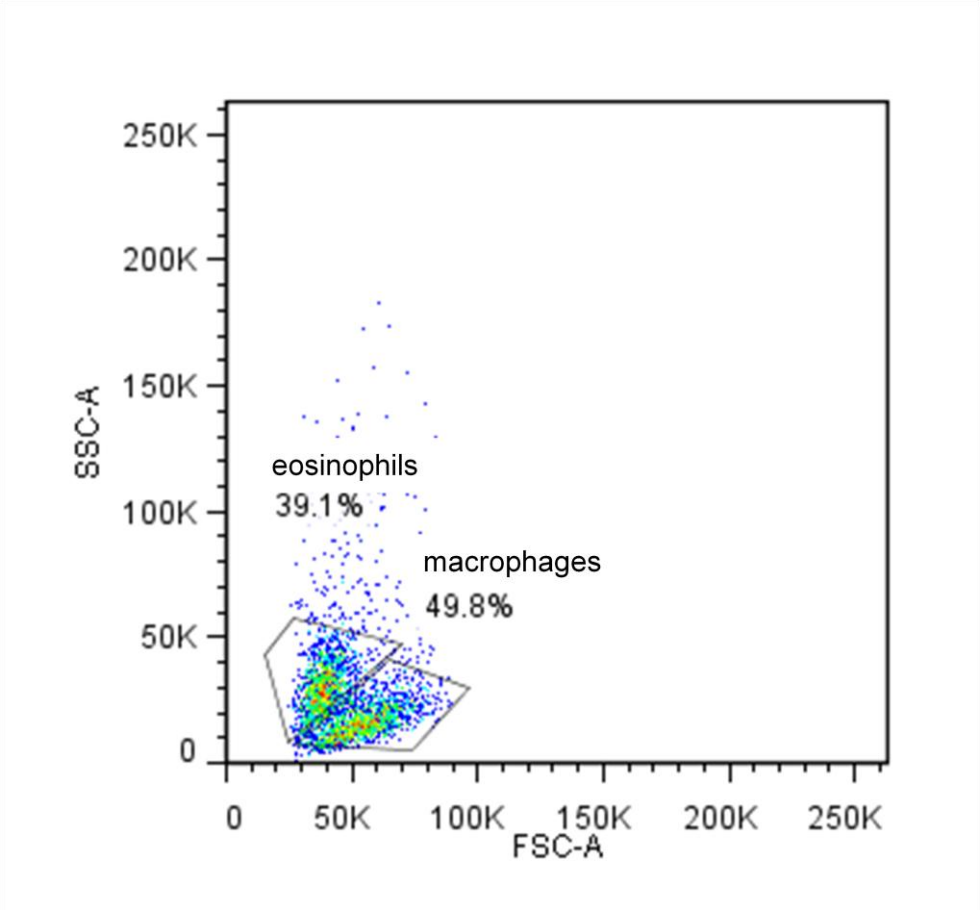

Figure 7.7 Revised gating strategy used to exclude F4/80$^+$ eosinophils Isolated lamina propria cells were stained with fluorescently labelled F4/80 antibody. Dead cells and doublets were exluded and F4/80$^+$ cells were further gated based on their FSC and SSC properties. Eosinophils are also F4/80$^+$ but they have the forward and side scatter properties of granulocytes, unlike macrophages.

APPENDIX F

Additional controls for Figure 4.7

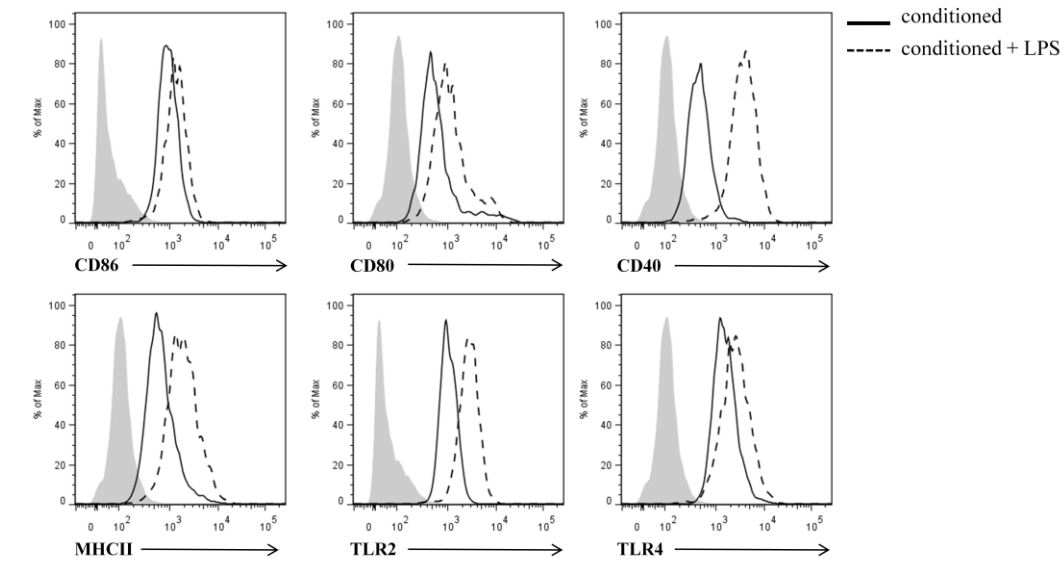

Figure 7.8 Expression of surface markers on CMT-93 conditioned macrophages following TLR4 ligation J774A.1 macrophages were incubated with CMT-93 conditioned medium for 2h before adding LPS (100ng/ml). After 24h cells were stained with fluorescently labelled antibodies for CD86, CD80, CD40, MHCII, TLR2 and TLR4 and expression was measured by flow cytometry. Histograms show surface marker expression of conditioned cells (black line) compared to conditioned LPS-stimulated cells (dashed line). Filled histograms represent fluorescence of unstained cells. Data are representative of three independent experiments.

Additional controls for Figure 5.19

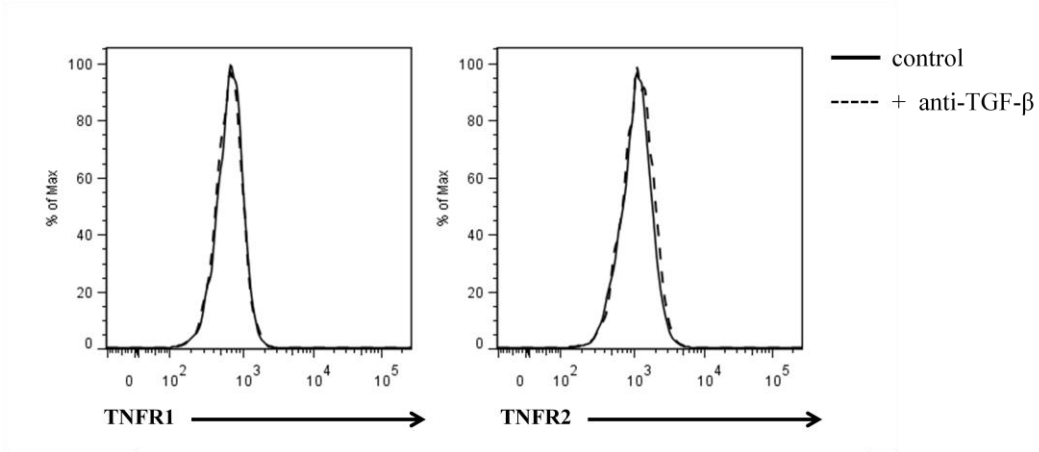

Figure 7.9 Neutralisation of TGF-β does not affect unconditioned cells TGF-β neutralising antibody (10μg/ml; R&D) was added to J774A.1 macrophage culture for 24h and the expression of TNFR1 and TNFR2 was measured by flow cytometry. Data are representative of three independent experiments

APPENDIX G

TNFR2 antagonist isotype control

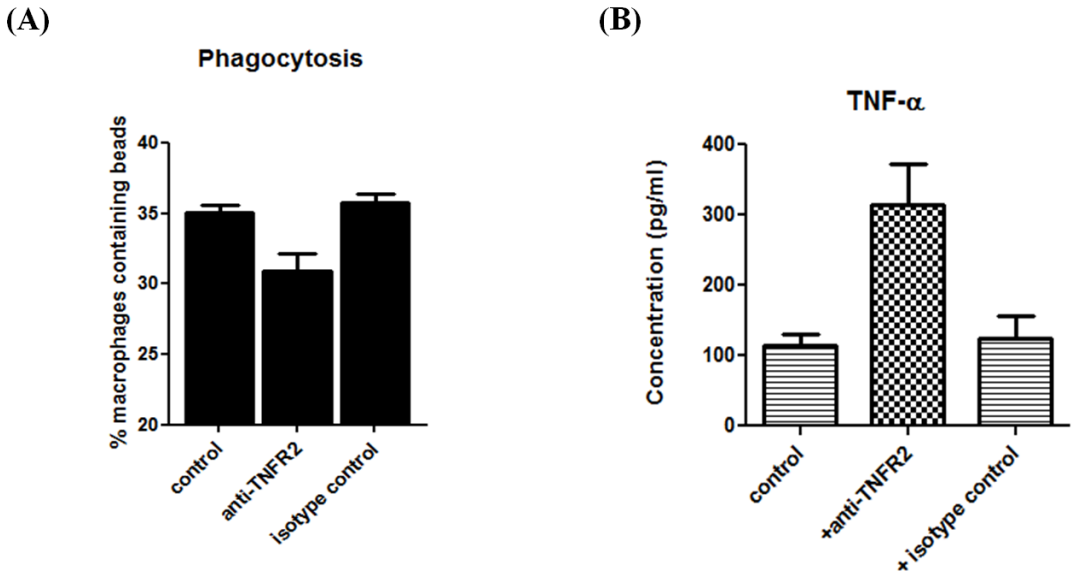

Figure 7.10 TNFR2 antagonist isotype control J774A.1 macrophages were incubated with TNFR2 antagonist (5µg/ml; Biolegend) or appropriate isotype control (5µg/ml; Biolegend) for 24h. Fluorescent latex beads (20beads/cell) were then added to the cell culture and macrophages were left to phagocytose for 1h at 37ºC. Uptake of beads was measured by flow cytometry (A). Concentration of TNF-α in cell supernatants was measured by ELISA (R&D) (B)

CHAPTER 8

BIBLIOGRAPHY

BIBLIOGRAPHY

ABREU, M. T. 2010. Toll-like receptor signalling in the intestinal epithelium: how bacterial recognition shapes intestinal function. *Nature Reviews Immunology,* 10**,** 131-143.

ADAMS, D. O. & HAMILTON, T. A. 1984. THE CELL BIOLOGY OF MACROPHAGE ACTIVATION. *Annual Review of Immunology,* 2**,** 283-318.

ADEREM, A. & UNDERHILL, D. M. 1999. Mechanisms of phagocytosis in macrophages. *Annual Review of Immunology,* 17**,** 593-623.

AGGARWAL, B. B. 2003. Signalling pathways of the TNF superfamily: a double-edged sword. *Nat Rev Immunol,* 3**,** 745-56.

AKIRA, S., TAKEDA, K. & KAISHO, T. 2001. Toll-like receptors: critical proteins linking innate and acquired immunity. *Nature Immunology,* 2**,** 675-680.

AL-LAMKI, R. S., WANG, J., VANDENABEELE, P., BRADLEY, J. A., THIRU, S., LUO, D. H., MIN, W., POBER, J. S. & BRADLEY, J. R. 2005. TNFR1- and TNFR2-mediated signaling pathways in human kidney are cell type-specific and differentially contribute to renal injury. *Faseb Journal,* 19**,** 1637-1645.

ALEXOPOULOU, L., HOLT, A. C., MEDZHITOV, R. & FLAVELL, R. A. 2001. Recognition of double-stranded RNA and activation of NF-kappaB by Toll-like receptor 3. *Nature,* 413**,** 732-8.

ARAKI, Y., MUKAISYO, K., SUGIHARA, H., FUJIYAMA, Y. & HATTORI, T. 2010. Increased apoptosis and decreased proliferation of colonic epithelium in dextran sulfate sodium-induced colitis in mice. *Oncol Rep,* 24**,** 869-74.

ARTIS, D. 2008. Epithelial-cell recognition of commensal bacteria and maintenance of immune homeostasis in the gut. *Nature Reviews Immunology,* 8**,** 411-420.

AUSTYN, J. M. & GORDON, S. 1981. F4-80, A MONOCLONAL-ANTIBODY DIRECTED SPECIFICALLY AGAINST THE MOUSE MACROPHAGE. *European Journal of Immunology,* 11**,** 805-815.

BAIN, C. C. & MOWAT, A. M. 2011. Intestinal macrophages - specialised adaptation to a unique environment. *European Journal of Immunology,* 41**,** 2494-2498.

BAIN, C. C., SCOTT, C. L., URONEN-HANSSON, H., GUDJONSSON, S., JANSSON, O., GRIP, O., GUILLIAMS, M., MALISSEN, B., AGACE, W. W. & MOWAT, A. M. 2013. Resident and pro-inflammatory macrophages in the colon represent alternative context-dependent fates of the same Ly6C(hi) monocyte precursors. *Mucosal Immunology,* 6**,** 498-510.

BARTLETT, J. G., MOON, N., CHANG, T. W., TAYLOR, N. & ONDERDONK, A. B. 1978. Role of Clostridium difficile in antibiotic-associated pseudomembranous colitis. *Gastroenterology,* 75**,** 778-82.

BELLOC, F., BELAUD-ROTUREAU, M. A., LAVIGNOLLE, V., BASCANS, E., BRAZ-PEREIRA, E., DURRIEU, F. & LACOMBE, F. 2000. Flow cytometry detection of caspase 3 activation in preapoptotic leukemic cells. *Cytometry,* 40**,** 151-60.

BLANCHARD, C. & ROTHENBERG, M. E. 2009. Biology of the Eosinophil. *In:* ALT, F. W. (ed.) *Advances in Immunology, Vol 101*.

BLUML, S., BINDER, N. B., NIEDERREITER, B., POLZER, K., HAYER, S., TAUBER, S., SCHETT, G., SCHEINECKER, C., KOLLIAS, G., SELZER, E., BILBAN, M., SMOLEN, J. S., SUPERTI-FURGA, G. & REDLICH, K. 2010. Antiinflammatory Effects of Tumor Necrosis Factor on Hematopoietic Cells in a Murine Model of Erosive Arthritis. *Arthritis and Rheumatism,* 62**,** 1608-1619.

BOGUNOVIC, M., GINHOUX, F., HELFT, J., SHANG, L., HASHIMOTO, D., GRETER, M., LIU, K., JAKUBZICK, C., INGERSOLL, M. A., LEBOEUF, M., STANLEY, E. R., NUSSENZWEIG, M., LIRA, S. A., RANDOLPH, G. J. & MERAD, M. 2009. Origin of the Lamina Propria Dendritic Cell Network. *Immunity,* 31**,** 513-525.

BRADLEY, J. R. 2008. TNF-mediated inflammatory disease. *Journal of Pathology,* 214**,** 149-160.

BRENNAN, F. M., MAINI, R. N. & FELDMANN, M. 1992. TNF-alpha - a pivotal role in rheumatoid-arthritis. *British Journal of Rheumatology,* 31**,** 293-298.

BROWN, S. L., RIEHL, T. E., WALKER, M. R., GESKE, M. J., DOHERTY, J. M., STENSON, W. F. & STAPPENBECK, T. S. 2007. Myd88-dependent positioning of Ptgs2-expressing stromal cells maintains colonic epithelial proliferation during injury. *The Journal of Clinical Investigation,* 117**,** 258-269.

BULL, D. M. & BOOKMAN, M. A. 1977. ISOLATION AND FUNCTIONAL CHARACTERIZATION OF HUMAN INTESTINAL MUCOSAL LYMPHOID-CELLS. *Journal of Clinical Investigation,* 59**,** 966-974.

BUTLER, M., NG, C. Y., VAN HEEL, D. A., LOMBARDI, G., LECHLER, R., PLAYFORD, R. J. & GHOSH, S. 2006. Modulation of dendritic cell phenotype and function in an in vitro model of the intestinal epithelium. *European Journal of Immunology,* 36**,** 864-874.

CADWELL, K., LIU, J. Y., BROWN, S. L., MIYOSHI, H., LOH, J., LENNERZ, J. K., KISHI, C., KC, W., CARRERO, J. A., HUNT, S., STONE, C. D., BRUNT, E. M., XAVIER, R. J., SLECKMAN, B. P., LI, E., MIZUSHIMA, N., STAPPENBECK, T. S. & VIRGIN, H. W. T. 2008. A key role for autophagy and the autophagy gene Atg16l1 in mouse and human intestinal Paneth cells. *Nature,* 456**,** 259-63.

CARADONNA, L., AMATI, L., LELLA, P., JIRILLO, E. & CACCAVO, D. 2000. Phagocytosis, killing, lymphocyte-mediated antibacterial activity, serum autoantibodies, and plasma endotoxins in inflammatory bowel disease. *Am J Gastroenterol,* 95**,** 1495-502.

CARIO, E., GERKEN, G. & PODOLSKY, D. K. 2007. Toll-like receptor 2 controls mucosal inflammation by regulating epithelial barrier function. *Gastroenterology,* 132**,** 1359-74.

CASTANOS-VELEZ, E., MAERLAN, S., OSORIO, L. M., ABERG, F., BIBERFELD, P., ORN, A. & ROTTENBERG, M. E. 1998. Trypanosoma cruzi infection in tumor necrosis factor receptor p55-deficient mice. *Infect Immun,* 66**,** 2960-8.

CHADBAN, S. J. & ATKINS, R. C. 2005. Glomerulonephritis. *Lancet,* 365**,** 1797-806.

CHAN, F. K., CHUN, H. J., ZHENG, L., SIEGEL, R. M., BUI, K. L. & LENARDO, M. J. 2000. A domain in TNF receptors that mediates ligand-independent receptor assembly and signaling. *Science,* 288**,** 2351-4.

CHEIFETZ, S., WEATHERBEE, J. A., TSANG, M. L., ANDERSON, J. K., MOLE, J. E., LUCAS, R. & MASSAGUE, J. 1987. The transforming growth factor-beta system, a complex pattern of cross-reactive ligands and receptors. *Cell,* 48**,** 409-15.

CHEN, X., BAUMEL, M., MANNEL, D. N., HOWARD, O. M. & OPPENHEIM, J. J. 2007. Interaction of TNF with TNF receptor type 2 promotes expansion and function of mouse CD4+CD25+ T regulatory cells. *J Immunol,* 179**,** 154-61.

CHEN, X., KATCHAR, K., GOLDSMITH, J. D., NANTHAKUMAR, N., CHEKNIS, A., GERDING, D. N. & KELLY, C. P. 2008a. A mouse model of Clostridium difficile-associated disease. *Gastroenterology,* 135**,** 1984-92.

CHEN, X., SUBLESKI, J. J., KOPF, H., HOWARD, O. M. Z., MANNEL, D. N. & OPPENHEIM, J. J. 2008b. Expression of TNFR2 defines a maximally suppressive subset of mouse CD4(+)CD25(+)FoxP3(+) T regulatory cells: Applicability to tumor-infiltrating T regulatory cells. *Journal of Immunology,* 180**,** 6467-6471.

CLARK, I. A. 2007. How TNF was recognized as a key mechanism of disease. *Cytokine & Growth Factor Reviews,* 18**,** 335-343.

COLOMBEL, J. F., SANDBORN, W. J., REINISCH, W., MANTZARIS, G. J., KORNBLUTH, A., RACHMILEWITZ, D., LICHTIGER, S., D'HAENS, G., DIAMOND, R. H., BROUSSARD, D. L., TANG, K. L., VAN DER WOUDE, C. J. & RUTGEERTS, P. 2010. Infliximab, azathioprine, or combination therapy for Crohn's disease. *N Engl J Med,* 362**,** 1383-95.

COOK, D. N. 1996. The role of MIP-1 alpha in inflammation and hematopoiesis. *Journal of Leukocyte Biology,* 59**,** 61-66.

COUPER, K. N., BLOUNT, D. G. & RILEY, E. M. 2008. IL-10: The master regulator of immunity to infection. *Journal of Immunology,* 180**,** 5771-5777.

DAS, L. M., TORRES-CASTILLO, M. D., GILL, T. & LEVINE, A. D. 2013. TGF-beta conditions intestinal T cells to express increased levels of miR-155, associated with down-regulation of IL-2 and itk mRNA. *Mucosal Immunol,* 6**,** 167-76.

DAVIES, D. 2007. Cell Sorting by Flow Cytometry. *In:* M. G. MACEY, H. P. I., TOTOWA, NJ (ed.) *Flow Cytometry: Principles and Applications.* NJ.

DAYER SCHNEIDER, J., SEIBOLD, I., SAXER-SEKULIC, N., PAREDES, B. E., SAURER, L. & MUELLER, C. 2009. Lack of TNFR2 expression by CD4(+) T cells exacerbates experimental colitis. *Eur J Immunol,* 39**,** 1743-53.

DECKERT-SCHLUTER, M., BLUETHMANN, H., RANG, A., HOF, H. & SCHLUTER, D. 1998. Crucial role of TNF receptor type 1 (p55), but not of

TNF receptor type 2 (p75), in murine toxoplasmosis. *Journal of Immunology,* 160**,** 3427-3436.

DEFIFE, K. M., JENNEY, C. R., COLTON, E. & ANDERSON, J. M. 1999. Disruption of filamentous actin inhibits human macrophage fusion. *Faseb Journal,* 13**,** 823-832.

DENNING, T. L., WANG, Y. C., PATEL, S. R., WILLIAMS, I. R. & PULENDRAN, B. 2007. Lamina propria macrophages and dendritic cells differentially induce regulatory and interleukin 17-producing T cell responses. *Nature Immunology,* 8**,** 1086-1094.

DEVARAJAN, P. 2006. Update on Mechanisms of Ischemic Acute Kidney Injury. *Journal of the American Society of Nephrology,* 17**,** 1503-1520.

DOE, W. F. 1989. The intestinal immune system. *Gut,* 30**,** 1679-85.

DUERR, R. H. 2007. Genome-wide association studies herald a new era of rapid discoveries in inflammatory bowel disease research. *Gastroenterology,* 132**,** 2045-9.

EA, C.-K., DENG, L., XIA, Z.-P., PINEDA, G. & CHEN, Z. J. 2006. Activation of IKK by TNFα Requires Site-Specific Ubiquitination of RIP1 and Polyubiquitin Binding by NEMO. *Molecular Cell,* 22**,** 245-257.

EBACH, D. R., RIEHL, T. E. & STENSON, W. F. 2005. Opposing effects of tumor necrosis factor receptor 1 and 2 in sepsis due to cecal ligation and puncture. *Shock,* 23**,** 311-8.

ERUSLANOV, E. & KUSMARTSEV, S. 2010. Identification of ROS using oxidized DCFDA and flow-cytometry. *Methods Mol Biol,* 594**,** 57-72.

FAUSTMAN, D. & DAVIS, M. 2010. TNF receptor 2 pathway: drug target for autoimmune diseases. *Nat Rev Drug Discov,* 9**,** 482-93.

FLYNN, J. L., GOLDSTEIN, M. M., CHAN, J., TRIEBOLD, K. J., PFEFFER, K., LOWENSTEIN, C. J., SCHREIBER, R., MAK, T. W. & BLOOM, B. R. 1995a. TUMOR-NECROSIS-FACTOR-ALPHA IS REQUIRED IN THE PROTECTIVE IMMUNE-RESPONSE AGAINST MYCOBACTERIUM-TUBERCULOSIS IN MICE. *Immunity,* 2**,** 561-572.

FLYNN, J. L., GOLDSTEIN, M. M., CHAN, J., TRIEBOLD, K. J., PFEFFER, K., LOWENSTEIN, C. J., SCHREIBER, R., MAK, T. W. & BLOOM, B. R. 1995b. Tumor necrosis factor-alpha is required in the protective immune response against Mycobacterium tuberculosis in mice. *Immunity,* 2**,** 561-72.

FONTAINE, V., MOHAND-SAID, S., HANOTEAU, N., FUCHS, L., PFIZENMAIER, K. & EISEL, U. 2002. Neurodegenerative and neuroprotective effects of tumor necrosis factor (TNF) in retinal ischemia: Opposite roles of TNF receptor 1 and TNF receptor 2. *Journal of Neuroscience,* 22.

FOTIN-MLECZEK, M., HENKLER, F., SAMEL, D., REICHWEIN, M., HAUSSER, A., PARMRYD, I., SCHEURICH, P., SCHMID, J. A. & WAJANT, H. 2002. Apoptotic crosstalk of TNF receptors: TNF-R2-induces depletion of TRAF2 and IAP proteins and accelerates TNF-R1-dependent activation of caspase-8. *J Cell Sci,* 115**,** 2757-70.

FRANKS, L. M. & HEMMINGS, V. J. 1978. CELL LINE FROM AN INDUCED CARCINOMA OF MOUSE RECTUM. *Journal of Pathology,* 124**,** 35-&.

FRÉDÉRICK, B., ULRICH, M., FABRICE, C., DOMINIQUE, B., MICHIKO, N.-K., MONIQUE, D., BENOIT, F., VINCENT, O., MARTINE, H., STÉPHANE, B., THECLA, L., GHISLAINE, S., MARCO, G. & JEAN-PIERRE, H. 2007. CARD15/NOD2 Is Required for Peyer's Patches Homeostasis in Mice. *Plos One,* 2.

FUKATA, M., HERNANDEZ, Y., CONDUAH, D., COHEN, J., CHEN, A., BREGLIO, K., GOO, T., HSU, D., XU, R. & ABREU, M. T. 2009. Innate immune signaling by Toll-like receptor-4 (TLR4) shapes the inflammatory microenvironment in colitis-associated tumors. *Inflamm Bowel Dis,* 15**,** 997-1006.

GAUTHO, K. 2003. BD FACSAria User's guide. Pushpa MacFarlane.

GEISSMANN, F., JUNG, S. & LITTMAN, D. R. 2003. Blood monocytes consist of two principal subsets with distinct migratory properties. *Immunity,* 19**,** 71-82.

GERSEMANN, M., BECKER, S., KUBLER, I., KOSLOWSKI, M., WANG, G., HERRLINGER, K. R., GRIGER, J., FRITZ, P., FELLERMANN, K., SCHWAB, M., WEHKAMP, J. & STANGE, E. F. 2009. Differences in goblet cell differentiation between Crohn's disease and ulcerative colitis. *Differentiation,* 77**,** 84-94.

GEWIRTZ, A. T., NAVAS, T. A., LYONS, S., GODOWSKI, P. J. & MADARA, J. L. 2001. Cutting edge: bacterial flagellin activates basolaterally expressed TLR5 to induce epithelial proinflammatory gene expression. *J Immunol,* 167**,** 1882-5.

GIBSON, P. R., HERMANOWICZ, A., VERHAAR, H. J. J., FERGUSON, D. J. P., BERNAL, A. L. & JEWELL, D. P. 1985. ISOLATION OF INTESTINAL MONONUCLEAR-CELLS - FACTORS RELEASED WHICH AFFECT LYMPHOCYTE VIABILITY AND FUNCTION. *Gut,* 26**,** 60-68.

GILL, S. R., POP, M., DEBOY, R. T., ECKBURG, P. B., TURNBAUGH, P. J., SAMUEL, B. S., GORDON, J. I., RELMAN, D. A., FRASER-LIGGETT, C. M. & NELSON, K. E. 2006. Metagenomic analysis of the human distal gut microbiome. *Science,* 312**,** 1355-9.

GORDON, S. 2007. The macrophage: past, present and future. *Eur J Immunol,* 37 Suppl 1**,** S9-17.

GORDON, S., HAMANN, J., LIN, H. H. & STACEY, M. 2011. F4/80 and the related adhesion-GPCRs. *Eur J Immunol,* 41**,** 2472-6.

GOTO, Y. & IVANOV, II 2013. Intestinal epithelial cells as mediators of the commensal-host immune crosstalk. *Immunol Cell Biol,* 91**,** 204-14.

GRIESS, P. 1879. Bemerkungen zu der abhandlung der H.H. Weselsky und Benedikt

"Ueber einige azoverbindungen. *Chem. Ber.,* 12**,** 426-8.

GUILBERT, L. J., WINKLERLOWEN, B., SMITH, A., BRANCH, D. R. & GARCIALLORET, M. 1993. Analysis of the synergistic stimulation of mouse macrophage proliferation by macrophage-colony-stimulating factor (CSF-1) and tumor-necrosis-factor-alpha (TNF-alpha). *Journal of Leukocyte Biology,* 54**,** 65-72.

GUM, J. R., JR., HICKS, J. W., TORIBARA, N. W., SIDDIKI, B. & KIM, Y. S. 1994. Molecular cloning of human intestinal mucin (MUC2) cDNA. Identification of the amino terminus and overall sequence similarity to prepro-von Willebrand factor. *J Biol Chem,* 269**,** 2440-6.

HADIS, U., WAHL, B., SCHULZ, O., HARDTKE-WOLENSKI, M., SCHIPPERS, A., WAGNER, N., MUELLER, W., SPARWASSER, T., FOERSTER, R. & PABST, O. 2011. Intestinal Tolerance Requires Gut Homing and Expansion of FoxP3(+) Regulatory T Cells in the Lamina Propria. *Immunity,* 34**,** 237-246.

HAFLER, D. A. & WEINER, H. L. 1989. MS: a CNS and systemic autoimmune disease. *Immunol Today,* 10**,** 104-7.

HALE, L. P. & CIANCIOLO, G. 2008. Treatment of experimental colitis in mice with LMP-420, an inhibitor of TNF transcription. *J Inflamm (Lond),* 5**,** 4.

HAMID, T., GU, Y., ORTINES, R. V., BHATTACHARYA, C., WANG, G., XUAN, Y.-T. & PRABHU, S. D. 2009. Divergent Tumor Necrosis Factor Receptor-Related Remodeling Responses in Heart Failure Role of Nuclear Factor-kappa B and Inflammatory Activation. *Circulation,* 119**,** 1386-1397.

HAUSMANN, M., KIESSLING, S., MESTERMANN, S., WEBB, G., SPOTTL, T., ANDUS, T., SCHOLMERICH, J., HERFARTH, H., RAY, K., FALK, W. & ROGLER, G. 2002. Toll-like receptors 2 and 4 are up-regulated during intestinal inflammation. *Gastroenterology,* 122**,** 1987-2000.

HAYASHI, F., SMITH, K. D., OZINSKY, A., HAWN, T. R., YI, E. C., GOODLETT, D. R., ENG, J. K., AKIRA, S., UNDERHILL, D. M. & ADEREM, A. 2001. The innate immune response to bacterial flagellin is mediated by Toll-like receptor 5. *Nature,* 410**,** 1099-103.

HE, B., XU, W., SANTINI, P. A., POLYDORIDES, A. D., CHIU, A., ESTRELLA, J., SHAN, M., CHADBURN, A., VILLANACCI, V., PLEBANI, A., KNOWLES, D. M., RESCIGNO, M. & CERUTTI, A. 2007. Intestinal bacteria trigger T cell-independent immunoglobulin A(2) class switching by inducing epithelial-cell secretion of the cytokine APRIL. *Immunity,* 26**,** 812-26.

HEAZLEWOOD, C. K., COOK, M. C., ERI, R., PRICE, G. R., TAURO, S. B., TAUPIN, D., THORNTON, D. J., PNG, C. W., CROCKFORD, T. L., CORNALL, R. J., ADAMS, R., KATO, M., NELMS, K. A., HONG, N. A., FLORIN, T. H., GOODNOW, C. C. & MCGUCKIN, M. A. 2008. Aberrant mucin assembly in mice causes endoplasmic reticulum stress and spontaneous inflammation resembling ulcerative colitis. *PLoS Med,* 5**,** e54.

HEINSBROEK, S. E. & GORDON, S. 2009. The role of macrophages in inflammatory bowel diseases. *Expert Rev Mol Med,* 11**,** e14.

HEMMI, H., TAKEUCHI, O., KAWAI, T., KAISHO, T., SATO, S., SANJO, H., MATSUMOTO, M., HOSHINO, K., WAGNER, H., TAKEDA, K. & AKIRA, S. 2000. A Toll-like receptor recognizes bacterial DNA. *Nature,* 408**,** 740-5.

HERSHBERG, R. M., CHO, D. H., YOUAKIM, A., BRADLEY, M. B., LEE, J. S., FRAMSON, P. E. & NEPOM, G. T. 1998. Highly polarized HLA class II

antigen processing and presentation by human intestinal epithelial cells. *Journal of Clinical Investigation,* 102**,** 792-803.

HERSHBERG, R. M. & MAYER, L. F. 2000. Antigen processing and presentation by intestinal epithelial cells - polarity and complexity. *Immunol Today,* 21**,** 123-8.

HIGUCHI, Y., MCTIERNAN, C. F., FRYE, C. B., MCGOWAN, B. S., CHAN, T. O. & FELDMAN, A. M. 2004. Tumor necrosis factor receptors 1 and 2 differentially regulate survival, cardiac dysfunction, and remodeling in transgenic mice with tumor necrosis factor-alpha-induced cardiomyopathy. *Circulation,* 109**,** 1892-7.

HINDRYCKX P, L. D. 2012. Intestinal barrier dysfunction : the primary driver of IBD? *In:* S, K. (ed.) *Inflammatory bowel disease : advances in pathogenesis and management.* Rijeka, Croatia: In-Tech.

HIROTANI, T., LEE, P. Y., KUWATA, H., YAMAMOTO, M., MATSUMOTO, M., KAWASE, I., AKIRA, S. & TAKEDA, K. 2005. The nuclear licB protein I kappa BNS selectively inhibits lipopolysaccharide-induced IL-6 production in macrophages of the colonic lamina propria. *Journal of Immunology,* 174**,** 3650-3657.

HOLT, P. G., ROBINSON, B. W. S., REID, M., KEES, U. R., WARTON, A., DAWSON, V. H., ROSE, A., SCHONHEGRAD, M. & PAPADIMITRIOU, J. M. 1986. EXTRACTION OF IMMUNE AND INFLAMMATORY CELLS FROM HUMAN-LUNG PARENCHYMA - EVALUATION OF AN ENZYMATIC DIGESTION PROCEDURE. *Clinical and Experimental Immunology,* 66**,** 188-200.

HOUSLEY, W. J., ADAMS, C. O., NICHOLS, F. C., PUDDINGTON, L., LINGENHELD, E. G., ZHU, L., RAJAN, T. V. & CLARK, R. B. 2011. Natural but not inducible regulatory T cells require TNF-alpha signaling for in vivo function. *J Immunol,* 186**,** 6779-87.

HUGOT, J. P., CHAMAILLARD, M., ZOUALI, H., LESAGE, S., CEZARD, J. P., BELAICHE, J., ALMER, S., TYSK, C., O'MORAIN, C. A., GASSULL, M., BINDER, V., FINKEL, Y., CORTOT, A., MODIGLIANI, R., LAURENT-PUIG, P., GOWER-ROUSSEAU, C., MACRY, J., COLOMBEL, J. F., SAHBATOU, M. & THOMAS, G. 2001. Association of NOD2 leucine-rich repeat variants with susceptibility to Crohn's disease. *Nature,* 411**,** 599-603.

HUME, D. A. 2006. The mononuclear phagocyte system. *Current Opinion in Immunology,* 18**,** 49-53.

HUME, D. A., PERRY, V. H. & GORDON, S. 1984. THE MONONUCLEAR PHAGOCYTE SYSTEM OF THE MOUSE DEFINED BY IMMUNOHISTOCHEMICAL LOCALIZATION OF ANTIGEN F4/80 - MACROPHAGES ASSOCIATED WITH EPITHELIA. *Anatomical Record,* 210**,** 503-512.

IKEDA, I., KASAJIMA, T., ISHIYAMA, S., SHIMOJO, T., TAKEO, Y., NISHIKAWA, T., KAMEOKA, S., HIROE, M. & MITSUNAGA, A. 1997. Distribution of inducible nitric oxide synthase in ulcerative colitis. *American Journal of Gastroenterology,* 92**,** 1339-1341.

ILIEV, I. D., MILETI, E., MATTEOLI, G., CHIEPPA, M. & RESCIGNO, M. 2009. Intestinal epithelial cells promote colitis-protective regulatory T-cell differentiation through dendritic cell conditioning. *Mucosal Immunology,* 2**,** 340-350.

INUI, M., ISHIDA, Y., KIMURA, A., KUNINAKA, Y., MUKAIDA, N. & KONDO, T. 2011. Protective Roles of CX3CR1-Mediated Signals in Toxin A-Induced Enteritis through the Induction of Heme Oxygenase-1 Expression. *Journal of Immunology,* 186**,** 423-431.

JACOBS, M., BROWN, N., ALLIE, N., CHETTY, K. & RYFFEL, B. 2000. Tumor necrosis factor receptor 2 plays a minor role for mycobacterial immunity. *Pathobiology,* 68**,** 68-75.

JIANG, Y., WORONICZ, J. D., LIU, W. & GOEDDEL, D. V. 1999. Prevention of constitutive TNF receptor 1 signaling by silencer of death domains. *Science,* 283**,** 543-6.

JOHANSSON, M. E., PHILLIPSON, M., PETERSSON, J., VELCICH, A., HOLM, L. & HANSSON, G. C. 2008. The inner of the two Muc2 mucin-dependent mucus layers in colon is devoid of bacteria. *Proc Natl Acad Sci U S A,* 105**,** 15064-9.

JUNG, C., HUGOT, J.-P., BARREAU, F., #233 & RICK 2010. Peyer's Patches: The Immune Sensors of the Intestine. *International Journal of Inflammation,* 2010.

JUNG, S., UNUTMAZ, D., WONG, P., SANO, G., DE LOS SANTOS, K., SPARWASSER, T., WU, S., VUTHOORI, S., KO, K., ZAVALA, F.,

PAMER, E. G., LITTMAN, D. R. & LANG, R. A. 2002. In vivo depletion of CD11c+ dendritic cells abrogates priming of CD8+ T cells by exogenous cell-associated antigens. *Immunity,* 17**,** 211-20.

KAFROUNI, M. I., BROWN, G. R. & THIELE, D. L. 2003. The role of TNF-TNFR2 interactions in generation of CTL responses and clearance of hepatic adenovirus infection. *J Leukoc Biol,* 74**,** 564-71.

KAMADA, N., HISAMATSU, T., OKAMOTO, S., SATO, T., MATSUOKA, K., ARAI, K., NAKAI, T., HASEGAWA, A., INOUE, N., WATANABE, N., AKAGAWA, K. S. & HIBI, T. 2005. Abnormally differentiated subsets of intestinal macrophage play a key role in Th1-dominant chronic colitis through excess production of IL-12 and IL-23 in response to bacteria. *Journal of Immunology,* 175**,** 6900-6908.

KANG, S., OKUNO, T., TAKEGAHARA, N., TAKAMATSU, H., NOJIMA, S., KIMURA, T., YOSHIDA, Y., ITO, D., OHMAE, S., YOU, D. J., TOYOFUKU, T., JANG, M. H. & KUMANOGOH, A. 2012. Intestinal epithelial cell-derived semaphorin 7A negatively regulates development of colitis via alphavbeta1 integrin. *J Immunol,* 188**,** 1108-16.

KARIN, M. & BEN-NERIAH, Y. 2000. Phosphorylation meets ubiquitination: the control of NF-[kappa]B activity. *Annu Rev Immunol,* 18**,** 621-63.

KASER, A., LEE, A. H., FRANKE, A., GLICKMAN, J. N., ZEISSIG, S., TILG, H., NIEUWENHUIS, E. E., HIGGINS, D. E., SCHREIBER, S., GLIMCHER, L. H. & BLUMBERG, R. S. 2008. XBP1 links ER stress to intestinal inflammation and confers genetic risk for human inflammatory bowel disease. *Cell,* 134**,** 743-56.

KASSIOTIS, G. & KOLLIAS, G. 2001. Uncoupling the proinflammatory from the immunosuppressive properties of tumor necrosis factor (TNF) at the p55 TNF receptor level: Implications for pathogenesis and therapy of autoimmune demyelination. *Journal of Experimental Medicine,* 193**,** 427-434.

KELLY, D., CAMPBELL, J. I., KING, T. P., GRANT, G., JANSSON, E. A., COUTTS, A. G., PETTERSSON, S. & CONWAY, S. 2004. Commensal anaerobic gut bacteria attenuate inflammation by regulating nuclear-cytoplasmic shuttling of PPAR-gamma and RelA. *Nat Immunol,* 5**,** 104-12.

KESHAVARZIAN, A., BANAN, A., FARHADI, A., KOMANDURI, S., MUTLU, E., ZHANG, Y. & FIELDS, J. Z. 2003. Increases in free radicals and cytoskeletal protein oxidation and nitration in the colon of patients with inflammatory bowel disease. *Gut*, 52**,** 720-8.

KIM, E. Y., PRIATEL, J. J., TEH, S. J. & TEH, H. S. 2006. TNF receptor type 2 (p75) functions as a costimulator for antigen-driven T cell responses in vivo. *Journal of Immunology*, 176**,** 1026-1035.

KOBAYASHI, K., TAKAHASHI, N., JIMI, E., UDAGAWA, N., TAKAMI, M., KOTAKE, S., NAKAGAWA, N., KINOSAKI, M., YAMAGUCHI, K., SHIMA, N., YASUDA, H., MORINAGA, T., HIGASHIO, K., MARTIN, T. J. & SUDA, T. 2000. Tumor necrosis factor alpha stimulates osteoclast differentiation by a mechanism independent of the ODF/RANKL-RANK interaction. *J Exp Med,* 191**,** 275-86.

KOLMODIN, L. A. & BIRCH, D. E. 2002. Polymerase Chain Reaction.

KONTOYIANNIS, D., PASPARAKIS, M., PIZARRO, T. T., COMINELLI, F. & KOLLIAS, G. 1999. Impaired on/off regulation of TNF biosynthesis in mice lacking TNF AU-rich elements: Implications for joint and gut-associated immunopathologies. *Immunity,* 10**,** 387-398.

KULLMANN, F., MESSMANN, H., ALT, M., GROSS, V., BOCKER, T., SCHOLMERICH, J. & RUSCHOFF, J. 2001. Clinical and histopathological features of dextran sulfate sodium induced acute and chronic colitis associated with dysplasia in rats. *International Journal of Colorectal Disease,* 16**,** 238-246.

KUPRASH, D. V., ALIMZHANOV, M. B., TUMANOV, A. V., ANDERSON, A. O., PFEFFER, K. & NEDOSPASOV, S. A. 1999. TNF and lymphotoxin beta cooperate in the maintenance of secondary lymphoid tissue microarchitecture but not in the development of lymph nodes. *Journal of Immunology,* 163**,** 6575-6580.

LEE, J., MO, J. H., KATAKURA, K., ALKALAY, I., RUCKER, A. N., LIU, Y. T., LEE, H. K., SHEN, C., COJOCARU, G., SHENOUDA, S., KAGNOFF, M., ECKMANN, L., BEN-NERIAH, Y. & RAZ, E. 2006. Maintenance of colonic homeostasis by distinctive apical TLR9 signalling in intestinal epithelial cells. *Nat Cell Biol,* 8**,** 1327-36.

LEE, S. H., STARKEY, P. M. & GORDON, S. 1985. QUANTITATIVE-ANALYSIS OF TOTAL MACROPHAGE CONTENT IN ADULT-MOUSE TISSUES - IMMUNOCHEMICAL STUDIES WITH MONOCLONAL-ANTIBODY F4/80. *Journal of Experimental Medicine,* 161**,** 475-489.

LEFRANCOIS, L. & LYCKE, N. 2001. Isolation of mouse small intestinal intraepithelial lymphocytes, Peyer's patch, and lamina propria cells. *Current protocols in immunology / edited by John E. Coligan ... [et al.],* Chapter 3.

LEY, R. E., PETERSON, D. A. & GORDON, J. I. 2006. Ecological and evolutionary forces shaping microbial diversity in the human intestine. *Cell,* 124**,** 837-48.

LI, H., KOBAYASHI, M., BLONSKA, M., YOU, Y. & LIN, X. 2006. Ubiquitination of RIP is required for tumor necrosis factor alpha-induced NF-kappaB activation. *J Biol Chem,* 281**,** 13636-43.

LIU, J., ZHAO, M. Q., XU, L., RAMANA, C. V., DECLERCQ, W., VANDENABEELE, P. & ENELOW, R. I. 2005. Requirement for tumor necrosis factor-receptor 2 in alveolar chemokine expression depends upon the form of the ligand. *Am J Respir Cell Mol Biol,* 33**,** 463-9.

LOFTUS, E. V., JR. 2004. Clinical epidemiology of inflammatory bowel disease: Incidence, prevalence, and environmental influences. *Gastroenterology,* 126**,** 1504-17.

LUCAS, A. D., CHADWICK, N., WARREN, B. F., JEWELL, D. P., GORDON, S., POWRIE, F. & GREAVES, D. R. 2001. The transmembrane form of the CX3CL1 chemokine fractalkine is expressed predominantly by epithelial cells in vivo. *Am J Pathol,* 158**,** 855-66.

LUO, J. C., SHIN, V. Y., YANG, Y. H., WU, W. K. K., YE, Y. N., SO, W. H. L., CHANG, F. Y. & CHO, C. H. 2005. Tumor necrosis factor-alpha stimulates gastric epithelial cell proliferation. *American Journal of Physiology-Gastrointestinal and Liver Physiology,* 288**,** G32-G38.

LYONS, A., LYNCH, A. M., DOWNER, E. J., HANLEY, R., O'SULLIVAN, J. B., SMITH, A. & LYNCH, M. A. 2009. Fractalkine-induced activation of the phosphatidylinositol-3 kinase pathway attentuates microglial activation in vivo and in vitro. *J Neurochem,* 110**,** 1547-56.

MA, X. J., SUN, J. W., PAPASAVVAS, E., RIEMANN, H., ROBERTSON, S., MARSHALL, J., BAILER, R. T., MOORE, A., DONNELLY, R. P.,

TRINCHIERI, G. & MONTANER, L. J. 2000. Inhibition of IL-12 production in human monocyte-derived macrophages by TNF. *Journal of Immunology,* 164**,** 1722-1729.

MACDONALD, T. T., BIANCHERI, P., SARRA, M. & MONTELEONE, G. 2012. What's the next best cytokine target in IBD? *Inflamm Bowel Dis,* 18**,** 2180-9.

MAHESHWARI, A., KELLY, D. R., NICOLA, T., AMBALAVANAN, N., JAIN, S. K., MURPHY-ULLRICH, J., ATHAR, M., SHIMAMURA, M., BHANDARI, V., APRAHAMIAN, C., DIMMITT, R. A., SERRA, R. & OHLS, R. K. 2011. TGF-beta2 suppresses macrophage cytokine production and mucosal inflammatory responses in the developing intestine. *Gastroenterology,* 140**,** 242-53.

MAHIDA, Y. R., PATEL, S., GIONCHETTI, P., VAUX, D. & JEWELL, D. P. 1989a. MACROPHAGE SUBPOPULATIONS IN LAMINA PROPRIA OF NORMAL AND INFLAMED COLON AND TERMINAL ILEUM. *Gut,* 30**,** 826-834.

MAHIDA, Y. R., WU, K. C. & JEWELL, D. P. 1989b. Respiratory burst activity of intestinal macrophages in normal and inflammatory bowel-disease. *Gut,* 30**,** 1362-1370.

MAJITHIA, V. & GERACI, S. A. 2007. Rheumatoid Arthritis: Diagnosis and Management. *The American journal of medicine,* 120**,** 936-939.

MALICH, G., MARKOVIC, B. & WINDER, C. 1997. The sensitivity and specificity of the MTS tetrazolium assay for detecting the in vitro cytotoxicity of 20 chemicals using human cell lines. *Toxicology,* 124**,** 179-92.

MANN, D. L. 2002. Inflammatory Mediators and the Failing Heart: Past, Present, and the Foreseeable Future. *Circulation Research,* 91**,** 988-998.

MARCINKIEWICZ, J. 1991. In vitro cytokine release by activated murine peritoneal macrophages: Role of prostaglandins in the differential regulation of tumor necrosis factor alpha, interleukin 1, and interleukin 6. *Cytokine,* 3**,** 327-332.

MARINO, M. W., DUNN, A., GRAIL, D., INGLESE, M., NOGUCHI, Y., RICHARDS, E., JUNGBLUTH, A., WADA, H., MOORE, M., WILLIAMSON, B., BASU, S. & OLD, L. J. 1997. Characterization of tumor necrosis factor-deficient mice. *Proceedings of the National Academy of Sciences,* 94**,** 8093-8098.

MARTIN, E. M., REMKE, A., PFEIFER, E., POLZ, J., PIETRYGA-KRIEGER, A., STEFFENS-WEBER, D., FREUDENBERG, M. A., MOSTBOCK, S. & MANNEL, D. N. 2013. TNFR2 maintains adequate IL-12 production by dendritic cells in inflammatory responses by regulating endogenous TNF levels. *Innate Immun*.

MARTINEZPOMARES, L., PLATT, N., MCKNIGHT, A. J., DASILVA, R. P. & GORDON, S. 1996. Macrophage membrane molecules: Markers of tissue differentiation and heterogeneity. *Immunobiology,* 195**,** 407-416.

MCDONALD, L. C., KILLGORE, G. E., THOMPSON, A., OWENS, R. C., KAZAKOVA, S. V., SAMBOL, S. P., JOHNSON, S. & GERDING, D. N. 2005. An epidemic, toxin gene-variant strain of Clostridium difficile. *New England Journal of Medicine,* 353**,** 2433-2441.

MCDONALD, L. C., OWINGS, M. & JERNIGAN, D. B. 2006. Clostridium difficile infection in patients discharged from US short-stay hospitals, 1996-2003. *Emerg Infect Dis,* 12**,** 409-15.

MCGOVERN, D. P., HYSI, P., AHMAD, T., VAN HEEL, D. A., MOFFATT, M. F., CAREY, A., COOKSON, W. O. & JEWELL, D. P. 2005. Association between a complex insertion/deletion polymorphism in NOD1 (CARD4) and susceptibility to inflammatory bowel disease. *Hum Mol Genet,* 14**,** 1245-50.

MEDINA-CONTRERAS, O., GEEM, D., LAUR, O., WILLIAMS, I. R., LIRA, S. A., NUSRAT, A., PARKOS, C. A. & DENNING, T. L. 2011. CX3CR1 regulates intestinal macrophage homeostasis, bacterial translocation, and colitogenic Th17 responses in mice. *J Clin Invest,* 121**,** 4787-95.

MEDZHITOV, R. 2007. Recognition of microorganisms and activation of the immune response. *Nature,* 449**,** 819-826.

MENNIGEN, R., NOLTE, K., RIJCKEN, E., UTECH, M., LOEFFLER, B., SENNINGER, N. & BRUEWER, M. 2009. Probiotic mixture VSL#3 protects the epithelial barrier by maintaining tight junction protein expression and preventing apoptosis in a murine model of colitis. *Am J Physiol Gastrointest Liver Physiol,* 296**,** G1140-9.

MENTEN, P., WUYTS, A. & VAN DAMME, J. 2002. Macrophage inflammatory protein-1. *Cytokine & Growth Factor Reviews,* 13**,** 455-481.

MENZEL, K., HAUSMANN, M., OBERMEIER, F., SCHREITER, K., DUNGER, N., BATAILLE, F., FALK, W., SCHOLMERICH, J., HERFARTH, H. &

ROGLER, G. 2006. Cathepsins B, L and D in inflammatory bowel disease macrophages and potential therapeutic effects of cathepsin inhibition in vivo. *Clin Exp Immunol,* 146**,** 169-80.

MICHEAU, O. & TSCHOPP, J. 2003. Induction of TNF receptor I-mediated apoptosis via two sequential signaling complexes. *Cell,* 114**,** 181-90.

MIZOGUCHI, E., MIZOGUCHI, A., TAKEDATSU, H., CARIO, E., DE JONG, Y. P., OOI, C. J., XAVIER, R. J., TERHORST, C., PODOLSKY, D. K. & BHAN, A. K. 2002. Role of tumor necrosis factor receptor 2 (TNFR2) in colonic epithelial hyperplasia and chronic intestinal inflammation in mice. *Gastroenterology,* 122**,** 134-144.

MOOTOO, A., STYLIANOU, E., ARIAS, M. A. & RELJIC, R. 2009. TNF-alpha in tuberculosis: a cytokine with a split personality. *Inflamm Allergy Drug Targets,* 8**,** 53-62.

MORA, J. R., IWATA, M., EKSTEEN, B., SONG, S.-Y., JUNT, T., SENMAN, B., OTIPOBY, K. L., YOKOTA, A., TAKEUCHI, H., RICCIARDI-CASTAGNOLI, P., RAJEWSKY, K., ADAMS, D. H. & VON ANDRIAN, U. H. 2006. Generation of Gut-Homing IgA-Secreting B Cells by Intestinal Dendritic Cells. *Science,* 314**,** 1157-1160.

MOWAT, A. M. 2011. Mucosal Macrophages in Intestinal Homeostasis and Inflammation. *Journal of Innate Immunity,* 3**,** 550-564.

MOWAT, A. M. & BAIN, C. C. 2010. The curious case of the intestinal eosinophil. *Mucosal Immunology,* 3**,** 420-421.

MUKHERJEE, S., VAISHNAVA, S. & HOOPER, L. V. 2008. Multi-layered regulation of intestinal antimicrobial defense. *Cell Mol Life Sci,* 65**,** 3019-27.

MURAI, M., TUROVSKAYA, O., KIM, G., MADAN, R., KARP, C. L., CHEROUTRE, H. & KRONENBERG, M. 2009. Interleukin 10 acts on regulatory T cells to maintain expression of the transcription factor Foxp3 and suppressive function in mice with colitis. *Nature Immunology,* 10**,** 1178-U61.

NAITO, Y., TAKAGI, T., HANDA, O., ISHIKAWA, T., NAKAGAWA, S., YAMAGUCHI, T., YOSHIDA, N., MINAMI, M., KITA, M., IMANISHI, J. & YOSHIKAWA, T. 2003. Enhanced intestinal inflammation induced by dextran sulfate sodium in tumor necrosis factor-alpha deficient mice. *J Gastroenterol Hepatol,* 18**,** 560-9.

NAKATA, K., INAGAWA, H., NISHIZAWA, T., HONDA, T., KOHCHI, C., TONOMOTO, Y., YOSHIMURA, H., NAGASUE, N., NATORI, S., TERADA, H. & SOMA, G. 2006a. Inherent potential for production of tumor necrosis factor-alpha by human intestinal macrophages. *Int J Colorectal Dis,* 21**,** 339-47.

NAKATA, K., INAGAWA, H., NISHIZAWA, T., KOHCHI, C. & SOMA, G. I. 2006b. Specific messenger RNA expression for signal transduction molecules by lipopolysaccharide in intestinal macrophages. *Clinical and Experimental Immunology,* 143**,** 484-493.

NAUDE, P. J., DEN BOER, J. A., LUITEN, P. G. & EISEL, U. L. 2011. Tumor necrosis factor receptor cross-talk. *FEBS J,* 278**,** 888-98.

NEISH, A. S., GEWIRTZ, A. T., ZENG, H., YOUNG, A. N., HOBERT, M. E., KARMALI, V., RAO, A. S. & MADARA, J. L. 2000. Prokaryotic regulation of epithelial responses by inhibition of IkappaB-alpha ubiquitination. *Science,* 289**,** 1560-3.

NISHITOH, H., SAITOH, M., MOCHIDA, Y., TAKEDA, K., NAKANO, H., ROTHE, M., MIYAZONO, K. & ICHIJO, H. 1998. ASK1 is essential for JNK/SAPK activation by TRAF2. *Mol Cell,* 2**,** 389-95.

NOTI, M., CORAZZA, N., MUELLER, C., BERGER, B. & BRUNNER, T. 2010. TNF suppresses acute intestinal inflammation by inducing local glucocorticoid synthesis. *J Exp Med,* 207**,** 1057-66.

O'DONNELL, M. A. & TING, A. T. 2011. RIP1 comes back to life as a cell death regulator in TNFR1 signaling. *FEBS J,* 278**,** 877-87.

OFENGEIM, D. & YUAN, J. 2013. Regulation of RIP1 kinase signalling at the crossroads of inflammation and cell death. *Nat Rev Mol Cell Biol,* 14**,** 727-36.

OKAYASU, I., HATAKEYAMA, S., YAMADA, M., OHKUSA, T., INAGAKI, Y. & NAKAYA, R. 1990a. A NOVEL METHOD IN THE INDUCTION OF RELIABLE EXPERIMENTAL ACUTE AND CHRONIC ULCERATIVE-COLITIS IN MICE. *Gastroenterology,* 98**,** 694-702.

OKAYASU, I., HATAKEYAMA, S., YAMADA, M., OHKUSA, T., INAGAKI, Y. & NAKAYA, R. 1990b. A novel method in the induction of reliable experimental acute and chronic ulcerative colitis in mice. *Gastroenterology,* 98**,** 694-702.

ORMEROD, M. G. 2008. *Flow cytometry A basic introduction* Michael G. Ormerod.

OTTE, J. M., CARIO, E. & PODOLSKY, D. K. 2004. Mechanisms of cross hyporesponsiveness to toll-like receptor bacterial ligands in intestinal epithelial cells. *Gastroenterology,* 126**,** 1054-1070.

OWENS, R. C., JR., DONSKEY, C. J., GAYNES, R. P., LOO, V. G. & MUTO, C. A. 2008. Antimicrobial-associated risk factors for Clostridium difficile infection. *Clin Infect Dis,* 46 Suppl 1**,** S19-31.

PABST, O. & BERNHARDT, G. 2010. The puzzle of intestinal lamina propria dendritic cells and macrophages. *European Journal of Immunology,* 40**,** 2107-2111.

PARAMESWARAN, N. & PATIAL, S. 2010. Tumor necrosis factor-alpha signaling in macrophages. *Crit Rev Eukaryot Gene Expr,* 20**,** 87-103.

PAVLI, P. 2001. Murine intestinal dendritic cell isolation. *Methods in molecular medicine,* 64**,** 63-72.

PERSSON, E. K., JAENSSON, E. & AGACE, W. W. 2010. The diverse ontogeny and function of murine small intestinal dendritic cell/macrophage subsets. *Immunobiology,* 215**,** 692-697.

PESCHON, J. J., TORRANCE, D. S., STOCKING, K. L., GLACCUM, M. B., OTTEN, C., WILLIS, C. R., CHARRIER, K., MORRISSEY, P. J., WARE, C. B. & MOHLER, K. M. 1998. TNF receptor-deficient mice reveal divergent roles for p55 and p75 in several models of inflammation. *Journal of Immunology,* 160**,** 943-952.

PFEFFER, K., MATSUYAMA, T., KUNDIG, T. M., WAKEHAM, A., KISHIHARA, K., SHAHINIAN, A., WIEGMANN, K., OHASHI, P. S., KRONKE, M. & MAK, T. W. 1993. Mice deficient for the 55 kd tumor necrosis factor receptor are resistant to endotoxic shock, yet succumb to L. monocytogenes infection. *Cell,* 73**,** 457-67.

PHILPOTT, D. J. & GIRARDIN, S. E. 2004. The role of Toll-like receptors and Nod proteins in bacterial infection. *Mol Immunol,* 41**,** 1099-108.

PIERIK, M., VERMEIRE, S., STEEN, K. V., JOOSSENS, S., CLAESSENS, G., VLIETINCK, R. & RUTGEERTS, P. 2004. Tumour necrosis factor-alpha receptor 1 and 2 polymorphisms in inflammatory bowel disease and their association with response to infliximab. *Aliment Pharmacol Ther,* 20**,** 303-10.

PINTO, D., GREGORIEFF, A., BEGTHEL, H. & CLEVERS, H. 2003. Canonical Wnt signals are essential for homeostasis of the intestinal epithelium. *Genes Dev,* 17**,** 1709-13.

PLATT, A. M., BAIN, C. C., BORDON, Y., SESTER, D. P. & MOWAT, A. M. 2010. An Independent Subset of TLR Expressing CCR2-Dependent Macrophages Promotes Colonic Inflammation. *Journal of Immunology,* 184**,** 6843-6854.

PLEVY, S. E., LANDERS, C. J., PREHN, J., CARRAMANZANA, N. M., DEEM, R. L., SHEALY, D. & TARGAN, S. R. 1997. A role for TNF-alpha and mucosal T helper-1 cytokines in the pathogenesis of Crohn's disease. *Journal of Immunology,* 159**,** 6276-6282.

PODOLSKY, D. K. 2002. Inflammatory bowel disease. *N Engl J Med,* 347**,** 417-29.

PORITZ, L. S., GARVER, K. I., GREEN, C., FITZPATRICK, L., RUGGIERO, F. & KOLTUN, W. A. 2007. Loss of the tight junction protein ZO-1 in dextran sulfate sodium induced colitis. *Journal of Surgical Research,* 140**,** 12-19.

POTT, J. & HORNEF, M. 2012. Innate immune signalling at the intestinal epithelium in homeostasis and disease. *EMBO Rep,* 13**,** 684-98.

PULL, S. L., DOHERTY, J. M., MILLS, J. C., GORDON, J. I. & STAPPENBECK, T. S. 2005. Activated macrophages are an adaptive element of the colonic epithelial progenitor niche necessary for regenerative responses to injury. *Proceedings of the National Academy of Sciences of the United States of America,* 102**,** 99-104.

QUALLS, J. E., KAPLAN, A. M., VAN ROOIJEN, N. & COHEN, D. A. 2006. Suppression of experimental colitis by intestinal mononuclear phagocytes. *Journal of Leukocyte Biology,* 80**,** 802-815.

RACHMILEWITZ, D., KATAKURA, K., KARMELI, F., HAYASHI, T., REINUS, C., RUDENSKY, B., AKIRA, S., TAKEDA, K., LEE, J., TAKABAYASHI, K. & RAZ, E. 2004. Toll-like receptor 9 signaling mediates the anti-inflammatory effects of probiotics in murine experimental colitis. *Gastroenterology,* 126**,** 520-528.

RAKOFF-NAHOUM, S., PAGLINO, J., ESLAMI-VARZANEH, F., EDBERG, S. & MEDZHITOV, R. 2004. Recognition of commensal microflora by toll-like receptors is required for intestinal homeostasis. *Cell,* 118**,** 229-241.

RALPH RAPLEY, D. L. M. 1998. RNA isolation and characterisation protocols. Humana Press.

RATH, P. C. & AGGARWAL, B. B. 1999. TNF-induced signaling in apoptosis. *Journal of Clinical Immunology,* 19**,** 350-364.

RAUERT, H., WICOVSKY, A., MUELLER, N., SIEGMUND, D., SPINDLER, V., WASCHKE, J., KNEITZ, C. & WAJANT, H. 2010. Membrane Tumor Necrosis Factor (TNF) Induces p100 Processing via TNF Receptor-2 (TNFR2). *Journal of Biological Chemistry,* 285**,** 7394-7404.

RAYMAEKERS, M., SMETS, R., MAES, B. & CARTUYVELS, R. 2009. Checklist for optimization and validation of real-time PCR assays. *J Clin Lab Anal,* 23**,** 145-51.

REES, A. J. 2010. Monocyte and macrophage biology: an overview. *Semin Nephrol,* 30**,** 216-33.

RESCIGNO, M., URBANO, M., VALZASINA, B., FRANCOLINI, M., ROTTA, G., BONASIO, R., GRANUCCI, F., KRAEHENBUHL, J. P. & RICCIARDI-CASTAGNOLI, P. 2001. Dendritic cells express tight junction proteins and penetrate gut epithelial monolayers to sample bacteria. *Nat Immunol,* 2**,** 361-7.

RICCIARDELLI, I., LINDLEY, K. J., LONDEI, M. & QUARATINO, S. 2008. Anti tumour necrosis-alpha therapy increases the number of FOXP3 regulatory T cells in children affected by Crohn's disease. *Immunology,* 125**,** 178-83.

RIMOLDI, M., CHIEPPA, M., SALUCCI, V., AVOGADRI, F., SONZOGNI, A., SAMPIETRO, G. M., NESPOLI, A., VIALE, G., ALLAVENA, P. & RESCIGNO, M. 2005. Intestinal immune homeostasis is regulated by the crosstalk between epithelial cells and dendritic cells. *Nature Immunology,* 6**,** 507-514.

RIVOLLIER, A., HE, J., KOLE, A., VALATAS, V. & KELSALL, B. L. 2012. Inflammation switches the differentiation program of Ly6Chi monocytes from antiinflammatory macrophages to inflammatory dendritic cells in the colon. *J Exp Med,* 209**,** 139-55.

RODA, G., SARTINI, A., ZAMBON, E., CALAFIORE, A., MAROCCHI, M., CAPONI, A., BELLUZZI, A. & RODA, E. 2010. Intestinal epithelial cells in inflammatory bowel diseases. *World Journal of Gastroenterology,* 16**,** 4264-4271.

ROGLER, G., HAUSMANN, M., VOGL, D., ASCHENBRENNER, E., ANDUS, T., FALK, W., ANDREESEN, R., SCHOLMERICH, J. & GROSS, V. 1998. Isolation and phenotypic characterization of colonic macrophages. *Clinical and Experimental Immunology,* 112**,** 205-215.

RUGTVEIT, J., BAKKA, A. & BRANDTZAEG, P. 1997a. Differential distribution of B7.1(CD80) and B7.2(CD86) costimulatory molecules on mucosal macrophage subsets in human inflammatory bowel disease (IBD). *Clinical and Experimental Immunology,* 110**,** 104-113.

RUGTVEIT, J., HARALDSEN, G., HOGASEN, A. K., BAKKA, A., BRANDTZAEG, P. & SCOTT, H. 1995. Respiratory burst of intestinal macrophages in inflammatory bowel disease is mainly caused by CD14+L1+ monocyte derived cells. *Gut,* 37**,** 367-73.

RUGTVEIT, J., NILSEN, E. M., BAKKA, A., CARLSEN, H., BRANDTZAEG, P. & SCOTT, H. 1997b. Cytokine profiles differ in newly recruited and resident subsets of mucosal macrophages from inflammatory bowel disease. *Gastroenterology,* 112**,** 1493-1505.

RYAN, A., LYNCH, M., SMITH, S. M., AMU, S., NEL, H. J., MCCOY, C. E., DOWLING, J. K., DRAPER, E., O'REILLY, V., MCCARTHY, C., O'BRIEN, J., NI EIDHIN, D., O'CONNELL, M. J., KEOGH, B., MORTON, C. O., ROGERS, T. R., FALLON, P. G., O'NEILL, L. A., KELLEHER, D. & LOSCHER, C. E. 2011. A role for TLR4 in Clostridium difficile infection and the recognition of surface layer proteins. *PLoS Pathog,* 7**,** e1002076.

SAKAGUCHI, S. 2005. Naturally arising Foxp3-expressing CD25(+) CD4(+) regulatory T cells in immunological tolerance to self and non-self. *Nature Immunology,* 6**,** 345-352.

SALZMAN, N. H., UNDERWOOD, M. A. & BEVINS, C. L. 2007. Paneth cells, defensins, and the commensal microbiota: a hypothesis on intimate interplay at the intestinal mucosa. *Semin Immunol,* 19**,** 70-83.

SANDBORN, W. J., HANAUER, S. B., KATZ, S., SAFDI, M., WOLF, D. G., BAERG, R. D., TREMAINE, W. J., JOHNSON, T., DIEHL, N. N. & ZINSMEISTER, A. R. 2001. Etanercept for active Crohn's disease: a randomized, double-blind, placebo-controlled trial. *Gastroenterology,* 121**,** 1088-94.

SANDHU PREMJEET1, GUPTA DEEPIKA1, BHARDWAJ SUDEEP1, JAIN SONAM2, KATARIA SAHIL1, RATHORE DEVASHISH3, KUMAR SUNIL1 2012. *Enzyme-Linked Immuno-Sorbent Assay (ELISA), basics and it's application : A comprehensive review*.

SASAOKA, T., ITO, M., YAMASHITA, J., NAKAJIMA, K., TANAKA, I., NARITA, M., HARA, Y., HADA, K., TAKAHASHI, M., OHNO, Y., MATSUO, T., KANESHIRO, Y., TANAKA, H. & KANEKO, K. 2011. Treatment with IL-27 attenuates experimental colitis through the suppression of the development of IL-17-producing T helper cells. *Am J Physiol Gastrointest Liver Physiol,* 300**,** G568-76.

SASHIO, H., TAMURA, K., ITO, R., YAMAMOTO, Y., BAMBA, H., KOSAKA, T., FUKUI, S., SAWADA, K., FUKUDA, Y., SATOMI, M., SHIMOYAMA, T. & FURUYAMA, J. 2002. Polymorphisms of the TNF gene and the TNF receptor superfamily member 1B gene are associated with susceptibility to ulcerative colitis and Crohn's disease, respectively. *Immunogenetics,* 53**,** 1020-7.

SCALDAFERRI, F. & FIOCCHI, C. 2007. Inflammatory bowel disease: progress and current concepts of etiopathogenesis. *J Dig Dis,* 8**,** 171-8.

SCHENK, M., BOUCHON, A., BIRRER, S., COLONNA, M. & MUELLER, C. 2005. Macrophages expressing triggering receptor expressed on myeloid cells-1 are underrepresented in the human intestine. *Journal of Immunology,* 174**,** 517-524.

SCHENK, M., BOUCHON, A., SEIBOLD, F. & MUELLER, C. 2007. TREM-1--expressing intestinal macrophages crucially amplify chronic inflammation in experimental colitis and inflammatory bowel diseases. *J Clin Invest,* 117**,** 3097-106.

SCHENK, M. & MUELLER, C. 2007. Adaptations of intestinal macrophages to an antigen-rich environment. *Seminars in Immunology,* 19**,** 84-93.

SCHULZ, O., JAENSSON, E., PERSSON, E. K., LIU, X., WORBS, T., AGACE, W. W. & PABST, O. 2009. Intestinal CD103(+), but not CX3CR1(+), antigen sampling cells migrate in lymph and serve classical dendritic cell functions. *Journal of Experimental Medicine,* 206**,** 3101-3114.

SECONDULFO, M., DE MAGISTRIS, L., FIANDRA, R., CASERTA, L., BELLETTA, M., TARTAGLIONE, M. T., RIEGLER, G., BIAGI, F.,

CORAZZA, G. R. & CARRATU, R. 2001. Intestinal permeability in Crohn's disease patients and their first degree relatives. *Dig Liver Dis,* 33**,** 680-5.

SEYRANTEPE, V., IANNELLO, A., LIANG, F., KANSHIN, E., JAYANTH, P., SAMARANI, S., SZEWCZUK, M. R., AHMAD, A. & PSHEZHETSKY, A. V. 2010. Regulation of phagocytosis in macrophages by neuraminidase 1. *J Biol Chem,* 285**,** 206-15.

SHALE, M. & GHOSH, S. 2009. How intestinal epithelial cells tolerise dendritic cells and its relevance to inflammatory bowel disease. *Gut,* 58**,** 1291-1299.

SHARPE, A. H. & FREEMAN, G. J. 2002. The B7-CD28 superfamily. *Nature Reviews Immunology,* 2**,** 116-126.

SHEN, C., ASSCHE, G. V., COLPAERT, S., MAERTEN, P., GEBOES, K., RUTGEERTS, P. & CEUPPENS, J. L. 2005. Adalimumab induces apoptosis of human monocytes: a comparative study with infliximab and etanercept. *Alimentary Pharmacology & Therapeutics,* 21**,** 251-258.

SMITH, P. D., OCHSENBAUER-JAMBOR, C. & SMYTHIES, L. E. 2005. Intestinal macrophages: unique effector cells of the innate immune system. *Immunological Reviews,* 206**,** 149-159.

SMITH, P. D., SMYTHIES, L. E., MOSTELLER-BARNUM, M., SIBLEY, D. A., RUSSELL, M. W., MERGER, M., SELLERS, M. T., ORENSTEIN, J. M., SHIMADA, T., GRAHAM, M. F. & KUBAGAWA, H. 2001. Intestinal macrophages lack CD14 and CD89 and consequently are down-regulated for LPS- and IgA-mediated activities. *Journal of Immunology,* 167**,** 2651-2656.

SMITH, P. D., SMYTHIES, L. E., SHEN, R., GREENWELL-WILD, T., GLIOZZI, M. & WAHL, S. M. 2011. Intestinal macrophages and response to microbial encroachment. *Mucosal Immunology,* 4**,** 31-42.

SMYTHIES, L. E., SELLERS, M., CLEMENTS, R. H., MOSTELLER-BARNUM, M., MENG, G., BENJAMIN, W. H., ORENSTEIN, J. M. & SMITH, P. D. 2005. Human intestinal macrophages display profound inflammatory anergy despite avid phagocytic and bacteriocidal activity. *Journal of Clinical Investigation,* 115**,** 66-75.

SMYTHIES, L. E., SHEN, R. Z., BIMCZOK, D., NOVAK, L., CLEMENTS, R. H., ECKHOFF, D. E., BOUCHARD, P., GEORGE, M. D., HU, W. K., DANDEKAR, S. & SMITH, P. D. 2010. Inflammation Anergy in Human Intestinal Macrophages Is Due to Smad-induced I kappa B alpha Expression

and NF-kappa B Inactivation. *Journal of Biological Chemistry,* 285**,** 19593-19604.

SWEET, M. J. & HUME, D. A. 2003. CSF-1 as a regulator of macrophage activation and immune responses. *Archivum Immunologiae Et Therapiae Experimentalis,* 51**,** 169-177.

TADA, Y., HO, A., KOARADA, S., MORITO, F., USHIYAMA, O., SUZUKI, N., KIKUCHI, Y., OHTA, A., MAK, T. W. & NAGASAWA, K. 2001. Collagen-induced arthritis in TNF receptor-1-deficient mice: TNF receptor-2 can modulate arthritis in the absence of TNF receptor-1. *Clin Immunol,* 99**,** 325-33.

TAKADA, Y., HISAMATSU, T., KAMADA, N., KITAZUME, M. T., HONDA, H., OSHIMA, Y., SAITO, R., TAKAYAMA, T., KOBAYASHI, T., CHINEN, H., MIKAMI, Y., KANAI, T., OKAMOTO, S. & HIBI, T. 2010. Monocyte Chemoattractant Protein-1 Contributes to Gut Homeostasis and Intestinal Inflammation by Composition of IL-10-Producing Regulatory Macrophage Subset. *Journal of Immunology,* 184**,** 2671-2676.

TAKEDA, K., CLAUSEN, B. E., KAISHO, T., TSUJIMURA, T., TERADA, N., FORSTER, I. & AKIRA, S. 1999. Enhanced Th1 activity and development of chronic enterocolitis in mice devoid of Stat3 in macrophages and neutrophils. *Immunity,* 10**,** 39-49.

TAKEUCHI, O., HOSHINO, K., KAWAI, T., SANJO, H., TAKADA, H., OGAWA, T., TAKEDA, K. & AKIRA, S. 1999. Differential roles of TLR2 and TLR4 in recognition of gram-negative and gram-positive bacterial cell wall components. *Immunity,* 11**,** 443-51.

TAMOUTOUNOUR, S., HENRI, S., LELOUARD, H., DE BOVIS, B., DE HAAR, C., VAN DER WOUDE, C. J., WOLTMAN, A. M., REYAL, Y., BONNET, D., SICHIEN, D., BAIN, C. C., MOWAT, A. M., REIS E SOUSA, C., POULIN, L. F., MALISSEN, B. & GUILLIAMS, M. 2012. CD64 distinguishes macrophages from dendritic cells in the gut and reveals the Th1-inducing role of mesenteric lymph node macrophages during colitis. *Eur J Immunol,* 42**,** 3150-66.

TARTAGLIA, L. A. & GOEDDEL, D. V. 1992. 2 TNF RECEPTORS. *Immunology Today,* 13**,** 151-153.

TARTAGLIA, L. A., PENNICA, D. & GOEDDEL, D. V. 1993. LIGAND PASSING - THE 75-KDA TUMOR-NECROSIS-FACTOR (TNF) RECEPTOR RECRUITS TNF FOR SIGNALING BY THE 55-KDA TNF RECEPTOR. *Journal of Biological Chemistry,* 268**,** 18542-18548.

TILL, A., ROSENSTIEL, P., KRIPPNER-HEIDENREICH, A., MASCHERETTI-CROUCHER, S., CROUCHER, P. J., SCHAFER, H., SCHEURICH, P., SEEGERT, D. & SCHREIBER, S. 2005. The Met-196 -> Arg variation of human tumor necrosis factor receptor 2 (TNFR2) affects TNF-alpha-induced apoptosis by impaired NF-kappaB signaling and target gene expression. *J Biol Chem,* 280**,** 5994-6004.

TRACEY, K. J. & CERAMI, A. 1993. Tumor necrosis factor, other cytokines and disease. *Annu Rev Cell Biol,* 9**,** 317-43.

TRAVIS, M. A., REIZIS, B., MELTON, A. C., MASTELLER, E., TANG, Q., PROCTOR, J. M., WANG, Y., BERNSTEIN, X., HUANG, X., REICHARDT, L. F., BLUESTONE, J. A. & SHEPPARD, D. 2007. Loss of integrin alpha(v)beta8 on dendritic cells causes autoimmunity and colitis in mice. *Nature,* 449**,** 361-5.

TROY, A. E., ZAPH, C., DU, Y., TAYLOR, B. C., GUILD, K. J., HUNTER, C. A., SARIS, C. J. & ARTIS, D. 2009. IL-27 regulates homeostasis of the intestinal CD4+ effector T cell pool and limits intestinal inflammation in a murine model of colitis. *J Immunol,* 183**,** 2037-44.

UEDA, Y., KAYAMA, H., JEON, S. G., KUSU, T., ISAKA, Y., RAKUGI, H., YAMAMOTO, M. & TAKEDA, K. 2010. Commensal microbiota induce LPS hyporesponsiveness in colonic macrophages via the production of IL-10. *International Immunology,* 22**,** 953-962.

ULLUWISHEWA, D., ANDERSON, R. C., MCNABB, W. C., MOUGHAN, P. J., WELLS, J. M. & ROY, N. C. 2011. Regulation of tight junction permeability by intestinal bacteria and dietary components. *J Nutr,* 141**,** 769-76.

VALLABHAPURAPU, S. & KARIN, M. 2009. Regulation and function of NF-kappaB transcription factors in the immune system. *Annu Rev Immunol,* 27**,** 693-733.

VAN HERREWEGHE, F., FESTJENS, N., DECLERCQ, W. & VANDENABEELE, P. 2010. Tumor necrosis factor-mediated cell death: to

break or to burst, that's the question. *Cellular and Molecular Life Sciences,* 67**,** 1567-1579.

VANDERHEIJDEN, P. J. & STOK, W. 1987. IMPROVED PROCEDURE FOR THE ISOLATION OF FUNCTIONALLY ACTIVE LYMPHOID-CELLS FROM THE MURINE INTESTINE. *Journal of Immunological Methods,* 103**,** 161-167.

VANDERPOLL, T., JANSEN, P. M., VANZEE, K. J., WELBORN, M. B., DEJONG, I., HACK, C. E., LOETSCHER, H., LESSLAUER, W., LOWRY, S. F. & MOLDAWER, L. L. 1996. Tumor necrosis factor-alpha induces activation of coagulation and fibrinolysis in baboons through an exclusive effect on the p55 receptor. *Blood,* 88**,** 922-927.

VARFOLOMEEV, E., GONCHAROV, T., FEDOROVA, A. V., DYNEK, J. N., ZOBEL, K., DESHAYES, K., FAIRBROTHER, W. J. & VUCIC, D. 2008. c-IAP1 and c-IAP2 are critical mediators of tumor necrosis factor alpha (TNFalpha)-induced NF-kappaB activation. *J Biol Chem,* 283**,** 24295-9.

VAROL, C., VALLON-EBERHARD, A., ELINAV, E., AYCHEK, T., SHAPIRA, Y., LUCHE, H., FEHLING, H. J., HARDT, W.-D., SHAKHAR, G. & JUNG, S. 2009. Intestinal Lamina Propria Dendritic Cell Subsets Have Different Origin and Functions. *Immunity,* 31**,** 502-512.

VIALA, J., CHAPUT, C., BONECA, I. G., CARDONA, A., GIRARDIN, S. E., MORAN, A. P., ATHMAN, R., MEMET, S., HUERRE, M. R., COYLE, A. J., DISTEFANO, P. S., SANSONETTI, P. J., LABIGNE, A., BERTIN, J., PHILPOTT, D. J. & FERRERO, R. L. 2004. Nod1 responds to peptidoglycan delivered by the Helicobacter pylori cag pathogenicity island. *Nat Immunol,* 5**,** 1166-74.

VIELHAUER, V., STAVRAKIS, G. & MAYADAS, T. N. 2005. Renal cell-expressed TNF receptor 2, not receptor 1, is essential for the development of glomerulonephritis. *Journal of Clinical Investigation,* 115**,** 1199-1209.

VIJAY-KUMAR, M., AITKEN, J. D., SANDERS, C. J., FRIAS, A., SLOANE, V. M., XU, J. G., NEISH, A. S., ROJAS, M. & GEWIRTZ, A. T. 2008. Flagellin treatment protects against chemicals, bacteria, viruses, and radiation. *Journal of Immunology,* 180**,** 8280-8285.

VOS, A. C., WILDENBERG, M. E., DUIJVESTEIN, M., VERHAAR, A. P., VAN DEN BRINK, G. R. & HOMMES, D. W. 2011. Anti-tumor necrosis factor-

alpha antibodies induce regulatory macrophages in an Fc region-dependent manner. *Gastroenterology,* 140**,** 221-30.

WAETZIG, G. H., SEEGERT, D., ROSENSTIEL, P., NIKOLAUS, S. & SCHREIBER, S. 2002. p38 mitogen-activated protein kinase is activated and linked to TNF-alpha signaling in inflammatory bowel disease. *J Immunol,* 168**,** 5342-51.

WAJANT, H., PFIZENMAIER, K. & SCHEURICH, P. 2003. Tumor necrosis factor signaling. *Cell Death and Differentiation,* 10**,** 45-65.

WANG, C., DENG, L., HONG, M., AKKARAJU, G. R., INOUE, J. & CHEN, Z. J. 2001. TAK1 is a ubiquitin-dependent kinase of MKK and IKK. *Nature,* 412**,** 346-51.

WANG, C., YU, X., CAO, Q., WANG, Y., ZHENG, G., TAN, T. K., ZHAO, H., ZHAO, Y. & HARRIS, D. 2013a. Characterization of murine macrophages from bone marrow, spleen and peritoneum. *BMC Immunol,* 14**,** 6.

WANG, K., HAN, G., DOU, Y., WANG, Y., LIU, G., WANG, R., XIAO, H., LI, X., HOU, C., SHEN, B., GUO, R., LI, Y., SHI, Y. & CHEN, G. 2012. Opposite role of tumor necrosis factor receptors in dextran sulfate sodium-induced colitis in mice. *Plos One,* 7**,** e52924.

WANG, L., DU, F. & WANG, X. 2008. TNF-alpha induces two distinct caspase-8 activation pathways. *Cell,* 133**,** 693-703.

WANG, Y., HAN, G., CHEN, Y., WANG, K., LIU, G., WANG, R., XIAO, H., LI, X., HOU, C., SHEN, B., GUO, R., LI, Y. & CHEN, G. 2013b. Protective role of tumor necrosis factor (TNF) receptors in chronic intestinal inflammation: TNFR1 ablation boosts systemic inflammatory response. *Lab Invest,* 93**,** 1024-35.

WANG, Y., ZHANG, H. X., SUN, Y. P., LIU, Z. X., LIU, X. S., WANG, L., LU, S. Y., KONG, H., LIU, Q. L., LI, X. H., LU, Z. Y., CHEN, S. J., CHEN, Z., BAO, S. S., DAI, W. & WANG, Z. G. 2007. Rig-I-/- mice develop colitis associated with downregulation of G alpha i2. *Cell Res,* 17**,** 858-68.

WATANABE, J., LIN, J. A., NARASIMHA, A. J., SHAHBAZIAN, A., ISHIKAWA, T. O., MARTIN, M. G., HERSCHMAN, H. R. & REDDY, S. T. 2010. Novel anti-inflammatory functions for endothelial and myeloid cyclooxygenase-2 in a new mouse model of Crohn's disease. *Am J Physiol Gastrointest Liver Physiol,* 298**,** G842-50.

WATANABE, N., HANABUCHI, S., SOUMELIS, V., YUAN, W., HO, S., DE WAAL MALEFYT, R. & LIU, Y. J. 2004. Human thymic stromal lymphopoietin promotes dendritic cell-mediated CD4+ T cell homeostatic expansion. *Nat Immunol,* 5**,** 426-34.

WEBER, B., SAURER, L. & MUELLER, C. 2009. Intestinal macrophages: differentiation and involvement in intestinal immunopathologies. *Seminars in Immunopathology,* 31**,** 171-184.

WEBER, B., SAURER, L., SCHENK, M., DICKGREBER, N. & MUELLER, C. 2011. CX3CR1 defines functionally distinct intestinal mononuclear phagocyte subsets which maintain their respective functions during homeostatic and inflammatory conditions. *Eur J Immunol,* 41**,** 773-9.

WEHKAMP, J., SALZMAN, N. H., PORTER, E., NUDING, S., WEICHENTHAL, M., PETRAS, R. E., SHEN, B., SCHAEFFELER, E., SCHWAB, M., LINZMEIER, R., FEATHERS, R. W., CHU, H., LIMA, H., JR., FELLERMANN, K., GANZ, T., STANGE, E. F. & BEVINS, C. L. 2005. Reduced Paneth cell alpha-defensins in ileal Crohn's disease. *Proc Natl Acad Sci U S A,* 102**,** 18129-34.

WEIGMANN, B., TUBBE, I., SEIDEL, D., NICOLAEV, A., BECKER, C. & NEURATH, M. F. 2007. Isolation and subsequent analysis of murine lamina propria mononuclear cells from colonic tissue. *Nature Protocols,* 2**,** 2307-2311.

WELLS, J. M., ROSSI, O., MEIJERINK, M. & VAN BAARLEN, P. 2011. Epithelial crosstalk at the microbiota-mucosal interface. *Proceedings of the National Academy of Sciences of the United States of America,* 108**,** 4607-4614.

WIRTZ, S. & NEURATH, M. F. 2007. Mouse models of inflammatory bowel disease. *Advanced Drug Delivery Reviews,* 59**,** 1073-1083.

WITSELL, A. L. & SCHOOK, L. B. 1992. Tumor-necrosis-factor-alpha is an autocrine growth-regulator during macrophage differentiation. *Proceedings of the National Academy of Sciences of the United States of America,* 89**,** 4754-4758.

XAVIER, R. J. & PODOLSKY, D. K. 2007. Unravelling the pathogenesis of inflammatory bowel disease. *Nature,* 448**,** 427-34.

YAKOVICH, A. J., HUANG, Q., DU, J., JIANG, B. & BARNARD, J. A. 2010. Vectorial TGF beta Signaling in Polarized Intestinal Epithelial Cells. *Journal of cellular physiology,* 224**,** 398-404.

YAPALI, S. & HAMZAOGLU, H. O. 2007. *Anti-TNF Treatment in Inflammatory Bowel Disease*.

ZAPH, C., TROY, A. E., TAYLOR, B. C., BERMAN-BOOTY, L. D., GUILD, K. J., DU, Y., YOST, E. A., GRUBER, A. D., MAY, M. J., GRETEN, F. R., ECKMANN, L., KARIN, M. & ARTIS, D. 2007. Epithelial-cell-intrinsic IKK-beta expression regulates intestinal immune homeostasis. *Nature,* 446**,** 552-6.

ZEUTHEN, L. H., FINK, L. N. & FROKIAER, H. 2008. Epithelial cells prime the immune response to an array of gut-derived commensals towards a tolerogenic phenotype through distinct actions of thymic stromal lymphopoietin and transforming growth factor-beta. *Immunology,* 123**,** 197-208.

ZHANG, D., ZHANG, G., HAYDEN, M. S., GREENBLATT, M. B., BUSSEY, C., FLAVELL, R. A. & GHOSH, S. 2004. A toll-like receptor that prevents infection by uropathogenic bacteria. *Science,* 303**,** 1522-6.

ZHANG, X., GONCALVES, R. & MOSSER, D. M. 2008. The isolation and characterization of murine macrophages. *Curr Protoc Immunol,* Chapter 14**,** Unit 14 1.

ZHAO, Y., CONZE, D. B., HANOVER, J. A. & ASHWELL, J. D. 2007. Tumor necrosis factor receptor 2 signaling induces selective c-IAP1-dependent ASK1 ubiquitination and terminates mitogen-activated protein kinase signaling. *J Biol Chem,* 282**,** 7777-82.